

**TEMPERATURE-DEPENDENT EFFICACY OF THE IFN- α/β RESPONSE AGAINST
CHIKUNGUNYA AND OTHER ARBOVIRUSES**

by

Whitney Christine Lane

B.S. in Biology, Purdue University-Fort Wayne, 2012

Submitted to the Graduate Faculty of
The School of Medicine in partial fulfillment
of the requirements for the degree of
Doctor of Philosophy in Molecular Virology and Microbiology

University of Pittsburgh

2018

UNIVERSITY OF PITTSBURGH
SCHOOL OF MEDICINE

This dissertation was presented

by

Whitney Lane

It was defended on

July 10, 2018

and approved by

William Klimstra, PhD, Associate Professor of Immunology

Neal DeLuca, PhD, Professor of Microbiology and Molecular Genetics

Robert Binder, PhD, Associate Professor of Immunology

Amy Hartman, PhD, Assistant Professor of Infectious Diseases and Microbiology

John Williams, MD, Professor of Pediatrics

Doug Reed, PhD, Associate Professor of Immunology

Dissertation Advisor: William Klimstra, PhD, Associate Professor of Immunology

Copyright © by Whitney Lane

2018

TEMPERATURE-DEPENDENT EFFICACY OF THE IFN- α/β RESPONSE AGAINST CHIKUNGUNYA AND OTHER ARBOVIRUSES

Whitney Christine Lane

University of Pittsburgh, 2018

Chikungunya virus (CHIKV) is a mosquito-transmitted arbovirus in the genus *Alphavirus* that has reemerged in recent years to cause explosive epidemics of acute and chronic arthritic disease across the globe. Like other arboviruses, CHIKV has evolved to replicate efficiently in both its arthropod vector and its vertebrate hosts, which represent two very different thermal environments. Arthritogenic alphaviruses such as CHIKV preferentially replicate and cause disease in distal small joints that are lower in temperature than the body core. The type-I interferon (IFN- α/β) system is a critical innate immune response for controlling arbovirus infection. Recent evidence suggests that IFN- α/β is less effective in controlling virus infection at temperatures below the body core temperature. Therefore, we hypothesized that arboviruses such as CHIKV may exploit a weakened innate immune environment in low-temperature joint tissues to fuel exacerbated viral replication and disease at these sites.

To address this hypothesis, we examined the efficacy of IFN- α/β induction and antiviral efficacy against CHIKV and other arboviruses at different temperatures within the normal physiological range. *In vitro*, we found that mild hypothermia significantly compromised both the induction and effector arms of the IFN- α/β response compared to normal or febrile-range temperatures against diverse arboviruses. We narrowed this effect to delayed and reduced transcription of effector genes, as upstream signaling pathways were not attenuated by hypothermia, and demonstrated differential temperature-sensitivity profiles of interferon-stimulated gene (ISG) induction versus some lipopolysaccharide (LPS)-inducible genes. Finally,

mice with reduced core temperatures suffered exacerbated CHIKV replication and disease compared with normal mice during the acute phase of infection, and this phenotype was dependent upon a functional IFN- α/β system. Reduced core temperature during the first few days of CHIKV infection also resulted in higher persistent viral signal at chronic time points, and temperature reduction >30 days post infection resulted in significantly increased viral protein production at persistently-infected sites. Together, these data indicate that reduced tissue temperature results in attenuated IFN- α/β and ISG gene transcription, leaving these tissues more vulnerable to arboviral infection than warmer sites. CHIKV can take advantage of this dynamic to infect and persist in low-temperature tissues *in vivo*.

TABLE OF CONTENTS

PREFACE.....	XIV
1.0 INTRODUCTION.....	1
1.1 ARBOVIRUSES	1
1.1.1 Major characteristics of arbovirus genera and associated diseases.....	3
1.1.1.1 Genus <i>Alphavirus</i>.....	3
1.1.1.2 Genus <i>Flavivirus</i>	5
1.1.1.3 Order Bunyavirales.....	6
1.1.1.4 Family <i>Reoviridae</i>	8
1.1.2 Common features of arbovirus transmission and ecology.....	9
1.1.3 Features of arbovirus pathogenesis and immune response in humans	11
1.2 CHIKUNGUNYA VIRUS.....	14
1.2.1 Cellular replication.....	15
1.2.2 Distribution and ecology	17
1.2.3 Pathogenesis and disease in humans.....	20
1.2.4 Adaptive immune response.....	27
1.2.4.1 T cell response	27
1.2.4.2 B cell response	29
1.2.5 Animal models of CHIKV infection.....	31

1.2.5.1	Neonatal and immunocompromised murine lethal challenge models	31
1.2.5.2	Adult wild-type murine acute arthritic models.....	31
1.2.5.3	Mouse models of chronic CHIKV infection.....	32
1.2.5.4	Nonhuman primate models.....	33
1.3	TYPE-I INTERFERON	33
1.3.1	Definition and classification.....	35
1.3.2	Induction pathways	36
1.3.2.1	Toll-like receptor signaling	36
1.3.2.2	RIG-I-like receptor signaling.....	38
1.3.2.3	IFN gene transcription.....	40
1.3.3	Effector pathways.....	41
1.3.3.1	Canonical JAK-STAT signaling	42
1.3.3.2	Accessory signaling pathways.....	42
1.3.3.3	ISG transcriptional regulation.....	44
1.3.4	ISG functions and the antiviral state.....	46
1.3.4.1	Myxovirus resistance (Mx).....	48
1.3.4.2	Interferon-induced protein with tetrapeptide repeats (IFIT).....	48
1.3.4.3	Interferon-inducible transmembrane (IFITM).....	49
1.3.4.4	Zinc finger antiviral protein (ZAP).....	50
1.3.4.5	Interferon-stimulated gene 15 kDa (ISG15).....	50
1.3.4.6	Interferon-stimulated gene 20 kDa (ISG20).....	50

1.3.4.7	Virus inhibitory protein, endoplasmic reticulum-associated, IFN-inducible (Viperin).....	51
1.3.5	Effects of IFN- α/β on innate and adaptive immunity.....	52
1.4	PHYSIOLOGICAL TEMPERATURE VARIATION.....	54
1.4.1	Mechanisms of thermoregulation for core temperature maintenance	55
1.4.1.1	Physiological and behavioral responses to cold exposure	56
1.4.2	Physiological and behavioral responses to heat exposure.....	60
1.4.3	Temperature variation between anatomical compartments	61
1.4.4	Physiological factors affecting human body temperature	64
1.4.4.1	Impaired circulation	64
1.4.4.2	Fever	65
1.4.5	Intracellular responses to temperature change	66
1.4.5.1	Heat shock response.....	67
1.4.5.2	Cold shock response.....	70
1.4.6	Effects of physiological temperature variation on immune responses	74
1.4.6.1	Fever/hyperthermia	74
1.4.6.2	Hypothermia.....	77
1.5	HYPOTHESIS	78
2.0	EFFICACY OF THE INTERFERON-A/B RESPONSE VERSUS ARBOVIRUSES IS TEMPERATURE-DEPENDENT.....	81
2.1	INTRODUCTION	81
2.2	RESULTS	83

2.2.1	Efficacy of IFN- α/β against arboviruses is reduced at subnormal temperatures.....	83
2.2.2	ISG protein and mRNA levels are reduced at subnormal temperatures .	89
2.2.3	Suppression of type I IFN signaling pathways is not associated with early temperature effects.....	95
2.2.4	Transcription of IFN response pathway genes is highly temperature-dependent.....	99
2.2.5	Reduced temperature also affects type I IFN induction	104
2.2.6	Lower temperatures <i>in vivo</i> suppress IFN- α/β responses	108
2.3	DISCUSSION.....	112
3.0	MODELING PERSISTENT CHIKUNGUNYA INFECTION IN MICE USING <i>IN VIVO</i> IMAGING	120
3.1	INTRODUCTION	120
3.2	RESULTS	125
3.2.1	High-sensitivity <i>in vivo</i> imaging reveals persistent CHIKV nLuc signal beyond four months post-infection.....	125
3.2.2	Exacerbation of CHIKV acute phase replication via body temperature reduction, IRF7 deficiency, or a mutant CHIKV (200R).....	130
3.2.3	Temperature reduction during chronic CHIKV infection induces flaring of persistent viral nLuc signal.....	134
3.3	DISCUSSION.....	138
3.3.1	Detection of a persistent infection	138
3.3.2	A flaring disease model	142

4.0	CONCLUSIONS	144
4.1	TEMPERATURE-DEPENDENT EFFICACY OF TYPE-I INTERFERON 145	
4.2	IMPACTS OF TEMPERATURE VARIATION AND ACUTE INFECTION SEVERITY ON CHIKUNGUNYA PERSISTENCE.....	146
4.3	CONCLUDING REMARKS	147
5.0	MATERIALS AND METHODS	148
	APPENDIX A	163
	BIBLIOGRAPHY	169

LIST OF TABLES

Table 1. List of primers used for qRT-PCR.....	154
Table 2. List of NanoString target genes and probe locations	155

LIST OF FIGURES

Figure 1: Example arbovirus transmission cycles (adapted with permission from (85))	11
Figure 2: Distribution of Chikungunya virus and its major epidemic vectors (adapted with permission from (33), Copyright Massachusetts Medical Society).....	18
Figure 3: Clinical signs of acute CHIKV disease: swollen joints and erythematous rash (adapted with permission from (126))	23
Figure 4: Pathogenesis of Chikungunya virus (adapted with permission from (153)).....	25
Figure 5: RNA-sensing type-I interferon induction pathways (adapted with permission from (285)).....	40
Figure 6: Signaling pathways stimulated by IFN- α/β (adapted with permission from (261)).....	44
Figure 7. Efficacy of type I IFN against arboviruses is reduced at subnormal temperatures.	86
Figure 8. Efficacy of type I IFN against arboviruses is reduced at subnormal temperatures in additional cell types.	88
Figure 9. At subnormal temperatures, ISG protein and mRNA levels are reduced.....	91
Figure 10. At subnormal temperatures, ISG protein and mRNA levels are reduced in additional cell types.	92
Figure 11. Temperature variation affects baseline transcription and translation rates.	94

Figure 12. Suppression of type I IFN signaling pathways is not associated with early temperature effects.....	97
Figure 13. Suppression of type I IFN signaling pathways is not associated with early temperature effects in additional cell types.....	99
Figure 14. NanoString analysis detects temperature-sensitive gene transcription.	101
Figure 15. Transcription of IFN response pathway genes is highly temperature-dependent.	103
Figure 16. Reduced temperature also affects IFN- α/β induction.....	107
Figure 17. Lower temperature in vivo suppresses IFN- α/β responses.....	110
Figure 18. Torpor and reserpine treatment reduce mouse core temperature.	111
Figure 19. High-sensitivity in vivo imaging reveals persistent CHIKV nLuc signal beyond four months post-infection.....	130
Figure 20. Exacerbation of CHIKV acute phase replication via body temperature reduction, IRF7 deficiency, or a mutant CHIKV (200R).....	134
Figure 21. Temperature reduction during chronic CHIKV infection induces flaring of persistent viral nLuc signal.	138

PREFACE

I owe many heartfelt thanks to those who helped me cross the finish line.

First, it is my firm belief that without the constant love and encouragement from my husband, Nishank Bhalla, I would not have made it through. His patience and belief in me far exceeded my own. And as a fellow member of the Klimstra lab, he provided me an enormous amount of scientific insight through our work-related conversations, not to mention good company for some very late nights in the lab. Thank you, and I love you.

Secondly, I would like to thank all my colleagues in the Klimstra lab, past and present, who formed an incredible support network throughout my graduate career. From technical and scientific to mental and emotional support, I could always count on my work family to be there for me. It meant the world on good days and bad days. Thank you. I also need to call out Matt Dunn by name, who single-handedly made sure I was adequately caffeinated through the dissertation writing process. Thank you for being not only an excellent co-worker and lab manager, but one of my very best friends, too.

Thirdly, a huge thanks to my parents, Ann and Matt Lane, my siblings, Paige Schonefeld and Nick Lane, and all my friends from back home whom I've been neglecting for the last six years. You've always been proud of me no matter what, cheering me on, reminding me to separate Whitney the person from Whitney the graduate student. I needed every last bit of it. Thank you, and I love you.

Lastly, I need to thank my mentor, Dr. William Klimstra, my dissertation committee, and the MVM program at University of Pittsburgh. William, thank you for being patient with me through this process. I learned an immense amount from you, and I am extremely grateful for that. To my dissertation committee, thank you for believing in my project and guiding my progress through helpful and congenial suggestions and constructive criticism. And finally, a big thank you to the University of Pittsburgh School of Medicine and the IBGP and MVM programs for giving me the opportunity to pursue my PhD and for the education and support I received during my time here.

1.0 INTRODUCTION

1.1 ARBOVIRUSES

The term *arbovirus* is an abbreviation used to refer to viruses transmitted biologically between vertebrate hosts by a hematophagous arthropod vector (*arthropod-borne virus*). The World Health Organization defines arboviruses as “viruses which are maintained in nature principally, or to an important extent, through biological transmission between susceptible vertebrate hosts by haematophagous arthropods; they multiply and produce viremia in the vertebrates, multiply in the tissues of arthropods, and are passed on to new vertebrates by the bites of arthropods after a period of extrinsic incubation” (1). This definition excludes arthropod-transmitted plant viruses as well as viruses that may be vectored by an arthropod but that do not replicate within the vector, a mode of transmission deemed mechanical rather than biological (2). However, the term arbovirus does not represent a taxonomic distinction, and in fact, arboviruses comprise a highly diverse group, with arthropod transmission evolving convergently among phylogenetically distant viruses belonging to several taxa. The clinically important arboviruses fall into one of four taxonomic groups; family *Togaviridae*, genus *Alphavirus*, family *Flaviviridae*, genus *Flavivirus*, several genera in the order *Bunyavirales* (formerly, family *Bunyaviridae*) and several in the *Reoviridae* family, however arboviruses of other vertebrates that rarely infect humans are

also found in the *Rhabdoviridae* (genus *Vesiculovirus*) and *Orthomyxoviridae* (genus *Thogotovirus*) families (3, 4).

One shared feature of all arboviruses is their ability to replicate efficiently across a broad temperature range due to their adaptation to both vertebrate hosts and invertebrate vectors, which represent two very different thermal environments. Many arboviruses, including all species known to infect humans, are transmitted between endothermic mammalian and/or avian hosts, whose core body tissues are actively maintained at a very high temperature, typically 37-39°C for mammals and 39-41°C for birds (5). By contrast, the arthropod vectors are ectotherms, and their temperatures are dependent on the ambient temperature of their environment. Within a human host, arboviral pathogenesis begins in the skin, at the site of the arthropod's bite, and from there the virus can use the lymphatics and bloodstream to disseminate systemically, traversing tissues in the body core and periphery and thus encountering variable tissue temperatures. In addition, while many arboviruses inhabit tropical and subtropical regions where transmission can occur year-round, others are subject to seasonality in more temperate climates, which may further impact their hosts' thermal environments, particularly during the transitions toward or away from peak (summer) transmission. It is currently unknown how arbovirus pathogenesis and disease are influenced by the thermal environment within a human host, but several lines of evidence suggest various components of innate and adaptive immunity are sensitive to temperature variation, which could, in turn, impact the course of an arbovirus infection. In this section, I will introduce some of the most medically and agriculturally impactful arboviruses and their associated diseases and describe the features of arbovirus ecology and pathogenesis that are common to most species.

1.1.1 Major characteristics of arbovirus genera and associated diseases

1.1.1.1 Genus *Alphavirus*

The alphaviruses are a genus of positive-sense single-stranded RNA (ssRNA) viruses in the family *Togaviridae*. The 60- to 70-nm, spherical alphavirus particle consists of a nucleocapsid core surrounded by a host cell plasma membrane-derived lipid envelope studded with glycoprotein spikes (6). The genomic RNA is contained in the nucleocapsid protein shell. 240 copies of the capsid protein are arranged around the genome in T=4 icosahedral symmetry (7-9). The viral envelope glycoproteins, E1 and E2, form trimers of heterodimers that protrude from the lipid envelope as 80 spike structures, such that 240 total copies each of E1 and E2 interact with the 240 copies of capsid (8, 10-12). The alphavirus genome measures between 11 and 12 kb in length (6) and bookended with a 5' type-0 7-methylguanosine cap and a 3' poly-A tail along with 5' and 3' untranslated regions (UTRs) (13-16). The nonstructural proteins, nsPs 1 through 4, are encoded as a single open reading frame in the 5' proximal end of the RNA, while the structural proteins, capsid, E3, E2, 6K/TF, and E1, are expressed off a subgenomic promoter 3' to the nonstructural proteins (6, 17). The *Alphavirus* genus (commonly, alphaviruses) comprises over 30 species, the vast majority of which are known to be arthropod-vector-borne (18). These species can be subdivided further into seven antigenically similar complexes, Barmah Forest, eastern equine encephalitis, Middleburg, Ndumu, Semliki Forest, Venezuelan equine encephalitis, and Western equine encephalitis serocomplexes (19). Most alphaviruses are transmitted between mammalian or avian hosts by mosquito vectors, but some are thought to be mite- or louse-borne (6, 20). Beyond antigenic complexes, alphaviruses historically have been grouped based on both geographic range and human or veterinary disease phenotype. Alphaviruses found predominantly on the continents of Australia, Africa, Europe, and/or Asia tend to cause a febrile illness

associated with joint pain and rash, and have thus been designated the Old World, arthritogenic alphaviruses (19, 21). Analogously, alphaviruses geographically restricted to the Americas primarily cause acute encephalitis, and thus became known as the New World, encephalitic alphaviruses (19, 22). However, these geographic designations do not accurately reflect the true distributions of all alphaviruses.

Members of both the Old World and New World alphaviruses are known to cause disease in humans and livestock. Eastern, western, and Venezuelan equine encephalitis viruses (EEEV, WEEV, and VEEV) are medically and agriculturally important New World alphaviruses while CHIKV, Ross River virus (RRV) and Sindbis virus (SINV) are the Old World alphaviruses most commonly associated with human infections. Most alphaviruses in fact do not infect humans and instead exhibit a very broad vertebrate host range, with various non-human primates, equids, rodents, birds, and fish serving as hosts for different alphaviruses (6, 23, 24). EEEV, VEEV, and WEEV are encephalitic alphaviruses that typically cause a low incidence of human disease but EEEV and VEEV have been known to cause large epizootic outbreaks in horses (25-27). VEEV has also been known to cause infrequent but explosive outbreaks of human disease in South America (28). The severity of human encephalitis caused by these viruses can range from subclinical to lethal. North American strains of EEEV, for example, have case-fatality rates between 35 and 75% (22, 29, 30). Nonfatal encephalitic cases of any of these viruses can result in mild to severe neurological sequelae (31). Most WEEV and VEEV cases in humans do not progress to encephalitis and are either asymptomatic or acute and mildly symptomatic, presenting with flu-like symptoms and fever and resolving within 1 to 2 weeks (22, 32). Unlike the encephalitic alphaviruses, the arthritogenic species are associated with low mortality but very high morbidity in humans. SINV, RRV, and CHIKV are examples of arthritogenic alphaviruses

commonly associated with human disease, especially CHIKV, which has reemerged on a pandemic scale in the last 15 years (33). These viruses cause an acute febrile illness and severe, debilitating joint pain that can persist for years after infection (21).

1.1.1.2 Genus *Flavivirus*

Viruses in the genus *Flavivirus*, family *Flaviviridae*, are, like the alphaviruses, enveloped, positive-sense ssRNA viruses. They are slightly smaller than alphaviruses, with particle diameters near 50 nm and a genome length of approximately 11 kb (34). Genomic RNA is contained within the nucleocapsid, encased by a coat of capsid proteins. Surrounding the nucleocapsid core is a host cell-derived lipid envelope in close association with the viral membrane protein (35). The surface of the flavivirus virion is covered completely with the envelope protein, which forms homodimers that lie parallel to the virion surface, giving mature flavivirus particles a smooth appearance (36, 37). The flavivirus genome is organized oppositely of that of the alphaviruses, with the structural proteins encoded 5' of the nonstructural proteins on a single ORF (38). The genomic RNA is capped at the 5' end but lacks a poly-A tail, and contains both 5' and 3' noncoding regions (39). Phylogenetic analysis has revealed that divergence from the ancestral virus occurred along two primitive lineages according to transmission vector, yielding sister taxa of tick-borne and mosquito-borne flaviviruses (40). The mosquito-borne flaviviruses further diverged according to usage of *Culex* versus *Aedes* species mosquitoes (40, 41). Today, there are over 60 recognized species of flaviviruses, many of which are pathogens of humans and livestock (42).

Many flaviviruses commonly associated with human disease are mosquito-borne species that cause exotic tropical fevers, such as Dengue virus (DENV), yellow fever virus (YFV) and Zika virus (ZIKV). However, other flaviviruses such as Japanese Encephalitis virus (JEV) and

West Nile virus (WNV) reside in more temperate regions as well as the tropics and subtropics (43). In addition, the tick-borne encephalitis viruses (TBEVs) cause frequent human infections throughout Europe and Asia (44). This diversity has given flaviviruses a near worldwide distribution. Human flavivirus diseases are typically either neurological/encephalitic or visceral/hemorrhagic (45). Acute flavivirus infection usually elicits fever, fatigue, body aches, and other nonspecific, flu-like symptoms, and many cases are asymptomatic (46).

1.1.1.3 Order Bunyavirales

The order Bunyvirales contains over 350 viral species divided into nine families (47). Of these families, only one, the *Hantaviridae*, is not a family of arthropod-transmitted viruses (48). The other eight families contain a huge diversity of arboviruses as well as arthropod-vectoring viruses of plants and invertebrates. Bunyaviruses are vectored by a plethora of different arthropods including mosquitoes, ticks, sand flies, and thrips, among others, and, as mentioned above, display incredible host diversity (48). Despite this variety, all bunyaviruses share common structural and genomic characteristics. Bunyavirus particles are enveloped and typically measure between 80 and 120 nm in diameter, with either spherical or pleiomorphic morphology (48-51). The nucleocapsid contains a tripartite genome of negative-sense or ambisense ssRNA, the large (L), medium (M), and small (S) segments, each encoding a single transcriptional unit flanked by 5' and 3' non-translated regions (48). The S segment encodes the nucleocapsid protein, which is responsible for packaging viral genomic RNA into virions, and, in many but not all bunyaviruses, the nonstructural protein NSs, which is involved in modulation of the host cell and innate immune evasion, making it a major virulence factor for pathogenic bunyaviruses (52, 53). The M segment encodes the two viral glycoproteins in a single ORF, along with NSm proteins in some genera, which may be involved in viral assembly (54, 55). The L segment of all

bunyaviruses codes for the RNA-dependent RNA polymerase (RdRp) without accessory nonstructural proteins (48). Aside from these shared features, the virion morphologies and protein coding strategies of bunyaviruses are as diverse as their vector and host ranges.

Many arthropod-borne bunyaviruses such as Rift Valley fever virus (RVFV), a phlebovirus, Crimean-Congo hemorrhagic fever virus (CCHFV), a nairovirus, and La Crosse virus (LACV), an orthobunyavirus, are of great public health and agricultural significance. RVFV is endemic to Africa and has recently expanded into the Middle East (56, 57). It infects various domesticated animal species such as goats, sheep, and cattle, as well as humans, and can be transmitted through direct contact with infected bodily fluids (58, 59) or by a large variety of mosquito genera including *Culex* and *Aedes* species (60). In humans, symptomatic cases can range from a mild febrile illness to rare cases of severe hemorrhagic fever syndrome or meningoencephalitis, with a case-fatality rate up to 20% (61). In livestock, RVFV infection is usually more serious and can result in higher fatality rates. It also induces 70-100% fetal loss in pregnant animals and 20-30% mortality in adult animals, which can be devastating for agricultural economies affected by a large outbreak (61). CCHFV can cause a similar hemorrhagic disease to RVFV, but it is transmitted by ticks, which also serve as the natural reservoir, in addition to body fluids (62). It is found in much of Europe, Africa, the Middle East, and Asia and can cause outbreaks of human disease that can reach a 30% case-fatality rate (62, 63). Unlike RVFV, domesticated ungulates that become infected with CCHFV do not experience disease (64). LACV is an encephalitic bunyavirus endemic to the United States that is transmitted between deciduous forest-dwelling rodents by the mosquito *Aedes triseriatus* (65). Human infection is associated with nonspecific summertime fevers that usually resolve within a

week, but a small subset of patients, typically children, progress to encephalitis characterized by seizure, paralysis, coma, and rarely, death (66, 67).

1.1.1.4 Family *Reoviridae*

The Reoviridae are a hugely diverse family of segmented, double-stranded RNA (dsRNA) viruses with a host range encompassing vertebrates, invertebrates, plants, protists, and fungi. There are two subfamilies of reoviruses containing 15 genera. Of these, four genera contain arboviruses; *Cardoreovirus*, *Coltivirus*, *Orbivirus*, and *Seadornavirus*, of which the latter three contain human pathogens. Rotavirus is probably the most-well known human reovirus, causing a common diarrheal disease in children, but it is transmitted via the oral-fecal route rather than by an arthropod vector. All reoviruses are nonenveloped and possess a single, double, or triple-layered virion structure with concentric inner and outer protein layers, and virions measure approximately 70 nm in diameter (68). The inner capsid is arranged as a T=2 icosahedron while the outer layer typically possesses T=13 icosahedral symmetry. The reovirus genome comprises 10-12 segments of dsRNA contained within the nucleocapsid, each encoding 1-3 proteins (68). Colorado tick fever virus (CTFV), a coltivirus, is one of the most important human reovirus transmitted by an arthropod, with 200-400 cases in the United States per year (69). It is transmitted to humans by the tick *Dermacentor andersoni*, which is endemic to the Rocky Mountains and the western United States (69). About 50% of human cases are symptomatic, characterized by biphasic fever, headache, muscle pain, and weakness, and disease is usually self-limiting (70). Rare severe complications such as encephalitis, hemorrhage, and pericarditis are sometimes observed in children, but associated mortality is very low (69).

1.1.2 Common features of arbovirus transmission and ecology

Most arbovirus transmission cycles involve a zoonotic reservoir or amplification in vertebrate hosts in addition to an arthropod vector, although some, such as dengue virus (DENV), Zika virus (ZIKV) and chikungunya virus (CHIKV), are capable of sustained human-mosquito-human spread in an urban transmission cycle in the absence of an intermediate zoonotic host (71, 72). Many characteristics of arbovirus existence – geographic range, ecological niche, potential for emergence in human populations, and epidemiology, to name a few – thus depend heavily on the lifestyles of its primary vectors and enzootic host(s). Birds are common enzootic reservoirs for arboviruses, and the avian arboviruses are transmitted by ornithophilic (bird-feeding) arthropods, frequently *Culex* and *Culiseta* species mosquitoes. The distribution of avian arboviruses such as the flaviviruses JEV and WNV is often subject to the migratory patterns of their host birds, and thus may exhibit very large or seasonal geographic ranges (71). The power of migratory birds to spread an emerging arbovirus was demonstrated recently with the single introduction of WNV into New York in 1999. Within only five years, WNV had established endemicity throughout the United States, southern Canada, Central and South America in large part due to the rapid infection of and dissemination through naïve migratory bird populations (73-76). In addition, many *Culex* mosquito species are anthropophilic (human-feeding) as well as ornithophilic, so humans living near arbovirus-infected bird populations are at risk of infection by the virus' primary vector species (71).

In contrast, arboviruses with mammalian reservoirs tend to be less naturally mobile than bird-borne arboviruses. Forest-dwelling rodents and nonhuman primates host various arbovirus species that are commonly transmitted by arboreal *Aedes* species mosquitoes in a sylvatic transmission cycle. Tick-borne viruses in temperate areas such as CTFV transmit in a similar

cycle between rodents and ticks that bite humans opportunistically. Historically, the risk of emergence of mammalian arboviruses in human populations has been relatively low, but recently, human encroachment into tropical forest habitats combined with the advent of rapid and prolific international air travel has greatly increased that risk (77-80). Interestingly, human interference in sylvatic arboviral transmission in Africa during the slave trade is responsible for bringing YFV and DENV and their principal vector *Aedes aegypti* to South America from Africa on ships (81-84), so humans have a rich history of aiding the spread of mammalian-borne arboviruses even before the age of air travel.

For mammalian arboviruses to cause an epidemic or epizootic outbreak, a spillover event out of their sylvatic cycle must occur. Most arboreal *Aedes* mosquitoes are not anthropophilic, so spillover into human or domesticated animal populations often occurs via a bridge or epizootic vector (85). For some arboviruses such as CHIKV and DENV, human epidemic spread can be maintained by direct human-mosquito-human transmission in an urban cycle by distinct, anthropophilic epidemic vectors such as *Aedes aegypti* or *Aedes albopictus* (85). Importantly, because most arboviruses evolved in an enzootic cycle that does not involve humans, human infections are typically not required for sustained viral transmission, and humans rarely establish a high enough viremia to reinfect a mosquito (except during urban CHIKV or DENV infections). Other factors beyond serum viremia, such as some heretofore unidentified aspects of human physiology or the feeding preferences of competent vector species, may also block human-to-vector transmission for some arboviruses. Thus, humans are usually dead-end hosts for arboviruses (71). However, lack of coevolution with arboviruses means that humans are more likely to become ill upon infection compared to an enzootic host, which typically replicates the

virus to high titer to enable transmission but does not develop disease (71). For some arboviruses, human infection can result in very severe disease and even death.

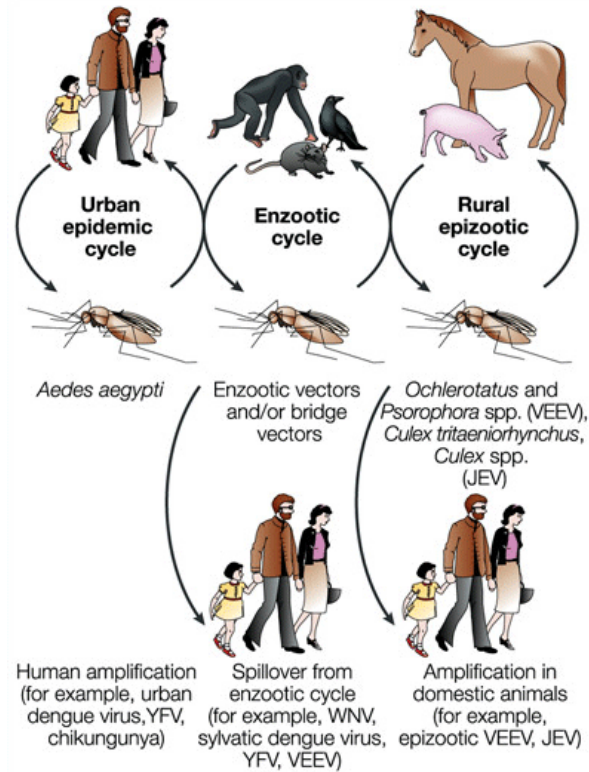


Figure 1: Example arbovirus transmission cycles (adapted with permission from (85))

1.1.3 Features of arbovirus pathogenesis and immune response in humans

Arbovirus infections of humans share many pathogenic features due to their similar routes of transmission. All arbovirus infections begin in the skin, at the site of the infected arthropod's bite. Many arboviruses replicate locally at the site of infection and then in secondary lymphoid organs, and from there disseminate systemically via the bloodstream. End-game organs vary by arbovirus and determine the presentation characteristics of severe disease. Encephalitic alphaviruses, flaviviruses, and bunyaviruses target tissues in the central nervous system including neurons, microglia, and astrocytes, depending on the virus (86, 87).

Meningoencephalitis is a common outcome of symptomatic encephalitic arbovirus disease. Arthritogenic alphaviruses exhibit preferential tropism for joint-associated musculoskeletal tissues in the distal limbs of patients, where they cause arthritis, arthralgia, and myalgia (88). Hemorrhagic arboviruses such as YFV and CCHFV infect a variety of the deep visceral organs like the liver and induce a strong inflammatory response associated with internal bleeding and eventual multiorgan failure (89, 90). CTFV targets hematopoietic cells in the bone marrow and can persist in the blood stream in erythrocytes that became infected as erythroblasts for months after infection (91, 92).

It bears repeating that the majority of arboviral infections of humans result in asymptomatic or mild disease, therefore, humans possess the immune capabilities to control and clear arbovirus infections. Type-I interferon (IFN- α/β) has been identified as a critical innate immune response for initial control of a plethora of arboviral infections. Evidence supporting the vital role of IFN- α/β against arboviruses comes from mouse models lacking various components of the IFN- α/β induction or effector pathways. Peripheral infection of adult wild-type mice with many arboviruses results in subclinical or mild nonlethal disease and viral replication is quickly controlled coincident with IFN- α/β induction. By contrast, arboviral infection of mice deficient in the IFN- α/β receptor or various components of its associated signaling pathways is often rapidly fatal with uncontrolled viral replication and systemic tissue invasion. This is true of the arthritogenic alphaviruses CHIKV (93, 94), o'nyong'nyong virus (ONNV) (95), Semliki Forest virus (96), and SINV (97, 98), the flaviviruses DENV (99-101), YFV (102), ZIKV (103, 104), TBEV (105), and Murray Valley encephalitis virus (106) and the bunyaviruses CCHFV (107) and LACV (108, 109). The encephalitic alphaviruses EEEV and VEEV, flaviviruses WNV and JEV, and the bunyavirus RVFV do cause fatal disease in adult IFN- α/β -competent mice, but

mean time-to-death is significantly shortened in its absence (110-114). Interestingly, mice with attenuated but not abrogated IFN- α/β responses have shown increased susceptibility to various arboviruses without the fatal outcome, indicating that the relative strength of the IFN- α/β response can determine pathogenic outcomes of arbovirus infections (115). Similarly, modest changes in IFN- α/β efficacy have been shown to influence the cellular tropism of highly IFN- α/β -sensitive arboviruses, such as SINV (98).

Additional support for the importance of the type-I IFN response against alphaviruses comes from the multitude of virally-encoded mechanisms to counteract the IFN- α/β response. For example, most alphaviruses are able to inhibit host cell macromolecular synthesis and thereby attenuate the cells' ability to produce IFN- α/β and its antiviral effectors (116). EEEV, by contrast, completely avoids replication in myeloid cells, which would otherwise be responsible for producing high levels of IFN- α/β (117, 118). Alphavirus and flavivirus proteins can also directly antagonize various components of the IFN- α/β signaling pathway (119-123). CCHFV encodes a protease that can directly cleave cellular ubiquitin and the antiviral effector protein ISG15 to suppress IFN- α/β responses (124) and LACV NSs can inhibit IFN- α/β production (125). Importantly, mutations that abrogate these activities result in greatly attenuated viruses. Together, these findings underline the role of type-I interferon as a critical first-line defense against most if not all arbovirus infections, and suggest that even modest variations in its efficacy can have meaningful impacts on arbovirus pathogenesis and disease.

1.2 CHIKUNGUNYA VIRUS

Chikungunya virus (CHIKV) is an Old World arthritogenic alphavirus that has recently extended its geographic range from sub-Saharan Africa and southeast Asia to include southern Europe, South and Central America, the Caribbean, and some areas of the southern United States. CHIKV causes an acute febrile syndrome in humans characterized by a debilitating polyarthritides/polyarthralgia, which can persist in the distal joints of the limbs and extremities for months or years after the initial infection has been cleared (21). It is well established that an effective IFN- α/β response, in concert with production of neutralizing antibody, is paramount to the control and clearance of the virus in the acute stage (126), but the mechanisms driving the chronic disease manifestations, including whether or not viable CHIKV persists in distal joint tissues, remain unknown and hotly debated. Among arboviruses, CHIKV is somewhat unique in its preferential infection of, and potentially, persistence in, cold peripheral musculoskeletal tissues. If reduced tissue temperature confers greater viral fitness, possibly through attenuation of IFN- α/β , then the cooler temperatures in distal joint tissues may facilitate CHIKV infection and disease at these sites. While this interaction would most likely manifest during the acute infection, indirect consequences of inefficient viral clearance from distal joint tissues due to weakened IFN- α/β may present a risk factor for chronic CHIKV arthritis. Alternatively, there is mounting evidence of chronic type-I interferon activity during persistent RNA virus infection, potentially due to continual stimulation of pattern recognition receptors by persistent viral RNA, which may contribute to chronic inflammatory phenotypes (127), but may also be necessary for long-term control of the virus. In this section, I will introduce the molecular and pathogenic characteristics of CHIKV, with a focus on its acute and chronic disease mechanisms in humans and in animal models.

1.2.1 Cellular replication

The major features of the CHIKV virion and genome are akin to those of the other alphaviruses, as described above. Viral attachment to host cells is mediated by the viral envelope glycoprotein E2. Though known to have a proteinaceous component, the identity of the cellular receptor(s) that bind to and promote infection by CHIKV, or indeed any alphavirus, has/have remained largely a mystery. Several candidate molecules including glycosaminoglycans have been proposed as attachment and/or entry factors (128-130), but none have been confirmed as universal receptors. It is clear that c-type lectins can facilitate the attachment of alphaviruses to immune cells such as dendritic cells via engagement of the high mannose carbohydrate modifications of mosquito-derived viruses (131), however, the role of lectins in mediating entry is unclear. As CHIKV displays a broad host and tissue tropism, it is likely that the cellular receptor is either a broadly conserved and widely expressed protein and/or carbohydrate modification, or that CHIKV uses different receptors depending on the host and cell type being infected, with the latter hypothesis most likely. Very recently, the cell adhesion molecule Mxra8 was identified in a CRISPR-Cas9 screen as a specific infection-promoting receptor for CHIKV and several other arthritogenic alphaviruses, but not for encephalitic alphaviruses or other, unrelated RNA viruses, both in relevant cell types *in vitro* and in a mouse model of CHIKV infection (132). After receptor binding, CHIKV is internalized by clathrin-mediated endocytosis, and uncoating and release of the viral genome into the cytoplasm occurs upon acidification of the endosomal compartment (133-137). A pH-dependent conformational change in the E1 glycoprotein exposes a fusion loop that enables viral envelope fusion with the endosomal membrane and release of the nucleocapsid core (136).

The alphavirus genomic RNA is recognized as an mRNA by host cell ribosomes and immediately translated, producing the nonstructural polyproteins P123 or P1234 via readthrough translation of an opal stop codon between nsP3 and nsp4 (6). Autoproteolytic processing through the protease activity of nsP2 frees nsP4, the RdRp, which, together with P123, forms an active replicase complex (6, 138, 139). Full-length negative strand synthesis is initiated by this replicase complex and is associated with membranous structures formed at the plasma membrane, termed spherules, which are thought to be the major sites of genome replication (140-144). These small, vesicular structures become large cytopathic vacuoles within the cytoplasm of the host cell as the infection proceeds and may serve as sites of viral assembly before egress (140-142). Further proteolytic processing of P123 by nsP2 results in a conformational change in the replicase complex that switches its activity from negative strand to positive strand synthesis, using negative strand genomes as a template for both full-length genomic RNA and the 26S subgenomic RNA that encodes the structural proteins (138, 141, 145).

The structural proteins are translated as a second polyprotein consisting of capsid (C), E3, E2, 6K, TF, and E1. C is released immediately from the polyprotein upon its completed translation by autoproteolytic processing, which enables it to associate with viral genomic RNA and begin the encapsidation process (146-149). The rest of the polyprotein is translated as E3-E2-6K-E1, but low-frequency ribosomal frameshifting also results in a secondary product, E3-E2-TF (150, 151). Host proteases cleave the viral structural polyprotein into pE2 (E3-E2 fusion), free 6K and TF, which share an N-terminus but have disparate C-termini due to ribosomal frameshifting (TF stands for transframe protein (151)), and E1 (138). E3 is a leader peptide fused to the N-terminus of E2 and is responsible for trafficking the other structural proteins through the secretory pathway and protecting the nascent spike heterodimer of E2/E1 from premature

membrane fusion in the low pH of the early secretory pathway (138, 152, 153). pE2 and E1 traverse the secretory pathway as a non-covalently-linked hetero-oligomer and acquire several post-translational modifications including palmitoylation and N-linked glycosylation (154-156). A host furin-like protease in the trans-Golgi cleaves E3 from pE2, leaving mature E2, which can then form mature heterodimers with E1 at the plasma membrane (157-159). Nucleocapsid cores containing a single copy of the genomic RNA bud into regions of plasma membrane studded with E1/E2 spikes, and emerge from cells as enveloped, infectious particles (138, 160, 161).

1.2.2 Distribution and ecology

CHIKV first evolved in sub-Saharan Africa at least several hundred years ago from an ancestral arbovirus that was likely transmitted between primate hosts, by *Aedes* species mosquitoes (33). Since its initial divergence from its closest relative, ONNV, CHIKV has further diverged along several distinct lineages. First, the ancestral West African lineage gave rise to the East/Central/South African (ESCA) genotype in sub-Saharan Africa (162). A third lineage evolved from an ESCA strain that was imported into India and Southeast Asia between 1879 and 1956 (163) and became the Asian genotype. Then, in 2004, an explosive outbreak involving another ESCA strain began in coastal Kenya and spread throughout the Indian Ocean basin, affecting millions of people (163, 164). These CHIKV strains comprised the newest lineage, the Indian Ocean Lineage (IOL), which is sometimes considered a sublineage of the ESCA genotype. Remarkably, the divergence of the IOL strains was associated with a mutation in the viral E1 protein that conferred enhanced fitness and transmissibility in a new vector species, *A. albopictus*, which was found to be the principal vector in the 2004 Indian Ocean outbreak, where *A. aegypti* is not common (165-167). The IOL outbreak also occurred in the era of unprecedented

increases in rapid air travel, and traveler-associated cases seeded autochthonous transmission in Italy and southern France (168, 169). Spread to the Americas was recognized in 2013 on the Caribbean island of St. Martin, ground zero for another massive outbreak that swept Central and South America and the Caribbean through 2014 (170, 171). Interestingly, the viruses circulating in the Americas were members of the Asian lineage, not the IOL, and transmission occurred via *A. aegypti* (172, 173). Subsequently, an ESCA-derived virus was imported to and established autochthonous spread in Brazil in 2014 (174).

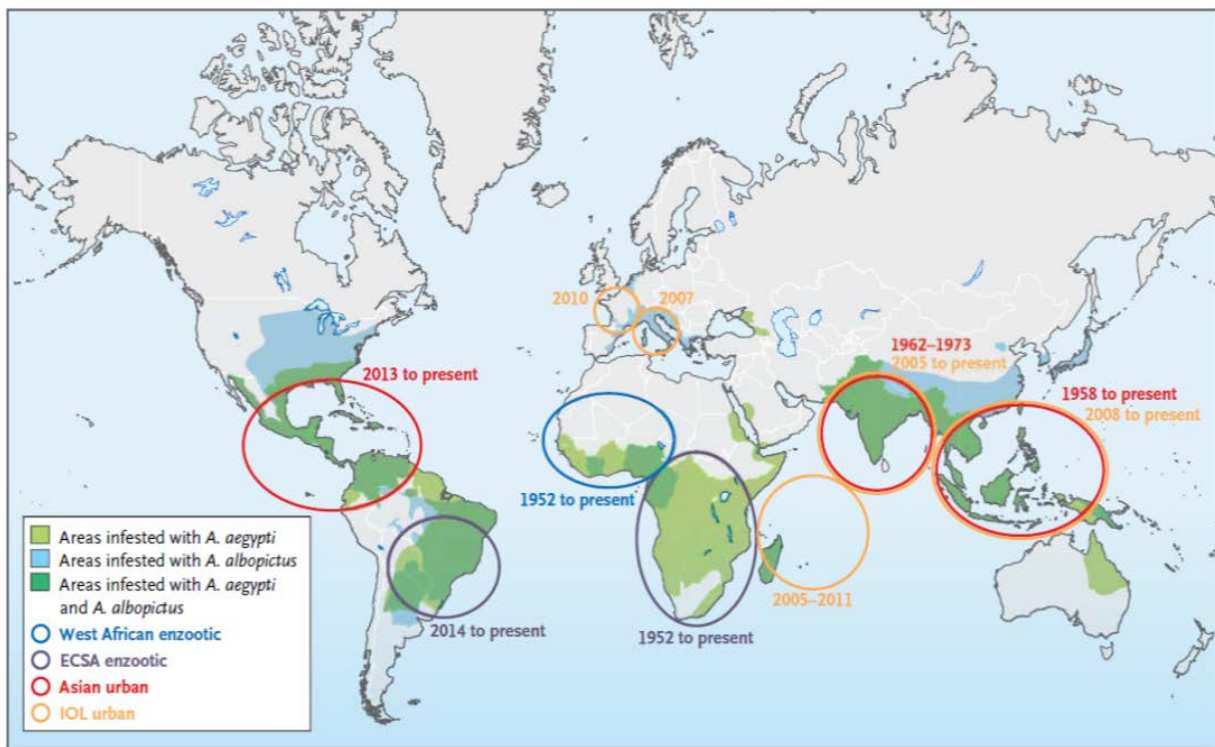


Figure 2: Distribution of Chikungunya virus and its major epidemic vectors (adapted with permission from (33), Copyright Massachusetts Medical Society)

Throughout its natural history, CHIKV has been maintained in two transmission cycles, a sylvatic cycle and an urban cycle. Sylvatic CHIKV transmission involves forest-dwelling

mosquitoes of the *Aedes* genus feeding on and transmitting the virus between enzootic, non-human primate (NHP) amplification hosts. The sylvatic cycle is considered the ancestral method of CHIKV transmission, occurring in Africa since CHIKV diverged and continuing there to the present day (173). In contrast, there is no evidence of sylvatic CHIKV transmission outside of Africa, despite its now worldwide distribution, save for its retention in these geographic areas between epidemics (173, 175). In areas of Asia and South America where sylvatic NHPs are endemic, the possibility of spillback into an enzootic cycle, as occurred with YFV in South America (83), is strong. In Asia and the Americas, CHIKV is known to be maintained in the urban cycle, which can also operate in Africa alongside sylvatic transmission. Originally, urban CHIKV transmission would occur as the result of a spillover event of the virus into a human population from the sylvatic cycle (176). That spillover event could be either a sylvatic mosquito vector biting a human or an anthropophilic mosquito biting an enzootic host, acquiring the virus, and then biting a human. The risk of spillover is greatly increased with human encroachment into or near arboreal habitats, which gives CHIKV vectors access to both humans and zoonotic/enzootic reservoirs. Once a human becomes infected, urban transmission can seed an epidemic outbreak fueled by human-mosquito-human transmission by the anthropophilic and domesticated *A. aegypti aegypti* subspecies (171). Domestication of *A. aegypti*, that is, the adaptation of this mosquito to live in and around human settlements and breed preferentially in standing water trapped in man-made vessels, probably coincided with the development of human-mosquito-human transmission and the urban transmission cycle (171). Recently, *A. albopictus* has joined *A. aegypti* as an urban cycle vector of IOL strains, which, as described above, have adapted to efficiently use this vector.

The recent establishment of urban transmission of CHIKV in the Americas and Europe did not result from enzootic spillover, but rather from importation of an infected human or mosquito from an urban transmission cycle elsewhere in the world. A major concern now is whether or not spillback into the sylvatic cycle from the urban cycle will occur and allow CHIKV to establish endemicity in new regions with robust NHP populations (173). Also troubling is the transition of IOL viruses into *A. albopictus*, as this mosquito inhabits a much larger geographic range than *A. aegypti*, which is confined to tropical and subtropical climates (177). *A. albopictus* is found worldwide from the tropics to much more temperate regions, posing a risk of CHIKV in previously risk-free populations should the IOL strains continue to expand geographically or additional lineages evolve to use this vector. There is also evidence that American strains of *A. albopictus* are more competent for transmission of CHIKV of any lineage, which adds another layer of risk to the expansion of CHIKV in the Americas (178). However, as NHPs are the major reservoirs for endemic CHIKV, it is unlikely that CHIKV would be able to establish endemicity in temperate climates in the absence of NHPs. Another possibility is that climate change may facilitate geographic expansion northward and southward for *A. aegypti*, which could pose its own risk for the introduction of CHIKV into new areas (179).

1.2.3 Pathogenesis and disease in humans

CHIKV infection of humans begins upon deposition of viral particles into the skin and superficial capillaries by an infected mosquito during a bloodmeal. The virus replicates initially at the site of infection in dermal fibroblasts, endothelial cells, and possibly macrophages, and is transported to the regional lymph node through the draining lymphatics, possibly aided by skin-resident dendritic cells (DCs) and macrophages (94, 135, 180, 181). Whether or not CHIKV can

infect myeloid cells *in vivo* is controversial, and transport by these cells may occur as a result of phagocytosis of infected cell debris (33). In the draining lymph node, CHIKV gains access to additional susceptible cells, where it replicates sufficiently to seed a primary serum viremia via the thoracic duct, and then utilizes the circulatory system for systemic spread. Major secondary sites of infection include musculoskeletal tissues, spleen, and skin, with rare involvement of liver, brain, and ocular tissues also possible (94, 181-186). Peripheral viral replication at these sites produces a high-titer viremia that can reach $>10^9$ genomes/mL (180, 186), allowing for direct human-mosquito-human transmission without the need for an intermediate amplifying host. Coincident with the high-titer viremia is a spike in circulating proinflammatory cytokines such as IFN- α , IL-1 β , tumor necrosis factor alpha (TNF α), monocyte chemoattractant protein 1 (MCP-1), and IL-6 and the onset of clinical symptoms (135, 187-193). Most patients experience a high fever (39-40°C) lasting up to 7 days, followed shortly by debilitating polyarthralgia, which is usually symmetrical and involving distal joints, although during the acute phase, axial and large joints can also be affected (21). A macropapular erythematous rash on the trunk and limbs is also a common manifestation of acute CHIKV (33). Incidence of subclinical CHIKV disease is very low, with seroconversion in the absence of overt disease occurring in less than 15% of infected individuals (194). Conversely, the incidence of fever and joint pain can reach as high as 90 and 95%, respectively (21). Rash is less common but still a hallmark sign of CHIKV infection, with 40-50% of infected individuals presenting with rash (21, 195). Atypical and severe manifestations include neurological and ocular involvement, hepatitis, hemorrhage, gastrointestinal disease, and myocarditis resulting on rare occasions of viral invasion of these tissues (186, 195-198). Severe CHIKV infection occurs almost exclusively in at-risk populations such as neonates, the elderly, and those with underlying comorbidities (199). Accordingly,

CHIKV infection results in very low mortality, less than 1 in 1000 infected, but very high morbidity; however, retrospective studies of CHIKV outbreaks in the Indian Ocean region and South America have revealed a higher-than-expected rate of neurological disease (e.g. Guillan-Barre syndrome) in previously healthy individuals after infection with CHIKV (196, 197, 200). This raises the possibility that more severe consequences of CHIKV infection are more common than previously thought.

Acutely-infected joint-associated musculoskeletal tissues contain numerous cell types that are targeted for CHIKV infection, including fibroblasts, osteoblasts, muscle satellite cells, myocytes, and endothelial cells (94, 180-184, 201-203). As a result, all articular and periarticular tissues are subject to infection and subsequent inflammation. Acute arthralgic symptoms can result from both direct cellular damage by the cytolytic virus (135, 204) and immune-mediated mechanisms. Immune cell infiltrates into infected joints are predominated by macrophages and contain neutrophils, natural killer (NK) cells and DCs, which contribute to inflammation and edema (180-184). High-titer viremia in patients coincides with elevated levels of several proinflammatory cytokines, with IL-6, MCP-1, and IL-1 β universally identified as markers of acute CHIKV disease in diverse patient cohorts from around the world, and their levels correlate with disease severity (192, 205). Interestingly, many of the features of CHIKV-induced arthritis are reminiscent of rheumatoid arthritis (RA), an autoimmune disorder marked by elevated levels of proinflammatory cytokines such as IL-6, synovial inflammation, focal bone erosions, damage to cartilage, and the production of autoantibodies (206). CHIKV arthritis is also associated with elevated IL-6 and synovial inflammation, and has been shown to lead to bone loss (207), but presence of RA-associated autoantibodies is rarely detected in CHIKV patients (208). However, it is not uncommon for patients experiencing chronic CHIKV-related rheumatic symptoms to

meet the clinical criteria for seronegative RA (208, 209), and significant overlap in gene expression profiles has been noted between a mouse model of CHIKV arthritis and human RA patients in affected musculoskeletal tissues (210). Thus, there may be a connection in the mechanisms driving RA and post-CHIKV rheumatism.



Figure 3: Clinical signs of acute CHIKV disease: swollen joints and erythematous rash (adapted with permission from (126))

Convalescence from the acute infection usually begins between 7 and 10 days after symptom onset. Viremia is cleared coincident with rising serum anti-CHIKV IgM, which usually appears within 5-7 days after infection (211). IgG is detectable between days 7 and 10 and contributes to viral clearance from circulation, if viremia is still present (212-214). Both CD4+ and CD8+ T cells are activated during acute CHIKV infection, but their roles in viral control and immune protection are unclear and may even contribute to CHIKV-associated pathology in the case of CD4+ T cells (180, 191, 215). A strong neutralizing antibody response is widely considered the best correlate of protection against secondary CHIKV infection (21). In most patients, acute symptoms resolve within two weeks of onset, and many patients report improvement or disappearance of joint and muscle pain (126). Many patients will reach full

recovery from joint symptoms within one month; however, between 15 and 87% of patients, with an average of 47% will report symptoms of persistent or flaring joint pain associated with the chronic phase of CHIKV disease (216).

Chronic CHIKV disease is characterized by persistent or flaring bouts of arthralgic symptoms (pain, swelling, stiffness) lasting for months or years beyond the acute infection. Unlike the acute phase, during which patients can experience arthritis/arthralgia in the large joints, chronic CHIKV manifests exclusively in the small joints of the extremities, namely the wrists, ankles, and phalanges (126, 217-219). Pain at these sites can be severe and debilitating. For example, many patients describe the inability to move from the position they were in when the pain started, which is indicative of the significant detriment to the affected person's quality of life (33, 220). Many risk factors for chronic CHIKV have been identified in various cohorts, with advanced age, acute-phase arthralgia persisting past one-month post-infection, and the presence of a pre-existing arthritic condition being universally associated with chronic disease (180, 218, 220-227). In addition, many studies have found the severity of acute disease, including high viral load, extreme joint pain, and atypical disease indicative of severe infection, to be strongly predictive of chronic arthralgia (180, 222, 226, 228-231). A few studies have also positively correlated female sex (222-224, 230), smoking (223), and chronic comorbidities such as cardiovascular disease and diabetes (220, 223) with increased risk of chronic CHIKV disease. Notably, one study determined that the most prominent factor associated with chronic CHIKV flaring disease (>40% of total) was a change in ambient temperature, indicating that external factors may influence disease progression (220).

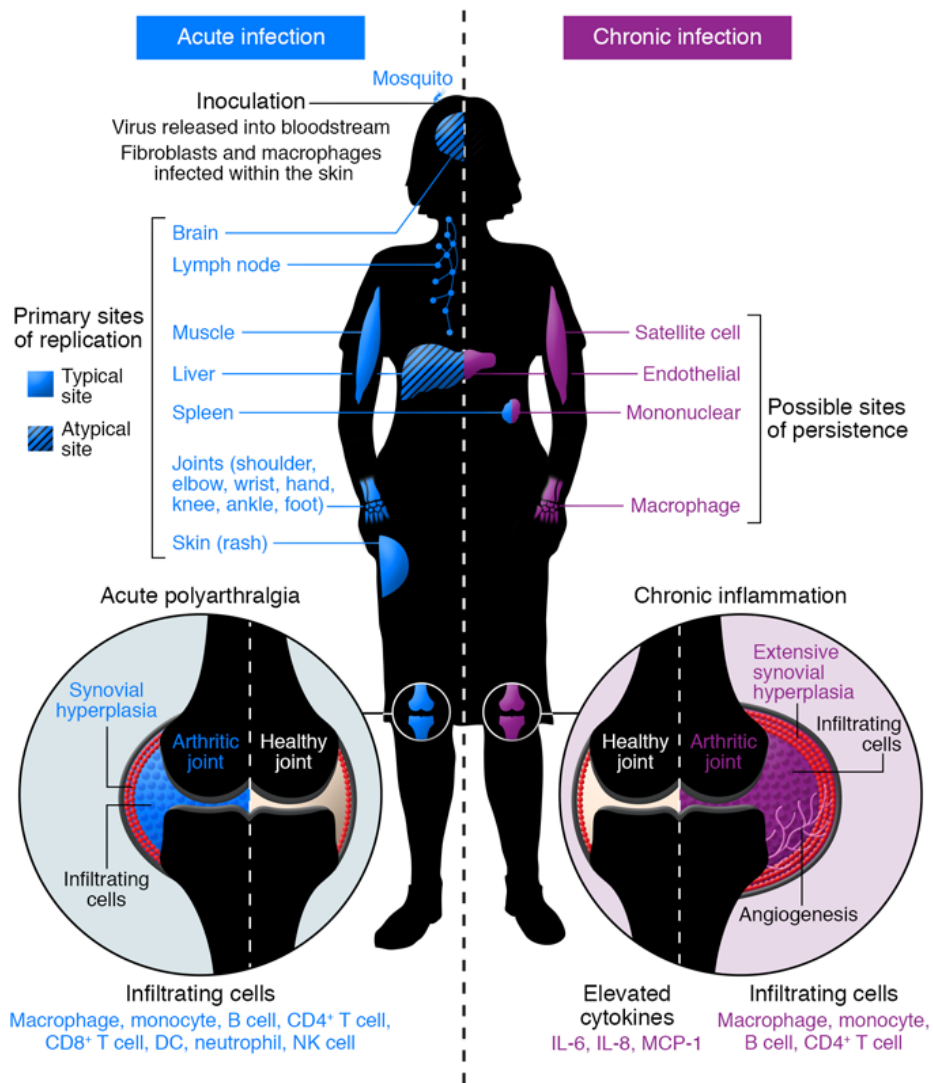


Figure 4: Pathogenesis of Chikungunya virus (adapted with permission from (153))

The underlying pathology and molecular mechanisms driving persistent and flaring joint pain in CHIKV patients have yet to be unraveled. It is generally accepted that much of the persistent CHIKV disease is immune-mediated, representing a chronic inflammatory state in the periarticular microenvironment, with some similarities to RA, as noted above. In patients with chronic CHIKV, the proinflammatory cytokines IL-6, IL-1, and MCP-1 remain elevated versus recovered patients, and increased levels of immune cells have been found in biopsies from these

patients (153). The possibility that chronic post-CHIKV arthralgia is an autoimmune condition has been explored, as it shares many features with RA, however, no autoantigens have yet been identified and affected patients are rarely positive for RA-associated autoantibodies (207). In contrast, viral genomes and, occasionally, antigens, have been found in both humans and animal models during the chronic phase of CHIKV infection, leading to the intriguing possibility that persistent CHIKV infection is responsible for driving the chronic inflammation. Specifically, CHIKV RNA and protein was detected in synovial and muscular biopsy specimens from one patient with chronic arthralgia 18 months post-infection (180). Similar findings have been reported in experimentally-infected macaques and mice (181, 202, 215, 232). However, infectious CHIKV has not been isolated from chronically infected humans or animals, except for persistent, low-level viremia in mice lacking B and T cells that lasted at least 84 days post-infection (202). No infectious virus has been successfully cultured from joint-associated tissues in any model past 6 weeks post-infection, and this was, again, in mice lacking adaptive immune responses (202). If the infectious virus was persisting in a cellular reservoir long-term, it would likely be at a low level and any infectious particles produced would likely be immediately neutralized by circulating antibody. Thus, while the presence of viral genomes at chronic time points in no way confirms the presence of an active infection, it warrants further investigation into its exact nature, and its relationship to the chronic inflammatory responses driving persistent post-CHIKV joint disease. The establishment of a tractable small animal model of chronic and/or flaring CHIKV infection will be of great aid in addressing these questions.

1.2.4 Adaptive immune response

The majority of information on the specific mechanisms by which CHIKV is controlled and cleared by the adaptive immune system comes from studies in mice, although some data is available from patient cohorts. Increasingly, it is becoming clear that adaptive immunity plays both protective and pathogenic roles in CHIKV infection, with different immune cell subsets contributing differently. As mentioned above, mice lacking B and T cells suffer a greater viral burden in several tissues during acute infection and sustain persistent viremia indefinitely, highlighting the importance of these adaptive immune cells in control and clearance of the virus (202, 215, 233, 234). However, these mice also display decreased musculoskeletal disease (foot swelling upon subcutaneous inoculation of CHIKV into the footpad), indicating that some subsets of adaptive immune cells may contribute to CHIKV disease.

1.2.4.1 T cell response

CD8⁺ T cells are activated in response to CHIKV infection in humans, with peak numbers observed in peripheral blood around the time of symptom onset and a sizeable circulating population persists until at least 7-10 weeks post-infection (191, 209). In mice, CD8⁺ T cells migrate into infected musculoskeletal tissues within the first week of infection (233). Despite this evidence for an active CD8⁺ T cell response, it is unclear what role, if any, CD8⁺ T cells play in the control or pathogenesis of CHIKV. In mice, genetic knockout or antibody-mediated depletion of CD8⁺ T cells have not resulted in differences in musculoskeletal disease or viral burden during the acute or chronic stages of CHIKV infection (233). However, it is possible that CD8⁺ T cells contribute to other aspects of anti-CHIKV immunity or pathogenesis, such as cytokine profiles or memory responses, that have not yet been studied.

In contrast to CD8⁺ T cells, distinct roles for effector CD4⁺ T cells and regulatory T cells have been described in mice. Large numbers of IFN- γ -producing CD4⁺ T cells migrate to synovial tissues of infected wild-type mice early after infection and contribute directly to disease pathology, as mice deficient in CD4⁺ T cells or MHC-II experience greatly reduced foot swelling compared to wild-type mice (215, 233). This reduction in musculoskeletal disease was not associated with any changes in viremia or recruitment of monocyte/macrophages or neutrophils to the site of infection, suggesting that effector CD4⁺ T cells are directly pathogenic during acute CHIKV infection (233). The role of CD4⁺ T cells during the chronic disease phase is unknown and has not been studied in mice, although one study of chronically-infected humans found a relatively high fraction of activated CD4⁺ T cells in synovial biopsies, suggesting that these cells may contribute to chronic disease manifestations, although no hypothesis for that mechanism has yet been posited (180). In contrast to effector CD4⁺ T cells, regulatory T cells appear to play a protective role against CHIKV-associated joint pathology. One study examined the effect of expanding the small regulatory T cell population found in the joints of CHIKV-infected mice by administration of an IL-2/anti-IL-2 complex, and found that increased numbers of regulatory T cells reduced foot swelling, proinflammatory cytokine expression, and IFN- γ + CD4⁺ T cell recruitment and expansion during acute CHIKV infection (235). $\gamma\delta$ T cells have also been implicated in protection from CHIKV-induced inflammation at the site of infection by limiting immune-mediated oxidative damage and proinflammatory cytokine induction (236). Thus, regulatory and $\gamma\delta$ T cells may limit immune-mediated pathology during acute CHIKV infection, although their roles during chronic infection remain unknown.

No epitopes for CHIKV-specific CD8⁺ or CD4⁺ T cells have yet been identified, and the antigen presenting cells (APCs) responsible for CD4⁺ T cell priming have not been defined.

However, CHIKV has been shown to infect monocytes and macrophages in humans and NHPs, and these cell types dominate immune infiltrates into infected tissues, so it is likely that these cell types contribute to antigen presentation (135, 181, 189). Less clear is the role of DCs in antigen presentation, as there is no evidence that CHIKV can productively infect these cells. It has been suggested, though, that skin-resident DCs may transport CHIKV and other arboviruses from the site of infection to the DLN, indicating that these cells may present antigen to T cells in the DLN (237). Other, nonclassical APCs such as neutrophils, which are abundant in immune cell infiltrates into CHIKV-infected tissues, may also contribute to antigen presentation, but no studies have addressed this possibility. B cells are refractory to CHIKV infection (135) and there is no evidence that they act as APCs in this context. Overall, additional studies are required to define the APC subsets important for CHIKV antigen presentation and how those interactions contribute to viral control and/or CD4+ T cell-mediated immunopathology.

1.2.4.2 B cell response

It is well-known that neutralizing antibodies are essential for clearance of infectious CHIKV from serum and tissues, as administration of neutralizing anti-CHIKV monoclonal antibodies is able to achieve viral clearance in B cell-deficient mice and even protect immunocompromised mice from lethal infection when given before or soon after infection (202, 215, 238-244). Most neutralizing antibodies so far identified target the viral envelope glycoproteins E2 and E1, which are exposed on the surface of the virion, and the most strongly neutralizing antibodies target the A and B domains of E2 and are cross-protective against other arthritogenic alphaviruses (245, 246). Different antibodies have been shown to inhibit the virus at various stages of infection *in vitro*, including attachment, entry, fusion at the endosome, virion assembly, budding, and cell-to-cell spread (240, 244, 246-249). In addition, antibodies may act

in other ways *in vivo*, including antibody-mediated cellular cytotoxicity, activation of complement, and opsonization of extracellular virus particles (250). CHIKV-specific IgM is detectable in mice within the first few days after infection and IgM levels fall during the second week of infection as class-switching to IgG occurs (251). In human patients, anti-CHIKV IgM remains detectable for months after the initial infection and isotype switching to IgG occurs more quickly than in mice, within the first week (180, 211).

Few studies have examined the specific characteristics of the anti-CHIKV IgG response, although one study found that the subtype IgG3 predominated the IgG response in both acutely- and chronically-infected CHIKV patients (252). These neutralizing antibodies were found to be directed against a single linear epitope near the N-terminus of the viral E2 glycoprotein (the E2EP3 peptide; STKDNFNVYKATRPYLAH), and immunization of NHPs and mice with this epitope reduced viremia and musculoskeletal disease upon CHIKV challenge (212, 253). A study in mice mapped the greatest number of antibody epitopes to the C-terminal region of E2, although a number of other epitopes were identified throughout the CHIKV structural proteins and the other domains of E2 (251). In addition, studies in mice lacking MHC-II expression have demonstrated that class switching from IgM to IgG occurs in the absence of T cell help, but the response is diminished compared to wild-type mice and predominated by the IgG2c isotype, indicating that development of normal antibody responses to CHIKV infection is partially dependent on T cells (215).

1.2.5 Animal models of CHIKV infection

1.2.5.1 Neonatal and immunocompromised murine lethal challenge models

Neonatal mice rapidly succumb to encephalitic disease upon infection with CHIKV, and therefore have proven useful in the past for vaccine candidate safety trials, but have little utility for more detailed studies of CHIKV pathogenesis or vaccine efficacy due to their immature immune systems and atypical disease course (254). However, due to increasing recognition of neurological involvement and encephalitis in human CHIKV cases that have been noted in recent human outbreaks, the neonatal mouse encephalitis model may prove serendipitously relevant yet, and has begun to be used for modeling neonatal human infection (94, 255). Adult mice lacking key components of the type-I IFN system also represent a lethal challenge model of CHIKV infection that may be somewhat less contrived than the neonatal model. Type-I IFN-deficient mice exhibit exacerbated arthritic disease compared to wild-type mice and uncontrolled viral replication and dissemination that ultimately results in death, underscoring the criticality of IFN- α/β in protecting mice from CHIKV (93, 94, 256, 257). Thus, these mice represent a useful control group against which to measure the contributions of individual components of IFN- α/β signaling or other immune mediators in protection from CHIKV challenge. In addition, these mice are useful in safety and efficacy studies of new vaccines and therapeutics (238, 258).

1.2.5.2 Adult wild-type murine acute arthritic models

Several related adult mouse models of CHIKV acute arthritis have been well-established. Studies in three- to eight-week-old outbred CD-1/NIH Swiss or inbred 129 and C57BL/6 (B6) background mice have yielded similar disease courses and findings, but the B6 model has proven more popular due to the availability of genetic knockouts in this background (93, 183, 184, 201).

Subcutaneous inoculation of CHIKV into the ventral side of the rear footpad of these mice results in a marked biphasic swelling of the infected foot and ankle region that resolves around day 8 post infection. Many features of human acute CHIKV arthritis are recapitulated in this model, including cell infiltrate and cytokine profiles, cellular tropism and musculoskeletal tissue involvement, and antibody-mediated clearance of viremia (183, 184). Such similarity to human disease has led to a plethora of information about the host and viral factors important for driving and controlling CHIKV infection, as well as pathogenic and pathologic details.

1.2.5.3 Mouse models of chronic CHIKV infection

In adult B6 mice infected with CHIKV, viral RNA has been detected in joint-associated tissues at least four months after infection and was associated with persistent synovitis (202), indicating that the B6 acute CHIKV model may also serve as a chronic disease model, if given the time. Additionally, several groups have attempted to encourage or exacerbate chronic CHIKV infection and disease through the use of various adaptive immune knockout strains, such as *Rag1/2^{-/-}* mice, which lack B and T cells, and μ MT mice, which are B cell deficient. The disease course in these mice does not differ appreciably from wild-type mice in the acute phase, but they do exhibit persistent viremia and elevated viral burden in several tissues at chronic time points attributable to the lack of effective clearing antibody responses (202, 215, 233, 234, 251). Importantly, infectious virus has been recovered from the ankle joints of *Rag1^{-/-}* mice as late as 6 weeks post-infection, indicating that persistent viral replication is possible in mouse models (202). However, whether or not alterations in the efficacy of human antibody responses underlie chronic disease manifestations is unknown.

1.2.5.4 Nonhuman primate models

Infection of cynomolgus macaques with CHIKV results in a clinical disease profile remarkably similar to that seen in humans. Kinetics of viremia and systemic dissemination closely followed the time course of human infection, and evidence of viral persistence in lymphoid tissues was detected at three months post infection (181). Signature cytokines such as IL-6 and MCP-1 were also elevated in macaques, and CHIKV-specific antibody epitopes were similar to those identified from human cases (181, 259). Rhesus macaques have also been used to study CHIKV pathogenesis and immune response and have provided important mechanistic insights regarding the route of dissemination from the site of infection and the kinetics of the adaptive immune response (232). This study also compared CHIKV disease in adult rhesus macaques to aged (>17 years old) animals in an effort to understand why and how elderly humans are more predisposed to severe and persistent CHIKV (232).

1.3 TYPE-I INTERFERON

The type-I interferon response is a critical component of antiviral innate immunity, and its efficacy during acute CHIKV infection is a major determinant of clinical outcome, particularly with respect to suppression of disseminated virus replication and morbidity prior to the development of effective neutralizing antibody responses (33). It is an ancient system, likely appearing very early in vertebrate evolution, as all known extant vertebrate genera possess homologous versions of this response (260). In humans and other mammals, nearly all somatic cells bear the type-I interferon receptor and are equipped with varying repertoires of antiviral genes responsive to these cytokines, allowing uninfected cells to preempt viral infection and

infected cells to suppress it (261). In response, viruses have collectively evolved extensive arsenals of molecular weapons that subvert or directly antagonize type-I interferon at every level of the response, from induction pathways to the actions of individual antiviral effectors (262). Substantial work since the discovery of type-I interferon in 1957 (263) has elucidated both its major signaling pathways and the finer details of its induction and effector phases, as well as mechanisms of action for many of its inducible effectors. Most of these studies have, necessarily, relied on genetic manipulation of model systems to knock out various components of the response and used the subsequent phenotypic changes to piece the signaling puzzle together. The resulting knowledge has proven invaluable to the fields of cell biology, innate immunology, and virology, among others, and the importance of these studies cannot be overstated. However, little of the research on type-I interferon has so far examined this system *in situ*, so to speak, or as a response of an intact organism, being activated and acting in diverse and spatially separated tissues with potentially variable physiological conditions. With mild hypothermia representing a near pervasive existence for peripheral and respiratory tissues in humans and other endotherms, at least in temperate and cooler climates, and with some viral infections preferentially affecting these tissues, the question of how immunity, and specifically type-I interferon, is influenced at variable temperatures becomes quite relevant. Importantly, type-I interferons are primary cytokines detected in the serum after virus infection and are responsible for systemic innate immune signaling and responses in tissues both near to and far from their site of production, which is commonly macrophages and DCs located in lymphoid organs (118).

1.3.1 Definition and classification

Type-I interferons (IFNs) are a family of secreted protein cytokines that act in an autocrine and paracrine manner to stimulate the production of a large subset of responsive gene products involved in its antiviral, antiproliferative, and immunomodulatory functions. They belong to the class II cytokine superfamily alongside interleukins -10, -19, -20, -22, -24, and -26, and the type-II and type-III IFNs (260, 264, 265). Despite modest amino acid sequence identity, these cytokines share structural similarity, in the form of a bundle of six α -helices, and functional similarity, as they all utilize heterodimeric transmembrane receptors that signal through the Janus kinase (JAK) – signal transducer and activator of transcription (STAT) pathway (265). There are multiple species within the type-I IFN family, including the IFNs α , β , ϵ , κ , ω in humans and additional types in other mammals, such as limitin/IFN- ζ in mice (266), but only the IFN- α subtypes and IFN- β are known to contribute substantially to antiviral innate immunity (261, 264). There are 13 IFN- α subtypes in humans and 14 in mice (266), which are likely to have diverged from the single, ancestral IFN- β -like gene through gene duplication events resulting in a type-I IFN gene cluster located on chromosome 9 (260, 265). While these distinct species of type-I antiviral IFNs demonstrate some degree of specificity in their stimulation and activities [reviewed in (267)], the amount of overlap between them in terms of induction and effector pathways is so vast and commonly simultaneous that unless otherwise specified, for the purposes of this discussion, they will be considered as one entity, which I will call IFN- α/β .

1.3.2 Induction pathways

IFN- α/β is produced in response to a variety of stimuli, and most body cells are capable of IFN- α/β induction (261). Induction pathways begin with the sensing of pathogen-associated molecular patterns (PAMPs) by membrane-bound or cytosolic pattern recognition receptors (PRRs). Three families of PRRs contribute to IFN- α/β induction in infectious contexts; the toll-like receptors (TLRs), the RIG-I-like receptors (RLRs), and the cytoplasmic DNA sensors. TLRs are expressed mainly on immune cells and some fibroblasts and epithelial cells, and exhibit specificity for viral, bacterial, or fungal antigens, while the cytoplasmic sensors bind nucleic acids and are therefore most important for detection of viruses (268). The diverse ligand specificity and broad expression patterns of these sensor molecules mediate innate detection of a wide variety of PAMPs and activate both distinct and overlapping signaling pathways tuned to elicit the appropriate response to a given stimulus. Though not all PRRs lead to appreciable IFN- α/β induction, those that do converge on the activation of interferon response factors (IRFs), the principal transcription factors for IFN- α/β mRNA upregulation. Translation and subsequent processing through the secretory pathway then ready the mature cytokines for export into the extracellular space, where they can bind receptors on the same or neighboring cells to exert their antiviral effects.

1.3.2.1 Toll-like receptor signaling

TLRs are class I integral membrane proteins that serve as sensors for a wide array of PAMPs and initiate appropriate cell-intrinsic immune responses through both distinct and overlapping signaling cascades. The N-terminal TLR extracellular domain contains between 19 and 25 leucine-rich-repeats that mediate ligand binding specificity. Intracellular signaling capacity is

conferred by the C-terminal cytoplasmic Toll/IL-1R homology (TIR) domain (268, 269). Humans possess ten TLRs (TLRs 1-10) with different substrate specificities and cell type distributions. Of these ten, TLRs 3, 4, 7, 8, and 9 induce a robust IFN- α/β response upon activation (261). TLR4 is expressed on the cell surface and exhibits relatively broad substrate specificity. Bacterial lipopolysaccharide is usually cited as the major ligand for TLR4, but several other agonists, such as fungal mannans and certain viral envelope proteins, have also been identified (268). Conversely, TLRs 3, 7, 8, and 9 are found in endosomal and lysosomal compartments and primarily engage nucleic acids including dsRNA (TLR3), ssRNA (TLRs 7 and 8), and unmethylated CpG DNA (TLR9). Thus, these TLRs are most suited for detection of viruses, which generally lack the complex, non-self signatures recognized by the other TLRs and often traffic through endolysosomal compartments (268). TLR3 is more widely expressed than the other endosomal TLRs, which are largely restricted to plasmacytoid and myeloid dendritic cells (pDCs and mDCs) (261, 270).

Upon ligand binding, TLR dimerization and conformational changes recruit TIR-containing adaptor molecules to the TLR TIR domain. All TLRs except for TLR3 utilize the TIR-containing adaptor myeloid differentiation factor 88 (MyD88) to initiate signaling leading to induction of proinflammatory cytokines (268, 271). TLR3 instead recruits TIR domain-containing adaptor protein inducing IFN- β (TRIF) (272, 273), which then activates TANK-binding kinase 1 (TBK1) and the inhibitor of kappa B kinase epsilon (IKK ϵ) through TRAF3 (274, 275). Active TBK1 is responsible for the phosphorylation and activation of IRF3, while IKK ϵ frees NF κ B from its cytoplasmic inhibitors (276, 277). Polyphosphorylated IRF3 then homodimerizes and translocates to the nucleus, where it induces the transcription of IFNs β and $\alpha 4$, among other innate immune genes such as IFIT1 and IRF7 (278). IFN gene transcription is

enhanced by NF κ B activity. Upregulation of IRF7 is a feed-forward mechanism to amplify the IFN induction pathway and its activation alongside IRF3 by TBK1 results in increased transcription of IFN β and $\alpha 4$ as well as induction of the other IFN α subtypes (279-281). In immune cells, IRF7 is constitutively expressed, leading to a more rapid induction of maximal IFN- α/β transcription (282). TLR4 is also able to recruit TRIF and uses a similar pathway to induce IFN- α/β , but can initiate MyD88-dependent signaling for induction of other proinflammatory cytokines (283). In DCs, MyD88 is found in complexes with IRF7 at the endosomal membrane and can directly activate it in response to ligation of TLR7 or 9, leading to particularly robust IFN- α/β responses in these cells (284).

1.3.2.2 RIG-I-like receptor signaling

While TLRs demonstrate a great deal of cell type-restricted expression, the RIG-I-like receptors (RLRs) are very widely expressed, allowing nearly any body cell to detect and respond to viral infection. The RLRs are a family of cytoplasmic DExD/H-box RNA helicases whose stimulation results primarily in the activation of IRF3 and/or IRF7 and IFN- α/β production (285). Humans express three RLRs; retinoic acid-inducible gene I (RIG-I), melanoma differentiation associated protein 5 (MDA5), and laboratory of genetics and physiology 2 (LGP2). RIG-I and MDA5 both contain caspase activation and recruitment domains (CARDs), which are essential for downstream antiviral signaling, but LGP2 lacks CARDs and cannot independently stimulate IFN- α/β production (286). Accordingly, RIG-I and MDA5 are the primary inducers of IFN- α/β in response to cytosolic RNA ligands, while LGP2 has been shown to enhance MDA5 signaling but repress RIG-I activity, making it an important regulator of the pathway downstream of these molecules (286-290).

Although RIG-I and MDA5 are structurally and functionally very similar, their roles as viral sensors are not completely redundant. They have demonstrated differential abilities to sense certain viral infections and have unique substrate specificities (291). RIG-I preferentially binds to short dsRNA and 5'-PPP ssRNA (292-294) while MDA5 recognizes longer, highly structured dsRNA (295-298) and possibly AU-rich RNA sequences (299, 300). In addition, both RIG-I and MDA5 can respond to viral and cellular cleavage products of the antiviral ISG RNase L (301). In the absence of an RNA ligand, RLRs exist in an autorepressed conformation wherein the C-terminal repressor domain obscures the N-terminal CARDs and prevents them from signaling (287). Upon engagement of the central helicase domain with a substrate, a conformational change exposes the CARDs, allowing homotypic interaction with CARDs of mitochondrial antiviral signaling protein (MAVS) (285). This CARD-CARD interaction induces the prion-like aggregation of MAVS, which is central to its activation and propagation of the signal to IKK ϵ and TBK1 (302). IKK ϵ and TBK1 then activate NF κ B and IRF3, as in the TLR pathways, to stimulate IFN- α/β transcription.

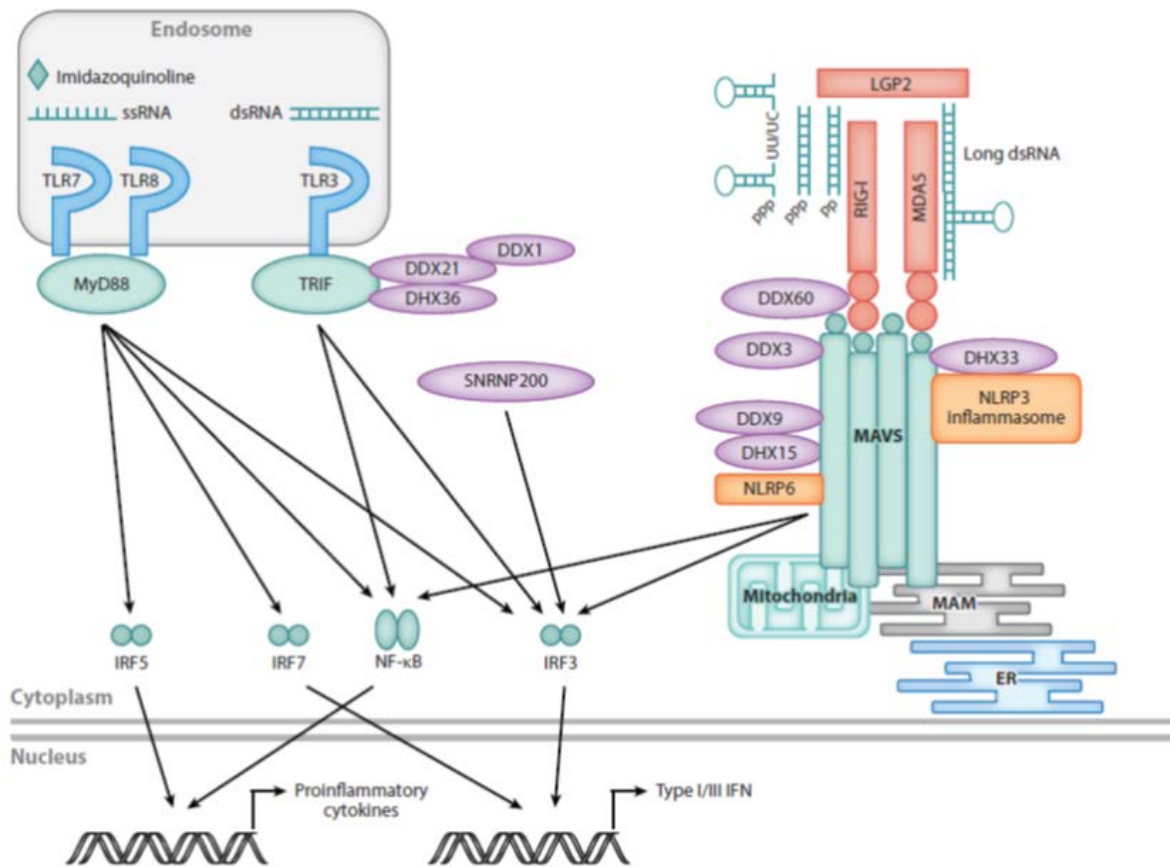


Figure 5: RNA-sensing type-I interferon induction pathways (adapted with permission from (285))

1.3.2.3 IFN gene transcription

In the absence of stimulation, the type-I IFN genes are near completely silenced by the presence of condensed chromatin, including nucleosome occlusion of the promoter and transcriptional start site, and constitutively-bound repressors (303). The IFN β promoter contains four *cis*-acting positive regulatory domains, PRDs I-IV (304). PRD-I and PRD-III are the binding sites for activated IRF dimers, while NF κ B and the transcription factor complex AP-1 bind to PRD-II and PRD-IV, respectively (304). Upon activation and translocation to the nucleus, IRF3/7, NF κ B, and AP-1 complex with the high mobility group (HMG) A1 protein to form the complete enhanceosome (304). The enhanceosome recruits the histone acetyl transferases (HATs) general

control of amino acid synthesis 5 (GCN5) and CREB binding protein (CBP) to the nucleosome, where they acetylate lysine residues on histones H3 and H4 (305). The acetylated histones allow a nucleosome modification complex to dislodge the IFN β transcription start site from the nucleosome, freeing the promoter for recognition by TFIID and assembly of the transcription machinery (305). The promoters for the IFN α genes only contain PRDI and PRDIII-like elements and are therefore fully activated by IRF binding alone (306). However, the IFN α promoters do exhibit differential affinities for IRF family members beyond IRF3 and 7, indicating a potential mechanism for gene-specific regulation, particularly in specific cell types, depending on the specific state of chromatin and transcription factor binding efficiency at different promoters under different conditions (307-309).

1.3.3 Effector pathways

While IFN- α/β inductive pathways concurrently produce some antiviral effectors in addition to IFNs, such as antiviral genes directly upregulated by IRF3, the full magnitude of the response, especially in uninfected bystander cells, is realized through subsequent autocrine and paracrine signaling of IFN- α/β . Binding of IFN- α/β to its cell surface receptor, which is expressed on nearly all cell types, initiates several distinct signaling cascades which, together, result in the induction of over 300 known effectors called interferon-stimulated genes (ISGs). The collective action of ISGs in IFN- α/β -primed cells constitutes the “antiviral state,” which renders uninfected cells largely refractory to subsequent viral infection and can greatly suppress viral replication in infected cells. The major pathway involved in this mass gene induction event is the JAK-STAT pathway, but secondary MAPK, CRK, and PI3K signaling serve to augment or regulate JAK-STAT-mediated responses to IFN- α/β .

1.3.3.1 Canonical JAK-STAT signaling

Upon engagement of the IFNAR by IFN- α/β , dimerization of the IFNAR1 and IFNAR2 receptor chains brings the nonreceptor tyrosine kinases Janus kinase 1 (JAK1) and tyrosine kinase 2 (Tyk2), which are constitutively associated with the receptor subunits, into close proximity (310, 311). JAK1 and Tyk2 then cross-phosphorylate, which activates their kinase domains and allows them to phosphorylate the IFNAR chains at multiple tyrosine residues, creating docking sites for signal transducer and activator of transcription (STAT) proteins via their Src homology 2 (SH2) domains (312-315). Type-I IFN binding most often recruits STAT1 and STAT2 to the receptor complex, which are themselves phosphorylated by JAK1 and Tyk2 at Tyr-701 and Tyr-690, respectively (310). Phosphorylated STAT1 and STAT2 then form a heterodimer, which joins with IRF9 to form the active transcriptional complex interferon stimulated gene factor 3 (ISGF3) (316). Phosphorylation of STAT1 at Tyr-701 exposes a nuclear localization signal (NLS), and assembled ISGF3 translocates into the nucleus, where it binds to interferon stimulated response elements (ISREs) in the promoters of ISGs (317, 318). STAT1 acquires a secondary phosphorylation at Ser-727 (319), which fully maximizes its transcriptional ability (320). Other homo- and hetero-dimers of STAT proteins can also be assembled in response to IFN- α/β signaling, often in an IFN- α subtype- and cell type-dependent manner, but these bind to another ISG promoter element, the IFN- γ -activated site (GAS), rather than ISREs (310, 316, 321-323).

1.3.3.2 Accessory signaling pathways

In addition to the JAK-STAT pathway, IFN- α/β stimulates other signaling cascades including mitogen activated protein kinase (MAPK) family members, and the CT10 regulator of kinase (Crk) and phosphoinositol-3-kinase (PI3K) pathways. Activation of multiple signaling cascades is thought to confer some of the diversity of cellular responses to IFN- α/β and allow fine-tuning

of the response in different contexts and cell types (324, 325). MAPK signaling pathways are quite diverse and involved in many cellular functions. In IFN- α/β signaling, activation of p38 MAPK is central to its antiviral and antiproliferative functions, with transcription of several ISGs shown to be dependent on downstream effectors of p38, including chromatin modifiers and histone kinases (325, 326). However, activation of the p38 pathway is not required for activation or nuclear translocation of STATs, indicating that this pathway operates independently of the JAK-STAT pathway in response to IFNs (327, 328). In addition, CrkL has been shown to interact directly with Tyk2 via its SH2 domain and become tyrosine-phosphorylated in response to IFN- α/β signaling, which then activates the small GTPase RAP1 through interaction with the guanine exchange factor C3G (329). RAP1 is thought to positively regulate p38MAPK signaling and contribute to the antiproliferative effects of IFNs (330). Finally, SH2-mediated activation of PI3K leads to activation of protein kinase c (PKC) isoforms, especially PKC- δ , which is responsible for phosphorylation of STAT1 at Ser727 (331). PI3K also regulates IFN-induced apoptosis through activation of AKT and mTOR, which can also selectively regulate ISG translation (325).

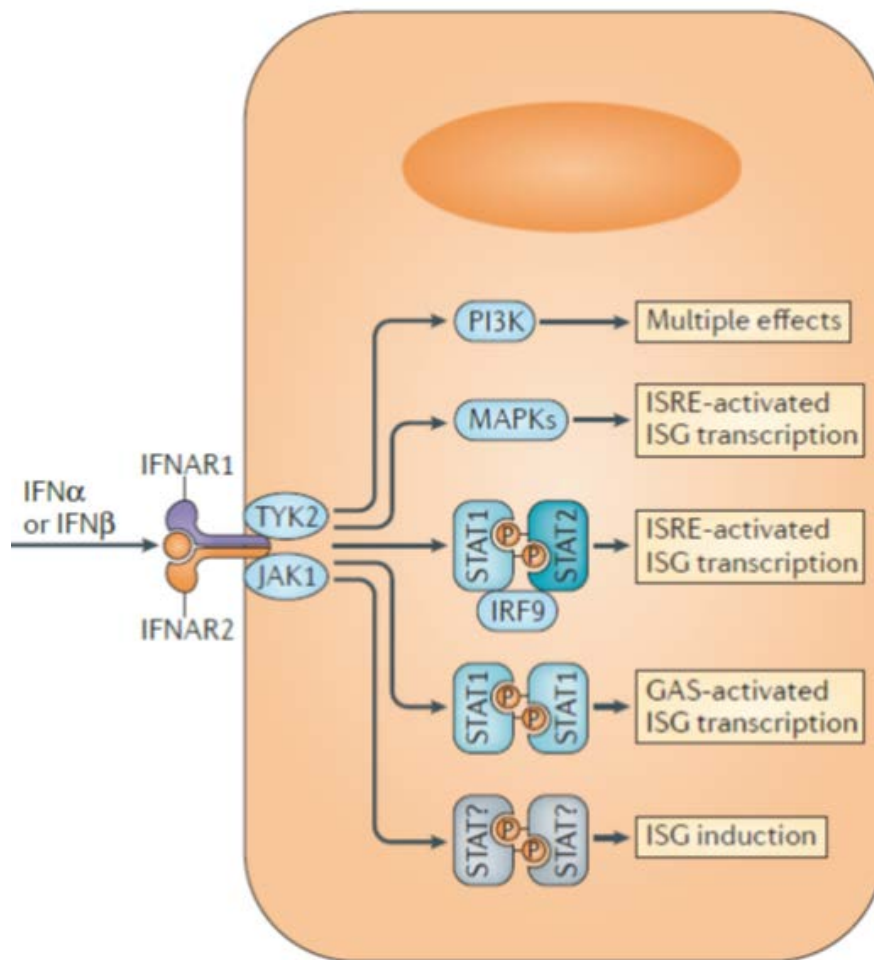


Figure 6: Signaling pathways stimulated by IFN- α/β (adapted with permission from (261))

1.3.3.3 ISG transcriptional regulation

Transcription of ISGs involves a multitude of regulators activated by the pathways described above. In the absence of an IFN- α/β signal, the chromatin structure around ISG promoters is kept closed by a ternary complex of repressors and higher-ordered nucleosomes (332). However, this is offset somewhat by the presence of the nucleosome remodeling complexes BAF and PBAF, which constitutively prime ISGs for rapid induction upon IFN- α/β signaling (333-335). When that signal occurs, ISGF3-associated IRF9 binds to ISRE regions in ISG promoters, and creates binding sites for STAT1 and STAT2, which exert strong pro-transcriptional activity (336). Some

ISG promoters contain either ISREs or GAS elements, while others have both, indicating that different STAT combinations determine optimal transcription of different ISGs (325). In addition to STATs, several other co-activators are required for ISG transcription. STATs in the nucleus interact with the HAT family members cAMP-responsive element binding protein (CREB)-binding protein (CBP)/p300 and GCN5, which further open the chromatin surrounding ISG promoters (337-342). STAT1 Ser727 phosphorylation is required for recruitment of these proteins, which probably contributes to the transcription-enhancing effects of p-Ser727. In addition, STAT-dependent gene induction has also been shown to be dependent on a number of other factors, including, paradoxically, histone deacetylases (HDACs) (343, 344), whose activity may be required for the recruitment of RNA polymerase II (345). Other coactivators, including minichromosome maintenance (MCM) 5 and 3 and N-Myc interactor, also facilitate ISG transcription, while several corepressors, including members of the protein inhibitor of activated STAT (PIAS) family of proteins act as corepressors (340, 341, 346, 347).

Beyond this canonical regulation of ISG transcription, numerous noncanonical transcription factors and transcriptional regulators have been identified that contribute to modulation of ISG expression. These include variants of the ISGF3 complex (348, 349), a CrkL-STAT5 dimer that binds GAS elements (350), and additional IRFs. IRF1, which is induced by IFN- α/β signaling, can bind to certain ISG promoters at a site that partially overlaps the ISRE, leading to their activation, while IRF2 can competitively inhibit this binding and negatively regulate ISG expression (351-353). IRF3, in addition to its crucial role in IFN- α/β induction, can also directly induce a subset of ISGs in an ISRE-dependent manner, as alluded to above (354, 355). Retinoic acid has also been shown to enhance IFN- α/β responses and ISG induction, and most ISG promoters contain retinoic acid response elements (RAREs) (356). It is thought that

retinoic acid facilitates binding of other transcription factors and works synergistically with IFNs to induce ISGs (356).

1.3.4 ISG functions and the antiviral state

ISGs are the functional units of the IFN- α/β response and their combined activities confer onto activated cells the ability to combat an existing intracellular infection or prevent the establishment of one. This heightened infection-refractory phenotype is known as the antiviral state. Over 300 ISGs have been identified, and their functions range from direct interference with viral processes and positive regulation of IFN-associated signaling pathways to pro-apoptotic mediators and direct inhibitors of IFN signaling. Most PRRs are present at low levels in the cell prior to viral infection to minimize the risk of aberrant activation and unnecessary inflammation, so their rapid upregulation in response to IFN- α/β greatly enhances the ability of infected and bystander cells to sense infection and mount an appropriately potent response (357). Both RLRs and TLRs are ISGs, as are the RNA-sensing molecules oligoadenylate synthetase (OAS) and double-stranded RNA-dependent protein kinase (PKR). OAS proteins detect foreign RNA species and produce 2'-5'-oligoadenylates, which act as second messengers to activate RNaseL, which promiscuously cleaves both host and viral RNAs, generating additional PAMPs for detection by PRRs and reinforcement of the IFN- α/β response (358). Concurrently, PKR activation leads to a global repression of translation in an effort to limit production of viral proteins while stabilizing IFN gene mRNAs to selectively enhance their translation (359) In addition, many IRFs and STATs are upregulated by IFN- α/β , including IRFs 1, 3, 7, and 9, and both STATs 1 and 2, each with crucial roles in enhancing IFN gene and ISG production (357).

Besides bolstering the innate and adaptive immune signaling capacity of activated cells, ISGs are also responsible for the opposite effect, that is, providing a means for efficient resolution of IFN responses and preventing cellular toxicity that can accompany prolonged activation. Endocytosis of the IFNAR and the actions of various non-ISG phosphatases also play important roles in limiting IFN responses (357). The PIAS proteins mentioned above also inhibit STAT function by preventing their interaction with DNA as well as targeting them for degradation via SUMOylation (360-362). Of the ISGs that negatively regulate IFN- α/β signaling, the suppressors of cytokine signaling (SOCS) family proteins and the ubiquitin-specific peptidase 18 (USP18) are the best characterized. SOCS proteins are SH2 domain-containing proteins that are induced rapidly by IFN- α/β signaling and inhibit the JAK-STAT pathway in two main ways. First, they bind to phosphorylated tyrosine residues on the IFNAR or JAKs, thereby preventing STAT binding (363). Secondly, their C-terminal SOCS box domains are involved in recruiting ubiquitin ligases to the receptor complex to target it for degradation (364). USP18 binds directly to the cytoplasmic tail of IFNAR2 and limit its interaction with JAK1 (365). In addition, USP18 binding to IFNAR2 appears to alter its extracellular conformation, abrogating its binding with IFN- α and reducing its affinity for IFN- β (366, 367). This differential binding phenotype has been suggested to be an example mechanism by which distinct IFN species can cause diverse cellular outcomes despite usage of the same receptor (357).

The antiviral ISGs comprise a highly varied set of effectors that are collectively known to target every stage of a viral life cycle. Several have been well-characterized and together exhibit highly diverse mechanisms of action, but the majority await detailed characterization. Additionally, efforts to parse out which ISGs are critical for restricting which viruses – and how – continue. Below, I will summarize the functions of a few select ISGs that are well-

characterized and/or have demonstrated anti-arboviral activity to illustrate the mechanistic diversity of this response.

1.3.4.1 Myxovirus resistance (Mx)

Mx proteins belong to a family of dynamin-like guanosine triphosphatases (GTPases) and are among the most recognizable of the “classical” ISGs. They were so named for their potent restriction of influenza virus, an orthomyxovirus. Humans encode two Mx proteins, Mx1 and Mx2, and neither of their mechanisms of action have been fully elucidated. Of the two, Mx1 is the more broadly-acting and better characterized. Mx1 is known to form oligomeric ring structures that are required for its ability to induce conformational changes in its binding partners and its antiviral activity (368, 369). Thus, Mx1 oligomers are thought to surround viral nucleocapsids at an early stage post-entry and direct them to degradation pathways, although the details of how this works are unknown (357). Less is known about Mx2, and it does not appear to be active against as many viruses as Mx1, ironically including influenza A. However, it has been shown to be a critical effector against HIV infection, but not other retroviruses, by preventing translocation of the reverse-transcribed genome into the nucleus and, as a result, integration of HIV into the host cell genome (370-372).

1.3.4.2 Interferon-induced protein with tetracopeptide repeats (IFIT)

The IFIT family of ISGs are broadly-acting translation suppressors and contain five members in humans, IFIT1, IFIT1B, IFIT2, IFIT3, and IFIT5 (373). They are not typically expressed under basal conditions in most cell types, but are rapidly and potently induced by both IRF3 and ISGF3 activation (354, 374). The best-characterized IFIT protein is murine Ifit1b (formerly Ifit1) (375). This protein restricts translation of RNA virus genomes that lack 2'-O-methylation on their 5'

guanosine cap (i.e. have a type-0 cap) either by directly binding to the RNA and preventing its association with the translational machinery or by preventing its recognition by the eIF3 complex (373, 376). Many RNA viruses, including flaviviruses and coronaviruses, subvert Ifit1b restriction by adding type-I caps to their genomic RNAs. Alphaviruses, however, have type-0 caps but evade recognition by Ifit1b due to conserved stem-loop structures in their 5' UTRs (377). The other IFIT family members are also translational repressors and may be involved in discrimination of self and non-self RNA, but their activities are not dependent on type-0 cap structures (378).

1.3.4.3 Interferon-inducible transmembrane (IFITM)

The IFITM family proteins were the first ISGs known to inhibit virus entry into cells. They are enriched in endosome and lysosome membranes, and have particularly potent effects on viruses that require endocytosis for cell entry (379, 380). Humans express four IFITM proteins, IFITMs 1-3 and IFITM 5, and each seems to selectively inhibit certain subsets of viruses (357). Although most of the viruses shown to be IFITM-sensitive have been enveloped, recently reovirus entry was reported to be inhibited by IFITM3 (381). The molecular details of IFITM-mediated viral entry restriction are unknown, but it has been proposed that IFITMs modify the physical properties of endolysosomal membranes, such as fluidity or curvature, that could impact viral escape from these compartments (382). IFITMs may also alter the kinetics of endosome maturation, such as acidification, and thereby interfere with the timing of viral processes necessary for efficient entry into cells (357, 373). The importance of IFITM3 against arboviruses was recently demonstrated in studies of alphaviruses and flaviviruses. In one study, *Ifitm3*^{-/-} mice were significantly more sensitive to CHIKV and VEEV infection than wild-type mice (383) and similar results were obtained in a mouse model of WNV (384).

1.3.4.4 Zinc finger antiviral protein (ZAP)

Like the IFITs, ZAP is transcriptionally induced by both ISGF3 and IRF3 (385, 386). It is a member of the poly(ADP-ribose) polymerase (PARP) family with activity against several RNA viruses including alphaviruses (387), retroviruses (388, 389), and filoviruses (390), and hepatitis B virus (391). ZAP is thought to prevent initial translation of incoming viral genomes by directly binding to viral RNA and targeting it for degradation by recruiting the RNA processing exosome (392). It may also inhibit viral RNA translation through interaction with different eukaryotic initiation factors (393).

1.3.4.5 Interferon-stimulated gene 15 kDa (ISG15)

ISG15 is a ubiquitin-like protein that is very highly induced by IFN- α/β and exerts pleiotropic effects on its vast array of protein targets. ISG15 becomes covalently attached to lysine residues of nascent polypeptide chains of both host and viral origin in a process termed ISGylation (394). ISGylation can have very different effects on its target proteins, and thus can exert antiviral activity in a variety of ways. For example, ISG15 linkage to IRF3 makes IRF3 more resistant to ubiquitin-mediated degradation and prolongs its transcriptional activity (395), but attachment to cyclin D1 results in destabilization and cell cycle inhibition (396). As the list of targets for ISG15 continues to expand, the view that ISGylation may represent a very broad and nonspecific mediator of antiviral defense strengthens, and it may be that all proteins are co-translationally ISGylated in IFN- α/β -primed cells, with largely undefined effects (397).

1.3.4.6 Interferon-stimulated gene 20 kDa (ISG20)

ISG20 is a 3'-5' exonuclease that can directly degrade ssRNA and ssDNA, with a substantial preference for ssRNA and little or no activity against dsRNA (398). ISG20 has reported antiviral

activity against a wide range of RNA viruses, including alphaviruses, vesicular stomatitis virus, influenza A, YFV, hepatitis A and C viruses, HIV, and several bunyaviruses (387, 399-402). Curiously, it is unlikely that ISG20 restricts these viruses by direct degradation of genomic or transcribed viral RNAs considering that ISG20 is localized to various intranuclear compartments (403). However, viral RNA degradation was demonstrated against hepatitis B virus, which transcribes viral RNA in the nucleus and uses it as a template for reverse-transcription of viral genomic DNA (404). Thus, direct degradation of viral RNA is an antiviral mechanism of ISG20, provided those RNAs are inside of the nucleus. For RNA viruses that replicate entirely in the cytoplasm, the mechanism(s) of ISG20-mediated restriction are less clear, but there is emerging evidence that ISG20 can globally enhance transcription of other ISGs, thus indirectly contributing to the cytoplasmic antiviral state (Weiss et al. 2018. mSphere. Under review).

1.3.4.7 Virus inhibitory protein, endoplasmic reticulum-associated, IFN-inducible (Viperin)

Viperin is induced by JAK-STAT signaling as well as activated IRF1 and IRF3 (405-409). It is localized to the ER and ER-derived lipid droplets and interferes with lipid-relevant steps in the replication cycles of diverse enveloped viruses (357). Mechanistically, viperin has been shown to inhibit genome replication of DENV, WNV, and the somewhat related flavivirus (genus hepacivirus) hepatitis C virus by binding to components of the viral replicase (410-412). As flaviviruses form extensive membranous structures in which to replicate, viperin gains access to the viral replicases by virtue of its association with lipid droplets, which are included in these structures (357). In addition, viperin has been reported to inhibit the budding process in HIV-1 and influenza-A infections (413, 414).

1.3.5 Effects of IFN- α/β on innate and adaptive immunity

Beyond the canonical induction of cell-intrinsic immunity, type-I IFNs work in other ways to promote innate and adaptive immune responses through action on DCs, B and T lymphocytes, and natural killer (NK) cells. In immature DCs, IFN- α/β signaling contributes to the maturation process by increasing cell surface expression of the major histocompatibility complexes and the costimulatory molecules CD80 and CD86, which are required for efficient antigen presentation and activation of T cells (415, 416). In T cells, the effects of IFN- α/β are very context-dependent and may be activating or inhibiting, either of which may lead to increased or decreased pathology. CD4⁺ T cell survival and B cell activating ability seem to be enhanced by IFN- α/β in response to viral infection (417), and IFN- α/β encourages a T_H1, IFN- γ -producing phenotype (418). CD8⁺ T cell responses to IFN- α/β depend on the relative levels of STAT1 versus other STATs, as predominant STAT1-mediated signaling leads to antiproliferative effects, while STAT3/5 activation promotes clonal expansion (419, 420). CD8⁺ T cell functionality may be regulated in similar manner, with IFN- γ production either repressed or enhanced depending on whether or not signaling occurs through STAT1 or STAT4 (421, 422), although cytotoxicity is generally positively regulated (423-425). IFN- γ expression in NK cells is also regulated this way (421, 426). It is increasingly clear that the effects of IFN- α/β on T cell expansion and function depend on the magnitude and timing of the IFN- α/β response itself, as well as the specific expression of different signaling intermediates in the target T cells (427-429). B cells, on the other hand, seem to be universally positively regulated by IFN- α/β , and display early activation and enhanced antibody class switching in response to various viral infections (430-434).

While there are certainly demonstrable positive effects of IFN- α/β signaling on the development of other innate and adaptive immune responses, our understanding of the fine

balances involved in these interactions is far from complete. For instance, much of the foundational information regarding the role of IFN- α/β on the development of adaptive immunity has come from a limited number of infectious models, such as lymphocytic choriomeningitis virus (LCMV) infections of mice. However, as specific effects are highly context-dependent and nuanced, it is probable that “known” effects of IFN- α/β on immune cells and its requirement for certain aspects of immune maturation may be quite different in other infections. For example, the IFN- α/β response is not stringently required for induction of adaptive immunity following vaccination with the yellow fever virus (YFV) vaccine strain 17D, as vaccinated IFNAR^{-/-} mice develop robust CD4⁺, CD8⁺, and antibody responses that confer protective immunity against a subsequent lethal challenge with wild-type YFV (435). In addition, the relationship between IFN- α/β and disease outcomes during chronic viral infections seems to be a detrimental one for the host. Simian immunodeficiency virus (SIV)-infected macaques and human immunodeficiency virus (HIV) patients with rapid disease progression display higher levels of IFN- α/β activation than non-progressors, which may lead to aberrant T cell recruitment or expansion and impede viral clearance (261, 436-438). Similarly, blocking of chronic IFN- α/β activation during LCMV infection aided CD4⁺ T cell-mediated viral control by preventing induction of inhibitory molecules such as IL-10 and PDL-1 (439, 440). This type of chronic immune suppression may very well operate in other chronic infections, but the details of other systems, including the potential contribution of IFN- α/β to chronic viral control as well as effects on other immune components, remain to be investigated.

1.4 PHYSIOLOGICAL TEMPERATURE VARIATION

The majority of human infectious disease research is conducted, naturally, under conditions aimed to recapitulate the homeostatic conditions of the human body. One parameter easily controlled during such applications as mammalian cell culture is ambient temperature, with 37°C, the historical average for the mammalian core body temperature, being the archetypal set point. However, other, equally valid physiological temperature states exist both within the human body and throughout the living world that may influence the cellular and organismal processes usually studied at 37°C. For example, other species may have elevated (birds) or depressed (reptiles, fish) core temperature optima, yet each has innate and adaptive immune responses that must function in these conditions. In the context of infectious diseases, conventional wisdom tells us to let a fever burn and that being out in the cold will make you catch a cold. Some studies have begun to explore the validity behind these statements, but our understanding of how temperature variation can affect immune system function, in response to an infection or otherwise, is far from complete. Of particular interest, and one of the central themes of this dissertation, is the extent to which, and by what mechanisms, temperature variation in host tissues may impact the fitness and pathogenesis of arboviruses, which have the ability to replicate efficiently across a broad temperature range due to their adaptation to both vertebrate hosts and invertebrate (arthropod) vectors. Within a human host, these viruses display a broad cellular tropism, invading myriad tissues in different thermal compartments, from the most superficial skin layers to deepest tissues of the visceral organs and central nervous system. In the following section, I will discuss the major mechanisms of human thermoregulation and how they result in temperature variation between anatomical compartments. I will also describe sources of tissue temperature variation under abnormal circumstances such as fever, and the

cellular responses to thermal stress. Finally, I will discuss known effects of temperature variation on immune responses that may influence arboviral pathogenesis and disease.

1.4.1 Mechanisms of thermoregulation for core temperature maintenance

Maintenance of core body temperature within a narrow, optimal range regardless of environmental conditions is among the most critical homeostatic requirements for endothermic organisms. Accordingly, humans have evolved a complex and multilayered thermoregulatory apparatus that has enabled the successful colonization of widely varied climatic regions across the globe. In any climate, successful core temperature maintenance is dependent upon the body's ability to balance metabolic heat production with heat loss to its surroundings. Under resting conditions, most metabolic heat is produced by deep organs such as the brain, heart, and liver, and delivered to the peripheral and superficial tissues (limbs, skeletal muscle, subcutaneous fat, and skin) primarily by convection from the bloodstream (441). Heat dissipation to the surroundings at the skin's surface can occur through evaporation, convection, radiation, and conduction with the relative contributions of each mechanism dependent on the magnitude and direction of the thermal gradient between the skin and the environment (442). Similarly, heat can be gained from the environment through the skin by radiation, and by conduction and convection if the temperature of the surroundings is higher than that of the skin. At rest in a thermoneutral environment, which in humans has been determined empirically to be between 24 and 28°C for air temperature (443-446), heat balance is achieved without dedicated energy expenditure on thermoregulatory processes because the rate of metabolic heat production equals the rate of heat dissipation and body temperature is maintained. When heat production exceeds dissipation, body tissues must store the excess heat, causing temperatures to rise. Conversely, when heat loss

occurs more rapidly than it can be replaced, body temperature falls (441). Human tolerance for these non-thermoneutral circumstances is borne from both physiological and behavioral responses to rising or falling body temperature, with opposing mechanisms (active heat conservation versus active heat dissipation) usually stimulated at threshold temperatures within just 0.2°C of one another (441, 447). These responses are aimed to curb the effects of the thermal stress and maintain deep (core) tissue temperature around 37°C, however, core temperature maintenance often comes at the expense of the peripheral tissues.

1.4.1.1 Physiological and behavioral responses to cold exposure

When the environmental temperature is lower than the skin surface temperature, convective heat loss from the bloodstream predominates skin surface cooling, with contributions from radiation and evaporation. Conduction of heat from static tissues to other static materials (solid objects or static fluids) usually accounts for very little of the total heat loss in any given environment (442). The skin contains a high density of cold-sensitive thermoreceptors, and thus autonomic thermoregulatory responses to cold are activated first upon reduction in skin temperature and are later reinforced by a subsequent drop in core temperature (441, 448). Afferent signals from cold-sensitive neurons in the skin are transmitted to the preoptic anterior hypothalamus, which is often described as the body's "thermostat," and which can centrally integrate thermal signals from all regions of the body (sometimes called "mean body temperature" (448)) to effect the appropriate responses (447, 448). Of note, local afferent signals can also elicit efferent responses without central integration at the hypothalamus, as different efferent responses appear to be activated at different core and skin threshold temperatures (449), resulting in localized thermoregulatory mechanisms acting independently of a systemic response (450). The sum of these local responses along with hypothalamic integration of thermal signals

yields the core body temperature balance point of 37°C, which is the product of the thermoregulatory efforts, rather than the standard against which they are measured (441). When skin temperature falls below a threshold of about 35°C (451), the body will attempt to limit further heat loss by employing cutaneous vasoconstriction. Smooth muscle contraction mediated by alpha-adrenergic sympathetic nerves innervating cutaneous blood vessels limits blood flow close to the skin surface (452). Thus, convective heat loss from the body core is reduced and the insulative effect of the periphery is increased, albeit at the expense of peripheral tissues, which continue to decrease in temperature (448). Although this mechanism operates in both non-glabrous (hairy) and glabrous skin, arteriovenous shunts specifically designed for thermoregulatory redirection of blood flow are concentrated in the glabrous (non-hairy) skin of acral regions (i.e. palms of hands, soles of feet, fingers, toes, tip of nose and ears) and make these regions the major contributors to heat conservation at the skin surface, especially during whole-body and reflexive vasoconstriction (441, 447, 448). These arteriovenous shunts are approximately 100 µm in diameter and close near completely during cold stress, effectively shunting 10,000 times more heat-carrying blood away from the skin surface than an equal length of constricted 10-µm capillary, making the shunts particularly efficient (447). Importantly, arteriovenous shunting under mild to moderate cold stress does not affect nutritional blood flow through distal capillary beds, nor does it impact systemic blood pressure, which is maintained by larger and more central arterioles (447). However, as these shunts are concentrated in acral regions, activation of vasoconstriction at these sites sharpens the temperature gradient between proximal and distal body tissues during cold stress and renders these regions particularly prone to damage and loss of dexterity due to severely lowered temperatures (441, 447, 453).

Peripheral vasoconstriction is the first-line defense against core temperature reduction, but is limited in its capacity to prevent hypothermia in the face of severe or prolonged cold exposure, as maximal vasoconstriction is reached at a skin temperature of approximately 31°C (451). When heat conservation alone is insufficient to maintain core temperature, thermogenic mechanisms must supplement vasoconstriction. Nonshivering thermogenesis is activated by catecholamine stimulation of beta-3 adrenergic nerves that terminate on brown adipose tissue (441). Rich in specialized mitochondria where oxidative metabolism can be uncoupled from ATP synthesis in response to cold signals, this tissue generates heat by increasing metabolic rate and energy expenditure (441, 454, 455). This mechanism of heat generation is critical in many small mammals and human infants, and plays a smaller but established role in thermogenesis in older children and adults, although the specific type of adipose tissue involved may be different (447, 456). In contrast, shivering thermogenesis is the principal source of autonomic heat generation in response to cold stress in humans older than a few years (447). Shivering serves to increase the resting metabolic rate 2-3-fold through involuntary, oscillating contractions of skeletal muscle (457). As these contractions hydrolyze ATP without coupling it to concurrent biochemical processes, that energy is released as heat (441). Shivering is initially stimulated upon cold exposure due to falling skin temperature, but is maintained and strengthened in response to falling core temperature (458), reaching maximal intensity with involvement of most skeletal muscle groups at a core temperature of approximately 34-35°C (459). Piloerection, or the contraction of the erector pili muscles at the base of hair follicles, causes hair normally lying parallel to the skin's surface to stand upright in response to cold signals to trap an insulating layer of air close to the skin's surface (441). Although by itself piloerection does little to conserve heat in humans versus other mammals due to our comparative lack of hair and

predilection for clothing, it has been suggested that this response may augment the effectiveness of shivering (442).

Together, vasoconstriction and shivering thermogenesis act to limit heat loss from the skin's surface and generate additional metabolic heat, which is conserved in the body core due to simultaneous peripheral vasoconstriction. The result is that deep body tissue temperature is preserved while skin and peripheral tissue temperatures are allowed to fall. However, these autonomic thermoregulatory processes are only effective to a point, and upon prolonged or severe cold exposure, heat dissipation will exceed heat production and both core and peripheral temperatures will continue to drop. Thus, the most effective responses to cold exposure are behavioral, motivated by feelings of thermal discomfort in response to afferent signals from the skin and processed through multiple brain regions (441). Heat-seeking activities such as finding shelter or building a fire combined with heat-conservatory efforts like covering the skin's surface with clothing and taking on a huddled posture are common behavioral responses to cold exposure. Voluntarily increasing activity levels through exercising or fidgeting is also effective in increasing metabolic heat production. When behavioral responses to cold exposure are inadequate or unavailable, or when thermoregulatory mechanisms have been disabled, such as due to blood loss from traumatic injury, heat dissipation from the body induces a hypothermic state, which is defined as a core temperature below 35°C (460). Continual drop in core temperature results in increasingly harmful physiological reactions, depending on the depth of the hypothermia, beginning with central nervous system and cardiovascular impairment at core temperatures above 33°C, and ending with death by cardiac failure (461).

1.4.2 Physiological and behavioral responses to heat exposure

In addition to cold stress, during which core heat conservation is paramount, humans are also regularly confronted with environmental or exertional heat stress, which demands efficient heat loss mechanisms to keep the core temperature from rising. When heat production and/or absorption by the body exceeds dissipation, heat stored by body tissues causes core and skin temperatures to increase. The increased temperature is sensed by heat-sensitive thermoreceptors located primarily in deep tissues such as the hypothalamus, spinal cord, viscera, and deep veins, but also to a lesser extent in the skin (450), which then activate sympathetic cholinergic nerves terminating on eccrine glands in the skin, causing the release of sweat onto the skin's surface (441, 447). Sweat is an ultrafiltrate of plasma comprised mostly of water (447). The ensuing evaporative cooling is an important defense against core temperature elevation regardless of ambient temperature, but becomes the body's sole heat loss mechanism when ambient temperature is higher than skin surface temperature, as convective and radiant heat loss rely on temperature gradients (442). Sweating efficiency is accompanied and enhanced by cutaneous vasodilation, which maximizes blood flow to the skin, bringing body heat as close to the skin surface as possible to encourage dissipation to the environment (447). Although the exact molecular mechanisms governing cutaneous vasodilation have not been confirmed, it is thought that the same cholinergic nerves that stimulate eccrine glands concomitantly induce vasodilation to rapidly maximize heat dissipation (441). In addition, the acral arteriovenous shunts that close in response to cold exposure passively open upon warming due to the absence of a cold signal (462, 463), further enhancing convective and evaporative heat loss. Combined, sweating and peripheral vasodilation are effective in preventing core temperature elevation under mild to moderate heat stress, but excessive heat exposure or physical exertion (especially in warm

conditions) requires behavioral responses to avoid overheating. Voluntary responses to heat stress can range from shedding of clothing and reduction in overall activity level to discourage metabolic heat production and storage, to movement to an area of lower ambient temperature. Unsurprisingly, behavioral thermoregulation is far more effective than autonomic mechanisms as it works to reduce or eliminate the thermal stress itself, rather than simply mitigating its effects (441).

1.4.3 Temperature variation between anatomical compartments

Maintenance of a stable core temperature often involves thermal instability in peripheral tissues. Even under conditions of thermoneutrality, there still exists a core-to-peripheral temperature gradient in which the deep tissues of the head and trunk (the body core compartment) maintain an elevated temperature versus the shell compartment (superficial and peripheral tissues of the skin and limbs), which is typically about 4°C cooler than the core (441, 464). At rest, most metabolic heat is produced in the central, deep organs, whereas heat loss to the environment occurs almost exclusively at the skin surface and respiratory passages (441). Thus, a thermal gradient exists in which body heat flows from the deep body core outward. Conduction of heat through and between adjacent tissues toward the skin surface accounts for very little of body heat redistribution, and instead heat redistribution relies most heavily on circulation by the bloodstream (442). Distal extremities (hands and feet) are the main sites for cutaneous heat loss and are also the last to be perfused with warm blood, after heat transfer to more proximal tissues has already occurred (447). Compounded by slow capillary perfusion rates, a high surface area-to-mass ratio, and little capacity for metabolic heat production, even “deep” tissues in the extremities are prone to heat loss and temperature reduction (126). The net result of these factors

is a well-documented core-to-peripheral temperature gradient, with the body core compartment maintained at 37°C, and peripheral tissues steadily decreasing in temperature as distance from the body core increases.

Many of the studies addressing the core-to-peripheral temperature gradient and heat flow and distribution within the human body have come from the field of anesthesiology. Under general anesthesia, thermoregulatory mechanisms are hindered or inhibited, resulting in a moderate core temperature depression that can be a complicating factor in patient well-being during and after surgery (465). Therefore, there has been interest in studying how core body heat is redistributed in anesthetized patients to develop strategies to counter or prevent intraoperative hypothermia. An ancillary but useful result of these studies has been their contribution to our knowledge of precise tissue temperatures within the peripheral thermal compartment, particularly the severity of temperature gradients between proximal and distal sites within a human limb under normal conditions. In one such study, an extensive series of thermocouples inserted at varying tissue depths in the periphery of healthy volunteers revealed that, upon induction of general anesthesia, core hypothermia resulted primarily from body heat shunting to distal limb compartments, rather than direct cutaneous heat loss (466). This finding reflects the capacity of peripheral tissues to gain heat from the body core along the core-peripheral temperature gradient when vasoconstrictor activity is abrogated by anesthetization. Importantly, this study also revealed that prior to induction of anesthesia, resting limb temperatures, calculated as a volume-weighted average of defined segments and tissue depths, were around 33°C with distal extremity temperatures as low as 31°C under room-temperature (22°C) conditions (466). These findings highlight an important point concerning human body

temperature in that, under room temperature conditions, tissue temperatures in the peripheral thermal compartment can be substantially lower than in the core compartment.

Other studies have recapitulated the peripheral tissue temperature measurements described above using similar methodology (467-469). As a result, attempts to define the exact physical volumes occupied by the core and peripheral thermal compartments, and how the sizes of those compartments change during general anesthesia, have been made. One study concluded that the core thermal compartment, carefully maintained at 37°C, includes tissues extending into the upper arm and thigh, with the core-peripheral temperature gradient extending radially from the interior of the proximal limbs toward the skin, and the core compartment reaching within 2.5-7 mm from the skin's surface (470). Another study examining more distal sites found that the core thermal compartment does not reach so close to the skin's surface, and tissues within 1.8 cm of the skin's surface (in this case, on the foot) display sub-core temperatures and the expected temperature gradient (471). Thus, in the extremities and acral regions, tissue depth is insufficient for maintenance of the core thermal compartment, and even relatively deep tissues at these sites, the muscles, bones, and joints, are fully immersed in the temperature variability of the peripheral thermal compartment. Of note, other bodily regions, namely the upper airways and the testes, also average tissue temperatures below 37°C. Inhalation of (usually) cooler ambient air results in high evaporative heat loss from the upper airways, and 33°C is considered a standard approximation of upper airway temperature (472). Testicular temperature between 33 and 35°C is optimal for spermatogenesis, and thus human testicles are separated spatially from the body core and designed for heat dissipation, with thin skin, minimal subcutaneous fat, and dense eccrine glands (473). In sum, humans experience a high degree of regional body temperature variation even under conditions of thermal comfort and thermoneutrality, and this variation is

exacerbated under conditions of cold stress. Heat stress can also result in increased whole-body temperatures, but this generally decreases regional temperature variation. However, many physiological conditions stemming from demographic factors, disease states, and voluntary behaviors can greatly impact human thermoregulatory mechanisms and cause abnormal variation in body temperature.

1.4.4 Physiological factors affecting human body temperature

1.4.4.1 Impaired circulation

As body heat redistribution from core tissues to the periphery is centrally dependent on blood circulation and convective heat transfer, any condition leading to impaired peripheral circulation will reduce heat delivery to peripheral tissues and steepen the core-peripheral thermal gradient. Poor circulation, regardless of the underlying cause, results from narrowing or blocking of blood vessels, such that blood flow through those vessels decreases and blood pressure increases. Unsurprisingly, cardiovascular diseases such as peripheral artery disease and atherosclerosis in peripheral vessels, by definition, result in decreased blood circulation in peripheral tissues. Thus, people with certain cardiovascular diseases may experience symptoms such as pain, numbness, and coldness in tissues suffering inadequate perfusion, most prominently in the limbs and extremities. Aging is also associated with circulatory dysfunction, in no small part due to higher incidences of cardiovascular diseases in the elderly (474). However, thermoregulatory mechanisms also degenerate with age, which contributes to decreased thermal tolerance and a higher risk for temperature-associated injury (475). In older individuals, the vasoconstrictor response becomes blunted due to decreased synthesis and release of noradrenaline (475) and falling muscle mass and glucose uptake lead to reduced shivering capacity (476). Combined with

a slowing of resting metabolic rate and decreased capacity to sense their thermal environment, elderly individuals are at a greater risk of hypothermia even in a mild climate (477).

Aging is not the only risk factor for poor circulation and cardiovascular disease. Smoking is strongly associated with deterioration of cardiac function and a primary risk factor for all manner of cardiovascular diseases, including atherosclerosis and peripheral artery disease (478, 479). Smoking also causes acute changes in peripheral circulation, such as a peripheral vasoconstrictor response during and immediately after smoking a cigarette (480). Further, smoking can cause the development of Buerger's disease, chronic inflammation of and thrombotic occlusions in the small and medium blood vessels, usually affecting the hands and feet, and starving these tissues of nutrition and heat (481). Additional disease states such as obesity, diabetes mellitus, and hypertension are also known to affect thermoregulatory cutaneous blood flow and may affect an individual's ability to control core and peripheral tissue temperatures (482, 483). Finally, Raynaud's syndrome is an example of peripheral vascular dysfunction that is not necessarily associated with underlying cardiovascular disease but can have profound effects on the temperature of the extremities. Individuals with Raynaud's syndrome experience vasospasm in the small arteries of the fingers and toes in response to cold exposure, emotional stress, or other stimuli, causing excessive narrowing of these vessels and severely limited blood supply to the affected tissues (484). Over time, this can result in permanently thickened vessel walls, which further limits blood supply to the extremities.

1.4.4.2 Fever

Fever is the programmed physiological elevation of core body temperature and most often occurs in response to infection. When the body senses invasion by a pathogen, innate immune cells release inflammatory, pyrogenic (fever-inducing) cytokines such as interleukins 1 and 6 (IL-1

and IL-6) and tumor necrosis factor (TNF) into the bloodstream, which stimulate production of prostaglandin E2 (PGE2) in the brain (485). PGE2 induces fever by decreasing the firing rate of certain heat-sensing neurons in the hypothalamus, which in turn activates cold effector responses (486). In other words, PGE2 signaling makes the hypothalamus less sensitive to heat signals, triggering heat generation and conservation mechanisms to compensate for the perceived temperature reduction, even though none exists. The result is that cutaneous vasoconstriction, shivering, and behavioral heat-seeking results in a 2-4°C increase in core body temperature (486). Temperatures in the peripheral thermal compartment may initially drop due to the vasoconstriction, but may also rise as core temperature increases, although still remaining cooler than the body core (487). The immune advantages conferred by fever induction in response to infection will be covered in a later section.

1.4.5 Intracellular responses to temperature change

Just as endothermic organisms have whole-body and local responses to thermal stress, so too do their cells. Mammalian cells are equipped with specific responses to mitigate potential temperature-related damage and as an adaptive mechanism to maintain homeostasis during variations in temperature. However, much of what is known about temperature stress responses comes from studies of cultured cells, which may behave differently from cells in an organismal context. For example, there is evidence of heat shock protein expression (detailed below) on the cellular level that contributes to whole-body protection from hyperthermia, and due to the narrow range of elevated temperature survivable by endotherms, it is likely that the heat shock responses observed *in vitro* are similar to those that operate *in vivo*. Less clear is the relationship between the response of cultured cells and body cells to cold stress. Near-freezing temperatures in

cultured cells are poorly tolerated and typically result in significant apoptotic or necrotic cell death. Conversely, core temperatures at or below 0°C are routine for deep hibernating mammals, and rapid and sporadic rewarming events can occur multiple times in a single hibernation cycle without detriment to the organism (488). On the other hand, cultured cells rapidly adapt to mildly hypothermic temperatures (28-34°C) and can continue to grow and divide indefinitely, while body core temperatures this low kill non-hibernating mammals, including humans, within hours. However, as discussed above, many peripheral tissues and cell types in humans regularly exist at both hypo- and hyper-thermic temperatures and are subject to rapid changes in their thermal environments according to ambient temperature conditions. Thus, it is plausible that different body cell types are differentially sensitive to temperature variation, and that modeling these responses in immortalized cultured cell lines might not accurately reflect *in vivo* responses. Conversely, the thermal stress responses observed in cultured cells may represent the homeostatic baseline for body cells under constant temperature stress.

1.4.5.1 Heat shock response

Under conditions of even mild heat stress, cells face significant challenges posed by the heat-labile nature of proteins. Heat-induced denaturation, misfolding of nascent proteins, entanglement, and nonspecific aggregation can deleteriously affect a vast number of cellular processes and, if left unmitigated, can lead to cell death (489). Cytoskeletal rearrangement and aggregation can cause incorrect localization of organelles and breakdown of proper cellular transport networks (490, 491). In the nucleus, ribosome assembly dysfunction in the nucleolus results in large granular deposits of ribosomal proteins and RNA (491). In the cytoplasm, mRNAs, translation initiation factors and ribosome components, and other proteins are sequestered in stress granules, which leads to a global decrease in protein translation (492).

Rising cellular temperatures can also cause damage to DNA and RNA, mitochondrial loss or dysfunction, fragmentation of the endomembrane system, and loss of plasma membrane integrity (493). The severity of these complications is directly related to the magnitude and duration of the heat stress (494). Severe ($>42^{\circ}\text{C}$) or prolonged heat stress results in cell cycle arrest and eventual cell death by apoptosis (494, 495). However, typical heat stress, such as febrile-range temperatures, rarely reaches that critical point and cells can survive and recover through induction of the heat shock response.

In a hyperthermic cell, changes in protein conformations and interactions, lipid membrane fluidity and permeability, and ion flux are sensed through various signaling events and trigger a coordinated stress response known as the heat shock response (HSR) (494). The HSR begins upon heat-induced activation of heat shock factor 1 (HSF1), which is constitutively expressed but is repressed in complexes with other regulatory proteins in the absence of heat stress (494). When rising temperature induces protein misfolding, those chaperones free HSF1 in favor of interaction with the misfolded proteins (496). Activated HSF1 is a homotrimer that translocates to the nucleus and binds to consensus heat shock elements (HSEs) in the promoters of heat shock genes and activates their transcription (497). Chief among heat shock responsive genes are the heat shock proteins (HSPs), which are protein chaperones involved in preventing protein misfolding and aggregation during thermal and other cell stresses. The HSP family consists of high molecular weight proteins (e.g. HSP70, HSP90) and low molecular weight proteins (e.g. HSP27), many of which are expressed in the absence of cellular stress to aid in protein folding and proper aggregation under normal conditions, but this function becomes paramount during heat stress (498, 499). Large HSPs such as HSP70 and HSP90 family members preferentially bind to hydrophobic regions of unfolded polypeptides and promote

proper refolding in an ATP-dependent manner (500), both in the cytoplasm and the nucleus (501). Small HSPs also act as molecular chaperones, but passively prevent aggregation of unfolded proteins under conditions of cell stress, rather than actively aiding in refolding (502). In addition to their role as chaperone proteins, HSPs can block apoptosis during heat stress through interaction with cytochrome c (HSP27) or through inhibition of downstream caspase-9 activation (HSP70/90) (503, 504).

In addition to HSPs, there are many other heat-shock inducible proteins, including many not dependent on HSF1 (505), that carry out important functions for cell survival during heat stress. These include proteasome components for clearing misfolded and aggregated proteins from the cell, nucleic acid-modifying enzymes for repairing DNA and RNA damage, various signaling molecules and transcription factors involved in maintenance of the stress response and repression of other signaling and metabolic pathways, and cytoskeleton- and membrane-stabilizing proteins (489). Despite the large number of genes upregulated upon heat stress, an even greater number are repressed, leading to a net decrease in overall transcription (505, 506). In sum, repression of cellular macromolecular synthesis in combination with preferential upregulation of pro-survival proteins such as chaperones and other stabilizers puts heat-stressed cells into a sort of “holding pattern,” during which the cell is protected from further damage until the thermal stress is relieved. HSE is self-limiting as thermal conditions return to normal. As the challenge of unfolded and misfolded proteins wanes in response to normal cellular temperatures, the highly upregulated chaperones HSP70 and HSP90 become excessive and re-associate with HSF1, blocking its transcription factor ability and curtailing the response (507).

1.4.5.2 Cold shock response

It has long been appreciated that under hypothermic conditions, cultured cells slow their growth rate, and with further temperature depression, enter cell cycle arrest and eventually die. At first this was attributed to generalized metabolic decline and cessation of vital cellular reactions. However, while metabolic slowing does indeed occur during cellular cold stress, it is in fact a part of a purposeful and carefully orchestrated set of responses. Like the heat shock response, the cold shock response in mammalian cells is designed to mitigate cellular damage that may occur in the wake of thermodynamic changes to cellular structures and processes under conditions of temperature stress. Cold shock rapidly and selectively induces the expression of a small group of cold responsive genes, and much of what is known about the cold shock response comes from studies on the functions of the two best-characterized cold-shock proteins, cold-inducible RNA binding protein (CIRP) and RNA binding motif protein 3 (RBM3).

CIRP and RBM3 are highly homologous, evolutionarily conserved glycine-rich RNA-binding proteins (508) that are expressed under normal homeostatic conditions in various tissues (509) and are upregulated in response to a variety of cellular stresses, including hypothermia, hypoxia, and ultraviolet and ionizing radiation (510-513). Peak expression of CIRP and RBM3 occurs at mildly hypothermic temperatures (28-34°) and further temperature reduction greatly decreases expression (510, 514, 515). Accordingly, both CIRP and RBM3 are highly expressed in mammalian testes, though in distinct cell types, where lowered temperatures are required for normal spermatogenic functions (516, 517). In warmer tissues, baseline levels of CIRP and RBM3 have a variety of functions and are involved in many processes, such as embryonic development, and their expression is tightly controlled both spatially and temporally (518). In adult humans, RBM3 expression is very low in most tissues except for actively proliferating

brain regions, where it is implicated in the maintenance of stemness, the ability to self-renew as well as differentiate, in neural progenitors (519, 520). Under conditions of cold stress, CIRP and RBM3 display some tissue-specific and cell-type-specific upregulation, indicating that different tissues may have distinct requirements for optimal responses to hypothermia (518). In hyperthermic conditions, expression of both proteins drops substantially (516, 521).

Induction of CIRP upon cold stress is mediated at the transcriptional, post-transcriptional, and translational levels. At 32°C, an increase in Sp1 recruitment to the mild-cold responsive element (MCRE) in the *CIRP* promoter region was observed versus 37°C (522). Post-transcriptionally, CIRP mRNA maturation is regulated by an alternative splicing mechanism wherein transcripts encoding the full-length CIRP are preferentially produced under hypothermic conditions, although the mechanism responsible for this preference was not identified (523). In addition, the cold-induced CIRP splice variants contain putative internal ribosomal entry sites (IRES) that may contribute to selective translation in the face of global translational slowing during cold stress (523). Much less is known regarding the cold-inducible properties of RBM3 transcription. The subcellular localization of CIRP is primarily nuclear under homeostatic conditions, but a fraction can shuttle to and from the cytoplasm (514). Nuclear CIRP regulates gene expression at the post-transcriptional level by binding to the 3' UTRs of certain target RNAs and stabilizing them (524). In addition, CIRP can contribute to alternative polyadenylation and splicing of certain genes (525, 526). CIRP targets often include other stress response genes and it can also enhance their translation through interaction with eIF4G after shuttling to the cytoplasm (527). However, CIRP has also been shown to reduce global translation through its binding to 3' UTRs, so its exact role in translational regulation is not fully understood (528, 529).

In addition to modulating gene expression, CIRP plays major roles in the promotion of cell survival and proliferation during hypothermia. Indeed, under the mild hypothermic conditions that induce maximal CIRP expression, cells continue to function and divide normally, albeit at a reduced rate. CIRP is intimately involved in preventing cell cycle arrest under mild to moderate cold stress, and has been shown to contribute to increased expression of cyclin E1 as well as prevent phosphorylation and inactivation of cyclin D1, which encourages progress through the G1/S checkpoint (530-532). In addition, CIRP is pro-survival in that it inhibits several apoptotic pathways and protects hypothermic cells from apoptotic death. In neurons, CIRP prevents cellular apoptosis by blocking mitochondrial apoptotic pathways (533, 534) and can also inhibit the activities of p53, Fas, and caspase-3 and their downstream pathways (535-537). CIRP overexpression or hypothermia-induced expression has also been shown to dramatically reduce apoptosis in hydrogen peroxide-treated neuronal cultures, in which the formation of reactive oxygen species (ROS) drive cell death (534, 535), and reduce ROS formation in hypothermic hepatocytes (538). Perhaps unsurprisingly, constitutively elevated CIRP is a common feature of many cancers, presumably due to its proliferative and pro-survival activities (518). To summarize, mild hypothermia (28-35°C) within a typical physiological range fails to induce cell cycle arrest and apoptotic cell death due in part to the activities of the cold-inducible CIRP. In contrast, severe hypothermia (<25°C) leads to dramatically decreased CIRP levels and does indeed result in cell cycle arrest and eventual apoptotic or necrotic cell death.

Like CIRP, RBM3 binds RNAs in the nucleus to modulate gene expression at post-transcriptional steps including alternative splicing and polyadenylation (525, 526). However, the most well-known impacts of RBM3 on gene expression are due to its effects on translation. At severely hypothermic temperatures, translation is arrested through the constitutive

phosphorylation of eIF2 α , which prevents assembly of the initiation complex (539). When RBM3 is upregulated under mild hypothermia, it enhances global translation through several mechanisms that promote translation initiation, including preventing the phosphorylation of eIF2 α (540, 541). Furthermore, RBM3 can promote cell cycle progression by facilitating the G2/M transition (542) and antagonize apoptosis. Hypothermia, like hyperthermia, can trigger ER stress and the unfolded protein response (UPR), which can lead to apoptosis through activation of the protein kinase RNA-like endoplasmic reticulum kinase (PERK), which arrests translation by phosphorylating eIF2 α and stimulates apoptosis through induction of the transcription factor C/EBP homologous protein (CHOP) (514, 543). RBM3 can traffic from the nucleus to the stressed ER and inhibit the activation of PERK, which mitigates the downstream translational arrest and suppresses pro-apoptotic pathways (544, 545).

Although CIRP and RBM3 are critical mediators of the cold shock response under mildly hypothermic conditions, other changes occur in cold stressed cells that appear to be independent of these proteins, and it is likely, as suggested above, that many functions of these proteins serve to prevent drastic changes to cell homeostasis that would otherwise occur, and indeed do occur with deeper hypothermia, in their absence. Common outcomes of mild cold stress observed in cultured mammalian cells include decreased oxygen and ATP consumption (slowed metabolism), attenuation of transcription and translation, increased mRNA stability and reduced degradation, extended doubling times, and prolonged viability (546). Some of these features, such as increased mRNA stability and prolonged viability, can be explained in part by the activities of CIRP and RBM3. Attenuation of global translation rates under mild cold stress was recently shown to be controlled at the elongation phase, rather than initiation, which is the target at lower temperatures, as discussed above (547). The molecular mechanisms leading to the other

changes are less clear, and may simply be attributable to the lowered temperature causing thermodynamic changes in macromolecule structure and interactions. However, if and how this assumed cold-induced, nonspecific slowing of cellular activity affects specific cellular components and processes is near completely unexplored. In addition, as nearly all studies of the cold-shock response in mammalian cells have been completed using cell culture models, the question of whether or not, and to what extent, these phenomena occur in cold-stressed cells *in vivo* remains open. Some studies in hibernating mammals under deep hypothermia have confirmed the metabolic, transcriptional, and translational arrest observed in cells under severe hypothermia, but without the accompanying apoptotic and necrotic injury (488). In addition, upregulation and functionality of CIRP and RBM3 have been noted in mouse testes (517, 548), indicating that these proteins are indeed inducible by mildly reduced temperatures *in vivo*. However, the effect of cold stress on the survival and functions other tissues, especially in humans, has yet to be extensively described.

1.4.6 Effects of physiological temperature variation on immune responses

1.4.6.1 Fever/hyperthermia

Fever, the purposeful elevation of body temperature in response to infection or injury, is evolutionarily conserved among many diverse animal taxa, with fever achieved biochemically in endotherms and behaviorally in ectotherms and poikilotherms (485, 486). The febrile response likely evolved around 600 million years ago and was retained in many lineages despite the considerable metabolic costs of raising one's temperature (486, 549-551), suggesting that hyperthermic body temperature is strongly pro-survival during infection. In 1927, Julius Wagner-Jauregg won the Nobel Prize in Physiology or Medicine for his successful treatment of

progressive neurosyphilis patients with malaria-induced fever, a strategy that built on the association between high fever and neurosyphilis remission known since Hippocrates' time (552). In the time since Dr. Wagner-Jauregg's discovery, the use of antipyretic medication to combat fever during infection has soared in popularity and become a staple of both at-home and clinical care for febrile patients (552). However, numerous studies have shown that the use of antipyretics has a detrimental effect on the patients' ability to control and clear various infections, including rhinovirus, varicella, and influenza (553-555), and that the immune response to vaccination may be weakened by antipyretics in children (556). In addition, numerous lethal challenge models of bacterial and viral infections in host species including goldfish, lizards, and mice can be rendered nonlethal by increasing the host's core temperature to a febrile range (486). Blocking fever with antipyretics in similar studies eliminated the survival benefit (486). However, there are some contexts in which fever or hyperthermia may be harmful to the host, such as during uncontrolled inflammatory states such as sepsis, or neural ischemic injury, when the proinflammatory effects of fever are no longer beneficial (557, 558). Together, these data argue for a host-protective role of fever in the context of many infections provided the febrile response and its downstream effects do not go uncontrolled and homeostasis can be restored.

The mechanisms that mediate fever's host-protective actions can be broadly categorized into anti-pathogen effects and pro-immune effects. In some cases, febrile-range temperature can directly inhibit a pathogen if the pathogen's ability to survive and grow is reduced at higher temperatures. For example, poliovirus replication in mammalian cells was reduced over 200-fold at 40-41°C compared to 37°C (485). Fever-range temperatures have also been shown to increase the susceptibility of Gram-negative bacteria to serum-induced lysis (559). Many pathogens,

however, are largely unaffected by the 2-4°C increase in body temperature caused by fever. For these infections, the survival benefit of the febrile response comes from its immune-enhancing effects. Numerous studies have characterized the molecular and cellular immune processes that benefit from hyperthermia, namely, those involved in inflammation and lymphocyte trafficking. Some of the pyrogenic molecules involved in the induction of the febrile response, such as IL-6, IL-1, and TNF α , are also classical proinflammatory cytokines that are upregulated in response to a variety of infections, thus providing a crucial link coordinating the febrile response and inflammation (485). In addition, activation of the heat shock response mediator HSF1 at febrile-range temperature (38-41°C) but not heat shock temperature (42-45°C) augments production of these cytokines (485) with mild activation of the heat shock response, indicating molecular crosstalk between the immune response to infection and pro-survival cellular responses to the heat stress (560). These are examples of feed-forward mechanisms driving both febrile and immune cytokine responses in a coordinated, complementary fashion.

While the specific response to a given infection can vary widely depending on the nature of the invading pathogen, the general innate inflammatory response typically involves recruitment of innate immune cells such as neutrophils, NK cells, macrophages, and DCs to the site of infection followed by relocation of antigen-presenting cells (APCs) to the local lymph node to activate pathogen-specific T cells near the high endothelial venule, the major port of entry for tissue-resident immune cells into lymphoid organs (561-563). In mouse models of fever induced by either LPS injection or external whole-body heating, neutrophil recruitment into bacteria-infected tissues and the respiratory burst associated with their activation were found to be enhanced by elevated temperature compared to normothermia (564-566). Similarly, increased NK cell cytotoxic activity and recruitment into tumor tissues was augmented by febrile

temperatures *in vivo* (567). Macrophage function is also enhanced by febrile-range temperature. HSP70 induction in macrophages at febrile temperatures is associated with prolonged activation in response to LPS and also increases the production of nitric oxide and inducible nitric oxide synthase upon activation by LPS and IFN- γ (568). Under febrile heat stress, HSP70 can also be released from cells and act as a damage-associated molecular pattern (DAMP) to stimulate macrophages and DCs to produce proinflammatory cytokines (569, 570). Fever-range hyperthermia has also been shown to improve the phagocytic, pathogen-sensing, and antigen-presenting abilities of DCs in part through heat-induced upregulation of TLRs and major histocompatibility complex (MHC) class I and II molecules (485). Trafficking of APCs from sites of infection to draining lymph nodes as well as extravasation of activated lymphocytes through endothelial gaps into sites of infection are also be improved by fever through more efficient chemotaxis (571, 572). Finally, T cell stimulatory function was enhanced in DCs under fever-range temperatures in an *ex vivo* assay (571). Together, these findings suggest that febrile temperatures can augment many functions of innate and adaptive immune cells and promote inflammatory responses to inflammation. However, most of these studies were completed in models of LPS-induced fever, and the specific mechanisms by which fever may enhance antiviral immunity, specifically the type-I IFN response, have not been extensively studied.

1.4.6.2 Hypothermia

Considerably less work has been undertaken on the effect of sub-normal temperatures on the immune response compared to fever-range temperatures. However, as alluded to above, there are certain situations in which hyperthermia becomes dangerous to the organism due to its contribution to uncontrolled inflammatory responses. In such cases as bacterial sepsis and neurologic injury, enhanced inflammation due to febrile temperatures can cause catastrophic

tissue damage, and therapeutic hypothermia have proven beneficial to patient outcomes in these contexts due in part to its anti-inflammatory effects in addition to induction of the pro-survival cold shock response (486, 573, 574). Hypothermia is generally considered to be immunosuppressive. Solid tumors can benefit from a hypothermic microenvironment due to dysfunctional T cell responses (575) and intraoperative hypothermia has been associated with increased risks of postoperative infection (576). However, few studies examining the mechanisms underlying these observations exist.

Recently, the type-I IFN response was shown to be attenuated by hypothermic temperatures in an *in vitro* model of rhinovirus infection (577). This study built upon previous observations that other viruses capable of infecting hypothermic tissues, such as a bovine herpesvirus, which was shown to induce less IFN but replicate to higher titers in experimentally cooled skin temperatures versus normal skin on two sides of the same cow (578). In addition, IFN- β has been implicated as one of the proinflammatory cytokines whose activity is dampened by therapeutic hypothermia in models of cerebral ischemia (579). Collectively, these studies suggest that type-I IFN induction and antiviral activity may be less at temperatures below 37°C, however, the mechanisms resulting in this phenotype have not been delineated.

1.5 HYPOTHESIS

The IFN- α/β response is one of the most critical innate immune systems in the protection of vertebrate hosts against viral infection; however, accumulating evidence suggests that its efficacy might be temperature-dependent. Many human viruses replicate and cause disease in anatomical sites that vary in temperature, such as the skin and respiratory tract, which are nearly always

lower in temperature than the body core. Arboviruses traverse variable thermal environments in a human host throughout their pathogenic course from the skin into the deeper organs, and therefore may be subject to temperature-regulated innate immune environments. In addition, many viral infections are associated with the febrile response, which results in an elevated body temperature and is generally considered to be immune-enhancing, although the mechanisms through which fever exerts its protective effects are incompletely understood. A recent study of human rhinovirus (RV) found that the increased replicative fitness of RV at the low upper airway temperature could be partially explained by hypothermia-mediated attenuation of IFN- α/β responses (577). However, the molecular mechanisms leading to reduced IFN- α/β efficacy remain unknown.

IFN- α/β is largely responsible for acute control of CHIKV and many other arboviral infections. CHIKV preferentially replicates and causes both acute and chronic arthritic/arthralgic disease in distal small joint tissues located in the extremities, such as those in the fingers, wrists, ankles, and toes. An underappreciated feature of these sites is their prominent role in whole-body thermoregulation in response to cold stress, which is constantly activated under room-temperature conditions. Peripheral vasoconstriction and arteriovenous blood shunts in the hands and feet render these regions much cooler in temperature than core tissues, and their large surface area-to-mass ratio and thin adipose insulation do little to protect the deeper bone and muscle tissues from experiencing these reduced temperatures. Therefore, CHIKV infection in these regions likely often occurs under conditions of mild hypothermia.

Overall, I hypothesized that the type-I IFN response against CHIKV and other arboviruses is less effective at subnormal temperatures and more effective at febrile

temperatures, compared to the normal 37°C mammalian core temperature. Specific aims for these studies were addressed in the following chapters:

- In Chapter 2, I explored the relationship between temperature variation and the ability of IFN- α/β to inhibit arbovirus infection. I hypothesized that temperature variation influences the sensitivity of diverse arboviruses to IFN- α/β responses as the result of temperature-dependent differences in the production of IFN- α/β and ISGs. In addition, I hypothesized that reduced temperatures *in vivo* contribute to acute CHIKV replication and disease through attenuation of the IFN- α/β response.
- In Chapter 3, I sought to better understand the factors that predispose CHIKV patients to developing chronic disease. One risk factor identified in human cohorts is the severity of acute phase viremia and disease. I hypothesized that body temperature reduction in the acute phase, chronic phase, or both could exacerbate chronic CHIKV infection in an adult wild-type mouse model as a result of its action on IFN- α/β -mediated viral control, dependent on the magnitude of viral replication during the acute phase.

The results of these studies revealed the mechanisms by which temperature variation influences the efficacy of the IFN- α/β response. They also demonstrated the impact of this relationship on the course and severity of arthritogenic alphavirus infection and suggest the utility of local or systemic temperature modulation as a therapeutic option for CHIKV or other arboviruses.

2.0 EFFICACY OF THE INTERFERON-A/B RESPONSE VERSUS ARBOVIRUSES IS TEMPERATURE-DEPENDENT

2.1 INTRODUCTION

Type I interferon is a critical early protector of vertebrate hosts from overwhelming viral replication and disease [reviewed in (357)]. This role has been abundantly demonstrated with arboviruses and other viruses by infection of *Ifnar1*^{-/-} mice that lack IFN- α/β signaling. In many cases, a completely benign localized infection of normal mice is rendered systemic and rapidly fatal by elimination of signaling through the IFN- α/β receptor (e.g., (97, 98, 190, 580)). Even minor changes in the characteristics of the IFN- α/β response greatly increase viral replication and disease (581).

The IFN- α/β response consists of an inductive phase in which virus infection stimulates infected and possibly uninfected cells to produce and secrete IFN- α and IFN- β proteins that signal through the dimeric IFN- α/β receptor and cause the transcriptional upregulation of antiviral effector genes (279, 582). This leads to production of proteins in infected and uninfected cells that, together, constitute an “antiviral state.” This response is the primary protector of vertebrate hosts from overwhelming virus replication prior to development of the adaptive immune response and is also involved in the clearance phase of infection (583, 584). Subclinical infections with arboviruses and other viruses that normally only affect regional

tissues can be rendered systemic and catastrophic by the absence of this response (98, 580, 585). The type I IFN response is so effective that it can determine apparent tissue tropism for highly IFN- α/β -sensitive viruses (98). This suggests that even minor increases or decreases in the efficacy of this response could have dramatic impacts upon the outcome of virus infection.

Previous studies have primarily focused upon the characteristics of IFN- α/β induction and effector phases in standard laboratory conditions mimicking mammalian core temperatures (e.g., 37°C). However, temperatures in peripheral tissues of humans can range as much as 5 degrees below 37°C under normal room temperature conditions (466), and can become much lower under more extreme conditions (586). In addition, few studies have examined IFN- α/β responses in the febrile conditions under which they commonly act *in vivo* during pathogen infection. Indeed, core (rectal) temperatures can rise to 42°C during extreme febrile or hyperpyrexia episodes, and febrile responses to infection typically range between 38 and 40°C (587). However, two recent studies have suggested that IFN- α/β responses may be lesser in upper airway epithelia where temperatures are substantially below core (577, 588). This work complemented several historical studies that also suggested temperature-mediated effects on IFN- α/β efficacy in other model systems (578, 589-594). Other early studies, however, including with arboviruses, that identified temperature variation as a factor in IFN- α/β effectiveness implicated temperature-altered virus replication rather than the IFN- α/β response (595-606).

Herein, we demonstrate that multiple arboviruses including alphaviruses, bunyaviruses, and flaviviruses, which have evolved to replicate at ambient temperatures in the invertebrate vector, are dramatically more resistant to the IFN- α/β system at temperatures below 37°C. Subnormal temperatures led to a considerable diminution of IFN- α/β efficacy and supranormal temperatures led to a modest enhancement of efficacy, possibly representing an evolutionary

mechanism for the febrile response. At the same time, induction of IFN- α/β was delayed and reduced at low temperatures and enhanced at higher temperatures *in vitro*. A primary mechanism underlying the temperature effect appeared to involve reduced rates of gene transcription at the lower temperatures. Furthermore, in a mouse model of chikungunya virus (CHIKV) infection and musculoskeletal disease (MSD), lowered temperatures induced in torpid or reserpine-treated mice resulted in exacerbation of virus replication and signs of MSD in an IFN- α/β response-dependent manner. The results of these studies will have impacts upon the understanding of pathogenesis of all arboviruses as well as other viruses that replicate in sites with altered temperature (e.g., rhinovirus, influenza virus, coronavirus) as well as other therapeutic contexts in which IFN is used (e.g., oncology). This may lead to improved therapeutic modalities involving localized or systemic temperature modification.

2.2 RESULTS

2.2.1 Efficacy of IFN- α/β against arboviruses is reduced at subnormal temperatures

To test the hypothesis that arboviruses are differentially sensitive to IFN- α/β treatment at different temperatures, we compared growth of wild-type strains from three distinct arbovirus genera, *Alphavirus*, *Flavivirus*, and *Phlebovirus*, in Vero cells treated with IFN- α/β at temperatures between 30 and 39°C with growth in temperature-matched untreated cells. Because Vero cells lack the IFN- α/β genes, they circumvent the potential confounding variable of temperature-dependent differences in IFN- α/β induction upon viral infection (577, 588). The arbovirus strains chosen, CHIKV La Reunion (CHIKV-LR), Sindbis virus TR339 (SINV-

TR339), Venezuelan equine encephalitis virus ZPC738 (VEEV-ZPC738), Eastern equine encephalitis virus FL93939 (EEEV-FL93), Dengue virus 2 16681 (DENV2-16681), Yellow Fever virus Angola (YFV-Angola) and Rift Valley fever virus ZH501 (RFVF-ZH501), are wild-type viruses that have undergone no or minimal passage *in vitro*, to limit potential selection for optimal replication under typical laboratory conditions, such as growth at 37°C. In the absence of IFN- α/β pretreatment in Vero cells, alphavirus growth was greatest at 37°C, the normal mammalian core body temperature, by 24 hours post infection (h.p.i.) compared to growth at 30 or 39°C, which was comparable to 37°C or slightly attenuated. (Fig 7A; 8A). This was also true in baby hamster kidney (BHK) cells (Fig 8B). Thus, in the absence of IFN- α/β , departure from 37°C conferred no advantage to alphavirus replication. Conversely, in cells pretreated with IFN- α/β , incubation at 30°C near uniformly conferred significant advantage to virus growth compared to 37°C, while incubation at 39°C, representing a febrile-range temperature, significantly reduced SINV and CHIKV growth compared to 37°C (Fig 7B). Accordingly, the replication ability of three alphaviruses, EEEV, CHIKV, and SINV, in IFN- α/β -treated cells was found to be significantly correlated to increasing IFN- α/β treatment temperature (Fig 7C). These results indicate that IFN- α/β efficacy was lowest at 30°C and increased with rising temperature. No such correlation was observed with VEEV, which is much more IFN- α/β -resistant than the other alphaviruses and minimally inhibited in Vero cells at the IFN- α/β concentration used (116, 607), further supporting the idea that decreased inhibition at 30°C is due to effects on IFN- α/β activity.

In addition, the EC₅₀ of IFN- α/β against SINV, CHIKV, EEEV, and VEEV on Vero cells was significantly correlated with incubation temperature, with substantially lower concentrations of IFN- α/β effectively inhibiting these viruses as temperature increased (Fig 7D-E). Finally, analogous temperature-dependent IFN- α/β sensitivity was observed in experiments with YFV

and DENV as well as RVFV, demonstrating that this effect is relevant to multiple families of arboviruses capable of replicating across a broad temperature spectrum (Fig 7F-I). Similar results were obtained in NIH/3T3 Tet-Off murine embryonic fibroblasts (MEFs) and primary murine osteoblasts, cell types representative of *in vivo* targets common to many of these viruses (Fig 8B-C). Collectively, these experiments suggest that the antiviral activities of IFN- α/β are most effective versus a variety of arboviruses at temperatures in the febrile range, and much less effective at subnormal temperatures in mammalian cells.

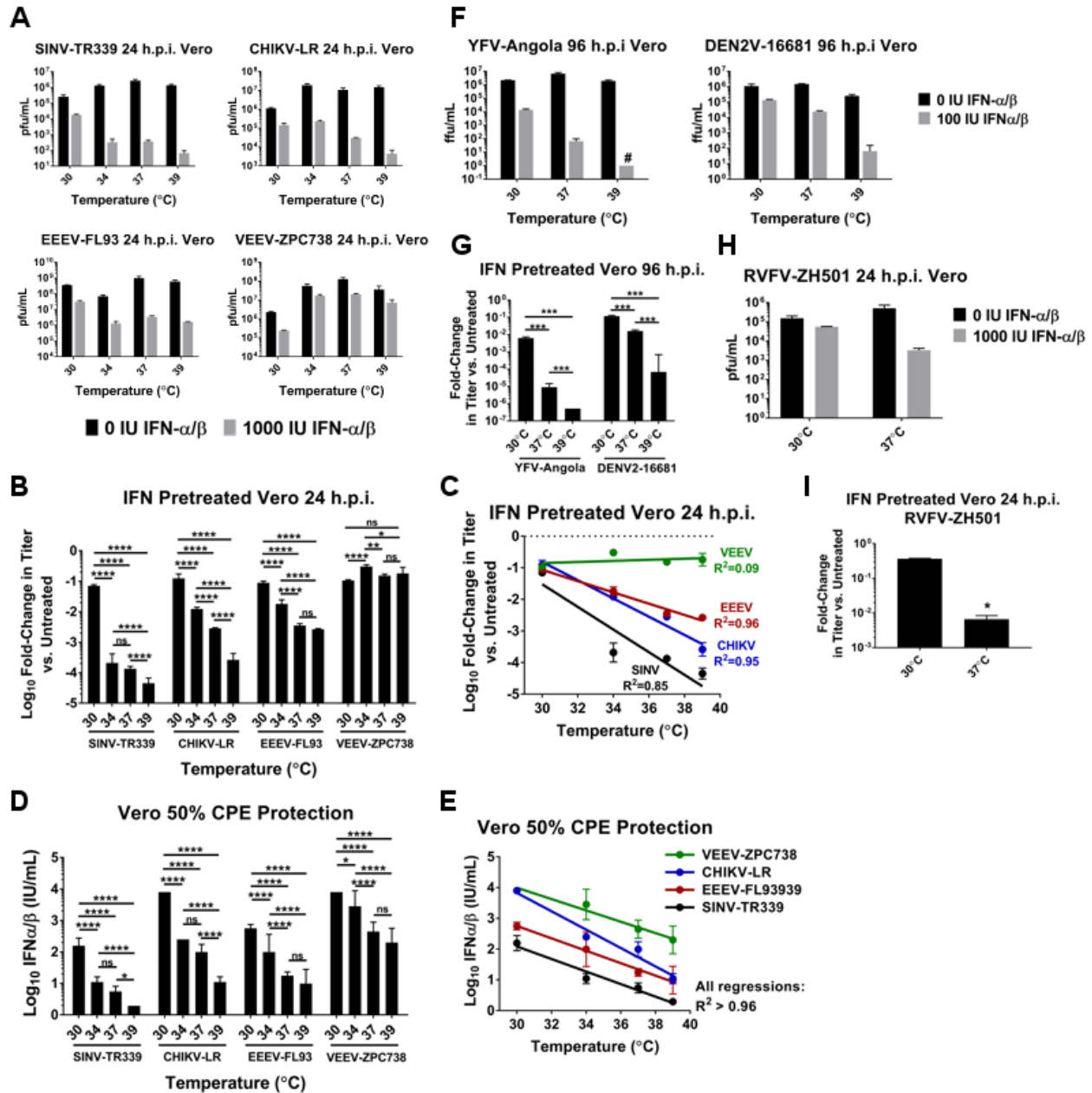


Figure 7. Efficacy of type I IFN against arboviruses is reduced at subnormal temperatures.

A-C: Vero cells were treated overnight with 0 or 1000 IU IFN- α/β at 30, 34, 37, or 39°C and infected with the indicated alphaviruses at a M.O.I. of 0.1. Supernatants were collected at 24 h.p.i. and viral titers were determined by plaque assay on BHK cells at 37°C. A: Comparison of viral growth at 24 h.p.i. between temperatures with and without IFN- α/β treatment. B: Log₁₀ fold-change in viral titer between IFN- α/β -treated and untreated cells at each temperature \pm SD. * p <0.05, ** p <0.01, *** p <0.001, **** p <0.0001, ns not significant by two-way ANOVA with Tukey's multiple comparison test on log-transformed fold-change values. C: Significant linear correlation between

increasing temperature and viral growth inhibition by IFN- α/β pretreatment for IFN- α/β -sensitive alphaviruses. Pearson's correlation $p < 0.02$ for EEEV and CHIKV, $p < 0.07$ for SINV. D-E: EC₅₀ of IFN- α/β in Vero cells at 30, 34, 37, and 39°C against the indicated alphaviruses was determined by IFN- α/β bioassay. D: Data are presented as log₁₀ mean IU/mL required to protect 50% of Vero cells from virus-induced cytopathic effect at each temperature \pm SD. * $p < 0.05$, ** $p < 0.01$, *** $p < 0.001$, **** $p < 0.0001$, ns not significant by two-way ANOVA with Tukey's multiple comparison test on log-transformed IU/mL values. E: Significant linear correlation between increasing temperature and decreasing IFN- α/β EC₅₀ was established using Pearson's correlation on log-transformed IU/mL values ($p < 0.02$ for all viruses). F-G: Vero cells were treated overnight with 0 or 100IU IFN- α/β at 30, 37, or 39°C and infected with YFV or DENV at a M.O.I. of 0.1. 96 h.p.i. supernatants were assayed for viral titer by focus forming assay at 37°C. F: Comparison of viral growth at 96 h.p.i. between temperatures with and without IFN- α/β treatment. G: Data are expressed as mean fold-change in titer between IFN- α/β -primed and unprimed cells at each temperature \pm SD. *** $p < 0.001$ two-way ANOVA with Tukey's multiple comparison test of log-transformed fold-change values. H-I: The procedure from (A) was repeated with RVFV at a M.O.I. of 5-10, using only 30 and 37°C temperature conditions. 24 h.p.i. supernatants were assayed for viral titer by plaque assay. H: Comparison of viral growth at 24 h.p.i. between temperatures with and without IFN- α/β treatment. I: Data are expressed as fold-change in titer between IFN- α/β -treated and untreated cells at each temperature \pm SD. * $p < 0.05$ two-tailed Student's *t* test of log-transformed fold-change values. All infections were performed in triplicate and data are representative of at least two independent experiments.

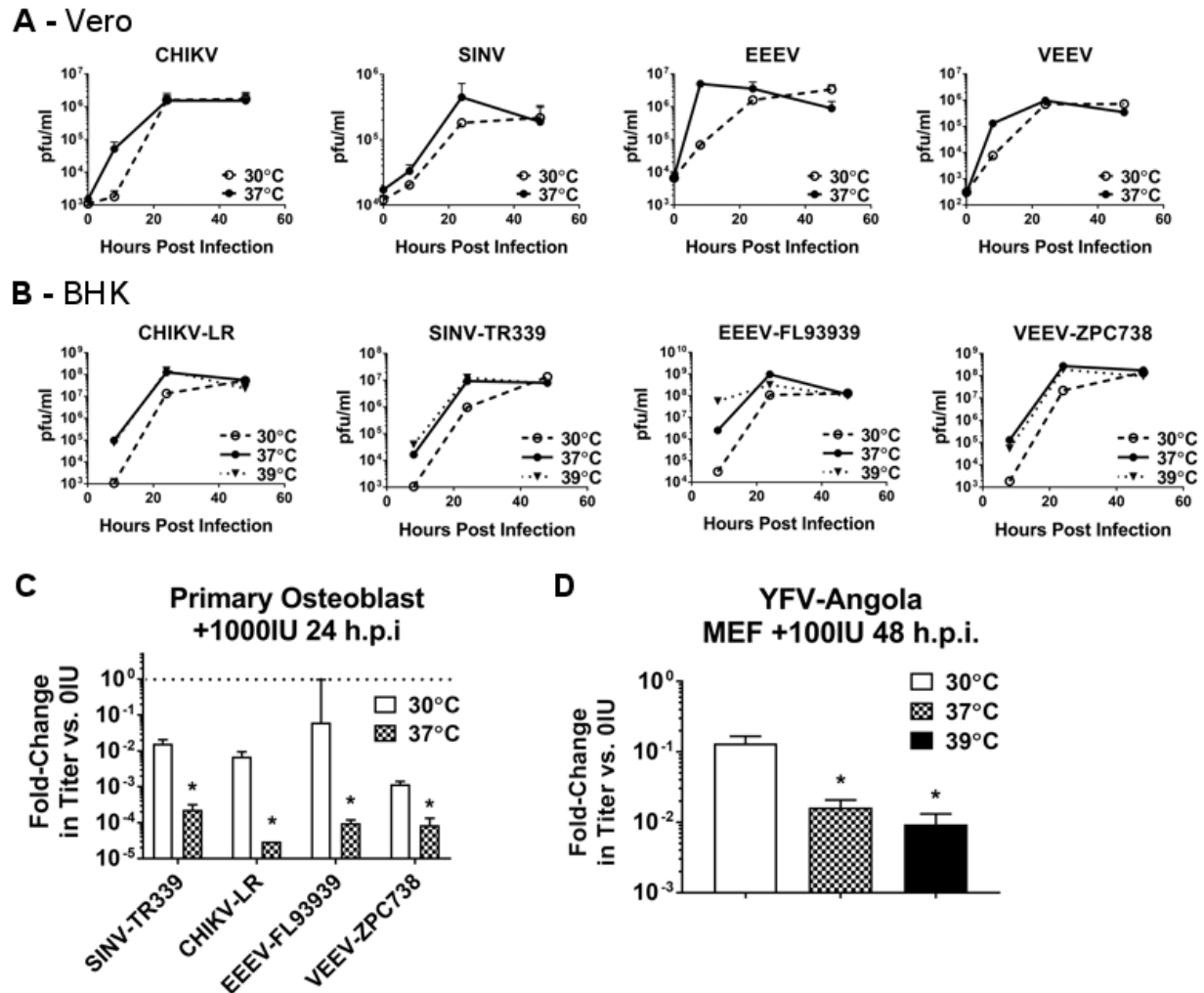


Figure 8. Efficacy of type I IFN against arboviruses is reduced at subnormal temperatures in additional cell types.

A-B: Unprimed Vero (A) or baby hamster kidney (BHK; B) cells were infected in triplicate with the indicated alphaviruses at a M.O.I. of 0.1 and incubated at 30, 37, or 39°C. At the indicated times post infection, supernatants were harvested and viral titer was determined by plaque assay on BHK cells at 37°C. C: Osteoblasts cultured from adult CD-1 mice were treated with 1000 IU/mL IFN- α/β at 30 or 37°C overnight and then infected at a M.O.I. of 0.1 with the indicated alphaviruses. 24 h.p.i. supernatants were assessed for viral titer by plaque assay at 37°C. Data are expressed as fold-change in titer between IFN- α/β -treated and untreated cells at each temperature. * $p < 0.001$ using multiple two-tailed t tests with Holm-Sidak correction of log-transformed fold-change values. D: MEFs were treated overnight with 100 IU/mL IFN- α/β at 30, 37, or 39°C and infected with YFV-Angola at M.O.I. 0.1. 48 h.p.i. supernatants were assayed for viral titer by focus-forming assay on Vero cells at 37°C. Data are presented as fold-

change in titer between IFN- α/β -treated and untreated cells at each temperature. * $p < 0.0001$ one-way ANOVA with Tukey's multiple comparison test of log-transformed fold-change values.

2.2.2 ISG protein and mRNA levels are reduced at subnormal temperatures

We hypothesized that the effect of temperature variation on IFN- α/β antiviral efficacy was most likely to result from differential expression levels of antiviral IFN-stimulated genes (ISGs). To test this, we treated cells with IFN- α/β at 30, 37, or 39°C for the time course indicated and performed western blots and qRT-PCR for protein and mRNA levels of several ISGs. STAT1, IFIT1, and ISG15 proteins were induced more slowly and to a lower peak expression level at 30°C compared to 37°C, and their expression was, in several cases, significantly increased at 39°C versus 37°C (Fig 9A-B, 10A-C). ISG mRNA expression patterns paralleled protein production at early timepoints, suggesting that temperature-dependent differences in ISG transcription efficiency contribute to differences in corresponding protein levels (Fig 9C 10D-E). However, ISG mRNA induced at 30°C did equalize to or surpass the levels induced at the higher temperatures at later times post IFN- α/β treatment, whereas protein levels did not. These data may suggest that both ISG transcription and subsequent translation are independently affected by cell temperature variation and that attenuation of both processes at 30°C contributes to the decreased magnitude of ISG production in response to IFN- α/β treatment.

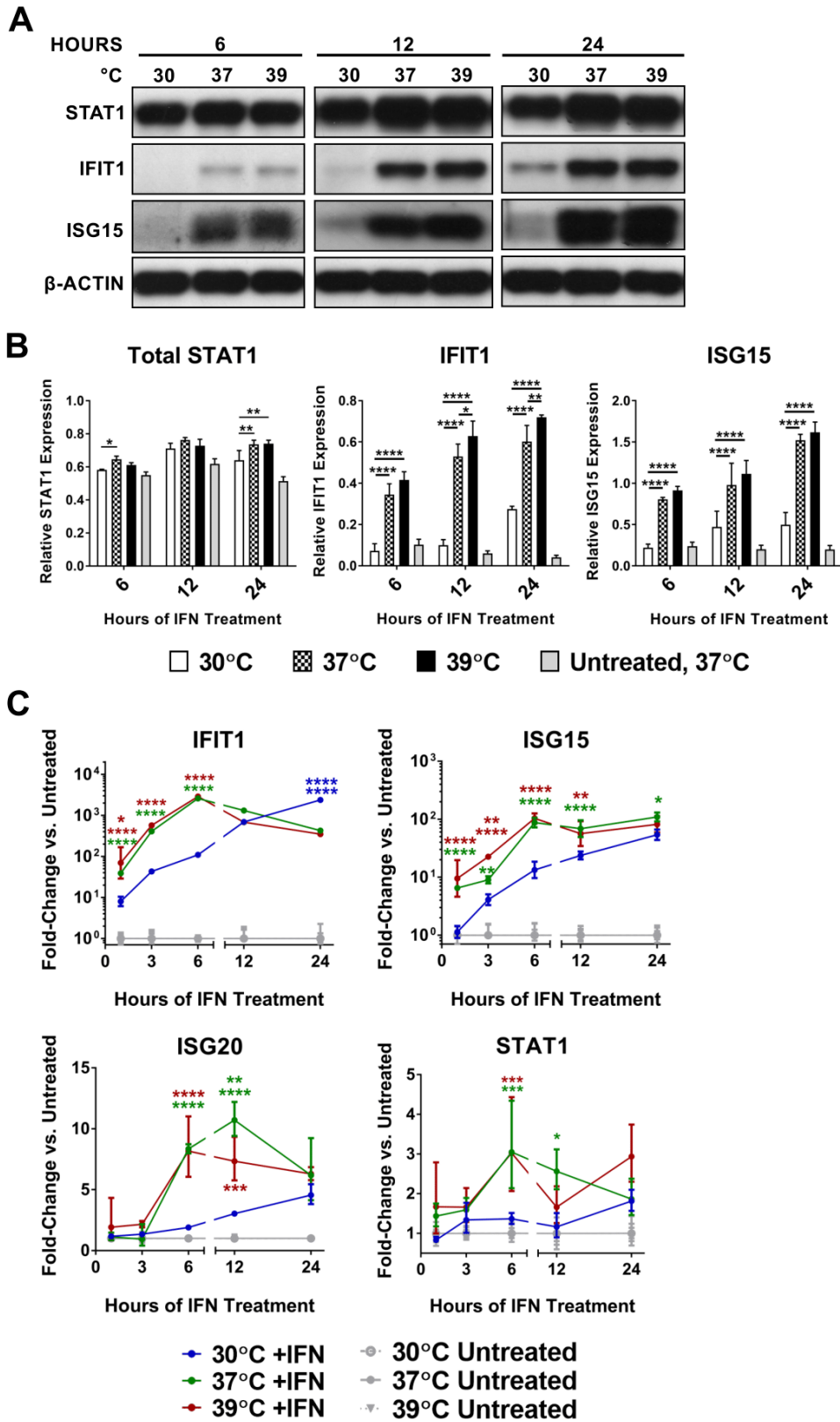


Figure 9. At subnormal temperatures, ISG protein and mRNA levels are reduced.

For all panels, Vero cells were treated with 1000 IU/mL IFN- α/β at 30, 37, or 39°C for 0-24 hours. A-B: Immunoblot of ISG protein levels (A) and corresponding densitometry quantification with ISG bands normalized to β -actin (B), presented as mean ratio of ISG to actin \pm SD. C: qRT-PCR was performed on total cellular RNA with specific primers for the indicated ISGs. Data are presented as fold-change in 18S-normalized Ct values between IFN- α/β -treated and untreated cells at each temperature \pm SD. Significance between groups is indicated with color-coordinated asterisks. For example, red and green asterisks indicate significance of 39 and 37°C results, respectively, over 30°C. Two sets of same-colored asterisks stacked over a single data point indicate significance of the results at that temperature over both others at that time point. Statistics: * $p < 0.05$, ** $p < 0.01$, *** $p < 0.001$, **** $p < 0.0001$, ns not significant by two-way ANOVA with Tukey's multiple comparison test. All experiments were done with triplicate samples and data are representative of at least two independent experiments.

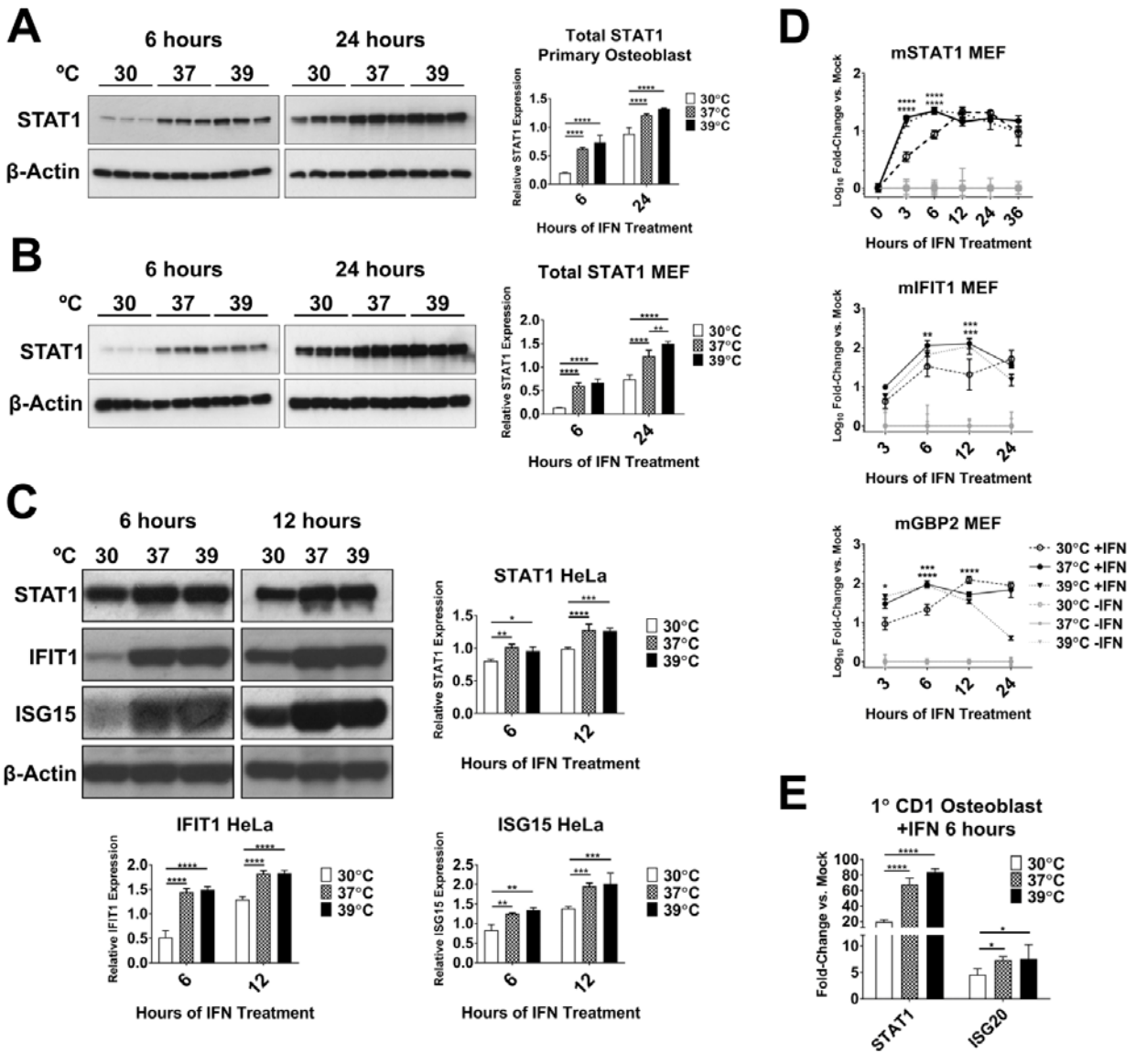


Figure 10. At subnormal temperatures, ISG protein and mRNA levels are reduced in additional cell types.

A-C: Primary CD-1 osteoblasts (A), MEFs (B), and HeLa cells (C) were treated with 100 IU/mL IFN- α/β at 30, 37, or 39°C for 6-24 hours. Lysates were analyzed for ISG protein production by immunoblot. Graphs display densitometry analysis of ISG bands at each temperature normalized to β -actin. D-E: The procedure from (A-C) was repeated and total cellular RNA was probed for ISG mRNA content by qRT-PCR. Data are presented as log₁₀ fold-change (D) or fold-change (E) between 18S-normalized Ct values for IFN- α/β -treated and untreated cells at each

temperature. Statistics: * $p < 0.05$, ** $p < 0.01$, *** $p < 0.001$, **** $p < 0.0001$, ns not significant by two-way ANOVA with Tukey's multiple comparison test.

To support this idea, we performed qRT-PCR for the gamma actin intron #3, as a proxy for basal transcriptional rate (116, 608), in cells incubated at different temperatures. We observed an approximate 2-fold decrease in intron transcript levels in cells incubated at 30°C compared to 37°C; however, raising the temperature to 39°C did not appear to influence basal transcription (Fig 11A). To test whether or not basal translation rate was also affected by temperature variation separately from effects on basal transcription, we transfected MEF cells with *in vitro*-transcribed RNAs expressing firefly luciferase (fLuc) and measured fLuc activity after 1 hour of incubation at 30, 37, and 39°C. At 30°C, fLuc reporter protein levels were slightly lower than those at 37°C, and fLuc activity was slightly increased at 39°C versus 37°C (Fig 11B). Beyond 1 hour, fLuc activity at 30°C met and surpassed the higher temperatures, and continued to rise through 6 hours post-transfection, while activity at the higher temperatures peaked and waned, indicating a defect in reporter RNA and/or fLuc protein degradation at 30°C. We confirmed this result in MEF cells lacking *Ifnar1* to rule out differential IFN- α/β responses to the reporter RNA at different temperatures accounting for this result (Fig 11B). To verify that basal translation rates vary with temperature in a native setting, we performed a [³⁵S]-methionine and -cysteine incorporation pulse-chase experiment in MEFs incubated at 30, 37, and 39°C. Equal volumes of total protein lysates were quantified by SDS-PAGE followed by autoradiography and densitometry analysis of all visible protein bands. In agreement with the fLuc reporter results, we observed an approximate 2-fold reduction in new protein synthesis at 30°C compared to the higher temperatures after 1 and 12 hours of incubation (Fig 11C). These results indicate that both basal transcription and translation are affected by cellular temperature and likely contribute to the effect of temperature variation on ISG expression.

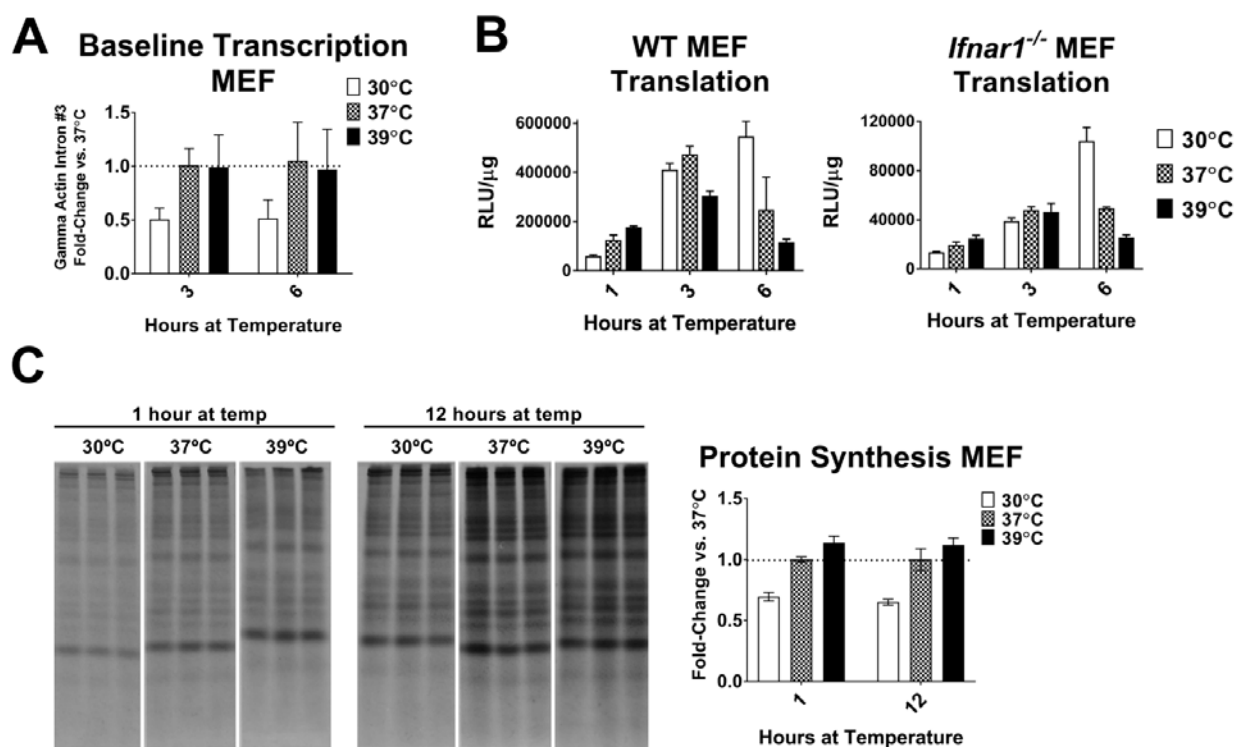


Figure 11. Temperature variation affects baseline transcription and translation rates.

A: Total cellular RNA from MEFs incubated at different temperatures were assayed for gamma actin intron #3 using qRT-PCR. Data are presented as fold-change in 18S-normalized Ct values versus 37°C. B: Wild-type or *Ifnar1^{-/-}* MEF cells were transfected with 5 µg of *in vitro*-transcribed firefly luciferase-expressing reporter RNA and divided among 30, 37, and 39°C temperature conditions for 1, 3, or 6 hours. Luciferase translation efficiency was quantified by luciferase activity assay and RLU values were normalized to total protein content determined by BCA assay. C: MEF cells were incubated at 30, 37, or 39°C for 1 or 12 hours and new protein production was marked by [³⁵S]-labeled cysteine and methionine incorporation. Lysates were separated using SDS-PAGE and total protein was quantified using autoradiography followed by densitometry analysis of all visible bands in each lane. Graph: Quantification of (C). Data are presented as fold-change versus mean protein content at 37°C at each time point.

2.2.3 Suppression of type I IFN signaling pathways is not associated with early temperature effects

In addition to the effects of temperature variation on global cellular transcription rates, we hypothesized that effects on one or more steps in the IFN- α/β signaling cascade may contribute to the temperature sensitivity of ISG transcription. IFN- α/β stimulates gene expression via activation of the JAK-STAT pathway, dependent upon the receptor tyrosine kinase activity of the IFN- α receptor complex (IFNAR1/2) and subsequent phosphorylation of primarily STAT1 and STAT2. It has been published previously that IFN-IFNAR binding characteristics do not vary significantly in the range of 30 to 37°C (609), so we decided first to examine the effect of temperature variation on the phosphorylation of STAT1 at Tyr-701. This step is mediated by the kinase Jak1 at the receptor complex and is required for assembly of the transcription factor complex ISGF3, which stimulates ISG transcription in the nucleus [reviewed in (325)]. Cells treated with IFN- α/β at 30, 37, or 39°C for 30 minutes showed similar levels of phosphorylated STAT1 (STAT1-p Tyr-701) by immunoblot (Fig 12A, 13A-B). By 60 minutes of IFN- α/β treatment, STAT1-p levels remained elevated in the 30°C samples but decreased at the higher temperatures (Fig 12A, 13B). Because phosphorylated STAT1 is required for ISG transcription, these findings did not fit with the attenuation of ISG transcription we observed at 30°C (Fig 9C, 10D-E). We reasoned that despite efficient phosphorylation of STAT1 at 30°C, its nuclear translocation might be negatively affected and result in less activated STAT1 in the nucleus available for ISG transcription. To test this, we examined the efficiency of STAT1-p Tyr-701 migration into the nucleus at different temperatures using confocal microscopy. In agreement with total STAT1-p levels, but in contrast to the observed effect on ISG transcription, IFN- α/β treatment of cells at 30°C resulted in significantly higher average content of STAT1-p per

nucleus compared to 37°C and 39°C by 30 minutes of IFN- α/β stimulation (Fig 12B, 13C). Furthermore, we noted similar levels of STAT1 phosphorylated at Ser-727, a modification required for maximal transcriptional activity of STAT1 that occurs in the nucleus, at all temperatures at 1-hour post-IFN- α/β (Fig 12C, 13D). Interestingly, late after IFN- α/β treatment, levels of STAT1-p Tyr-701 at 37 and 39°C were significantly increased over those at 30°C, indicating a potential mechanism for greater sustenance of the response at higher temperatures and (Fig 12D). This finding could perhaps be a consequence, in part, of the increased level of total STAT1 present at the higher temperatures compared to 30°C at this timepoint (Fig 9A-B).

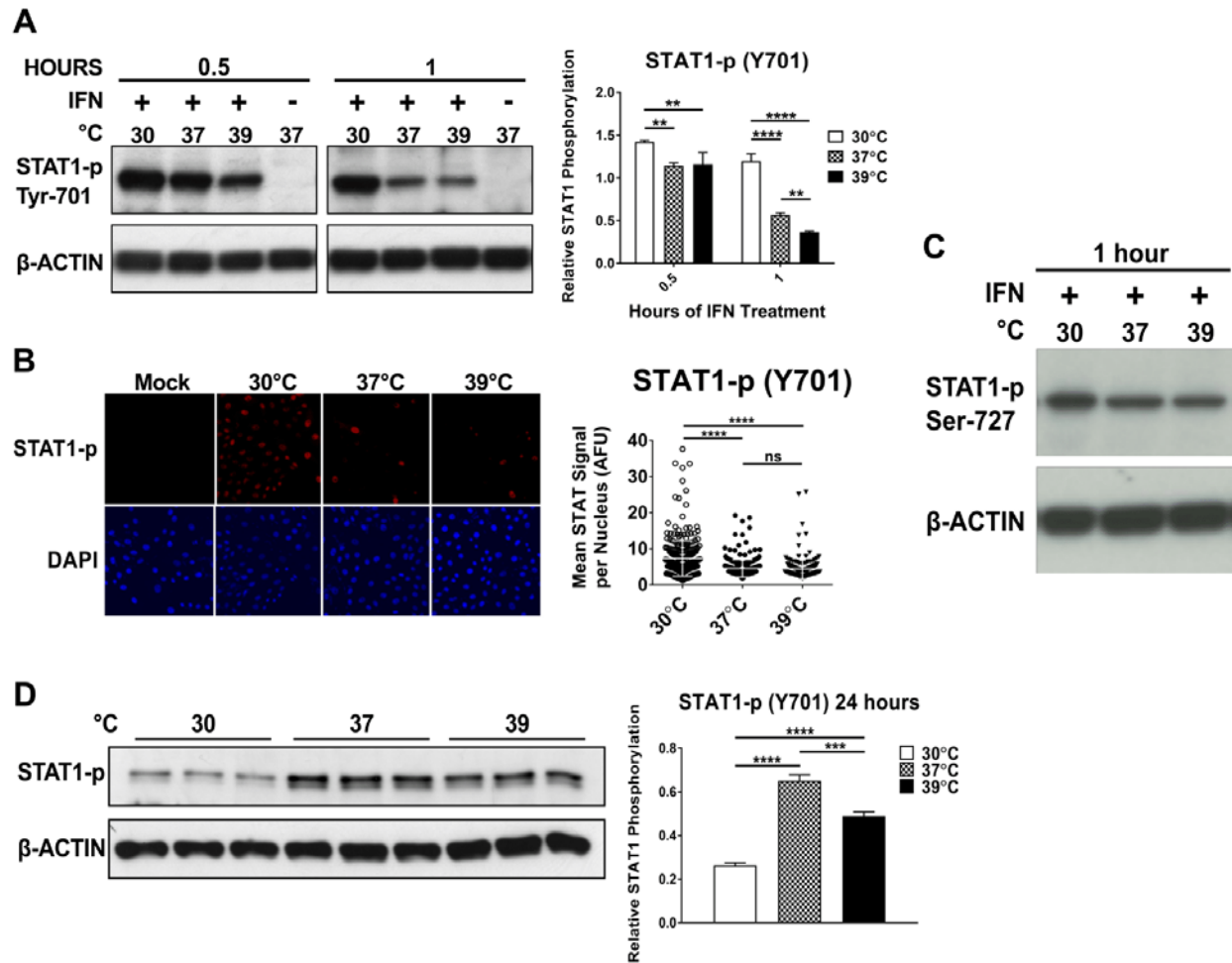


Figure 12. Suppression of type I IFN signaling pathways is not associated with early temperature effects.

A, C, and D: Immunoblot of STAT1 phosphorylated at Tyr-701(A and D) or Ser-727 (C) from Vero cells treated with 1000 IU/mL IFN- α/β at 30, 37, or 39°C and corresponding densitometry quantification with STAT1-p bands normalized to β -actin. Data are presented as mean STAT1-p/actin ratio \pm SD. B: Vero cells treated with 1000 IU/mL IFN- α/β for 30 minutes at 30, 37, or 39°C were subjected to immunocytochemistry staining for STAT1-p (Y701). Confocal imaging shows phosphorylated STAT1 nuclear translocation. Graph displays average nuclear STAT1-p signal intensity per imaged nuclear area at each temperature. At least 199 cells/nuclei were analyzed in each temperature group. Statistics for A: ** $p < 0.01$, **** $p < 0.0001$ two-way ANOVA with Tukey's multiple comparison test. Statistics for B and D: *** $p < 0.001$, **** $p < 0.0001$, ns not significant by one-way ANOVA with Tukey's multiple comparison test. All experiments were done with triplicate samples and data are representative of at least two independent experiments.

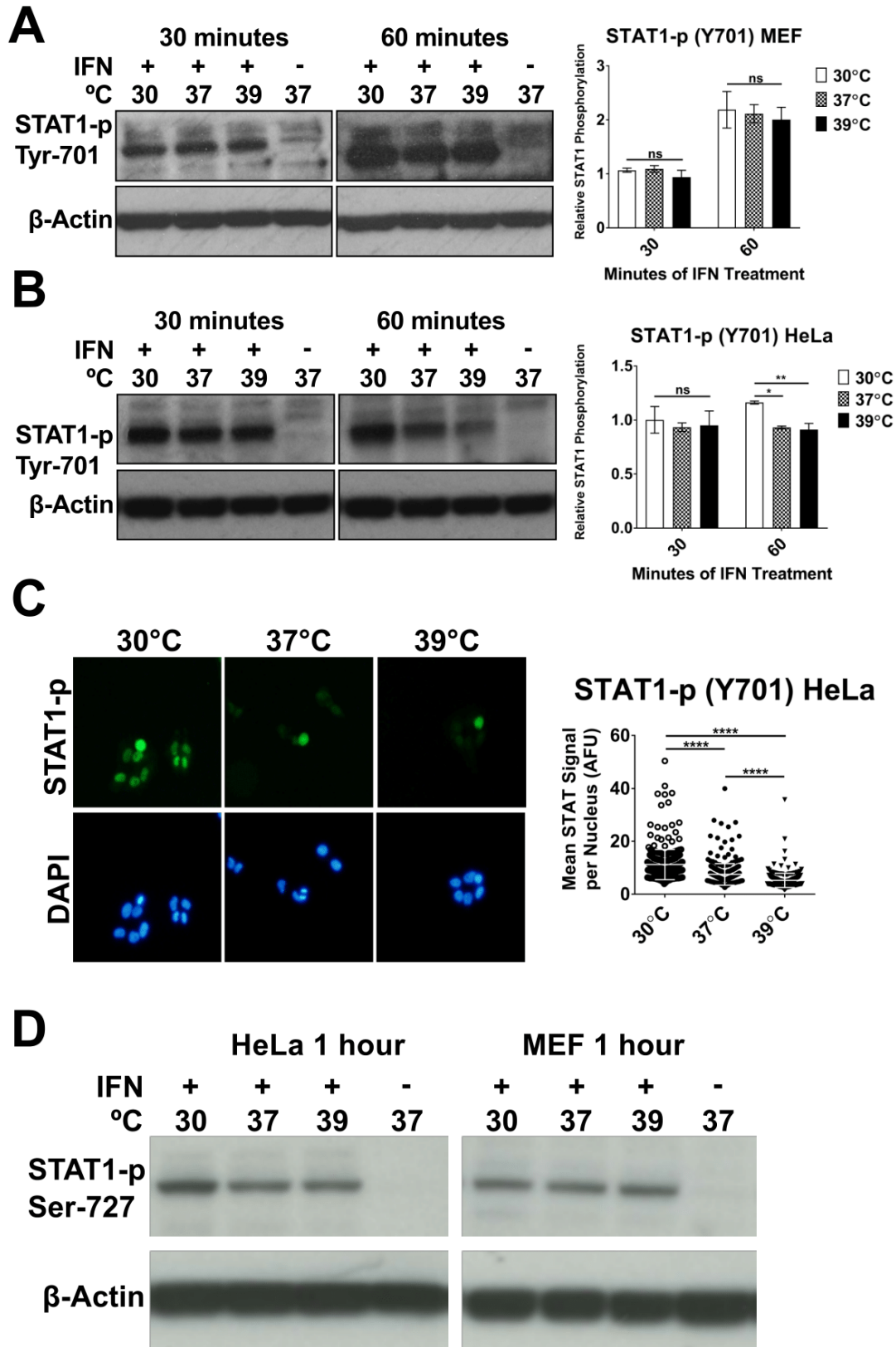


Figure 13. Suppression of type I IFN signaling pathways is not associated with early temperature effects in additional cell types.

A, B, and D: MEF and HeLa cells were treated with 100 IU/mL IFN- α/β for 30 or 60 minutes at 30, 37, or 39°C and lysates were probed for STAT1 phosphorylated at Tyr-701 (A-B) or Ser-727 (D) by immunoblot. Graphs display densitometry analysis of STAT1-p bands normalized to β -actin at each temperature. Statistics for A and B: * $p < 0.05$, ** $p < 0.01$, *** $p < 0.001$, **** $p < 0.0001$, ns not significant by two-way ANOVA with Tukey's multiple comparison test. C: HeLa cells treated with 1000 IU/mL IFN- α/β for 30 minutes at 30, 37, or 39°C were subjected to immunocytochemistry staining for STAT1-p (Y701). Confocal imaging shows phosphorylated STAT1 nuclear translocation. Graph displays average nuclear STAT1-p signal intensity per imaged nuclear area at each temperature. **** $p < 0.0001$ one-way ANOVA with Tukey's multiple comparison test.

2.2.4 Transcription of IFN response pathway genes is highly temperature-dependent

Because the IFN- α/β signaling pathway upstream of ISG transcription was not attenuated by subnormal cellular temperature, we decided to focus more closely on the effect of temperature variation on ISG transcription. Specifically, we examined whether or not ISG mRNA induction was unique in its temperature sensitivity compared to other inducible and constitutively-expressed genes, or if this phenotype might be solely attributable to a slowdown in global transcription rates. We performed direct mRNA quantification analysis via the NanoString platform on total RNA derived from MEF cells treated at 30, 37, or 39°C with IFN- α/β or lipopolysaccharide (LPS) for 3-12 hours. NanoString is a high-throughput mRNA quantification method that utilizes fluorescently-barcoded hybridization probes to simultaneously detect and count hundreds of distinct mRNA species in a given sample. Our multiplexed gene target panel included a variety of inducible genes from each stimulus, as well as signaling intermediates, feedback and regulatory genes, and cell homeostatic components such as transcription and

translation factors (see Table 2 for a complete list of target genes). Most constitutive genes were not appreciably affected by changing temperature or the addition of either stimulus (data not shown), including genes selected for normalization (Fig 14A). Expression of known temperature-responsive genes, including the cold-inducible CIRP and RBM3, and the heat-inducible HSP70, displayed the expected temperature-dependent patterns, but expression was not influenced by IFN- α/β or LPS treatment (Fig 14B). Gamma actin intron #3 levels also followed the temperature-sensitive trend we observed in our qRT-PCR assays (Fig 14C). These results combine to validate the NanoString platform as a reliable method for quantitating the effect of temperature variation on gene expression.

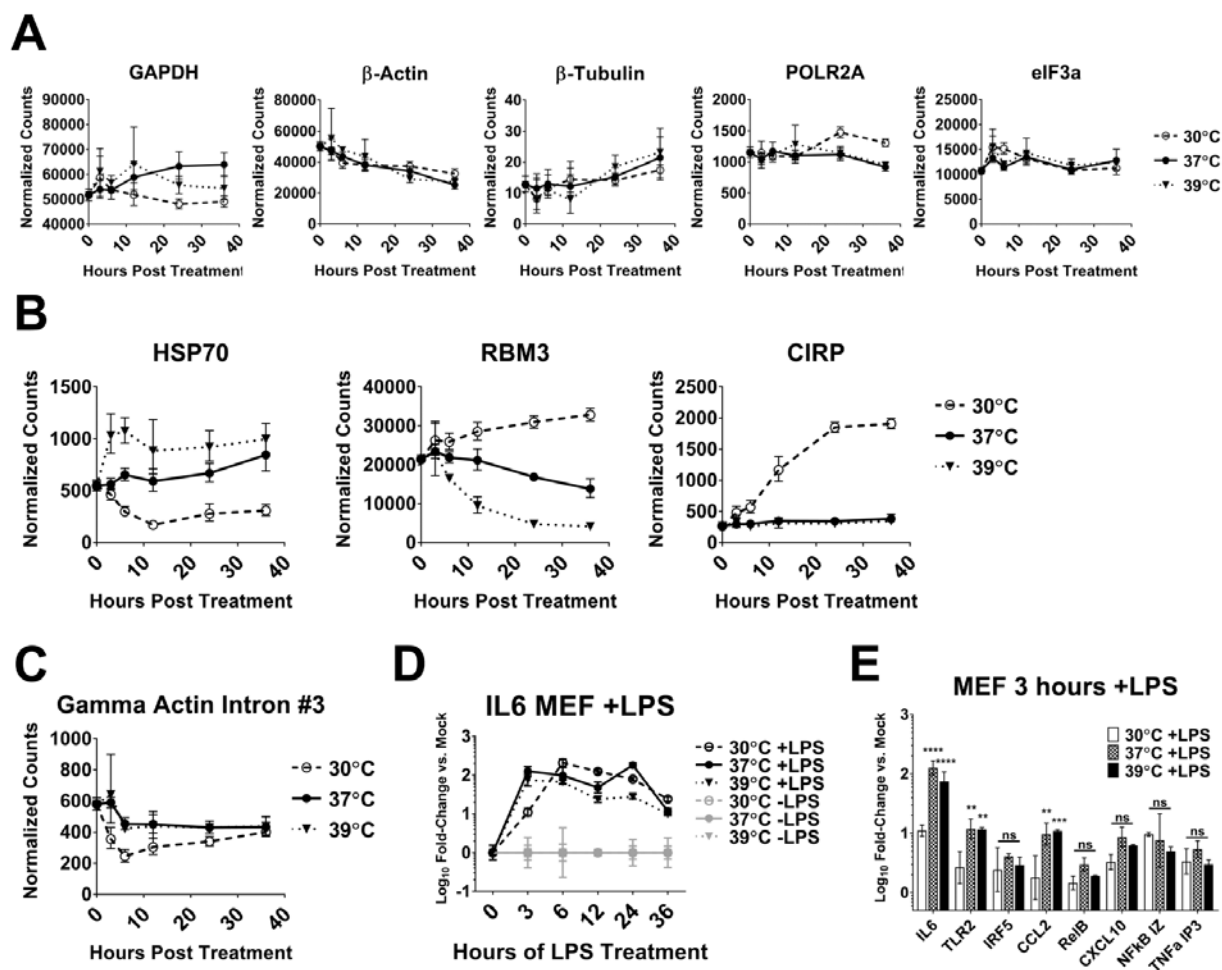


Figure 14. NanoString analysis detects temperature-sensitive gene transcription.

MEF cells were treated in with 100IU IFN- α/β or 250 ng/mL LPS, or were left untreated, at 30, 37, or 39°C for the time course indicated in duplicate samples. At each time point, total cellular RNA was harvested and subjected to direct mRNA quantification of 125 gene targets (see Table S2) using the NanoString platform. Raw mRNA counts in each sample were subject to background subtraction followed by normalization to the geometric mean of five normalization genes (B-actin, GAPDH, B-Tubulin, POLR2A, and eIF3a) in the same sample. A: Background-subtracted mRNA count values of the five genes used for normalization, with IFN- α/β - or LPS-stimulated and unstimulated samples pooled at each temperature. B: Normalized expression profile of three known temperature-responsive genes, with IFN- α/β - or LPS-stimulated and unstimulated samples pooled at each temperature. C: Gamma actin intron #3 expression. D: IL6 expression in LPS-treated MEFs in an independent experiment, quantified by qRT-PCR. E: Verification of expression of other LPS-responsive genes in MEFs at 3 hours post-LPS treatment in an independent experiment, quantified by qRT-PCR.

Figure 15A shows the fold-induction of IFN- α/β -responsive genes at 30, 37, and 39°C versus temperature-matched mock-treated samples at 3, 6, and 12 hours post IFN- α/β treatment, respectively. Panel B shows analogous results for LPS-treated cells. Only genes upregulated at least 2-fold over mock at any temperature are shown and included in subsequent analyses. After 3 hours of stimulation with IFN- α/β or LPS, both IFN- α/β -induced and LPS-induced genes displayed similar patterns of temperature-sensitive expression in general, with optimal induction at 37°C or 39°C and dramatically reduced induction at 30°C (Fig 15A-B). Upon closer examination, however, differences became apparent. Most ISGs in our panel displayed decreased expression at 30°C compared to 37°C far below the 2-fold decrease in basal transcriptional rate that we observed (Fig 11A, 14C), indicating that the temperature sensitivity of ISG transcription may be attributable to additional mechanisms. Although this was also true of some LPS-inducible genes, there were several examples (IKBA, NFKBIZ, and TNFAIP3) upon which temperature variation seemed to have little or no effect (Fig 15B). These results contrasted with the reliable temperature sensitivity of all ISGs in the panel. In addition, induction kinetics varied between ISGs and LPS-induced genes throughout the rest of the time course. For LPS-induced genes, apart from known ISGs also induced by LPS (GBP1, GBP2), expression in the 30°C group matched or exceeded expression at the higher temperatures by just 6 hours of LPS treatment (Fig 15B-C). At 30°C in IFN- α/β -treated cells, by contrast, ISG induction remained significantly lower than at higher temperatures until 12 hours of IFN- α/β treatment (Fig 15C). These differences in gene induction by LPS and IFN- α/β at different temperatures could indicate gene- or pathway-specific responses to changing cellular temperature beyond simple changes to basal transcriptional rates.

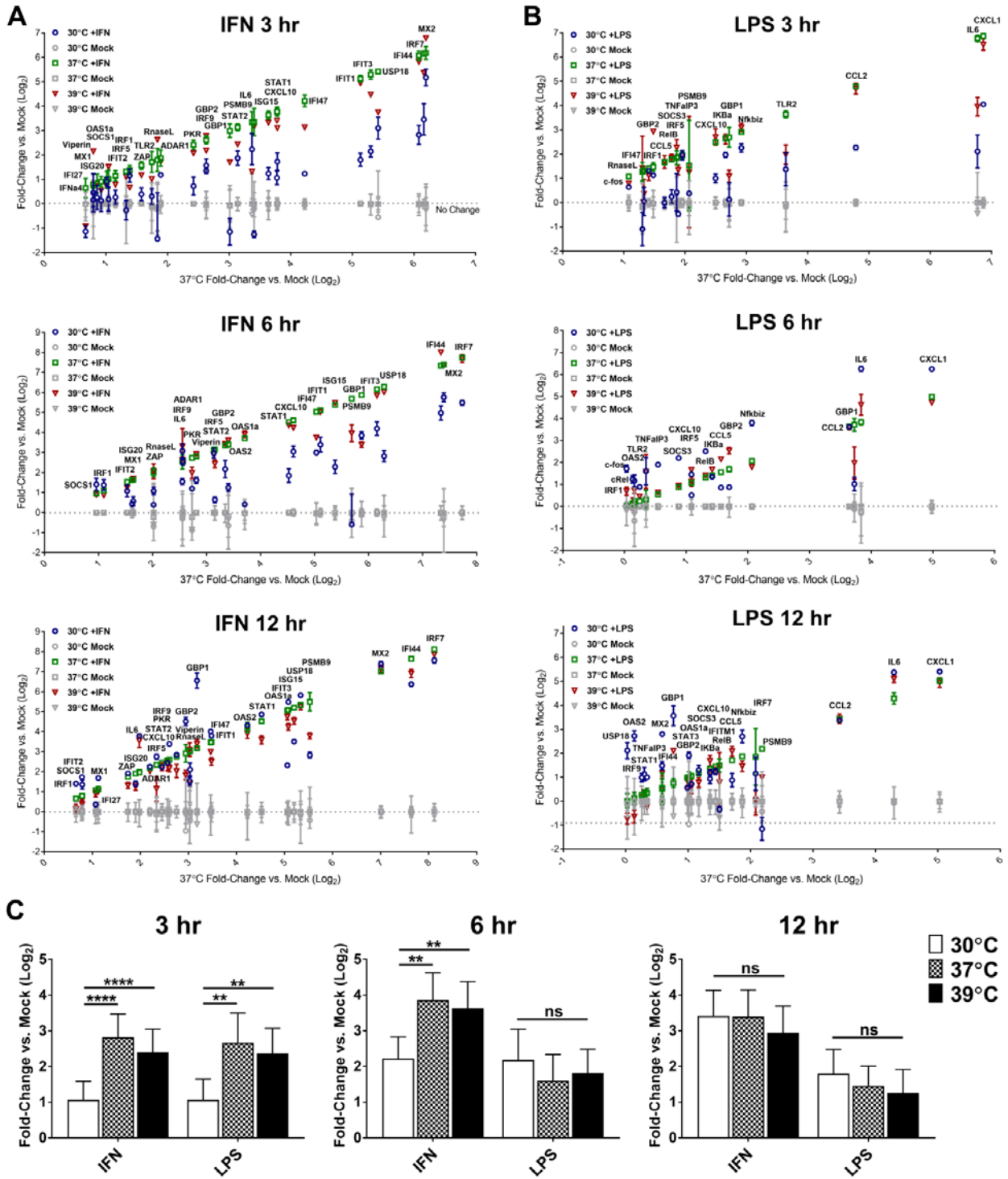


Figure 15. Transcription of IFN response pathway genes is highly temperature-dependent.

NIH/3T3 MEF cells were treated with 100IU IFN- α/β or 250 ng/mL LPS, or were left untreated, at 30, 37, or 39°C for the time course indicated in duplicate samples. At each time point, total cellular RNA was harvested and

subjected to direct mRNA quantification of 125 gene targets (see Table S2) using the NanoString platform. Raw mRNA counts in each sample were subject to background subtraction followed by normalization to the geometric mean of five normalization genes (B-actin, GAPDH, B-Tubulin, POLR2A, and eIF3a) in the same sample. A-B: Genes upregulated at least 2-fold in treated cells versus mock at any temperature are shown as log₂ mean fold-change of duplicate samples versus mock. Genes are ordered along the x-axis by log₂ fold-change in expression at 37°C. C: Bar graphs show geometric mean ± SD of ≥2-fold upregulated genes at each temperature at each time point. Statistics: **p<0.01, ****p<0.0001, ns not significant by Mann-Whitney rank test.

2.2.5 Reduced temperature also affects type I IFN induction

Thus far, our studies have focused on the effect of temperature variation on the signaling/effector phase of the IFN- α/β response. However, as the effector phase is preceded by the IFN- α/β inductive phase in response to infection *in vivo*, it is relevant to examine the effect of temperature in this context as well, as IFN- α/β efficacy *in vivo* depends concurrently on both phases. It has been published previously that IFN- α/β induction by rhinovirus is diminished at the subnormal temperatures of airway epithelial cells, which could contribute to enhanced rhinovirus fitness in the upper airways (577). To avoid temperature-dependent differences in viral replication that could influence IFN- α/β production, we electroporated poly-I:C into MEFs and then incubated the cells at 30, 37, or 39°C. We observed the earliest detectable IFN- α/β activity in cell supernatants from the 39°C samples, and IFN- α/β activity remained highest at this temperature throughout the time course (Fig 16A). IFN- α/β induction at 37°C was slightly but significantly reduced compared to 39°C at early time points, but still far exceeded levels of IFN- α/β produced 30°C, which did not surpass the limit of detection until 8 hours post transfection (Fig 16A). We also performed qRT-PCR analysis for *Ifna4*, *Ifnb*, and *Ifit1* mRNAs and found a similar trend in temperature dependent expression at early time points (Fig 16B). Interestingly,

while transcript levels of the IFN- α/β genes fell dramatically at the higher temperatures by 8 hours post poly-I:C, they continued to rise at 30°C (Fig 16B); however, this did not correspond to increased secreted IFN- α/β at this temperature (Fig 16A), suggesting that translation suppression and/or attenuation of the secretory pathway may also play a role in temperature-dependent IFN- α/β induction.

The IFN- α/β genes are downstream targets of IRF3, which is activated in response to polyI:C, therefore, we examined IRF3 activation by western blot for IRF3 phosphorylated at Ser-396 (IRF3-p). Temperature variation had no impact on levels of IRF3-p initially, but surprisingly, IRF3-p levels were maintained at 30°C through 6 hours post-stimulation, while all but disappearing at the higher temperatures (Fig 16C). In the same samples, however, IFIT1, which is directly IRF3-inducible (279), was much more highly expressed at 37 and 39°C compared to 30°C (Fig 16C). These results underline the discrepancy between activation of the IFN- α/β induction pathway and functional IRF3 responsive gene expression and highlight differences in gene transcription and translation as the major mediators of the effects of temperature variation on these pathways.

The above experiments served to examine the effect of temperature variation on the cytosolic IFN- α/β induction pathway with equal initial stimulation of the pathway at all temperatures (i.e. an equal dose of the nonreplicating poly-I:C). However, this does not accurately represent the context of a viral infection, in which differences in viral replication rates at different temperatures could lead to variation in pathway stimulation and likely compound the effect of temperature on IFN- α/β induction that we observed with poly-I:C. To verify that viral infection at different temperatures also stimulates differential IFN- α/β induction, we infected cells at 30°C for the first hour to allow equal attachment and entry. After washing, infected wells

were divided among 30, 37, and 39°C temperature treatments for 12 to 24 hours, at which times supernatants were collected and assayed for IFN- α/β activity as described in Materials and Methods. Infections of MEF cells required the use of mutant viruses whose transcription and translation inhibitory mechanisms have been disabled (SINV-nsP2-726G (Fig 16D) and VEEV-CD/nsP2-739L (Fig 16E)) (116). However, we also tested a wild-type alphavirus, SINV-TR339 (Fig 5F), in the murine monocyte/macrophage RAW 264.7 cell line, which, unlike MEFs, can still produce IFN- α/β upon wild-type alphavirus infection. Unlike the results with poly-I:C, we observed greatest IFN- α/β activity from the 37°C infections, and IFN- α/β levels produced at 39°C either did not differ from or were significantly lower than those observed from the 37°C treatment (Fig 16D-F). In agreement with the poly-I:C results, however, viral infection at 30°C resulted in greatly delayed and stunted IFN- α/β production (Fig 16D-F). Surprisingly, viral titers did not vary appreciably between temperatures, in general, indicating that differences in pathway stimulation may not have contributed much to differences in IFN- α/β output in this context. Viral growth at any temperature did not seem to be impacted by IFN- α/β induction by 24 h.p.i., which may be explained by the fact these viruses are competent for some inhibition of downstream IFN- α/β signaling in MEFs. The exception was SINV-nsP2-726G at 39°C, which did suffer some inhibition compared to the other temperatures, a possible indication of the increased efficacy of IFN- α/β at 39°C apparent against this virus. Importantly, these results demonstrate that IFN- α/β induction is also sensitive to temperature variation, and that a viral infection occurring at subnormal temperatures may benefit both from diminished detection and IFN- α/β induction, and from reduced ISG upregulation leading to a weakened antiviral state relative to higher temperatures. Combined, these two factors may create an environment in which the virus can replicate uninhibited by the IFN- α/β response long enough to produce IFN- α/β antagonists,

which could then combat subsequent IFN- α/β -mediated restriction, an interplay that could be particularly relevant *in vivo*.

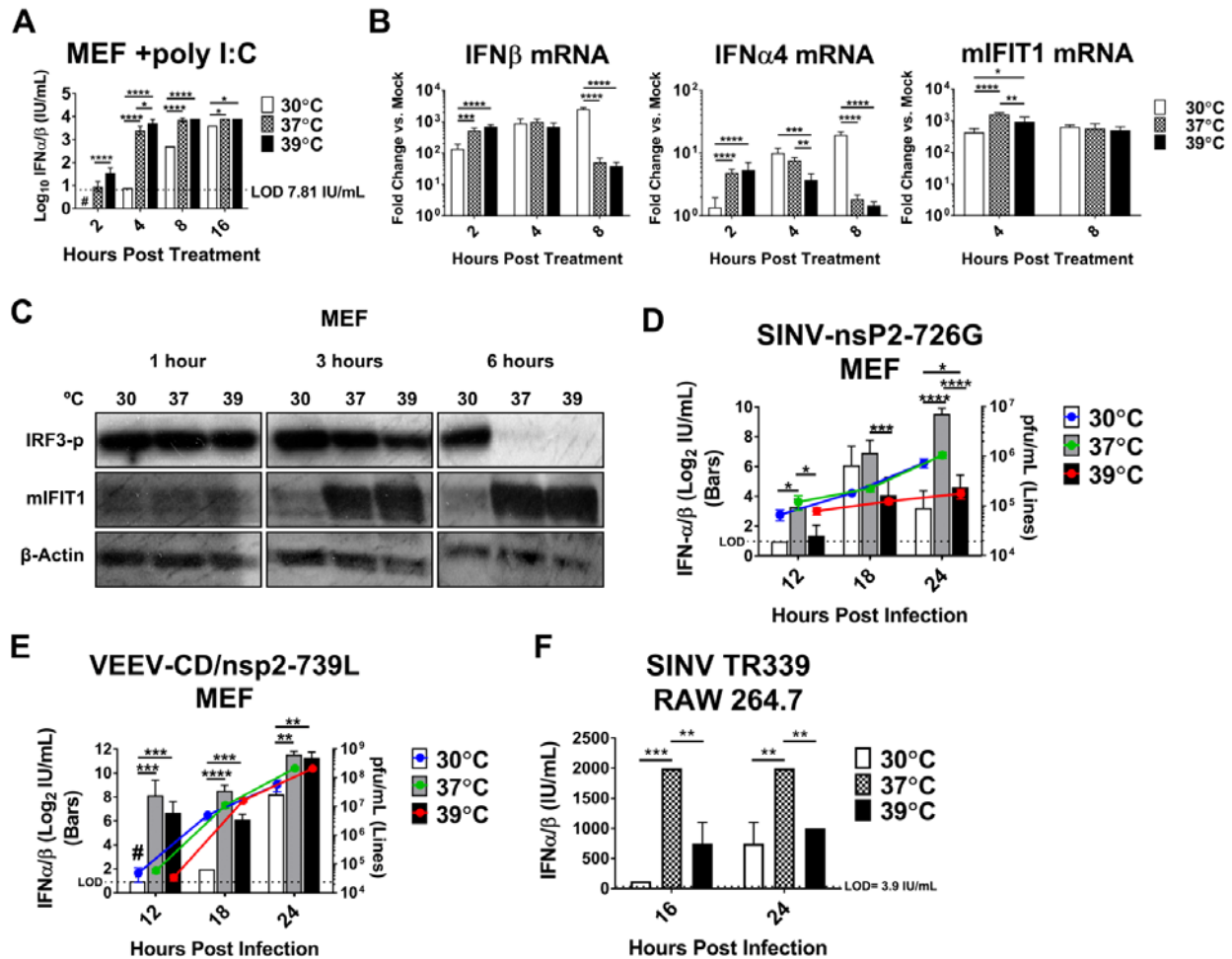


Figure 16. Reduced temperature also affects IFN- α/β induction.

A-C: MEFs were transfected with 50 μ g polyI:C per million cells using electroporation. Pooled transfections were then divided among 30, 37, and 39 $^{\circ}$ C temperature conditions. A: Supernatants were assayed for biologically active IFN- α/β as described in the Materials and Methods. Data are presented as log₁₀ mean IU/mL \pm SD. B: qRT-PCR was used to quantify IFN- α/β and IFIT1 mRNA induction. Data are presented as mean fold-change in 18S-normalized Ct values in polyI:C-treated versus untreated cells at each temperature \pm SD. C: Immunoblot of IRF3 phosphorylated at Ser-396 and IFIT1 from polyI:C-treated MEF lysates. D-F: Supernatants from virus-infected MEFs or Raw 264.7 cells were assayed for IFN- α/β as in A. IFN- α/β induction data are presented on the left Y-axis

as \log_2 mean IU/mL \pm SD. Statistics: * p <0.05, ** p <0.01, *** p <0.001, **** p <0.0001, ns not significant by two-way ANOVA with Tukey's multiple comparison test of log-transformed IU/mL values. Viral titer data for (D) and (E) was determined by plaque assay on BHK cells at 37°C from the same supernatants assayed for IFN- α/β activity and is presented along the right y-axis of those panels, \pm SD. # indicates the result was below the limit of detection of the assay. All experiments were done in duplicate or triplicate, and results shown are representative of at least two independent experiments.

2.2.6 Lower temperatures *in vivo* suppress IFN- α/β responses

To test the possibility that temperature variation might affect the pathogenesis and disease outcomes of a relevant infection *in vivo*, we adapted the C57BL/6 adult murine model of CHIKV infection and musculoskeletal disease (MSD) (183) to include systemic body temperature reduction. One of two strategies was used to achieve core temperature reduction depending on the experimental setup: either induction of metabolic torpor, a prolonged state of inactivity and energy conservation that attenuates heat-generating mechanisms (610), or administration of the small molecule reserpine (RES), which depletes peripheral monoamine neurotransmitters by antagonizing the vesicular monoamine transporter (VMAT), leading to dysregulation of temperature regulatory mechanisms (611, 612). Both methods effectively reduced mouse subcutaneous (scruff) temperature in both wild-type C57BL/6 (B6) and IFNAR1^{-/-} (AB6) mice (Fig 18). For assessing the effect of reduced temperature on CHIKV-induced MSD, torpid and normal mice were infected in the left rear footpad and cross-sectional area was measured daily to track foot swelling. In wild-type mice, torpor induction resulted in significantly greater MSD between 6 and 8 days post infection, whereas in IFNAR1^{-/-} AB6 animals, MSD was slightly reduced by torpor (Fig 17A). These results suggest that the effect of reduced body temperature

on CHIKV-induced disease signs manifests in an IFN- α/β -dependent manner, with low temperature leading to more severe disease only when functional IFN- α/β is present.

Next, we used RES treatment to extend the duration of temperature reduction and examine viral growth kinetics using a nanoluciferase-expressing CHIKV (613) and *in vivo* imaging. In B6 mice, viral signal in both the infected (ipsilateral) and contralateral footpads rose similarly over time between RES-treated and normal animals until 3 days post infection, beyond which signal in the RES-treated group increased significantly over the signal in the warm group (Fig 17B). An opposite trend was observed in AB6 mice, with viral signal in RES-treated animals significantly lower than in the warm mice for the entire course of infection, until the mice were about to succumb to the infection (Fig 17B). In addition, viral titers from dissected tissues were not significantly different between normal and torpid B6 mice at 2 d.p.i., but remained high in the infected footpad and spleen of the torpid mice by 6 d.p.i., indicating dysfunctional viral clearance in those tissues at reduced temperature (Fig 17C). Finally, torpid mice failed to induce a robust serum IFN- α/β response at 2 days post-CHIKV infection compared to normal mice, suggesting that impaired IFN- α/β inductive pathways *in vivo* at low temperatures likely contribute to the observed effects on CHIKV infection (Fig 17D), although kinetic differences in virus replication brought on by the altered temperatures may have contributed to this result.

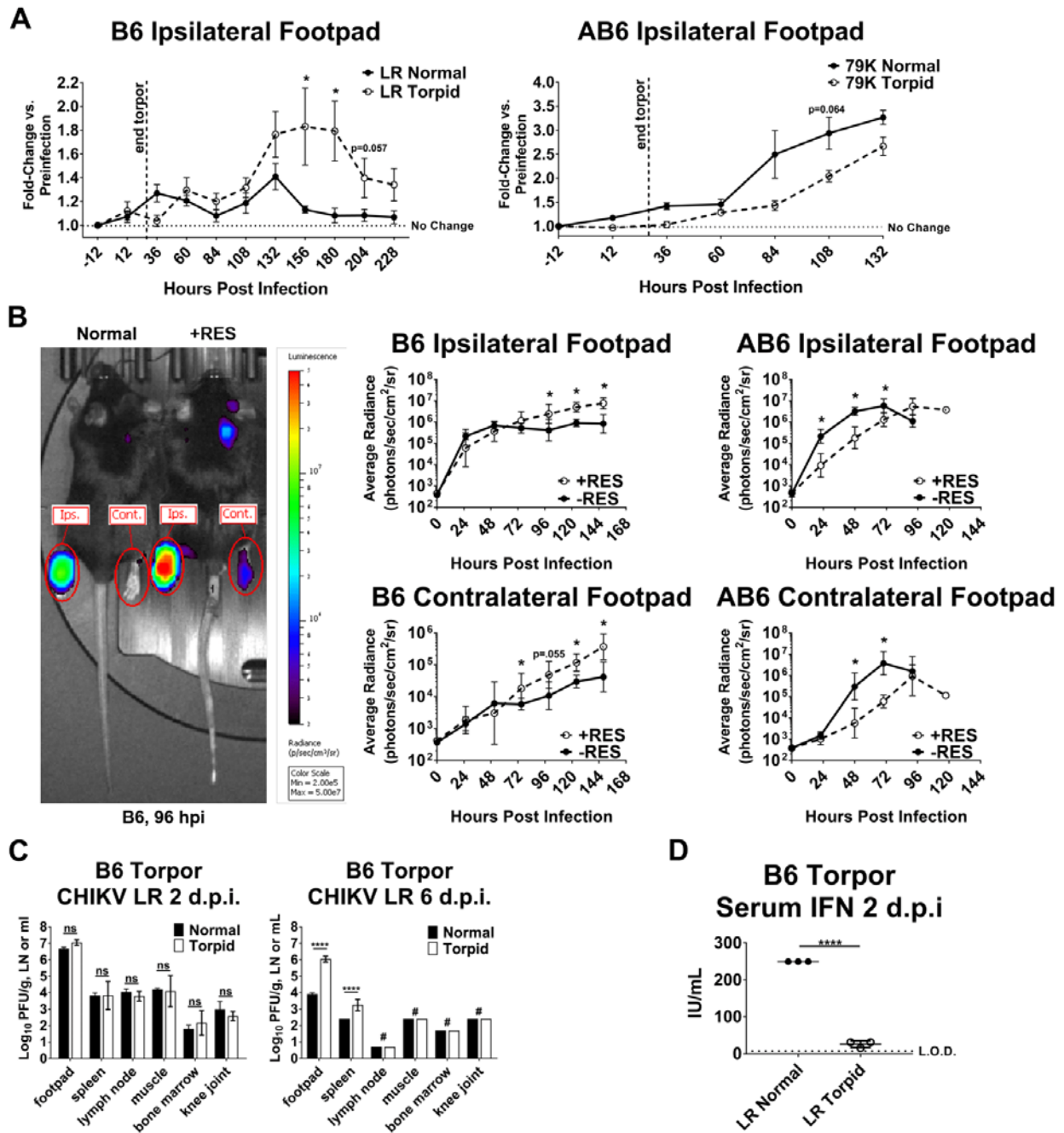


Figure 17. Lower temperature *in vivo* suppresses IFN- α/β responses.

A: Core temperature reduction in 6-week-old C57BL/6 mice and *Ifnar1*^{-/-} AB6 mice was achieved by induction of metabolic torpor. Torpid and normal mice were then infected in the left hind footpad with 1000 p.f.u. of wild-type CHIKV-LR (B6 mice) or the attenuated variant CHIKV-LR-E279K (AB6 mice). Virus-induced musculoskeletal disease was quantified daily by manual caliper measurement of footpad width and thickness to determine cross-

sectional area. Data are presented as fold-change in infected footpad cross sectional area versus pre-infection area \pm SEM. B: Mouse core temperature reduction was induced with intraperitoneal administration of reserpine approximately 3 hours prior to infection as in (A) with 1000 p.f.u of CHIKV-LR-nluc TaV and viral replication was tracked over time using *in vivo* imaging. Data are presented as the geometric mean of average footpad radiance in each group \pm geometric SD. Statistics for A and B: * $p < 0.05$ Mann-Whitney rank test at individual time points. C: Tissues from CHIKV-LR infected normal and torpid B6 mice were assayed for viral load by plaque assay at day 2 and day 6 post infection. Data shown are mean viral titer \pm SD. **** $p < 0.0001$, ns not significant by two-tailed Student's *t* test of log-transformed titer values. # indicates titer was below the limit of detection. D: Serum from CHIKV-LR infected normal and torpid B6 mice was assayed for biologically active IFN- α/β as described in the Materials and Methods. Data are shown as mean IU/mL \pm SD. **** $p < 0.0001$ by two-tailed Student's *t* test. For all experiments, $n = 3-6$ mice per group and data are representative of at least two independent experiments.

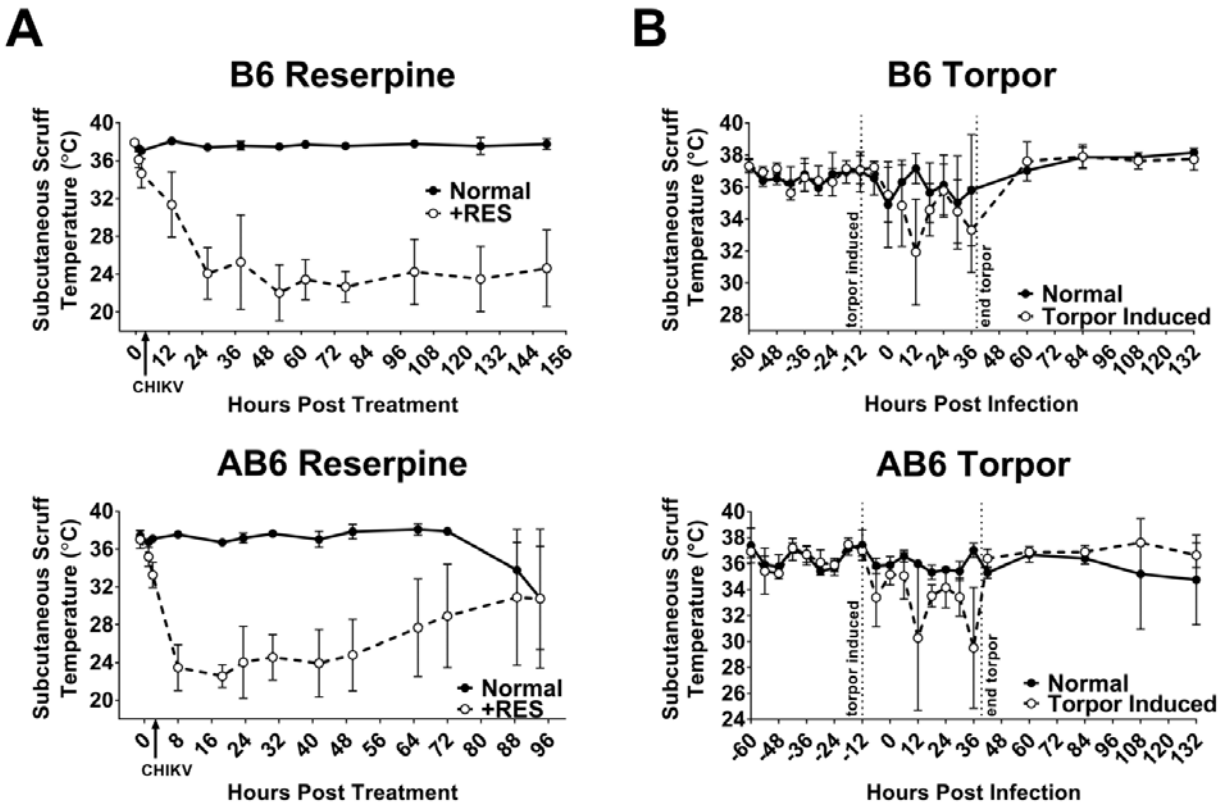


Figure 18. Torpor and reserpine treatment reduce mouse core temperature.

Mice were implanted subcutaneously in the scruff with temperature transponders (BMDS) prior to administration of reserpine (A) or induction of metabolic torpor (B) as described in the Materials and Methods. Temperature was monitored regularly throughout the course of all experiments, and graphs represent the typical temperature profiles of reserpine-treated or torpid animals versus normal.

2.3 DISCUSSION

Historically, studies of the IFN- α/β response have largely relied on genetic knockout strategies to examine the roles of individual mediators and effectors in various infection and disease models. However, there is a growing body of literature focused on intact innate immune mechanisms within the variable physiological contexts in which they operate *in vivo* and how this variability may affect efficacy (577, 579, 588, 591, 592, 594, 614-616). The results presented here indicate that ambient temperature can have broad impacts on the effectiveness of the mammalian IFN- α/β antiviral response. Many human pathogens, such as respiratory viruses, and other pathologies, such as certain malignancies (575), cause disease in tissues regularly exposed to temperatures below the normal core temperature of 37°C and may take advantage of a weakened innate immune environment. In these studies, we examined whether or not arboviruses, which are replication-competent across a wide range of temperatures due to their evolution in both arthropod vectors and mammalian or avian hosts, represented another type of pathogen capable of subverting IFN- α/β responses occurring at subnormal temperatures. *In vitro*, we found that arboviruses representing three distinct viral families had increased fitness at 30°C relative to 37°C, but only when cells had been pretreated with IFN- α/β at each temperature. Without IFN- α/β present, lowered temperature conferred no advantage to viral replication. These findings parallel trends observed with human rhinovirus (RV) and influenza virus (577, 588), although

the increased fitness of RV at low temperature is attributable to additional mechanisms as well (617). Uniquely, our studies demonstrate that temperature-dependent IFN- α/β efficacy alone is sufficient to alter arbovirus fitness and effectively overcome the small disadvantage posed to these viruses by low temperature in the absence of IFN- α/β . Collectively, these data suggest that the effect of temperature on IFN- α/β efficacy is widely applicable to any IFN- α/β -sensitive infection or pathology that occurs in a reduced-temperature environment.

To examine the effect of temperature on the entirety of the IFN- α/β response, we examined both IFN- α/β gene upregulation and ISG upregulation phases. Mechanistically, it has been shown previously (577, 588) that several ISGs were less robustly induced at the mRNA level when cells are treated with IFN- α/β at temperatures below 37°C, but the mechanism(s) leading to decreased ISG transcription, as well as whether or not reductions in ISG transcript are functionally relevant to the antiviral state at the protein level, were not addressed. We found that activation of the Jak-STAT pathway resulting in phosphorylation, nuclear translocation, and nuclear phosphorylation of STAT1 to the transcription-promoting state was not attenuated by subnormal temperature. In fact, IFN- α/β signaling at 30°C resulted in more phosphorylated STAT1 present in the nucleus relative to 37°C. Thus, differences in IFN- α/β signaling efficiency were not responsible for the observed reduction in ISG transcript induction at subnormal temperature. Importantly, marked temperature-dependent differences in ISG expression were observed at the protein level, indicating that differences in ISG transcription and possibly subsequent translation result in differential functionality of the antiviral state at different temperatures. It is also possible that the activities of individual ISGs may be affected by temperature variation and that this could contribute to differences in their efficacy. If true, this idea may help explain the enhanced antiviral activity of IFN- α/β observed at 39°C versus 37°C,

when ISG protein levels were only modestly higher at this temperature. Moreover, enhanced induction of ISGs known to strengthen the IFN- α/β response, such as RIG-I or RNaseL, at higher temperatures may also contribute to increased efficacy versus lower temperatures, although this idea would presumably apply also to negative feedback ISGs, such as SOCS. Further studies will be needed to test this idea for individual ISGs and to determine the relative contributions these differences may have to immunity against specific pathogens. In sum, we conclude that transcription is the first step in both the IFN- α/β inductive and effector ISG inductive pathways affected by low cellular temperature that lead to attenuation of the antiviral activity of the IFN- α/β response.

Although detailed examination of the transcription factor activities for individual ISGs that account for the effect of temperature was beyond the scope of our current studies, our results comparing baseline transcriptional rate with ISG and LPS-responsive gene transcriptional efficiency did reveal some relevant trends. Transcript levels of the constitutively-expressed genes included in our NanoString analysis did not change appreciably upon temperature shift, while initial transcription of genes induced upon IFN- α/β or LPS treatment were highly affected by incubation temperature. We observed an approximate 2-fold reduction in basal transcriptional rate at 30°C versus 37°C by intron qPCR, and this may account for a portion of the reduction in inducible gene expression. However, it does not fully explain the dramatic differences in induction of all ISGs that were highly upregulated, nor does it account for the subset of LPS-responsive genes whose expression was not temperature-sensitive. In general, these results point to a model in which inactive genes are much more susceptible to transcription attenuation by low temperature than genes actively being transcribed. Potentially, chromatin remodeling around inducible promoters and initial assembly of transcription machinery represent additional

obstacles to inducible genes being “turned on” that are absent from constitutively active genes (618). In addition, variation in the chromatin environments around different promoters, as well as in the transcription factors required for transcription of different genes, would allow for differential temperature sensitivity of inducible genes. Indeed, increased sp1 recruitment to a hypothermia-responsive element upstream of the cold-responsive RNA binding protein (*Cirp*) locus has been identified in the preferential upregulation of this gene at low temperature (522), indicating that temperature shift can impact transcription initiation at the chromatin level. In this view, the reliable temperature sensitivity we observed with ISGs is consistent with the presumption that ISRE-containing promoters reliant on similar transcription factors and chromatin modifications (619-621) would be subject to the same challenges of transcription initiation at subnormal temperatures, yielding the phenotype of temperature-sensitive ISG transcription. By contrast, the chromatin remodeling events and transcription factors required for LPS-responsive genes can vary considerably (618, 622), allowing for the possibility of different effects of temperature shift on individual genes or subsets of genes. Consistent with this idea, several genes that responded to both LPS and IFN- α/β treatment followed the same temperature-dependent expression patterns regardless of the stimulus. Examination of additional signaling cascades with known repertoires of inducible genes, particularly those that stimulate distinct sets of transcription factors and co-factors to effect transcription of different gene subsets, will be helpful in elucidating gene-specific versus pan-regulatory effects of temperature variation.

The initial lag in ISG transcription at 30°C was largely overcome by 12 hours post-IFN- α/β treatment, and in some cases, ISG transcript levels at this temperature continued to increase as they began to stabilize or wane at the higher temperatures. Similarly, LPS-inducible gene transcript levels at 30°C also initially lagged behind those at higher temperatures on average, but

drew level by just 6 hours of LPS treatment, with many genes exhibiting greater expression at 30°C by this timepoint. Although the mechanisms behind this temporal difference in ISG and LPS-induced gene regulation by temperature are unclear, this observation represents another piece of evidence that the effect of temperature on gene transcription is likely gene- and/or pathway-specific. That levels of gene transcripts induced at 30°C eventually met or exceeded peak expression at the higher temperatures and remained elevated over a longer period of time could be the result of a generalized increase in mRNA stability at subnormal temperatures (623-625), and/or due to a defect in negative feedback pathways responsible for curtailing these signaling pathways. Regardless, there did not appear to be a functional consequence of ISG mRNA levels “catching up” at 30°C, as ISG protein levels remained reduced at this temperature compared to 37 and 39°C, even as late as 48 hours post-IFN- α/β treatment. It is likely that protein translation was also attenuated separately from transcription, accounting for this difference, as translational slowing is generally considered a hallmark feature of the cellular cold stress response (547, 624). This idea is supported by our *in vitro* RNA translation reporter and protein synthesis radiolabel assays (Fig 11). Differences in translational efficiency may also explain instances of enhanced ISG protein production at 39°C over 37°C when there was no difference at the transcript level. We conclude that general suppression of translation likely contributes to the suppression of ISG protein production at 30°C independently from effects on transcription. Whether or not ISG transcripts are specifically sensitive to temperature induced changes to translation efficiency, or if these effects manifest with all mRNAs, is still unclear.

We also investigated the effect of temperature variation on IFN- α/β induction efficiency upon stimulation with either poly-I:C or viral infection. Poly-I:C, a non-replicating stimulus, was used for examination of IFN- α/β induction with equal RLR stimulation at each temperature. In

agreement with previous studies (577), poly-I:C treatment of cells at subnormal temperatures resulted in delayed and stunted IFN- α/β production compared to 37°C. That study attributed this difference to a modest reduction in the enzymatic activities of the cytosolic sensors Rig-I and MDA-5 at low temperature, as determined in *in vitro* ATPase assays (577). In contrast, we found that a downstream consequence of Rig-I/MDA-5 stimulation, the phosphorylation of IRF3, was not suppressed at the low temperature, suggesting that any effect on the enzymatic activity of these sensors is functionally inconsequential in this context. Rather, the effect of temperature on this pathway, as in the Jak-STAT pathway, likely manifests first at the level of transcription of responsive genes. We observed delayed transcription of *IfnB*, *Ifna4*, and *Ifit1* genes, each primarily dependent on IRF3 in fibroblasts (279), at 30°C versus the higher temperatures at early time points, but levels surpassed those at the higher temperatures quickly thereafter. However, IFN- α/β protein release was drastically slowed and reduced at 30°C, both initially and well after mRNA levels had recovered, as was IFIT1 protein expression, indicating that efficiency of translation and/or secretory mechanisms also contributed to the reduction in IFN- α/β secretion at the lower temperature. Further studies are required to determine whether or not translation or secretory suppression by low temperature represents a universal effect or if different mRNAs are affected to varying degrees. Poly-I:C treatment at 39°C resulted in the highest induction of IFN- α/β and IFIT1 proteins, indicating that enhanced IFN- α/β production may be an evolutionary aspect of the febrile response *in vivo*. As IFN- α/β is itself a pyrogenic cytokine, this relationship could be evidence of a feed-forward loop in which innate immune responses and fever co-regulate to mount a more rapid response to infection.

IFN- α/β induction was similarly temperature-dependent upon alphavirus infection, with the cells infected at 30°C resulting in delayed and diminished IFN- α/β production compared to

37°C. Interestingly, we did not observe the same enhancement of peak IFN- α/β production at 39°C compared to 37°C that we did with poly-I:C treatment. It is reasonable to hypothesize that an enhanced downstream antiviral state at a febrile temperature could lead to more efficient control of the infection, possibly with lower peak IFN- α/β induction. Indeed, we did observe greater viral control of SINV-nsP2-726G at 39°C compared to 37 or 30°C in our MEF cultures, even with IFN- α/β levels well below those at 37°C. In contrast, at 30°C, IFN- α/β induction and subsequent effector phase are both delayed and attenuated. Because alphaviruses have evolved to grow efficiently at this temperature (and colder) in arthropods, virus replication largely resists the low-temperature environment, and initial replication proceeds largely uninhibited by IFN- α/β . During this window, the virus can produce sufficient levels of IFN- α/β antagonists before a strong antiviral response can be mounted. IFN- α/β antagonism by most alphaviruses depends on the activities of nonstructural protein 2 (nsP2) or capsid proteins (116, 626, 627) and the viruses can also interfere with Jak-STAT signaling (119, 122, 607).

In a murine model of CHIKV infection, we demonstrated that hypothermia can exacerbate virus replication and associated musculoskeletal disease, but only in the presence of a functional IFN- α/β response. In mice lacking IFNAR1, lowered body temperatures reduced both viral replication and disease signs, indicating that the effect of the reduced temperatures on the virus was acting through its effects on IFN- α/β , and serum IFN- α/β levels were much reduced in cold mice versus their warm counterparts. Surprisingly, differences in MSD in wild-type mice manifested several days after hypothermic mice had recovered to a normal body temperature, indicating that, as predicted from our cell culture models, influences of reduced temperature on viral infection occur at an early stage of the virus-host interaction, in the window before IFN- α/β can control the infection. As MSD in CHIKV infection is a complicated process driven by both

viral and host factors (183), it is tempting to speculate that subnormal temperatures early during infection allowed the virus to establish a more severe infection in the face of a weakened IFN- α/β response, which then attracted increased immune cell infiltrates and induced greater inflammation at the site of infection. We did observe delayed viral clearance in the infected footpad and the draining lymph node of the hypothermic mice compared to the normal mice at 6 d.p.i., which could help drive the exacerbated MSD at later timepoints. Together, these results demonstrate that CHIKV or other arbovirus pathogenesis and disease can be altered by variation in tissue temperature, with subnormal temperatures benefitting, and supranormal temperatures impairing, virus infection via effects on the IFN- α/β response. This suggests that local or systemic warming could represent a viable therapeutic for infection with CHIKV or other arthritogenic arboviruses if applied early after infection. However, other, off-target effects of reserpine treatment or torpor induction, such as systemic stress responses or altered hormone levels, may have contributed to our results through unknown mechanisms. Thus, future experiments using localized or external methods of temperature reduction may be useful for controlling for any off-target effects of reserpine or torpor. In addition, experiments involving external heating of reserpine-treated or torpid mice to mitigate temperature depression may be warranted to confirm the direct influence of temperature, and not other effects of reserpine or torpor, on viral phenotypes. Finally, it is also worth noting that early studies of temperature and interferon responses focused on the establishment of persistent infection and its relationship to temperature-dependent interferon induction *in vitro* (628-632). It will be of interest to determine if temperature effects on the innate immune system influence the establishment of arboviral persistence in sites such as the testes (Zika (633-635)) and peripheral joints (CHIKV (180)) that may differ from core temperatures.

3.0 MODELING PERSISTENT CHIKUNGUNYA INFECTION IN MICE USING *IN VIVO* IMAGING

3.1 INTRODUCTION

The reemergence of Chikungunya virus (CHIKV) in previously endemic areas and expansion globally within the last 15 years has caused massive outbreaks affecting millions of people across the globe (33). Its 2004-2005 rampage across the Indian Ocean territories resulted in a new sublineage of the virus containing a mutation in its E1 envelope glycoprotein that was shown to confer enhanced fitness and transmissibility by a new species of mosquito vector, *Aedes albopictus* (165). This development is of major public health relevance because *A. albopictus* inhabits a much larger geographic range than the usual vector for CHIKV, *Aedes aegypti*, which is found only in tropical and subtropical regions (177). *A. albopictus* thrives across temperate climatic areas in Europe and North America as well as at equatorial latitudes across the globe, so its new role as a major vector for CHIKV puts an enormous number of naïve hosts at risk for infection, should the Indian Ocean Lineage CHIKV continue to expand its range (177). It has already been imported to southern Europe by infected travelers and seeded autochthonous spread by *A. albopictus* in multiple instances, however, it is not known to have established endemicity in these areas (168, 169). CHIKV made its way to the Western Hemisphere in 2013, when an Asian lineage virus caused an outbreak that started on St. Martin

island in the Caribbean and rapidly engulfed much of Central and South America, causing millions of suspected or confirmed cases (636, 637). Transmission during this outbreak was mediated by *A. aegypti* (636) and did not spread north of Florida (638), however, it did result in nearly 4000 traveler-associated cases reported in 49 states and the District of Columbia between 2014 and 2016 (639), which suggests there is a real risk of CHIKV spreading into the greater United States, particularly if an *A. albopictus*-adapted virus emerges here.

CHIKV causes an acute febrile illness characterized by intense and debilitating joint pain associated with direct cytolytic tissue damage and destructive inflammatory responses (153). In approximately half of acute CHIKV patients, arthritic/arthralgic symptoms will persist into a chronic disease phase after other acute symptoms have resolved and virus has been cleared from circulation (216). Chronic joint symptoms post-CHIKV infection may be persistent and unrelenting, or may reappear intermittently between periods of recovery. In either case, CHIKV-induced chronic arthralgia is nontrivial and significantly decreases perceived quality of life in affected patients (220). Unlike acute CHIKV infection, during which any joint can be involved, chronic CHIKV-associated arthropathy is localized almost exclusively in the small, distal joints – ankles, wrists, fingers, and toes – and is usually polyarticular and symmetrical (33). Advanced age has been universally identified as one of the strongest risk factors for progressing to chronic CHIKV disease (222, 229, 640). Other age-associated comorbidities such as cardiovascular disease, obesity, and diabetes are also independent risk factors, and may contribute to the strength of the association between chronic CHIKV and age (199). In addition, severity of acute disease strongly correlates with chronic CHIKV incidence, which may also be age-related, as elderly individuals account for a higher proportion of severe acute CHIKV cases than younger

age groups (180, 231, 640). Smoking, female sex, and changing ambient temperature have also been identified as predictors of post-CHIKV chronic arthralgia or arthralgic episode (220, 223).

In the previous chapter, we demonstrated that acute CHIKV replication in an arthritic mouse model was enhanced by systemic temperature reduction in both the inoculated and contralateral footpads of wild-type, but not *Ifnar1*^{-/-} mice, indicating that lowered body temperature tempered the IFN- α/β response against CHIKV and contributed to increased viral fitness *in vivo*. It is known that adult wild-type mice can harbor CHIKV RNA, including negative-strand RNA, in joint-associated tissues as late as 4 months post-infection (202, 215). CHIKV RNA has also been detected in synovial biopsy samples from patients suffering chronic CHIKV-associated arthralgia, as well as one patient with CHIKV protein staining in synovial macrophages at 18 months post-infection (180). This study also found upregulated innate immune cytokines such as IFN- α , IL8, TNF α , and IL1 β in PBMCs harvested from patients experiencing chronic CHIKV arthralgia, as well as in synovial fluid from one patient, indicating a persistent activation of innate immune responses that could be driving chronic inflammation (180). CHIKV antigen was also detected in muscle satellite cells in a quadriceps biopsy from one patient at 3 months post-infection (182). These findings suggest that CHIKV RNA capable of gene expression may persist in musculoskeletal tissues in humans. However, whether or not the viral RNA is a full-length conventional viral replicative entity, a dormant, infectious genome, or a defective replicative intermediate, are open questions. It is also unknown if all chronic CHIKV patients harbor the same type of persistent viral entity, or if persistent viral components differ between patients. Also, it is unlikely but possible that persistent virus infection is unrelated to chronic arthritis symptoms, which may reflect an autoimmune process originally stimulated by acute infection. Some studies have attempted to address these questions using mice deficient for

one or more components of the adaptive immune response to discourage viral clearance from joint-associated and lymphoid tissues and promote persistence, as viral clearance from circulation and most tissues is dependent on a strong neutralizing antibody response (251). CHIKV infection of *Rag1*^{-/-}, *Rag2*^{-/-}, or μ MT mice results in higher initial viral burden in target organs that persists to chronic time points, a low-level serum viremia that in one study was found to last over 500 days, and infectious CHIKV virions recoverable from joint-associated tissues as late as 42 d.p.i. in *Rag1*^{-/-} mice (202, 215, 233, 234, 251). *Rag1*^{-/-} mice also showed histological signs of arthritis, metatarsal muscle inflammation and necrosis, and tendonitis at 12 weeks post-infection, whereas these pathologies had resolved much earlier in wild-type B6 mice, although both strains still had synovitis at that time point (202). These results indicate that abrogation of adaptive immunity, particularly B cell responses, augments CHIKV and CHIKV RNA persistence and exacerbates chronic joint inflammation in ways that parallel human infections, but they have yet to address the underlying viral mechanisms that may be driving the inflammation and model the flaring of arthritis found in a large portion of humans suffering from chronic disease.

In light of the established association between acute disease severity and risk of developing chronic CHIKV symptoms and the potential for virus replication as a driver of chronic and/or flaring disease, we hypothesized that factors that altered virus replication at acute or chronic time points might influence viral persistence and disease manifestations. To address this hypothesis, we have used a CHIKV expression vector newly developed in our laboratory that is similarly virulent to the unmodified parental virus and very stably expresses reporters of infection (613).

Initially, we used a wild-type CHIKV strain expressing nanoluciferase (nLuc) and an IVIS Spectrum CT *in vivo* imaging instrument (IVIS) to establish a sensitive method for tracking viral replication, spread, and persistence in adult wild-type C57BL/6 (B6) mice. We found that positive nLuc signal, a direct indicator of virus gene expression in this virus, was detectable throughout a 136-day experimental period. This is much longer than previously demonstrated and suggests that viral proteins are expressed in the mouse model during much, if not all, of the time viral genomes are present. Furthermore, to address the effect of the severity of acute infection upon subsequent chronic replication and disease, we have varied the intensity of initial replication by 1) reducing mouse core temperature during the first few days of disease, 2) infecting *Irf7*^{-/-} transgenic mice that are more susceptible to initial virus replication and 3) infecting wild-type mice with a recently described CHIKV mutant (E2 K200R) that exhibits greater early replication and spread than normal CHIKV strains (641).

Temperature reduction caused by reserpine treatment during the first few days of infection was found to exacerbate CHIKV replication and spread at early time points and led to higher persistent viral signal compared to untreated mice at 30 days after infection. Similarly, use of innate-immune compromised *Irf7*^{-/-} mice or the CHIKV 200R mutant enhanced initial virus replication and spread as measured by IVIS. Most notably, we observed that viral protein production at late time points could also be significantly increased by hypothermia induction during the chronic disease phase, potentially recapitulating a CHIKV infection “flare” and identifying temperature reduction as a potential driver of recurrent disease. Consistent with our hypothesis, the mice with the highest viral signal during the first two weeks of infection, either due to hypothermia at the time of infection or by genetic deletion of IRF7, tended to show the largest increases in signal upon temperature reduction later on, supporting the link between acute

disease severity and the risk of progressing to the chronic phase in humans. Studies of chronic infection with the CHIKV 200R mutant are in progress.

To our knowledge, this is the first demonstration of active viral protein production during the chronic disease stage in any model, and it is suggestive that CHIKV can and does establish a *bona fide* persistent, productive infection in musculoskeletal tissues. This is also the first evidence that the “flaring” arthralgia phenotype observed in some human cases might be reasonably modeled in an animal and associated with potential viral reactivation events, possibly directly related to alterations in the efficacy of the IFN system as modulated by temperature. This is consistent with survey data of humans exhibiting chronic disease in that the most common factor associated with flaring disease was altered ambient temperature (220). Clearly, these initial observations come with many caveats and open questions, especially whether or not the persistent phenotypes in mice are analogous to those operating and driving persistent disease in human CHIKV patients. Further study and development of this model are necessary to address these questions.

3.2 RESULTS

3.2.1 High-sensitivity *in vivo* imaging reveals persistent CHIKV nLuc signal beyond four months post-infection

Recent attempts to develop of a mouse model of chronic CHIKV infection have largely relied on the use of mouse strains deficient in various components of the adaptive immune system to delay or inhibit viral clearance from joint-associated (and other) tissues. This strategy is and will

continue to be valuable for understanding how CHIKV might establish persistence at various sites and especially whether or not chronic CHIKV represents a true, active persistent infection or retention of viral RNA or proteins in the absence of productive gene expression or replication. However, adaptive immunity plays a key role in viral clearance and protection from secondary infection. Thus, in its absence in these immunodeficient mouse models, CHIKV persistence phenotypes such as cell and tissue tropism may not accurately represent the situation in human patients. For example, antibody-deficient mice establish persistent, low-level viremia that lasts indefinitely, but this is not observed in human infections (202, 215). Therefore, we employed the use of wild-type adult C57BL/6 (B6) mice to establish an immunocompetent model of chronic CHIKV infection. It has been shown previously that CHIKV RNA is recoverable from the ankle joints of these mice at least 16 weeks post-infection, suggesting that this model does reflect some aspects of human infection (202).

To maximize the sensitivity of CHIKV detection, we employed a strain of CHIKV-La Reunion (LR) expressing nanoLuciferase (Promega) for use with *in vivo* imaging (Fig 19A, (613)). The nLuc protein is fused in-frame between the capsid and pE2 proteins and gets autoproteolytically (amino terminus, capsid protease) and co-translationally (carboxy terminus, *Thosea asigna* viral 2A-like protease) cleaved from the structural polyprotein during virus replication. NanoLuciferase (nLuc) is a small, 19.1 kDa luminescent enzyme that exhibits enhanced stability and 150-fold greater luminescent output per molecule compared to firefly or renilla luciferases (642). Importantly, it also shows remarkable stability within the alphavirus genome and is less likely to be deleted from the genome than larger proteins, even over the course of a lengthy infection (613). Because nLuc was inserted into the CHIKV structural gene subgenomic region and was constructed as an in-frame fusion with the viral structural proteins, it

is produced concomitantly with viral proteins only after the synthesis of negative strand RNA. Therefore, its presence is suggestive of both productive viral gene expression and successful genome replication. Thus, our viral nLuc reporter system should reveal active viral replication and gene expression even when infection levels are very low or if relatively few cells become persistently infected during the chronic phase of CHIKV disease. Importantly, it should also be very sensitive to changes in chronic virus replication associated with altered host or environmental factors.

To test the ability of the CHIKV-LR-nLuc reporter virus to persist in mice and our ability to detect persistence by *in vivo* imaging, we infected 5-week-old male B6 mice subcutaneously on the left rear footpad with 1000 pfu of CHIKV-LR-nLuc and imaged them regularly through 136 days post-infection. Viral nLuc signal was highest in the inoculated (ipsilateral) rear footpad and the opposite rear (contralateral) footpad very early after infection (day 3 in our imaging time course) and decreased sharply over the first two weeks (Fig 1C-D). As expected from previous virus titrations and examination of musculoskeletal disease (93, 184), ipsilateral nLuc signal was always higher than contralateral. Interestingly, the primary footpad signal in both footpads at chronic time points was localized between the fibulare/intermedium bones and in the base metatarsal region adjacent to, but not in, the phalanges, and possibly not associated with a synovial joint (Fig 1B-C). In the ipsilateral footpad, viral signal at 14 days post-infection (dpi) was still over 2 logs above mock-infected background levels and remained well above background until very late time points, steadily decreasing throughout the rest of the time course (Fig 1C). In contrast, signal in the contralateral footpad was much lower and became indistinguishable from background signal by 58 dpi. Interestingly, similar localization of signal was observed regardless of whether or not the footpad was infected artificially (ipsilateral) or

through natural spread of the virus (contralateral). However, it is possible that the localization of signal within the footpad as well as footpad signal being prominent versus other sites on the mouse is related to technical aspects of IVIS imaging as well as precise sites of maximal virus replication. Indeed, other locations such as the snout, forelimbs, and popliteal lymph nodes can also become positive for viral signal, and signal may persist and flare at these sites as well (Fig 20B, D; data not quantified). For the remainder of the chapter, I will focus on the footpad signal as an indicator of persistent virus replication that may well also be occurring at other sites as levels below the limit of detection of the IVIS instrument.

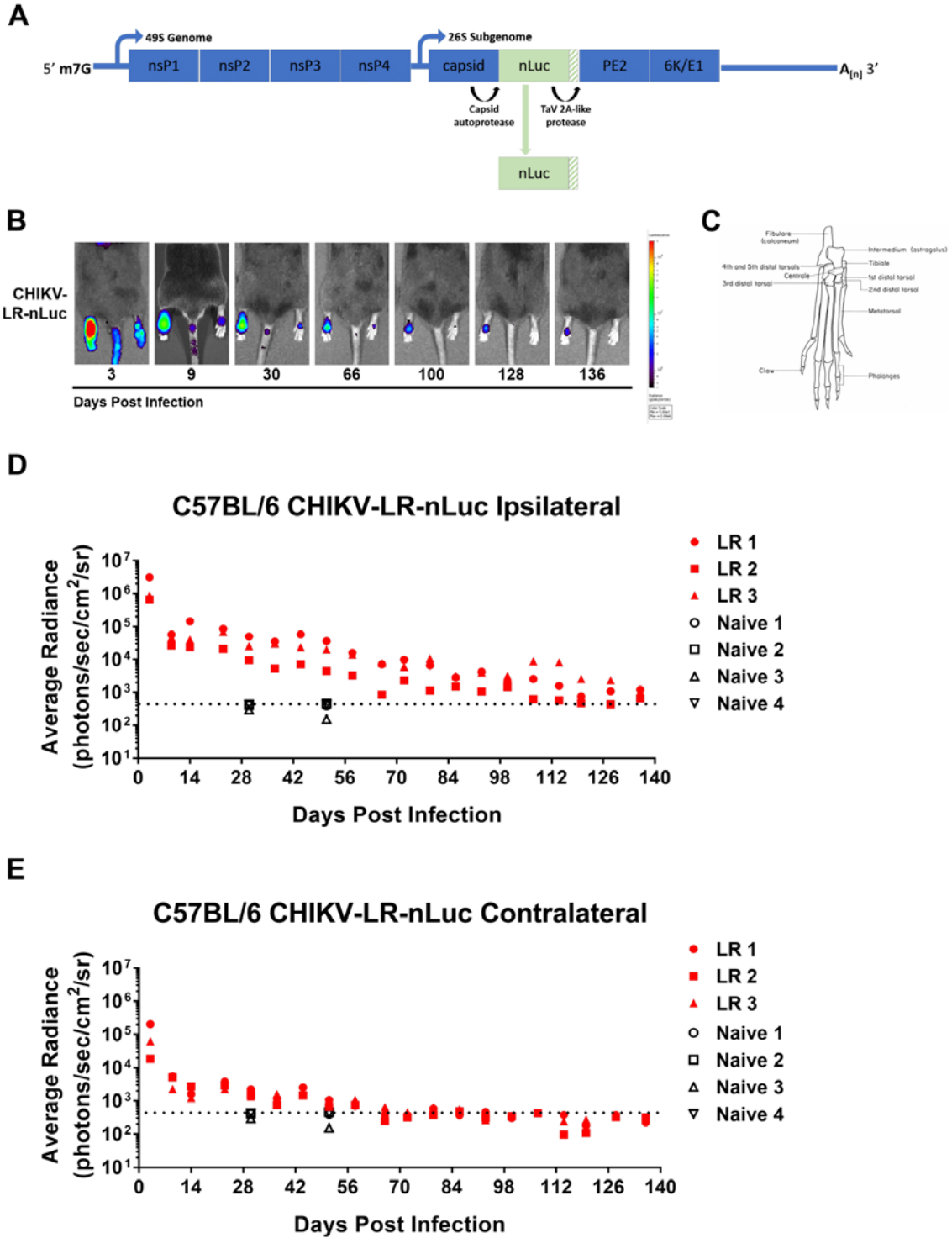


Figure 19. High-sensitivity *in vivo* imaging reveals persistent CHIKV nLuc signal beyond four months post-infection.

A: Diagram of the genome structure of CHIKV-LR-nLuc (adapted from [sun 2013]). B: 5-week-old male C57BL/6 mice were infected in the ventral left hind footpad with 1000 p.f.u. CHIKV-LR-nLuc and viral replication and spread was tracked over time using *in vivo* imaging. C: Dorsal view of murine hind foot bone anatomy (diagram adapted from (643)). D-E: Regions of interest encompassing the entire visible ventral foot were quantified for average radiant signal.

3.2.2 Exacerbation of CHIKV acute phase replication via body temperature reduction, IRF7 deficiency, or a mutant CHIKV (200R)

To test the hypothesis that the magnitude of CHIKV replication during the acute infection phase leads to higher viral signal during the chronic phase, we first tested three strategies aimed at increasing acute CHIKV replication versus a normal infection with CHIKV-LR-nLuc in B6 mice: 1) reserpine (RES)-induced body temperature reduction during the first few days of CHIKV-LR-nLuc infection in B6 mice, 2) CHIKV-LR-nLuc infection of mice lacking IRF7 (*Irf7*^{-/-}), and 3) infection of B6 mice with a CHIKV strain containing a mutation that has been shown to increase virulence in mice versus the parental virus (641) (CHIKV-LR-200R-nLuc). In addition, we infected another group with the related arthritogenic alphavirus Sindbis virus strain TR339 (SINV-TR339-nLuc) with the intent to evaluate the persistence phenotype of a related alphavirus that does not commonly cause severe or chronic arthritis. Each of these groups was infected with 1000 p.f.u. of either CHIKV-LR-nLuc, CHIKV-LR-200R-nLuc, or SINV-TR339-nLuc subcutaneously in the left hind footpad on day 0 and viral replication, spread, and persistence was monitored by *in vivo* imaging.

As expected, reserpine treatment four hours prior to infection resulted in a period of hypothermic body temperature corresponding to the first few days of CHIKV infection (Fig 20A), and these mice exhibited higher viral signal in the ipsilateral footpad than normal mice on days 3 and 9 post-infection (Fig 20B-C, * $p < 0.05$ Kruskal-Wallis rank test). Similarly, both CHIKV-LR-nLuc-infected *Irf7*^{-/-} mice and B6 mice infected with the 200R mutant CHIKV had significantly higher viral nLuc signal in the ipsilateral footpad than the LR-infected B6 control mice at 3 d.p.i. (Fig 20D-E, *** $p = 0.0008$, * $p = 0.0424$ unpaired two-tailed t tests of log-transformed radiance values). Note that the same normal B6 + LR control group mice were used across all experiments in figure 20. The visual differences in the nLuc signal for these mice in figure 20 panels B and D reflect different ranges of the pseudocolor scales that were necessary to accurately depict differences in the experimental groups, which varied greatly in signal strength. These results validate all three of our methods for exacerbating acute CHIKV replication to test the effect of the magnitude of acute phase replication of chronic or persistent phenotypes. The experimental groups for two of these strategies, temperature reduction and IRF7 deficiency, were followed by *in vivo* imaging to approximately 1-month post-infection. Interestingly, ipsilateral footpad nLuc signal became significantly higher in the reserpine-treated B6 mice than the normal mice on day 30 after two weeks of insignificant difference, possibly resulting from a slower rate of signal diminution during this time (Fig 20C, * $p < 0.05$ Kruskal-Wallis rank test). Ipsilateral footpad nLuc signal in *Irf7*^{-/-} mice remained higher than that in B6 mice throughout the entire time course, although direct comparison at chronic time points was not possible because the groups were imaged on slightly different days (Fig 20F). SINV-TR339-nLuc signal was comparable to CHIKV-LR-nLuc at 3 d.p.i., but decreased more rapidly thereafter (Fig 20C). Surprisingly, SINV-TR339-nLuc signal was still detectable in the infected footpad at 30 d.p.i.,

suggesting that this virus may have heretofore unrecognized potential to persist in host tissues, though it could be an artifact of undegraded nLuc that may remain active in tissues for a time after it is produced. No direct evidence exists for either of these possibilities, however, and it will be important to answer this question in the future. Collectively, these results indicate that increased acute CHIKV replication can lead to higher levels of persistent viral signal at a chronic time point. Studies with the 200R mutant are ongoing, but we expect that those results will lend further support to this conclusion. However, whether greater acute viral replication results in a greater number of persistently-infected cells compared to baseline or a similar number of infected cells that are producing more viral proteins on a per-cell basis is unknown and either possibility could underlie our findings. Future immunohistochemical/immunocytochemical analysis of persistently-infected cell populations in these different experimental groups will be needed to resolve this question.

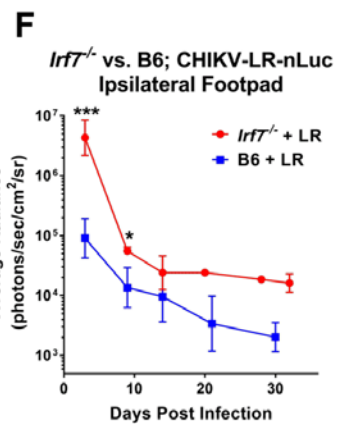
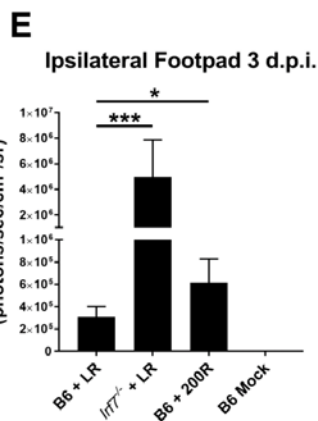
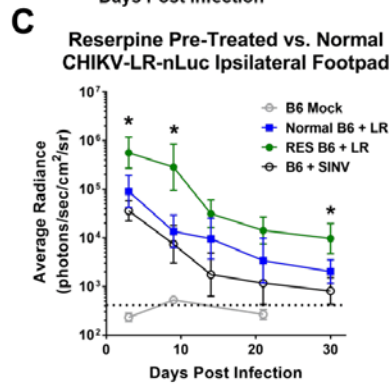
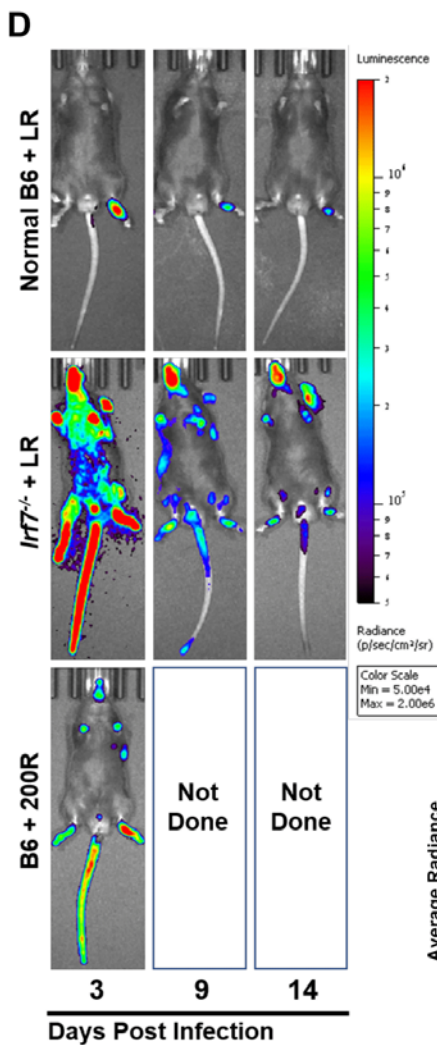
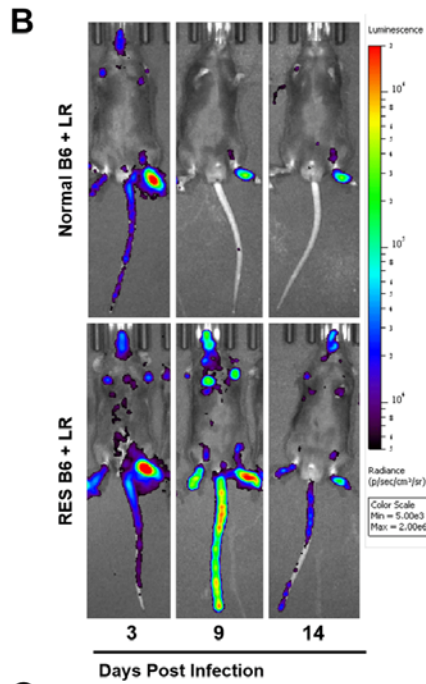
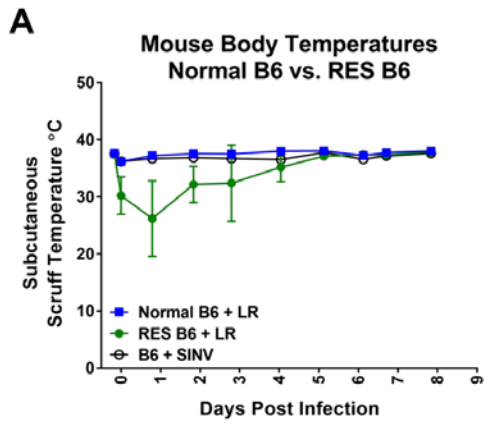


Figure 20. Exacerbation of CHIKV acute phase replication via body temperature reduction, IRF7 deficiency, or a mutant CHIKV (200R).

5-6-week-old male C57BL/6 and *Irf7*^{-/-} mice were infected in the left rear footpad with 1000 p.f.u. of nLuc-expressing CHIKV strains LR or LR-200R, as indicated. A subset of the C57BL/6 mice were treated with reserpine four hours prior to infection with CHIKV-LR-nLuc. Viral replication and spread were monitored over the course of 1 month by *in vivo* imaging on an IVIS-Ct machine. A: Subcutaneous (scruff) temperature profiles of reserpine-treated and normal C57BL/6 mice during the first 8 days of infection. B and D: Pseudocolored IVIS images show nLuc signal strength and distribution in infected mice. C, E, and F: Average radiant signal was quantified from the ipsilateral hind foot region and compared between experimental groups. Statistics for C: * $p < 0.05$ Kruskal-Wallis rank test. Statistics for E and F: * $p < 0.05$, *** $p < 0.001$ unpaired two-tailed t tests of log-transformed average radiance values.

3.2.3 Temperature reduction during chronic CHIKV infection induces flaring of persistent viral nLuc signal

CHIKV RNA persistence has been associated with chronic immune activation in humans and in animal models, evidenced by cellular infiltrates into musculoskeletal tissues and elevated levels of proinflammatory cytokines, including type-I IFNs (180, 215). Chronic IFN- α/β activation has been suggested to contribute to inflammatory tissue damage or adaptive immune suppression associated with several persistent viral infections (127, 644, 645), but it may also be playing a virus-suppressive role, and its role in chronic CHIKV infection and disease has not been defined. In addition, temperature change has been associated with the onset of chronic CHIKV arthralgia flare-ups in humans (220), and we have demonstrated that temperature reduction increases CHIKV fitness *in vivo* by suppressing IFN- α/β (previous chapter). Therefore, we hypothesized that temperature reduction during the chronic phase of CHIKV infection will cause a flare in viral nLuc signal in our mouse model, potentially through attenuation of IFN- α/β . To test this,

we treated a subset of the CHIKV-LR-nLuc-infected B6 control mice from the previous experiment (Fig 20 group normal B6 + LR) with reserpine at 1-month post-infection and performed IVIS imaging one day before and four days after treatment to observe any changes in nLuc signal associated with the temperature reduction. Reserpine treatment caused the expected four-day period of hypothermia (Fig 21A) and resulted in modest but significant increases in ipsilateral footpad nLuc signal compared to signal one day before treatment (Fig 21B-C; group Normal B6 + LR RES d31; *** $p < 0.001$ paired ratio t test). To our knowledge, this is the first demonstration of active changes in viral protein expression levels in a chronic CHIKV infection model.

We also observed ipsilateral footpad signal flares post-reserpine treatment in the CHIKV-LR-nLuc-infected B6 mice that had been treated with reserpine at the outset of infection (RES B6 + LR RES d31) and the reserpine-treated *Irf7*^{-/-} mice (Fig 21B-C; RES B6 + LR RES d31 ** $p < 0.01$ paired ratio t test; *Irf7*^{-/-} + LR RES d32 – statistical analysis could not be performed due to n of only 2). Additionally, increases in nLuc signal were clearly visible post-reserpine treatment in other locations as well, such as the snout region, front footpads, and the popliteal lymph nodes (Fig 21B, white arrows). Curiously, a much smaller but significant ipsilateral footpad signal increase from pre- to post-reserpine was also observed in CHIKV-LR-nLuc-infected B6 mice that had not received reserpine treatment at any point (Fig 21C; Normal B6 + LR * $p < 0.05$ paired ratio t test). These mice were co-housed with reserpine-treated mice, and as a result, they suffered slight reductions (~1°C) in body temperature during this window potentially due to a dearth of shared body heat available to them (Fig 21A). This may underlie the small signal increases in this group, although it may also reflect the presence of naturally-occurring flares in viral activity in this model. Finally, we observed that the mice with the highest levels of

viral replication during the acute phase of CHIKV infection (B6 mice treated with reserpine on the day of infection and *Irf7*^{-/-} mice) also had the largest fold-change in ipsilateral footpad nLuc signal post-reserpine treatment versus pre-reserpine at 1-month post-infection (Fig 21D). Reserpine-induced fold-change in viral signal in *Irf7*^{-/-} mice was significantly higher than in the normal B6 group (p=0.006 two-tailed t test). While the fold-change in signal was not statistically different between the initially reserpine-treated B6 + LR group and the control B6 + LR group in this experiment, we are confident that significance will be achieved once more mice are tested, and experiments to address this are currently in-progress. In addition, two of the reserpine-treated B6 + LR mice exhibited much larger signal flares than the others, which resulted in a high variance and contributed to the lack of statistical significance. In any case, these results support our hypothesis that acute infection severity is a determinant of chronic CHIKV persistence phenotypes. In sum, these data are highly suggestive of an active CHIKV infection persisting in multiple musculoskeletal and/or lymphoid tissue at least one-month post-infection and confirm that hypothermic temperature can influence both the establishment of chronic CHIKV infection and elicit flaring events. In addition, the data support an association of acute infection severity with the intensity of flaring disease, either via stochastic aspects due to differing infected cell numbers or the actual intensity of the viral gene expression increase.

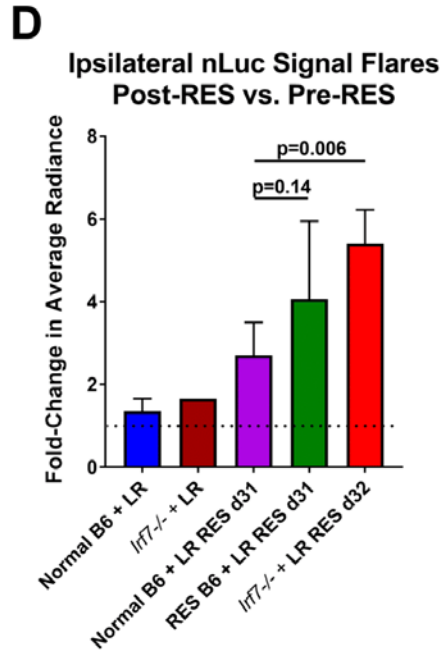
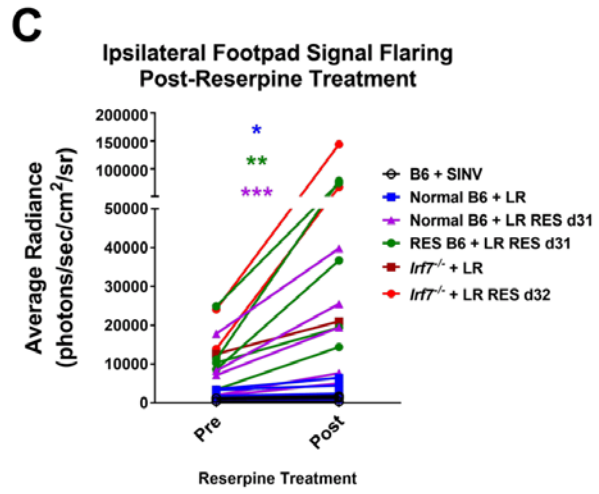
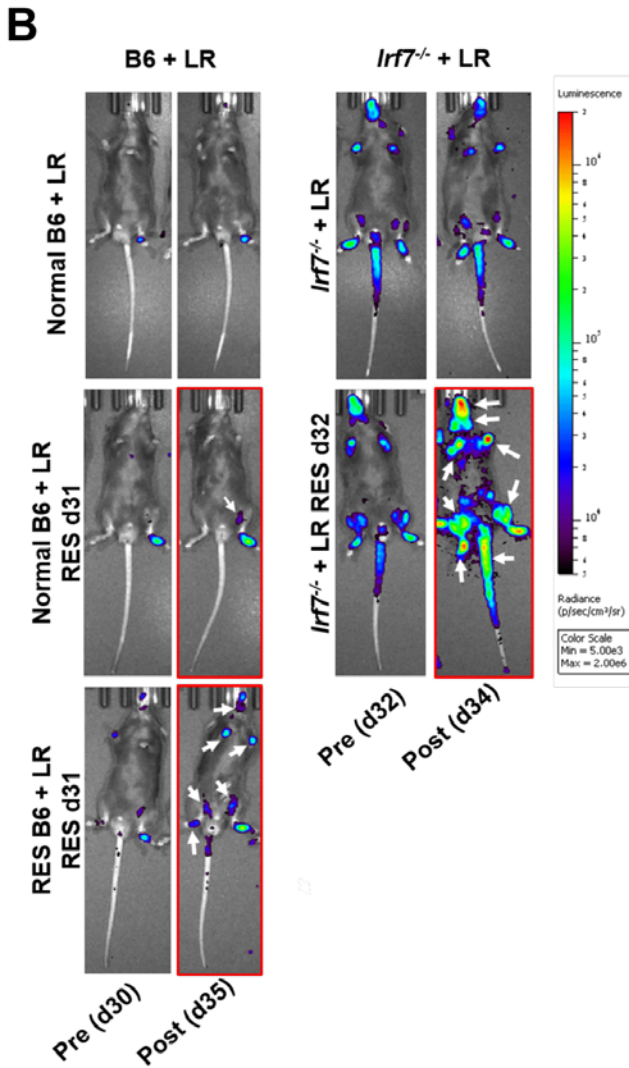
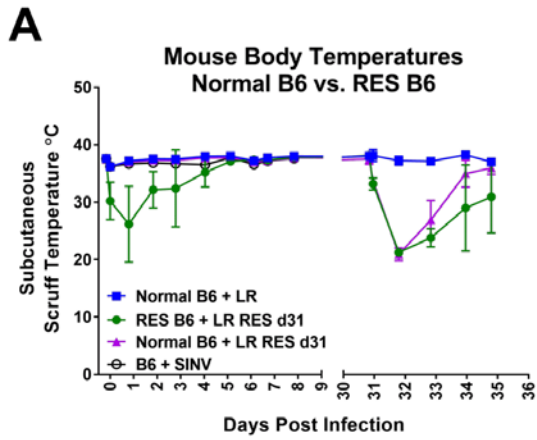


Figure 21. Temperature reduction during chronic CHIKV infection induces flaring of persistent viral nLuc signal.

A subset of the mice from each experimental group from Figure 20 were treated with reserpine at ~1-month post-infection and changes in nLuc signal between pre- and post-reserpine were observed by *in vivo* imaging. A: Subcutaneous (scruff) temperature profiles of reserpine-treated and normal C57BL/6 mice. B: Pseudocolored IVIS images show nLuc signal strength and distribution in infected mice pre- and post-reserpine treatment at 1-month. White arrows indicate sites of visible signal increases other than the ipsilateral footpad. C: Average radiant signal was quantified from the ipsilateral hind foot region and compared between pre- and post-reserpine time points for each animal. * $p < 0.05$, ** $p < 0.01$, *** $p < 0.001$ paired ratio t test. D: Mean fold-change in ipsilateral footpad signal post-reserpine vs. pre- for each experimental group. P values reported are from two-tailed t tests.

3.3 DISCUSSION

3.3.1 Detection of a persistent infection

Using a CHIKV that expresses an nLuc reporter within its structural proteins, we successfully detected positive viral protein signal over four months post-infection using *in vivo* imaging. As alphavirus structural proteins are produced from a subgenomic mRNA transcribed only after negative strand RNA synthesis and genome replication, nLuc signal in this context is highly suggestive of persistent, productive viral genome replication and protein production in the inoculated footpad and other sites where signal could be detected. However, a significant caveat exists in this interpretation that will need to be addressed before this chronic CHIKV model can be validated as evidence for a true, persistent CHIKV infection. Specifically, our experiments did not rule out the possibility that nLuc might be remarkably stable in mouse tissues, and the long-term signal we observed was not due to new gene expression from the virus, but rather from

undegraded nLuc protein produced earlier in the infection. It is unknown how long nLuc protein can remain active in tissues once it is produced, and what the limit of detection of nLuc is on the IVIS, as no studies have addressed these issues so far. Direct injection of nLuc protein from a transfected cell lysate that gives an initial IVIS signal equivalent to CHIKV infection into the footpad and tracking how quickly its activity wanes via *in vivo* imaging might be a productive strategy for answering the question of *in vivo* nLuc stability, although presumably, the majority of injected protein would be extracellular as opposed to intracellular virus-produced protein and the clearance rates of these two groups may not be similar. Alternatively, the addition of a PEST sequence to the nLuc insert would theoretically speed up nLuc turnover and reduce its potential for giving a false positive signal.

Infection of mice with SINV-TR339-nLuc did result in diminished nLuc signal compared to CHIKV-LR-nLuc at 30 d.p.i. despite similar signal strength at 3 d.p.i., but signal was still detectable in a subset of SINV-infected mice (Fig 20C). This experiment was intended to address the similarity or differences in persistent replication produced by a related alphavirus that causes a less severe manifestation of musculoskeletal disease (MSD) in humans. Along these lines, we have never detected swelling of the ipsilateral (or any) footpad when mice are infected with SINV in the same context as CHIKV, where we do see easily detectable increases in footpad cross-sectional area (93). The results we obtained suggest that SINV may also exhibit persistent genome replication and protein expression. Indeed, previous studies have demonstrated the capacity to RT-PCR amplify SINV sequences from the brains of infected normal mice for their lifetimes (646). Therefore, multiple alphaviruses may have persistent replicative cycles in vertebrates. However, the mechanisms underlying the differences in disease elicited by SINV versus CHIKV remain to be elucidated

Naturally, the most compelling evidence for a truly persistent CHIKV infection in our model would be isolation of infectious virus from persistently-infected sites such as the ipsilateral footpad. Although we did not attempt to culture live virus from a chronic time point in our studies, several unsuccessful attempts have been made in other studies using normal mice (201, 202, 215). Whether or not these failures reflect the scale of the persistent infection in the studies or the effects of neutralizing antibodies on the characteristics of persistent infection or the capacity to detect infectious virus is unclear. Since mice incapable of producing a neutralizing antibody response do yield infectious virus for long periods post infection (202, 215, 234, 251), it does appear that detection of viable virions at late times post infection of normal mice should be technically possible and that in the absence of clearance pressures exerted by antibodies, the virus infection can productively persist. We could approach these issues in antibody-competent mice by increasing the magnitude of acute disease through use of early reserpine treatment or IRF7-deficient mice or by reducing antibody responses at late times post infection through B cell and IgG depletions followed by sensitive co-culture of nLuc-positive tissues with susceptible cells. Alternatively, transplantation of an infected foot from a chronic timepoint onto a naïve, immunocompromised mouse, such as a *Rag*^{-/-} or *Ifnar*^{-/-}, may be a very sensitive method for determining if infectious virus persists in our model. Presumably, in the absence of these immune components, any infectious CHIKV would be able to replicate and spread uninhibited from the transplanted foot, and would be readily detectable in its new host by IVIS imaging.

Barring detection of cell-free virus, PCR could be used to amplify both the genome and antigenome from tissues showing persistent nLuc signal to confirm the presence of viral RNA and active replication. Deep sequencing could reveal whether the whole CHIKV genome is present in these tissues. If the intact CHIKV genome is not present, then that would strongly

suggest that infectious virions are not being produced during the chronic phase, and persistence of CHIKV RNA does not represent a true persistent or latent infection. In addition, it will be of interest to identify the cell type(s) that harbor persistent viral RNA or protein using immunohistochemistry on tissue sections from chronically-infected hindlimbs and feet. However, this has not been achieved previously, likely due to the limited number of infected cells or the low level of virus gene expression in cells subjected to antibody-mediated clearance pressure (647, 648). Indeed, only the high sensitivity of the nLuc/IVIS approach has allowed us to reproducibly detect chronic gene expression in normal mice. As indicated above, antibodies to viral proteins are insufficiently sensitive to detect persistent gene expression and no antibody to nLuc has been described. However, we are attempting to detect long-term virus gene expression by use of CHIKVs expressing fluorescent reporters of infection (e.g., GFP, mCherry, iRFP) followed by tissue cryosectioning and confocal microscopy. However, it remains to be determined if these approaches will yield the increased sensitivity required to detect virus gene expression in individual cells. Interestingly, the prevailing hypothesis is that synovial macrophages are the most likely cell type supporting persistent CHIKV infection (180, 181), but our IVIS images indicate that the most prominent viral signal may not always be associated with synovial joints at chronic time points. One of our hypotheses was that persistent viral nLuc signal could be enhanced by increasing the severity of acute CHIKV infection and replication. We used reserpine-induced hypothermia in B6 mice and IRF7-deficient mice as two distinct methods for achieving higher acute replication and spread than a typical B6 infection, and found that both strategies resulted in higher persistent signal at least one-month post-infection. In addition, we infected B6 mice with a mutant CHIKV strain, 200R, that exhibits increased pathogenicity in mice and found increased replication and spread versus the parental LR strain at 3 d.p.i. This

represents another strategy for exacerbating acute CHIKV infection, but the results pertaining to its effect on persistence are still pending. Effecting a more intense acute infection through one of these methods to enhance persistent infection/signal may improve the ability to detect individual cells or populations that are persistently infected, as those cells/populations are likely to be higher in number and/or viral antigens versus a typical infection.

3.3.2 A flaring disease model

We used reserpine treatment and the resultant reduction in body temperature to cause temporary flares in viral nLuc signal at chronic time points, however, the cellular and molecular mechanisms leading to the flare are unknown. Presumably, the low temperature caused by the reserpine treatment temporarily attenuated an immune mechanism that dampens viral gene expression during the chronic phase. It is possible that this mechanism is the type-I IFN response, as we have shown previously that temperature-sensitive IFN- α/β responses can alter acute CHIKV infection (Chapter 2). This would also make sense in the context of intracellular viral products driving continual stimulation of IFN- α/β inductive and effector pathways, as has been noted for other persistent viral infections and are proposed for CHIKV inflammatory arthritis (127). To test this, type-I IFN neutralizing antibody or a blocking antibody against the IFN receptor could be administered to chronically-infected mice to assess their effects upon nLuc signal flares either in normal mice or in those stimulated to undergo reserpine-induced flares. Similarly, other components of the immune system such as B cells, T cells, and NK cells could be systematically depleted during chronic CHIKV infection to determine which immune cell types contribute to the control or persistence of CHIKV. Effects of these depletions on the virus could be tracked over time using IVIS in normal mice and in mice with exacerbated acute

infections (e.g. reserpine-treated or IRF7-deficient). Presumably, flaring caused by any of these immune system modulations would be greater in magnitude following a more severe acute infection.

Although temperature reduction at chronic time points resulted in flares in viral signal, we have not yet detected overt signs of MSD typical of the acute phase (i.e. visually evident foot swelling) in any mice, regardless of acute infection severity, although cross-sectional footpad area measurements would be needed to confirm or refute the presence of any swelling. Histological analysis of affected mouse tissues may reveal exacerbated MSD (e.g. edema, cell infiltration, inflammation damage, apoptosis) concurrent with a signal flare, but a model of chronic CHIKV arthritis/arthralgia with the obvious joint pain and swelling observed in humans would be useful in the future. To this end, we will be testing multiple factors that may affect the magnitude and duration of flaring signal as well as much more detailed assessment of the characteristics of the flare to determine if conventional signs of MSD (e.g. foot swelling, histological changes) become apparent in the chronic infection model, possibly dependent upon intensity of signal reactivation. Currently, mouse models of chronic CHIKV disease have been focused on the cellular and molecular underpinnings of viral persistence, and none have assessed disease symptoms such as pain. DigiGate analysis of chronic CHIKV-infected mice with and without viral signal flaring may reveal pain-associated alterations in gate (walking) attributable to chronic CHIKV disease, which would be a valuable parameter to measure 1) the relevance of a mouse model to human disease, and 2) the effectiveness of potential therapeutics aimed at treating CHIKV-associated chronic joint pain.

4.0 CONCLUSIONS

Arboviruses such as CHIKV have evolved to tolerate a broad range of host tissue temperatures due to their transmission cycles through endothermic vertebrate hosts and ectothermic arthropod vectors. In a human host, these viruses encounter variable thermal environments throughout their pathogenesis from the skin into deeper tissues, and control of acute arboviral replication and spread is largely dependent on type-I IFN responses. As CHIKV is able to establish infection and cause chronic disease in distal joint tissues that are lower in temperature than the body core, we questioned whether or not the ability of type-I IFN to control CHIKV and other arboviruses was temperature-dependent. We found that the induction and antiviral efficacy of IFN- α/β was sensitive to changes in ambient temperature, and that transcription of inducible genes in these pathways, but not upstream signaling events, was the main cellular process regulated by temperature. In addition, we found that the interplay between temperature and the type-I IFN response could influence acute and chronic CHIKV infection *in vivo*. This work demonstrates that physiologically-relevant temperature variation can have meaningful impacts on innate immune pathways and potentially influence the severity of viral infections in humans.

4.1 TEMPERATURE-DEPENDENT EFFICACY OF TYPE-I INTERFERON

In Chapter 2, we examined the effect of mildly hypothermic and febrile-range temperatures on the induction and antiviral efficacy of IFN- α/β , and the mechanism leading to observed differences. We conclude that diverse arboviruses are universally more resistant to the IFN-induced antiviral state produced at sub-normal (30°C) temperatures compared to 37°C, and somewhat more sensitive to IFN- α/β treatment at a febrile-range temperature (39°C) *in vitro*. This finding can be explained by the delayed and blunted induction of ISG proteins we observed at 30°C versus 37°C, however, ISG levels at 39°C were modestly and non-uniformly higher than those at 37°C, indicating ISG expression alone may not underlie the enhanced antiviral activity of IFN- α/β at a febrile-range temperature. Both mRNA and protein levels of ISGs were affected by ambient temperature, but upstream JAK-STAT signaling steps including STAT1 phosphorylation and nuclear translocation were not attenuated at 30°C. Thus, we conclude that, along the pathway of establishment of the antiviral state, ISG induction is initially temperature-regulated at the transcription step. We obtained similar results for IFN- α/β gene induction, with bioactive IFN- α/β and IFN- α/β transcript levels both sensitive to ambient temperature, but not the upstream activation of IRF3. We also found that IFNs and ISGs may be somewhat unique in their temperature-sensitive transcription, as LPS-inducible genes did not reliably share the same temperature-regulated phenotype. Finally, we demonstrated that CHIKV replication and MSD can be exacerbated by reducing core temperature in an IFN- α/β -dependent manner in a mouse model of acute CHIKV arthritis. In sum, we conclude that low temperature associated with certain anatomical sites and tissues dampens IFN- α/β responses and provides an advantage for viruses such as CHIKV to replicate and cause disease there. These studies suggest that

exogenous heat application or tolerance of virally-induced fever may prove beneficial for controlling CHIKV or other infections through its enhancement of IFN- α/β .

4.2 IMPACTS OF TEMPERATURE VARIATION AND ACUTE INFECTION SEVERITY ON CHIKUNGUNYA PERSISTENCE

In Chapter 3, we extended our studies of the impact of reduced tissue temperature on acute CHIKV infection *in vivo* to possible effects on viral persistence. We established that adult wild-type mice remain positive for CHIKV reporter protein (nLuc) expression in the infected footpad past four months post-infection using IVIS, indicating their use as a model for chronic CHIKV infections. In addition, we achieved higher persistent nLuc signal using temperature reduction during the acute phase as well as infections of IRF7-deficient mice, supporting the idea that the magnitude of viral replication during the acute phase is predictive of progression to chronic disease, as has been observed in human cases. Finally, we used temperature reduction at chronic time points to cause significant increases in persistent nLuc signal, reminiscent of the flaring chronic arthralgia common in CHIKV patients. We conclude that IVIS is a sensitive method for tracking chronic CHIKV phenotypes and will be useful for further developments of a chronic CHIKV mouse model. In adult wild-type mice, it is likely that CHIKV persists as a RNA entity capable of continued gene expression whose presence may be driving chronic inflammation, but it is unknown if this results in infectious virion production.

4.3 CONCLUDING REMARKS

In conclusion, we have verified previous reports that IFN- α/β responses are attenuated at hypothermic temperatures and revealed that the mechanism of temperature regulation of these responses occurs at the transcription of the IFN- α/β genes and ISGs. We also showed increased efficacy of IFN- α/β against arboviruses at a fever-range temperature. In a mouse model of CHIKV, temperature reduction exacerbated viral replication during the acute phase and caused flares in viral reporter signal during the chronic phase, indicating that temperature variation can impact the pathogenesis of CHIKV *in vivo*. These studies contribute to our understanding of how environmental factors such as temperature can influence innate immune responses and impact viral infection.

5.0 MATERIALS AND METHODS

Cell lines

Baby Hamster Kidney (BHK-21) cells (ATCC; RRID CVCL_1915) and L929 murine fibrosarcoma cells (RRID CVCL_0462) were maintained in RPMI-1640 supplemented with 10% donor calf serum (DCS) and 10% tryptose phosphate broth (TBP). RAW264.7 murine monocyte/macrophage (RRID CVCL_0493), African Green Monkey Kidney (Vero; RRID CVCL_0059), and human cervical carcinoma (HeLa; ATCC; RRID CVCL_0058) cells were maintained in Dulbecco's modified Eagle's medium (DMEM) supplemented with 10% fetal calf serum (FCS). MEF/3T3 Tet-Off murine embryonic fibroblasts (simply called MEFs throughout; Clontech; CVCL_KS91) and immortalized primary MEFs from *Ifnar1*^{-/-} animals (MEF isolation and immortalization are described in (649)) were maintained in DMEM containing 10% FCS, 100 mM HEPES buffer, 0.075% sodium bicarbonate, and 0.05 mg/mL G418 sulfate (Mediatech). All media also contained 100 U/mL penicillin G sodium and 100 µg/mL streptomycin sulfate. Except for instances of experimental temperature variation, all cells were grown at 37°C in a humidified chamber with 5% CO₂.

Primary cell cultures

Primary murine osteoblast cultures were generated from 3- to 5-day old suckling CD1 mice and maintained as described previously (117). Briefly, dissected calvaria were triply digested with

collagenase P and cultured for 5 days in AMEM containing 15% FCS at 37°C and 5% CO₂ in a humidified chamber to allow osteoblast outgrowth. Osteoblasts were detached by trypsinization, strained to remove bone fragments, seeded into 150-mm culture dishes and allowed to expand under the same growth conditions as above. Upon reaching confluency, the osteoblasts were trypsinized and seeded into multiwell plates for experimentation.

Virus stocks

cDNA clones of SINV-TR339 (650), CHIKV-LR (651), EEEV-FL93-939 (626), and VEEV-ZPC738 (652) have been described. Mutant viruses SINV-nsP2-726G (653), VEEV-CD-nsP2-739L (116), and CHIKV-E2-79K (654) were generated by site-directed mutagenesis with appropriate overlapping primers and Quikchange kit (Agilent) according to the manufacturer's instructions. The nanoluciferase-expressing CHIKV-LR-nluc-TaV and CHIKV-LR-E2-79K-nluc-TaV viruses are described in (613). To generate virus stocks, infectious, capped RNA was generated by *in vitro* transcription from linearized clones (mMessage mMachine; Ambion) and electroporated into BHK-21 cells using a GenePulser II (Biorad) as previously described (655). Virus-containing supernatants were collected after 24 hours and titered on BHK-21 cells using a standard plaque assay. The DENV-2 strain 16681 was a gift from Jared Evans. Viral stocks were generated from a single passage on C6/36 mosquito cells and titers were determined by focus forming assay on human hepatocarcinoma Huh7 cells using anti-flavivirus D1-4G2-4-15 antibody (ATCC). The YFV-Angola strain was a gift from Alan Barrett and stocks were made and titered as described (435). Experiments involving RFVF strain ZH501 (656) were conducted in the laboratory of Dr. Amy Hartman. Propagation and titration of this virus is described in (657).

Animals

All experiments involving animals were carried out under approval of the Institutional Animal Care and Use Committee of the University of Pittsburgh and in accordance with the recommendations found in the Guide for the Care and Use of Laboratory Animals published by the National Institutes of Health. 5-6-week-old adult male and female C57BL/6 mice were purchased from Jackson Laboratories (RRID IMSR_JAX:000664) and 5-7-week-old adult male and female *Ifnar1*^{-/-} mice on the C57BL/6 background were bred in-house. Mice were housed socially (maximum 5/cage for females and 4/cage for males) in SPF microisolator cages in our ABSL3 facility. Animals were kept on a 12-hour light/12-hour dark cycle with access to food and water *ad libitum* except in instances of experimental induction of metabolic torpor (detailed below). All mice weighed between 15 and 25 grams and were drug and test naïve prior to use in these studies. Prior to and upon initiation of experiments, all mice were weighed and checked for disease signs (lethargy, ruffled fur, hunching) daily to ensure maximal animal welfare in accordance with approved IACUC procedures. Animals of both sexes were divided randomly into experimental groups, such that experiments reflect pooled data from both sexes.

Antibodies and other reagents

The following antibodies were used for Western blotting and/or immunostaining: mouse anti- β -actin (BA3R; Invitrogen; RRID AB_10979409), rabbit anti-STAT1 (M-22; Santa Cruz; RRID AB_632434), rabbit anti-ISG15 (H-150; Santa Cruz; RRID AB_2126309), rabbit anti-IFIT1 (Invitrogen CAT# PA5-27907 for human/nonhuman primate samples; RRID AB_2545383), rabbit anti-IFIT1 (Invitrogen CAT# PA3-846 for murine samples; RRID AB_1958734), rabbit

anti-phospho-STAT1 (Tyr-701) (#9171; Cell Signaling Technology; used for Western blots; RRID AB_561284), rabbit anti-phospho-STAT1 (Tyr-701) (D4A7; Cell Signaling Technology; used for immunofluorescence; RRID AB_10950970), rabbit anti-phospho-STAT1 (Ser-727) (#9177; Cell Signaling Technology; RRID AB_2197983), rabbit anti-phospho-IRF3 (Ser-396) (#29047; Cell Signaling Technology). Anti-flavivirus group antigen D1-4G2-4-15 (ATCC HB-112 hybridoma; RRID CVCL_J890) and mouse anti-YFV ascites fluid were used in flavivirus focus-forming assays. Human and murine IFNs α 4 and β were prepared in-house as described (607). Lipopolysaccharides (LPS) from *E. coli* 0111:B4 were purchased from Sigma. Poly-I:C was purchased from R&D Systems.

Treatment of cells with IFN- α / β , LPS, poly-I:C, and virus

For experiments involving IFN or LPS treatment of cells, IFN- α / β (1:1 ratio of IFN- α 4 to IFN- β ; called IFN- α / β throughout) or LPS was applied directly to cells in media pre-warmed to room temperature or 30°C. IFN- α / β dosages selected for individual experiments represent the range of concentrations of IFN- α / β empirically determined to elicit robust ISG induction as well as observable dose-dependent anti-arboviral activity. The required dosage, then, necessarily varied according to the cell type used, the IFN- α / β sensitivity of individual viruses, murine vs. human, and the experimental aim. Dosages used for specific experiments are noted in the text and figure legends. LPS was used at a concentration of 250 ng/mL. After addition of the stimulus, cells were moved immediately to the appropriate temperature treatments and the stimulus was left until sample collection. For experiments involving poly-I:C treatment of cells, 50 μ g poly-I:C was transfected into MEF cells using the Neon Transfection system (Invitrogen) at room temperature according to the manufacturer's instructions and recommended settings. Pooled

transfections were then divided among temperature conditions. For experiments involving virus infection at different temperatures, all infections were performed for 1 hour at 30°C to minimize temperature-dependent variation in attachment and entry efficiency, unless otherwise noted. Cells were then washed in PBS and placed in fresh growth media before being placed in different temperature conditions.

Viral growth curves

Vero, MEF, or primary murine osteoblast cells were treated for 12-16 hours at 30, 37, or 39°C with 0 or 100-1000 IU/mL human (Vero) or murine (MEF/osteoblast) IFN- α/β , rinsed in room-temperature PBS, and infected at a multiplicity of infection (MOI) of 0.1 as described above. Supernatants were harvested at the indicated time points and viral growth was determined by plaque assay on BHK-21 cells for alphaviruses, by focus-forming assay on Vero cells for flaviviruses, and by plaque assay on Vero cells for RVFV. All quantification assays were performed at 37°C.

CPE inhibition assays

Vero cells were treated for 12-16 hours at 30, 34, 37, or 39°C with 2-fold decreasing concentrations of human or mouse IFN- α/β in 96-well plates, beginning with 4000 IU. Cells were then infected at a MOI of 10 and returned to the original temperature condition for 96 hours. The concentration of IFN- α/β necessary to inhibit 50% of cell death was determined visually by crystal violet staining.

Western blotting

Protein lysates were taken in radioimmunoprecipitation assay (RIPA) buffer (50 mM Tris, pH 7.4; 150 mM NaCl, 1% NP-40, 0.5% sodium deoxycholate, 0.1% sodium dodecyl sulfate (SDS), 1 mM EDTA, 1 mM EGTA) supplemented with protease inhibitors (1 mM phenylmethylsulfonyl fluoride, 1 µg/mL leupeptin, 1 µg/mL pepstatin), and a phosphatase inhibitor cocktail (Sigma). Protein concentrations were determined by bicinchoninic acid (BCA) assay (Pierce) according to the manufacturer's instructions. Equal amounts of protein (15 µg) per sample were resolved by SDS-PAGE on a 10% polyacrylamide gel and proteins were transferred to a PVDF membrane (BioRad). Membranes were blocked in Tris-buffered saline with 0.1% Tween-20 (TBS-T) containing 5% milk for at least 1 hour. Primary antibody was diluted in TBS-T containing 3% bovine serum albumin (BSA) and applied to membranes overnight at 4°C, then washed 4x in TBS-T (15 minutes per wash) and replaced with horseradish peroxidase (HRP)-conjugated secondary antibody, diluted in a 2% milk/TBS-T solution. Secondary antibody was incubated at room temperature for at least 1 hour at room temperature or overnight at 4°C, then washed 4x in TBS-T, as above. Finally, membranes were exposed to Pierce ECL Western Blotting Substrate and signal was captured on x-ray film (GE Healthcare). Densitometry analysis was performed using ImageJ software (NIH).

Quantitative PCR and NanoString

Total cellular RNA was isolated from samples taken in TRIzol reagent (Ambion) per the manufacturer's protocol using 1-Bromo-3-chloropropane (BCP) and isopropanol. For qRT-PCR, 10 µg of RNA per sample was reverse-transcribed into cDNA using random hexamer primers and semi-quantitative PCR was performed using the Sybr Green method on an ABI 7900 Real-Time PCR machine (Applied Biosystems) using gene-specific primers. See Table 1 for a

complete list of primer sequences. Ct values were normalized to 18S rRNA and compared using the $\Delta\Delta C_t$ method (658).

Table 1. List of primers used for qRT-PCR.

Gene Name	Sense (5' → 3')	Antisense (5' → 3')
Primate <i>STAT1</i>	CACGCACACAAAAGTGATGA	ACATGTTTCAGCTGGTCCACA
Primate <i>IFIT1</i>	TCTCAGAGGAGCCTGGCTAAG	CCACACTGTATTTGGTGTCTAGG
Primate <i>ISG20</i>	CTCCTGCACAAGAGCATCCA	CGTTGCCCTCGCATCTTC
Primate <i>ISG15</i>	CACCGTGTTTCATGAATCTGC	CTTTATTTCCGGCCCTTGAT
Murine <i>Stat1</i>	TTCAGAGCTCCTTCGTGGT	TCGACTCTTGCAATTCACC
Murine <i>Ifit1</i>	TGGCTCACATAGAGCAGGA	AGTTTCTCCAAGCAAAGGA
Murine <i>Gbp2</i>	TGAGAAGGGTGACAACCAGA	AGCTCCGTCACATAGTGCAG
Murine <i>Isg20</i>	GGCACTGAGACAGGGCTT	CCATGGATGTTTACAATGCT
Murine <i>Il6</i>	TTCCATCCAGTTGCCTTCTT	CAGAATTGCCATTGCACAAC
Murine <i>Tlr2</i>	ACAACCTTACCGAAACCTCAGAC	ACCCAGAAAGCATCACATG
Murine <i>Irf5</i>	CACCTCAGCCGTACAAGATC	GCCTGGTAGCATTCTCTGG
Murine <i>Ccl2</i>	GTCCCTGTCATGCTTCTGG	GCTCTCCAGCCTACTCATTG
Murine <i>Relb</i>	GCTGTACTTGCTCTGTGACA	TGGCGTTTTGAACACAATGG
Murine <i>Cxcl10</i>	TCAGCACCATGAACCCAAG	CTATGGCCCTCATTCTCACTG
Murine <i>Nfkbiz</i>	GGAATAAGAGCCTGGTAGACAC	AAGAGGCGAATGAGTTCAG
Murine <i>Tnfaip3</i>	ACAGGACTTTGCTACGACAC	CTGAGGATGTTGCTGAGGAC
Murine Gamma Actin Intron #3	ACAGAACGCAAGCAGAAACG	TGGCATTTCCTCCCTGAAGC
Murine <i>Ifnb</i>	GAACATTTCGGAAATGTCAGG	ACTGTCTGCTGGTGGATGTC
Murine <i>Ifna4</i>	CTGCTGGCTGTGAGGAAATA	GAAGACAGGGCTCTCCAGAC
18S rRNA	CGCCGCTAGAGGTGAATTTCT	CGAACCTCCGACTTTCGTTCT

For NanoString, 100 ng RNA from each sample was subjected to fluorescent probe hybridization (see Table 2 for complete list of gene targets and probe sequences) and fluorescent barcodes corresponding to individual target mRNA molecules were counted automatically with a nCounter Analysis System (NanoString Technologies). All mRNA quantification steps were performed by the Genomics Research Core at the University of Pittsburgh. Raw mRNA counts for each target gene underwent background subtraction and housekeeping gene normalization using nSolver 2.6 software (NanoString Technologies).

Table 2. List of NanoString target genes and probe locations

Gene Name	Accession Number	Probe Position
β -Actin	NM_007393.3	42-141
γ -Actin	ENSMUST00000071555.2	1090-1189
ADAR1	NM_001146296.1	24-123
AKT1	NM_001165894.1	899-998
AKT2	NM_001110208.1	2505-2604
ATF-1	NM_007497.3	1217-1316
CCL2	NM_011333.3	416-515
CCL5	NM_013653.1	166-265
IKK α	NM_001162410.1	223-322
CIRP	NM_007705.2	203-302
CREB1	NM_001037726.1	2735-2834
CREBBP	NM_001025432.1	3771-3870
CSE1L	NM_023565.3	907-1006
CXCL1	NM_008176.1	561-660
CXCL10	NM_021274.1	116-215
eEF2	NM_007907.2	1520-1619
eEF2K	NM_007908.3	1167-1266
PKR	NM_011163.4	407-506
PERK	NM_010121.3	503-602
eIF2 α	NM_026114.3	666-765
eIF3 α	NM_010123.3	755-854
eIF4A1	NM_144958.4	1006-1105
eIF4E	NM_007917.3	697-796
eIF4EBP1	NM_007918.3	555-654
eIF4EBP2	NM_010124.2	236-335
eIF4G1	NM_145941.3	1981-2080
p300	NM_177821.6	4306-4405
c-fos	NM_010234.2	1331-1430
GAPDH	NM_008084.2	216-315
GBP2	NM_010260.1	1997-2096
GBP1	NM_010259.2	677-776
HSP90ab1	NM_008302.3	1355-1454
HSP70	NM_010478.2	2470-2569
IFI27	NM_026790.2	167-266
IFI44	NM_133871.2	991-1090
IFI47	NM_008330.1	710-809
IFIT1	NM_008331.2	891-990
IFIT2	NM_008332.2	231-330
IFIT3	NM_010501.1	1291-1390
IFITM1	NM_001112715.1	413-512

IFN α 4	NM_010504.2	262-361
IFNAR1	NM_010508.1	1196-1295
IFNAR2	NM_001110498.1	726-825
IFN β	NM_010510.1	336-435
IKK β	NM_010546.2	499-598
IKK ϵ	NM_019777.3	619-718
IKK γ	NM_178590.2	526-625
IL6	NM_031168.1	41-140
IRAK1	NM_008363.2	952-1051
IRAK4	NM_029926.5	251-350
IRF1	NM_008390.1	366-465
IRF2	NM_008391.2	441-540
IRF3	NM_016849.4	527-626
IRF5	NM_001252382.1	491-590
IRF7	NM_016850.2	706-805
IRF9	NM_008394.2	1406-1505
ISG15	NM_015783.1	396-495
ISG20	NM_020583.5	553-652
JAK1	NM_146145.2	4081-4180
c-jun	NM_010591.2	2213-2312
Importin α 1	NM_008465.5	2671-2770
Importin β 1	NM_008379.3	5136-5235
MEK	NM_008927.3	1696-1795
MAP2K3	NM_008928.4	1116-1215
MAP2K6	NM_011943.2	321-420
TAK1	NM_009316.1	823-922
ERK2	NM_011949.3	1211-1310
p38 α	NM_011951.2	1421-1520
ERK1	NM_011952.2	826-925
MCM5	NM_008566.2	2610-2709
MKKNK1	NM_021461.4	636-735
MKKNK2	NM_021462.3	2877-2976
mTOR	NM_020009.2	2433-2532
MX1	NM_010846.1	2486-2585
MX2	NM_013606.1	2096-2195
MyD88	NM_010851.2	1596-1695
I κ B α	NM_010907.1	941-1040
Nf κ biz	NM_030612.1	1306-1405
OAS1a	NM_145211.2	472-571
OAS2	NM_145227.3	1149-1248
PABP	NM_008774.3	863-962
PAP	NM_011112.3	4117-4216
PIAS1	NM_019663.3	1291-1390

PIAS3	NM_001165949.1	1137-1236
PI3K p100 α	NM_008839.1	1256-1355
PI3K p85	NM_001024955.1	5665-5764
POLR2A	NM_001291068.1	2769-2868
PKC δ	NM_011103.2	1266-1365
PSMB9	NM_013585.2	541-640
PTPN1	NM_011201.3	510-609
SHP-2	NM_011202.3	3711-3810
PTPN2	NM_001127177.1	1013-1112
SHP-1	NM_013545.2	1692-1791
Ran	NM_009391.3	1756-1855
RBM3	NM_001166409.1	537-636
cRel	NM_009044.2	1291-1390
RelA	NM_009045.4	646-745
RelB	NM_009046.2	2014-2113
18S rRNA	NR_003278.3	1019-1118
RnaseL	NM_011882.2	2387-2486
RPS6	NM_009096.3	1196-1295
S6K1	NM_028259.4	1079-1178
Viperin	NM_021384.4	341-440
SOCS1	NM_009896.2	1021-1120
SOCS3	NM_007707.2	586-685
STAT1	NM_009283.3	1591-1690
STAT2	NM_019963.1	363-462
STAT3	NM_213659.2	2131-2230
TBK1	NM_019786.4	441-540
TBP	NM_013684.3	71-170
TRIF	NM_174989.4	2160-2259
TRAM	NM_173394.2	1244-1343
TIRAP	NM_001177845.1	1109-1208
TLR2	NM_011905.2	256-355
TLR4	NM_021297.2	2511-2610
TNF α IP3	NM_009397.2	233-332
TRADD	NM_001033161.2	563-662
TRAF3	NM_011632.3	885-984
TRAF6	NM_009424.2	981-1080
β -Tubulin	NM_009451.3	1820-1919
Tyk2	NM_001205312.1	1533-1632
USP18	NM_011909.2	1191-1290
Exportin 1	NM_134014.3	1905-2004
ZAP	NM_028864.2	2586-2685

Biological interferon assays

Concentrations of biologically active murine IFN- α/β was measured by bioassay as previously described (659). Briefly, supernatants or serum samples (200 μ L) were acidified to pH 2.0 with 2N HCl overnight at 4°C and then neutralized to pH 7.4 using 2N NaOH. Samples were serially diluted 2-fold across 96-well plates seeded with L929 cells and incubated at 37°C for 24 hours. Cells were then infected with 3×10^4 plaque-forming units (pfu) per well of encephalomyocarditis virus (EMCV) and incubated for an additional 24 hours at 37°C prior to fixation and staining with crystal violet. The concentration of IFN- α/β in each sample was calculated from the dilution required to protect 50% of cells from CPE, compared with a standard IFN- α/β dilution series of known concentrations.

Immunofluorescence

IFN- α/β - or poly-I:C-treated cells seeded on glass microscope slides were fixed in 4% paraformaldehyde at 4°C for at least 1 hour at the indicated times post-stimulation. Cells were permeabilized in 100% methanol at -20°C for 10 minutes and blocked in blocking buffer (phosphate-buffered saline with 3% BSA and 0.1% Triton X-100) containing 10% normal serum corresponding to the species of the secondary antibody for at least 1 hour at room temperature. Cells were then incubated overnight at 4°C with primary antibody diluted in blocking buffer, washed, and incubated with fluorescently-labeled secondary antibody and DAPI nuclear stain for 1 hour at room temperature. Images were acquired on a Nikon A1 Confocal microscope or an Olympus CKX41 inverted epifluorescence microscope. Image analysis was performed in NIS Elements v4.51.00. The DAPI channel was used to create a binary mask that identified both the nuclear location and individual cells. The intensity of the STAT-p channel for all pixels within

the nuclear mask was summed and then divided by the total number of pixels to produce the mean STAT-p signal per nucleus expressed as arbitrary fluorescence units (AFU). Mean STAT-p signal was plotted for individual cells.

Protein radiolabel

MEF cells were incubated at 30, 37, or 39°C for 1 or 12 hours. At each time point, growth media was replaced with labeling media (DMEM lacking cysteine and methionine (Cellgro) supplemented with 1% FBS and 1% Pen-Strep), and cells were returned to their temperature conditions for 15 minutes. Supernatants were then replaced with labeling media containing 100 μ Ci/mL [³⁵S]-cys/met (MP Biomedicals) and plates were returned to their temperature conditions for another 15 minutes. Cells were rinsed in PBS and lysates were prepared with equal volumes of RIPA buffer. 20 μ L per sample was resolved on an 8% SDS-PAGE gel, which was then fixed and dried to allow for autoradiographic signal capture of x-ray film (GE Healthcare). Gels were exposed for 7 days at -80°C and resulting protein signal was quantified by densitometry analysis of all visible proteins in each lane using ImageJ software (NIH).

Translation reporters

Construction and production of host-mimic firefly luciferase-expressing mRNA translation reporter constructs have been described (385, 660, 661). MEFs or *Infar1*^{-/-} MEFs were transfected with 5 μ g RNA reporter per reaction using the Neon transfection system (Invitrogen) according to the manufacturer's instructions and recommended settings. Single transfections were divided among 30, 37, and 39°C temperature treatments for the appropriate time course and cell lysates were collected in passive lysis buffer (Promega). Firefly luciferase activity was

quantified using the Dual Luciferase Reporter assay kit (Promega) and light production measured on an Orion Microplate Luminometer (Berthold). Relative light unit (RLU) values were normalized to protein concentration in each sample, as determined by bicinchoninic acid assay (Pierce). Data are expressed at RLU/ μ g protein.

Mouse core temperature reduction and infection

5-6-week-old male and female C57BL/6 mice (Jackson Laboratories), *Ifnar1*^{-/-} or *Irf7*^{-/-} mice (bred in-house) were used for all experiments. For induction of metabolic torpor, mice were housed for 4.5 days in 24-hour low red light before torpor was induced by food withdrawal. Non-torpid mice were also housed in red light but had access to food and water *ad libitum*. Food and normal light conditions (12h light/12h dark) were restored 48 hours after food withdrawal. For pharmacological temperature reduction, mice were given 300 μ L intraperitoneal injections of 1.5-2 mg/kg reserpine (U.S. Pharmacopeia Standard; Sigma) dissolved in 0.5% acetic acid. Reserpine solutions were prepared fresh by first dissolving the powder in 100% glacial acetic acid and then diluting to the desired concentration in sterile ddH₂O. Final reserpine solutions underwent 0.22-micron filter sterilization before being injected into mice. Mice were given 0.5 mg/kg booster doses as needed (when subcutaneous scruff temperature exceeded 30°C) to maintain core temperature reduction throughout an experiment. Control mice were given equal volumes of sterile 0.5% acetic acid only. Isoflurane-anesthetized mice were infected with 1000 p.f.u. CHIKV-LR, CHIKV-LR-E2-79K, CHIKV-LR-E2-200R, SINV-TR339, or nanoluciferase (nLuc)-TaV viruses (described in (613)) in a 10 μ L volume injected subcutaneously into the left rear footpad. For torpor experiments, infections took place 12 hours after food withdrawal. For reserpine experiments, infections were done 3 hours after reserpine treatment. All mice were

weighed and monitored for disease signs daily. Musculoskeletal disease in infected feet was quantified every 12 to 24 hours as described (93).

On days 2 and 6 post-infection, groups of mice were sacrificed by isoflurane overdose and blood samples were collected by cardiac puncture before perfusion of tissues with PBS. Perfused tissues were extracted and homogenized, and viral load in each tissue was determined by plaque assay on BHK-21 cells. Serum was separated from whole blood samples using microtainer tubes (BD Biosciences) and IFN- α/β concentrations were determined by biological IFN- α/β assay, as described above.

***In vivo* bioluminescence imaging**

Mice were anesthetized with a low-dose continuous stream of isoflurane using the Xenogen XGI-8 Gas Anesthesia System (Caliper Life Sciences). The nLuc substrate furimazine (Nano-Glo Luciferase Assay System; Promega) was diluted in sterile DPBS without Ca²⁺ and Mg²⁺ (Corning) and injected subcutaneously in the scruff (5 μ L substrate in 500 μ L total volume per mouse) and allowed to circulate for 4 minutes. After 4 minutes, bioluminescence was imaged using an IVIS Spectrum CT instrument (PerkinElmer). Exposure time was determined automatically according to signal strength using Living Image Acquisition Software (PerkinElmer). Resulting pseudocolored images, normalized for exposure time, were marked with regions of interest (ROIs) around the hind feet of each mouse, and luciferase signal was quantitated as average radiance (photons/sec/cm²/sr) in each ROI using Living Image software (PerkinElmer).

Quantification and statistical analysis

Statistical significance for all experiments was determined using GraphPad PRISM software. Results were declared statistically significant when p was less than or equal to 0.05, for all statistical tests employed across experiments. Specific tests used as well as demarcations of additional levels of significance are detailed in the figure legends. All experiments were performed with at least two replicate samples per group, and all experiments were performed at least twice to confirm results, except for the NanoString analysis, which was performed once and select results were confirmed by qPCR. Data from single representative experiments are shown in the figures, and pooled data are presented as either mean \pm SD or geometric mean \pm geometric SD as appropriate.

APPENDIX A

ABBREVIATIONS GLOSSARY

AKT – protein kinase B

APC – antigen-presenting cell

AP-1 – activator protein 1

Arbovirus – arthropod-borne virus

C – capsid protein

CARD – caspase recruitment domain

CBP – CREB binding protein

CCHFV – Crimean-Congo hemorrhagic fever virus

CHIKV – chikungunya virus

CIRP – cold-inducible RNA binding protein

Crk – CT-10 regulator of kinase

DC – dendritic cell

DENV – dengue virus

DLN – draining lymph node

DPI – days post infection

dsRNA – double-stranded RNA

E1/E2/E3 – alphavirus envelope proteins

ECSA – East/Central/South African

EEEV – eastern equine encephalitis virus

eIF – eukaryotic initiation factor

GAS – gamma interferon activated site

GCN5 – gene control non-derepressible 5

HAT – histone acetyltransferase

HDAC – histone deacetylase

HIV – human immunodeficiency virus

HMG – high mobility group

HSP – heat shock protein

IFIT – interferon-inducible protein with tetraco peptide repeat

IFITM – interferon-induced transmembrane

IFN – interferon

IFNAR – IFN- α receptor

Ig – immunoglobulin

IKK ϵ – inhibitor of NF κ B kinase subunit epsilon

IL – interleukin

IOL – Indian Ocean lineage

IRF – interferon regulatory factor

ISG – interferon-stimulated gene

ISG15 – interferon-stimulated gene 15 kDa

ISG20 – interferon-stimulated gene 20 kDa

ISGF3 – interferon-stimulated gene factor 3

ISRE – interferon-stimulated response element

IVIS – *in vivo* imaging system

JAK – Janus kinase

JEV – Japanese encephalitis virus

LACV – LaCrosse virus

LGP2 – laboratory of genetics and physiology 2

LPS – lipopolysaccharide

MAPK – mitogen activated protein kinase

MAVS – mitochondrial antiviral signaling protein

MCM – minichromosome maintenance

MCP – macrophage chemoattractant protein

MDA5 – melanoma differentiation associated protein 5

MOI – multiplicity of infection

mRNA – messenger RNA

MSD – musculoskeletal disease

mTOR – mammalian target of rapamycin

Mx – myxomavirus resistance protein

MyD88 – myeloid differentiation primary response 88

NFκB – nuclear factor kappa-light chain-enhancer of activated B cells

NHP – nonhuman primate

NK – natural killer cell

NLS – nuclear localization signal

nLuc – nanoluciferase

nsP – nonstructural protein

OAS – oligoadenylate synthetase

ONNV – o'nyong'nyong virus

PAMP – pathogen-associated molecular pattern

PI3K – phosphatidylinositol-3-kinase

PIAS – protein inhibitor of activated STAT

PKC – protein kinase C

PKR – interferon-induced double-stranded RNA-activated protein kinase

Poly-A – polyadenylate

PRD – positive regulatory domain

PRR – pattern recognition receptor

qRT-PCR – quantitative reverse-transcription polymerase chain reaction

RA – rheumatoid arthritis

RAP1 – Ras-proximate 1

RBM3 – RNA binding motif protein 3

RdRp – RNA-dependent RNA polymerase

RES – reserpine

RIG-I – retinoic acid-inducible gene I

RLR – RIG-I-like receptor

RNaseL – ribonuclease latent

ROI – region of interest

RRV – Ross River virus

RVFV – Rift Valley fever virus

Ser – serine

SINV – Sindbis virus

SOCS – suppressor of cytokine signaling

ssRNA – single-stranded RNA

STAT – signal transducer and activator of transcription

TBEV – tick-borne encephalitis virus

TBK1 – TANK-binding kinase 1

TFIID – transcription factor II D complex

TF – transframe protein

TIR – toll/IL-1 receptor

TLR – toll-like receptor

TNF – tumor necrosis factor

TRAF – TNF receptor-associated factor

TRIF – TIR-domain containing adapter inducing interferon- β

Tyk2 – tyrosine kinase 2

Tyr – tyrosine

USP18 – ubiquitin-specific peptidase 18

VEEV – Venezuelan equine encephalitis virus

Viperin – virus inhibitory protein, endoplasmic reticulum-associated, interferon-inducible

WNV – West Nile virus

YFV – yellow fever virus

ZAP – zinc finger antiviral protein

ZIKV – zika virus

BIBLIOGRAPHY

1. Organization WSGoA-BaR-BVDWH. 1985. Arthropod-borne and rodent-borne viral diseases. Report of a WHO Scientific Group. World Health Organ Tech Rep Ser 719:1-116.
2. Kuno G, Chang GJ. 2005. Biological transmission of arboviruses: reexamination of and new insights into components, mechanisms, and unique traits as well as their evolutionary trends. *Clin Microbiol Rev* 18:608-37.
3. Cleton N, Koopmans M, Reimerink J, Godeke GJ, Reusken C. 2012. Come fly with me: review of clinically important arboviruses for global travelers. *J Clin Virol* 55:191-203.
4. Weaver SC, Reisen WK. 2010. Present and future arboviral threats. *Antiviral Res* 85:328-45.
5. Prinzinger R, Preßmar A, Schleucher E. 1991. Body temperature in birds. *Comparative Biochemistry and Physiology Part A: Physiology* 99:499-506.
6. Strauss JH, Strauss EG. 1994. The Alphaviruses: Gene Expression, Replication, and Evolution. *Microbiological Reviews* 58:491-562.
7. Paredes AM, Simon MN, Brown DT. 1992. The mass of the Sindbis virus nucleocapsid suggests it has T = 4 icosahedral symmetry. *Virology* 187:329-32.
8. Paredes AM, Brown DT, Rothnagel R, Chiu W, Schoepp RJ, Johnston RE, Prasad BV. 1993. Three-dimensional structure of a membrane-containing virus. *Proc Natl Acad Sci U S A* 90:9095-9.
9. Cheng RH, Kuhn RJ, Olson NH, Rossmann MG, Choi HK, Smith TJ, Baker TS. 1995. Nucleocapsid and glycoprotein organization in an enveloped virus. *Cell* 80:621-30.
10. Rice CM, Strauss JH. 1982. Association of sindbis virion glycoproteins and their precursors. *J Mol Biol* 154:325-48.
11. Ziemiecki A, Garoff H. 1978. Subunit composition of the membrane glycoprotein complex of Semliki Forest virus. *J Mol Biol* 122:259-69.

12. Fuller SD. 1987. The T=4 envelope of Sindbis virus is organized by interactions with a complementary T=3 capsid. *Cell* 48:923-34.
13. Hefti E, Bishop DHL, Dubin DT, Stollar V. 1976. 5' Nucleotide Sequence of Sindbis Viral RNA. *J Virol* 17:149-59.
14. Donaghue TP, Faulkner P. 1973. Characterisation of the 3'-terminus of Sindbis virion RNA. *Nat New Biol* 246:168-70.
15. Raju R, Hajjou M, Hill KR, Botta V, Botta S. 1999. In vivo addition of poly(A) tail and AU-rich sequences to the 3' terminus of the Sindbis virus RNA genome: a novel 3'-end repair pathway. *J Virol* 73:2410-9.
16. Hyde JL, Chen R, Trobaugh DW, Diamond MS, Weaver SC, Klimstra WB, Wilusz J. 2015. The 5' and 3' ends of alphavirus RNAs--Non-coding is not non-functional. *Virus Res* 206:99-107.
17. Simmons DT, Strauss JH. 1972. Replication of Sindbis virus. I. Relative size and genetic content of 26 s and 49 s RNA. *J Mol Biol* 71:599-613.
18. Chen R, Mukhopadhyay S, Merits A, Bolling B, Nasar F, Coffey LL, Powers A, Weaver SC, Ictv Report C. 2018. ICTV Virus Taxonomy Profile: Togaviridae. *J Gen Virol* 99:761-762.
19. Powers AM, Brault AC, Shirako Y, Strauss EG, Kang W, Strauss JH, Weaver SC. 2001. Evolutionary relationships and systematics of the alphaviruses. *J Virol* 75:10118-31.
20. La Linn M, Gardner J, Warrilow D, Darnell GA, McMahon CR, Field I, Hyatt AD, Slade RW, Suhrbier A. 2001. Arbovirus of marine mammals: a new alphavirus isolated from the elephant seal louse, *Lepidophthirus macrorhini*. *J Virol* 75:4103-9.
21. Suhrbier A, Jaffar-Bandjee MC, Gasque P. 2012. Arthritogenic alphaviruses--an overview. *Nat Rev Rheumatol* 8:420-9.
22. Zacks MA, Paessler S. 2010. Encephalitic alphaviruses. *Vet Microbiol* 140:281-6.
23. McLoughlin MF, Graham DA. 2007. Alphavirus infections in salmonids--a review. *J Fish Dis* 30:511-31.
24. Nasar F, Palacios G, Gorchakov RV, Guzman H, Da Rosa AP, Savji N, Popov VL, Sherman MB, Lipkin WI, Tesh RB, Weaver SC. 2012. Eilat virus, a unique alphavirus with host range restricted to insects by RNA replication. *Proc Natl Acad Sci U S A* 109:14622-7.
25. Weaver SC, Powers AM, Brault AC, Barrett AD. 1999. Molecular epidemiological studies of veterinary arboviral encephalitides. *Vet J* 157:123-38.

26. Powers AM, Oberste MS, Brault AC, Rico-Hesse R, Schmura SM, Smith JF, Kang W, Sweeney WP, Weaver SC. 1997. Repeated emergence of epidemic/epizootic Venezuelan equine encephalitis from a single genotype of enzootic subtype ID virus. *J Virol* 71:6697-705.
27. Silva ML, Galiza GJ, Dantas AF, Oliveira RN, Iamamoto K, Achkar SM, Riet-Correa F. 2011. Outbreaks of Eastern equine encephalitis in northeastern Brazil. *J Vet Diagn Invest* 23:570-5.
28. Rivas F, Diaz LA, Cardenas VM, Daza E, Bruzon L, Alcala A, De la Hoz O, Caceres FM, Aristizabal G, Martinez JW, Revelo D, De la Hoz F, Boshell J, Camacho T, Calderon L, Olano VA, Villarreal LI, Roselli D, Alvarez G, Ludwig G, Tsai T. 1997. Epidemic Venezuelan equine encephalitis in La Guajira, Colombia, 1995. *J Infect Dis* 175:828-32.
29. Deresiewicz RL, Thaler SJ, Hsu L, Zamani AA. 1997. Clinical and neuroradiographic manifestations of eastern equine encephalitis. *N Engl J Med* 336:1867-74.
30. Armstrong PM, Andreadis TG. 2013. Eastern equine encephalitis virus--old enemy, new threat. *N Engl J Med* 368:1670-3.
31. Ronca SE, Dineley KT, Paessler S. 2016. Neurological Sequelae Resulting from Encephalitic Alphavirus Infection. *Front Microbiol* 7:959.
32. de la Monte S, Castro F, Bonilla NJ, Gaskin de Urdaneta A, Hutchins GM. 1985. The systemic pathology of Venezuelan equine encephalitis virus infection in humans. *Am J Trop Med Hyg* 34:194-202.
33. Weaver SC, Lecuit M. 2015. Chikungunya virus and the global spread of a mosquito-borne disease. *N Engl J Med* 372:1231-9.
34. Brinton MA. 1986. Replication of Flaviviruses, p 327-374. *In* Schlesinger S, Schlesinger MJ (ed), *The Togaviridae and Flaviviridae* doi:10.1007/978-1-4757-0785-4_11. Springer New York, Boston, MA.
35. Zhang W, Chipman PR, Corver J, Johnson PR, Zhang Y, Mukhopadhyay S, Baker TS, Strauss JH, Rossmann MG, Kuhn RJ. 2003. Visualization of membrane protein domains by cryo-electron microscopy of dengue virus. *Nat Struct Biol* 10:907-12.
36. Rey FA, Heinz FX, Mandl C, Kunz C, Harrison SC. 1995. The envelope glycoprotein from tick-borne encephalitis virus at 2 Å resolution. *Nature* 375:291.
37. Kuhn RJ, Zhang W, Rossmann MG, Pletnev SV, Corver J, Lenches E, Jones CT, Mukhopadhyay S, Chipman PR, Strauss EG, Baker TS, Strauss JH. 2002. Structure of Dengue Virus: Implications for Flavivirus Organization, Maturation, and Fusion. *Cell* 108:717-25.

38. Rice CM, Lenches EM, Eddy SR, Shin SJ, Sheets RL, Strauss JH. 1985. Nucleotide sequence of yellow fever virus: implications for flavivirus gene expression and evolution. *Science* 229:726-33.
39. Rice CM, Strauss EG, Strauss JH. 1986. Structure of the Flavivirus Genome, p 279-326. *In* Schlesinger S, Schlesinger MJ (ed), *The Togaviridae and Flaviviridae* doi:10.1007/978-1-4757-0785-4_10. Springer New York, Boston, MA.
40. Kitchen A, Shackelton LA, Holmes EC. 2011. Family level phylogenies reveal modes of macroevolution in RNA viruses. *Proc Natl Acad Sci U S A* 108:238-43.
41. Grard G, Moureau G, Charrel RN, Holmes EC, Gould EA, de Lamballerie X. 2010. Genomics and evolution of Aedes-borne flaviviruses. *J Gen Virol* 91:87-94.
42. Simmonds P, Becher P, Bukh J, Gould EA, Meyers G, Monath T, Muerhoff S, Pletnev A, Rico-Hesse R, Smith DB, Stapleton JT. 2017. ICTV Virus Taxonomy Profile: Flaviviridae. *J Gen Virol* 98:2-3.
43. Daep CA, Muñoz-Jordán JL, Eugenin EA. 2014. Flaviviruses, an expanding threat in public health: focus on Dengue, West Nile, and Japanese encephalitis virus. *J Neurovirol* 20:539-60.
44. Bogovic P, Strle F. 2015. Tick-borne encephalitis: A review of epidemiology, clinical characteristics, and management. *World J Clin Cases* 3:430-41.
45. Sips GJ, Wilschut J, Smit JM. 2012. Neuroinvasive flavivirus infections. *Rev Med Virol* 22:69-87.
46. Turtle L, Griffiths M, Solomon T. 2012. Encephalitis caused by flaviviruses. *QJM* 105:219-23.
47. Adams MJ, Lefkowitz EJ, King AMQ, Harrach B, Harrison RL, Knowles NJ, Kropinski AM, Krupovic M, Kuhn JH, Mushegian AR, Nibert M, Sabanadzovic S, Sanfacon H, Siddell SG, Simmonds P, Varsani A, Zerbini FM, Gorbalenya AE, Davison AJ. 2017. Changes to taxonomy and the International Code of Virus Classification and Nomenclature ratified by the International Committee on Taxonomy of Viruses (2017). *Arch Virol* 162:2505-2538.
48. Elliott RM, Schmaljohn CS. 2013. Bunyaviridae, p 1244-1282. *In* Knipe DM, Howley PM (ed), *Fields Virology*, 6 ed, vol 1. Lippincott Williams and Wilkins, Philadelphia.
49. Talmon Y, Prasad BV, Clerx JP, Wang GJ, Chiu W, Hewlett MJ. 1987. Electron microscopy of vitrified-hydrated La Crosse virus. *J Virol* 61:2319-21.
50. Overby AK, Pettersson RF, Grunewald K, Huiskonen JT. 2008. Insights into bunyavirus architecture from electron cryotomography of Uukuniemi virus. *Proc Natl Acad Sci U S A* 105:2375-9.

51. Freiberg AN, Sherman MB, Morais MC, Holbrook MR, Watowich SJ. 2008. Three-dimensional organization of Rift Valley fever virus revealed by cryoelectron tomography. *J Virol* 82:10341-8.
52. Walter CT, Barr JN. 2011. Recent advances in the molecular and cellular biology of bunyaviruses. *J Gen Virol* 92:2467-84.
53. Ly HJ, Ikegami T. 2016. Rift Valley fever virus NSs protein functions and the similarity to other bunyavirus NSs proteins. *Virology* 533:118.
54. Alexander WS. 2002. Suppressors of cytokine signalling (SOCS) in the immune system. *Nat Rev Immunol* 2:410-6.
55. Shi X, Kohl A, Léonard VHJ, Li P, McLees A, Elliott RM. 2006. Requirement of the N-Terminal Region of Orthobunyavirus Nonstructural Protein NSm for Virus Assembly and Morphogenesis. *Journal of Virology* 80:8089-8099.
56. Flick R, Bouloy M. 2005. Rift Valley fever virus. *Curr Mol Med* 5:827-34.
57. Bird BH, Khristova ML, Rollin PE, Ksiazek TG, Nichol ST. 2007. Complete genome analysis of 33 ecologically and biologically diverse Rift Valley fever virus strains reveals widespread virus movement and low genetic diversity due to recent common ancestry. *J Virol* 81:2805-16.
58. Nicolas G, Durand B, Rakotoarimanana TT, Lacote S, Chevalier V, Marianneau P. 2014. A 3-year serological and virological cattle follow-up in Madagascar highlands suggests a non-classical transmission route of Rift Valley fever virus. *Am J Trop Med Hyg* 90:265-6.
59. Nicholas DE, Jacobsen KH, Waters NM. 2014. Risk factors associated with human Rift Valley fever infection: systematic review and meta-analysis. *Trop Med Int Health* 19:1420-9.
60. Pepin M, Bouloy M, Bird BH, Kemp A, Paweska J. 2010. Rift Valley fever virus (Bunyaviridae: Phlebovirus): an update on pathogenesis, molecular epidemiology, vectors, diagnostics and prevention. *Vet Res* 41:61.
61. Bird BH, Nichol ST. 2012. Breaking the chain: Rift Valley fever virus control via livestock vaccination. *Curr Opin Virol* 2:315-23.
62. Bente DA, Forrester NL, Watts DM, McAuley AJ, Whitehouse CA, Bray M. 2013. Crimean-Congo hemorrhagic fever: history, epidemiology, pathogenesis, clinical syndrome and genetic diversity. *Antiviral Res* 100:159-89.
63. Hoogstraal H. 1979. The epidemiology of tick-borne Crimean-Congo hemorrhagic fever in Asia, Europe, and Africa. *J Med Entomol* 15:307-417.

64. Gunes T, Poyraz O, Vatansever Z. 2011. Crimean-Congo hemorrhagic fever virus in ticks collected from humans, livestock, and picnic sites in the hyperendemic region of Turkey. *Vector Borne Zoonotic Dis* 11:1411-6.
65. Borucki MK, Kempf BJ, Blitvich BJ, Blair CD, Beaty BJ. 2002. La Crosse virus: replication in vertebrate and invertebrate hosts. *Microbes Infect* 4:341-50.
66. McJunkin JE, Khan RR, Tsai TF. 1998. California-La Crosse encephalitis. *Infect Dis Clin North Am* 12:83-93.
67. Rust RS, Thompson WH, Matthews CG, Beaty BJ, Chun RW. 1999. La Crosse and other forms of California encephalitis. *J Child Neurol* 14:1-14.
68. Dermody TS, Parker JSL, Sherry B. 2013. Orthoreoviruses, p 1304-1346. *In* Knipe DM, Howley PM (ed), *Fields Virology*, 6 ed, vol 2. Lippincott Williams and Wilkins, Philadelphia.
69. Romero JR, Simonsen KA. 2008. Powassan encephalitis and Colorado tick fever. *Infect Dis Clin North Am* 22:545-59, x.
70. Klasco R. 2002. Colorado tick fever. *Med Clin North Am* 86:435-40, ix.
71. Gould E, Pettersson J, Higgs S, Charrel R, de Lamballerie X. 2017. Emerging arboviruses: Why today? *One Health* 4:1-13.
72. Kenney JL, Brault AC. 2014. Chapter Two - The Role of Environmental, Virological and Vector Interactions in Dictating Biological Transmission of Arthropod-Borne Viruses by Mosquitoes, p 39-83. *In* Maramorosch K, Murphy FA (ed), *Advances in Virus Research*, vol 89. Academic Press.
73. Gould EA, de Lamballerie X, Zanotto PMdA, Holmes EC. 2003. Origins, evolution, and vector/host coadaptations within the Genus *Flavivirus*, p 277-314, *Advances in Virus Research*, vol 59. Academic Press.
74. Lanciotti RS, Roehrig JT, Deubel V, Smith J, Parker M, Steele K, Crise B, Volpe KE, Crabtree MB, Scherret JH, Hall RA, MacKenzie JS, Cropp CB, Panigrahy B, Ostlund E, Schmitt B, Malkinson M, Banet C, Weissman J, Komar N, Savage HM, Stone W, McNamara T, Gubler DJ. 1999. Origin of the West Nile Virus Responsible for an Outbreak of Encephalitis in the Northeastern United States. *Science* 286:2333-2337.
75. Roehrig JT. 2013. West Nile Virus in the United States — A Historical Perspective. *Viruses* 5:3088-108.
76. Owen J, Moore F, Panella N, Edwards E, Bru R, Hughes M, Komar N. 2006. Migrating Birds as Dispersal Vehicles for West Nile Virus. *EcoHealth* 3:79.
77. Gould EA, Higgs S. 2009. Impact of climate change and other factors on emerging arbovirus diseases. *Trans R Soc Trop Med Hyg* 103:109-21.

78. Kilpatrick AM, Randolph SE. 2012. Drivers, dynamics, and control of emerging vector-borne zoonotic diseases. *The Lancet* 380:1946-1955.
79. Gubler DJ. 2002. The Global Emergence/Resurgence of Arboviral Diseases As Public Health Problems. *Archives of Medical Research* 33:330-342.
80. Liang G, Gao X, Gould EA. 2015. Factors responsible for the emergence of arboviruses; strategies, challenges and limitations for their control. *Emerg Microbes Infect* 4:e18.
81. Moureau G, Cook S, Lemey P, Nougairede A, Forrester NL, Khasnatinov M, Charrel RN, Firth AE, Gould EA, de Lamballerie X. 2015. New Insights into Flavivirus Evolution, Taxonomy and Biogeographic History, Extended by Analysis of Canonical and Alternative Coding Sequences. *PLOS ONE* 10:e0117849.
82. Zanotto PM, Gould EA, Gao GF, Harvey PH, Holmes EC. 1996. Population dynamics of flaviviruses revealed by molecular phylogenies. *Proceedings of the National Academy of Sciences* 93:548-553.
83. Bryant JE, Holmes EC, Barrett ADT. 2007. Out of Africa: A Molecular Perspective on the Introduction of Yellow Fever Virus into the Americas. *PLOS Pathogens* 3:e75.
84. Tabachnick WJ. 1991. Evolutionary genetics and arthropod-borne disease: The yellow fever mosquito. *Am Entomol* 37:14-24.
85. Weaver SC, Barrett AD. 2004. Transmission cycles, host range, evolution and emergence of arboviral disease. *Nat Rev Microbiol* 2:789-801.
86. Hollidge BS, Gonzalez-Scarano F, Soldan SS. 2010. Arboviral encephalitides: transmission, emergence, and pathogenesis. *J Neuroimmune Pharmacol* 5:428-42.
87. Beckham JD, Tyler KL. 2015. Arbovirus Infections. *Continuum (Minneapolis, Minn)* 21:1599-611.
88. Suhrbier A, La Linn M. 2004. Clinical and pathologic aspects of arthritis due to Ross River virus and other alphaviruses. *Curr Opin Rheumatol* 16:374-9.
89. Meltzer E. 2012. Arboviruses and viral hemorrhagic fevers (VHF). *Infect Dis Clin North Am* 26:479-96.
90. Paessler S, Walker DH. 2013. Pathogenesis of the viral hemorrhagic fevers. *Annu Rev Pathol* 8:411-40.
91. Philipp CS, Callaway C, Chu MC, Huang GH, Monath TP, Trent D, Evatt BL. 1993. Replication of Colorado tick fever virus within human hematopoietic progenitor cells. *J Virol* 67:2389-95.
92. Hughes LE, Casper EA, Clifford CM. 1974. Persistence of Colorado tick fever virus in red blood cells. *Am J Trop Med Hyg* 23:530-2.

93. Gardner CL, Burke CW, Higgs ST, Klimstra WB, Ryman KD. 2012. Interferon-alpha/beta deficiency greatly exacerbates arthritogenic disease in mice infected with wild-type chikungunya virus but not with the cell culture-adapted live-attenuated 181/25 vaccine candidate. *Virology* 425:103-12.
94. Couderc T, Chretien F, Schilte C, Disson O, Brigitte M, Guivel-Benhassine F, Touret Y, Barau G, Cayet N, Schuffenecker I, Despres P, Arenzana-Seisdedos F, Michault A, Albert ML, Lecuit M. 2008. A mouse model for Chikungunya: young age and inefficient type-I interferon signaling are risk factors for severe disease. *PLoS Pathog* 4:e29.
95. Seymour RL, Rossi SL, Bergren NA, Plante KS, Weaver SC. 2013. The Role of Innate versus Adaptive Immune Responses in a Mouse Model of O'Nyong-Nyong Virus Infection. *The American Journal of Tropical Medicine and Hygiene* 88:1170-1179.
96. Hwang SY, Hertzog PJ, Holland KA, Sumarsono SH, Tymms MJ, Hamilton JA, Whitty G, Bertoncello I, Kola I. 1995. A null mutation in the gene encoding a type I interferon receptor component eliminates antiproliferative and antiviral responses to interferons alpha and beta and alters macrophage responses. *Proceedings of the National Academy of Sciences* 92:11284-11288.
97. Ryman KD, Meier KC, Gardner CL, Adegboyega PA, Klimstra WB. 2007. Non-pathogenic Sindbis virus causes hemorrhagic fever in the absence of alpha/beta and gamma interferons. *Virology* 368:273-85.
98. Ryman KD, Klimstra WB, Nguyen KB, Biron CA, Johnston RE. 2000. Alpha/Beta Interferon Protects Adult Mice from Fatal Sindbis Virus Infection and Is an Important Determinant of Cell and Tissue Tropism. *Journal of Virology* 74:3366-3378.
99. Züst R, Toh Y-X, Valdés I, Cerny D, Heinrich J, Hermida L, Marcos E, Guillén G, Kalinke U, Shi P-Y, Fink K. 2014. Type I Interferon Signals in Macrophages and Dendritic Cells Control Dengue Virus Infection: Implications for a New Mouse Model To Test Dengue Vaccines. *Journal of Virology* 88:7276-7285.
100. Shresta S, Sharar KL, Prigozhin DM, Snider HM, Beatty PR, Harris E. 2005. Critical Roles for Both STAT1-Dependent and STAT1-Independent Pathways in the Control of Primary Dengue Virus Infection in Mice. *The Journal of Immunology* 175:3946-3954.
101. Johnson AJ, Roehrig JT. 1999. New mouse model for dengue virus vaccine testing. *J Virol* 73:783-6.
102. Meier KC, Gardner CL, Khoretonenko MV, Klimstra WB, Ryman KD. 2009. A mouse model for studying viscerotropic disease caused by yellow fever virus infection. *PLoS Pathog* 5:e1000614.
103. Lazear HM, Govero J, Smith AM, Platt DJ, Fernandez E, Miner JJ, Diamond MS. 2016. A Mouse Model of Zika Virus Pathogenesis. *Cell Host Microbe* 19:720-30.

104. Dowall SD, Graham VA, Rayner E, Atkinson B, Hall G, Watson RJ, Bosworth A, Bonney LC, Kitchen S, Hewson R. 2016. A Susceptible Mouse Model for Zika Virus Infection. *PLoS Negl Trop Dis* 10:e0004658.
105. Weber E, Finsterbusch K, Lindquist R, Nair S, Lienenklaus S, Gekara NO, Janik D, Weiss S, Kalinke U, Överby AK, Kröger A. 2014. Type I Interferon Protects Mice from Fatal Neurotropic Infection with Langkat Virus by Systemic and Local Antiviral Responses. *J Virol* 88:12202-12.
106. Lobigs M, Müllbacher A, Wang Y, Pavy M, Lee E. 2003. Role of type I and type II interferon responses in recovery from infection with an encephalitic flavivirus. *Journal of General Virology* 84:567-572.
107. Bente DA, Alimonti JB, Shieh W-J, Camus G, Ströher U, Zaki S, Jones SM. 2010. Pathogenesis and Immune Response of Crimean-Congo Hemorrhagic Fever Virus in a STAT-1 Knockout Mouse Model. *Journal of Virology* 84:11089-11100.
108. Hefti HP, Frese M, Landis H, Di Paolo C, Aguzzi A, Haller O, Pavlovic J. 1999. Human MxA protein protects mice lacking a functional alpha/beta interferon system against La crosse virus and other lethal viral infections. *J Virol* 73:6984-91.
109. Taylor KG, Woods TA, Winkler CW, Carmody AB, Peterson KE. 2014. Age-dependent myeloid dendritic cell responses mediate resistance to la crosse virus-induced neurological disease. *J Virol* 88:11070-9.
110. Grieder FB, Vogel SN. 1999. Role of interferon and interferon regulatory factors in early protection against Venezuelan equine encephalitis virus infection. *Virology* 257:106-18.
111. Daffis S, Samuel MA, Suthar MS, Keller BC, Gale M, Jr., Diamond MS. 2008. Interferon regulatory factor IRF-7 induces the antiviral alpha interferon response and protects against lethal West Nile virus infection. *J Virol* 82:8465-75.
112. Aguilar PV, Paessler S, Carrara AS, Baron S, Poast J, Wang E, Moncayo AC, Anishchenko M, Watts D, Tesh RB, Weaver SC. 2005. Variation in interferon sensitivity and induction among strains of eastern equine encephalitis virus. *J Virol* 79:11300-10.
113. Lathan R, Simon-Chazottes D, Jouvion G, Godon O, Malissen M, Flamand M, Bruhns P, Panthier JJ. 2017. Innate Immune Basis for Rift Valley Fever Susceptibility in Mouse Models. *Sci Rep* 7:7096.
114. Aoki K, Shimada S, Simantini DS, Tun MM, Buerano CC, Morita K, Hayasaka D. 2014. Type-I interferon response affects an inoculation dose-independent mortality in mice following Japanese encephalitis virus infection. *Virol J* 11:105.
115. Larena M, Lobigs M. 2017. Partial dysfunction of STAT1 profoundly reduces host resistance to flaviviral infection. *Virology* 506:1-6.

116. Bhalla N, Sun C, Metthew Lam LK, Gardner CL, Ryman KD, Klimstra WB. 2016. Host translation shutoff mediated by non-structural protein 2 is a critical factor in the antiviral state resistance of Venezuelan equine encephalitis virus. *Virology* 496:147-165.
117. Gardner CL, Burke CW, Tesfay MZ, Glass PJ, Klimstra WB, Ryman KD. 2008. Eastern and Venezuelan equine encephalitis viruses differ in their ability to infect dendritic cells and macrophages: impact of altered cell tropism on pathogenesis. *J Virol* 82:10634-46.
118. Trobaugh DW, Gardner CL, Sun C, Haddow AD, Wang E, Chapnik E, Mildner A, Weaver SC, Ryman KD, Klimstra WB. 2014. RNA viruses can hijack vertebrate microRNAs to suppress innate immunity. *Nature* 506:245-8.
119. Simmons JD, White LJ, Morrison TE, Montgomery SA, Whitmore AC, Johnston RE, Heise MT. 2009. Venezuelan equine encephalitis virus disrupts STAT1 signaling by distinct mechanisms independent of host shutoff. *J Virol* 83:10571-81.
120. Jones M, Davidson A, Hibbert L, Gruenwald P, Schlaak J, Ball S, Foster GR, Jacobs M. 2005. Dengue virus inhibits alpha interferon signaling by reducing STAT2 expression. *J Virol* 79:5414-20.
121. Munoz-Jordan JL, Laurent-Rolle M, Ashour J, Martinez-Sobrido L, Ashok M, Lipkin WI, Garcia-Sastre A. 2005. Inhibition of alpha/beta interferon signaling by the NS4B protein of flaviviruses. *J Virol* 79:8004-13.
122. Fros JJ, Liu WJ, Prow NA, Geertsema C, Ligtenberg M, Vanlandingham DL, Schnettler E, Vlak JM, Suhrbier A, Khromykh AA, Pijlman GP. 2010. Chikungunya virus nonstructural protein 2 inhibits type I/II interferon-stimulated JAK-STAT signaling. *J Virol* 84:10877-87.
123. Liu WJ, Wang XJ, Mokhonov VV, Shi PY, Randall R, Khromykh AA. 2005. Inhibition of interferon signaling by the New York 99 strain and Kunjin subtype of West Nile virus involves blockage of STAT1 and STAT2 activation by nonstructural proteins. *J Virol* 79:1934-42.
124. Scholte FEM, Zivcec M, Dzimianski JV, Deaton MK, Spengler JR, Welch SR, Nichol ST, Pegan SD, Spiropoulou CF, Bergeron É. 2017. Crimean-Congo Hemorrhagic Fever Virus suppresses Innate Immune Responses via a Ubiquitin and ISG15 Specific Protease. *Cell Rep* 20:2396-407.
125. Blakqori G, Delhaye S, Habjan M, Blair CD, Sanchez-Vargas I, Olson KE, Attarzadeh-Yazdi G, Fragkoudis R, Kohl A, Kalinke U, Weiss S, Michiels T, Staeheli P, Weber F. 2007. La Crosse bunyavirus nonstructural protein NSs serves to suppress the type I interferon system of mammalian hosts. *J Virol* 81:4991-9.
126. Burt FJ, Chen W, Miner JJ, Lenschow DJ, Merits A, Schnettler E, Kohl A, Rudd PA, Taylor A, Herrero LJ, Zaid A, Ng LFP, Mahalingam S. 2017. Chikungunya virus: an update on the biology and pathogenesis of this emerging pathogen. *Lancet Infect Dis* 17:e107-e117.

127. McCarthy MK, Morrison TE. 2017. Persistent RNA virus infections: do PAMPS drive chronic disease? *Curr Opin Virol* 23:8-15.
128. Silva LA, Khomandiak S, Ashbrook AW, Weller R, Heise MT, Morrison TE, Dermody TS. 2014. A Single-Amino-Acid Polymorphism in Chikungunya Virus E2 Glycoprotein Influences Glycosaminoglycan Utilization. *Journal of Virology* 88:2385-2397.
129. Ashbrook AW, Burrack KS, Silva LA, Montgomery SA, Heise MT, Morrison TE, Dermody TS. 2014. Residue 82 of the Chikungunya Virus E2 Attachment Protein Modulates Viral Dissemination and Arthritis in Mice. *Journal of Virology* 88:12180-12192.
130. Acharya D, Paul AM, Anderson JF, Huang F, Bai F. 2015. Loss of Glycosaminoglycan Receptor Binding after Mosquito Cell Passage Reduces Chikungunya Virus Infectivity. *PLoS Negl Trop Dis* 9:e0004139.
131. Klimstra WB, Nangle EM, Smith MS, Yurochko AD, Ryman KD. 2003. DC-SIGN and L-SIGN can act as attachment receptors for alphaviruses and distinguish between mosquito cell- and mammalian cell-derived viruses. *J Virol* 77:12022-32.
132. Zhang R, Kim AS, Fox JM, Nair S, Basore K, Klimstra WB, Rimkunas R, Fong RH, Lin H, Poddar S, Crowe JE, Doranz BJ, Fremont DH, Diamond MS. 2018. Mxra8 is a receptor for multiple arthritogenic alphaviruses. *Nature* 557:570-574.
133. Marsh M, Kielian MC, Helenius A. 1984. Semliki forest virus entry and the endocytic pathway. *Biochem Soc Trans* 12:981-3.
134. Kolokoltsov AA, Fleming EH, Davey RA. 2006. Venezuelan equine encephalitis virus entry mechanism requires late endosome formation and resists cell membrane cholesterol depletion. *Virology* 347:333-42.
135. Sourisseau M, Schilte C, Casartelli N, Trouillet C, Guivel-Benhassine F, Rudnicka D, Sol-Foulon N, Le Roux K, Prevost M, Fsihi H, Frenkiel M, Blanchet F, Afonso PV, Ceccaldi P, S. O, Gessain A, Schuffenecker I, Verhasselt B, Zamborlini A, Saïb A, Rey FA, Arenzana-Seisdedos F, Desprès P, Michault A, Albert ML, Schwartz O. 2007. Characterization of Reemerging Chikungunya Virus. *PLoS Pathogens* 3:0804-0817.
136. van Duijl-Richter MK, Hoornweg TE, Rodenhuis-Zybert IA, Smit JM. 2015. Early Events in Chikungunya Virus Infection-From Virus Cell Binding to Membrane Fusion. *Viruses* 7:3647-74.
137. Bernard E, Solignat M, Gay B, Chazal N, Higgs S, Devaux C, Briant L. 2010. Endocytosis of chikungunya virus into mammalian cells: role of clathrin and early endosomal compartments. *PLoS One* 5:e11479.
138. Kuhn JH. 2013. Togaviridae, p 629-650. *In* Knipe DM, Howley PM (ed), *Fields Virology*, 6 ed, vol 1. Lippincott Williams and Wilkins, Philadelphia.

139. Barton DJ, Sawicki SG, Sawicki DL. 1991. Solubilization and immunoprecipitation of alphavirus replication complexes. *J Virol* 65:1496-506.
140. Frolova EI, Gorchakov R, Pereboeva L, Atasheva S, Frolov I. 2010. Functional Sindbis virus replicative complexes are formed at the plasma membrane. *J Virol* 84:11679-95.
141. Spuul P, Balistreri G, Kaariainen L, Ahola T. 2010. Phosphatidylinositol 3-kinase-, actin-, and microtubule-dependent transport of Semliki Forest Virus replication complexes from the plasma membrane to modified lysosomes. *J Virol* 84:7543-57.
142. Kujala P, Ikaheimonen A, Ehsani N, Vihinen H, Auvinen P, Kaariainen L. 2001. Biogenesis of the Semliki Forest virus RNA replication complex. *J Virol* 75:3873-84.
143. Thaa B, Biasiotto R, Eng K, Neuvonen M, Gotte B, Rheinemann L, Mutso M, Utt A, Varghese F, Balistreri G, Merits A, Ahola T, McInerney GM. 2015. Differential Phosphatidylinositol-3-Kinase-Akt-mTOR Activation by Semliki Forest and Chikungunya Viruses Is Dependent on nsP3 and Connected to Replication Complex Internalization. *J Virol* 89:11420-37.
144. Utt A, Quirin T, Saul S, Hellstrom K, Ahola T, Merits A. 2016. Versatile Trans-Replication Systems for Chikungunya Virus Allow Functional Analysis and Tagging of Every Replicase Protein. *PLoS One* 11:e0151616.
145. Shirako Y, Strauss JH. 1994. Regulation of Sindbis virus RNA replication: uncleaved P123 and nsP4 function in minus-strand RNA synthesis, whereas cleaved products from P123 are required for efficient plus-strand RNA synthesis. *J Virol* 68:1874-85.
146. Choi HK, Tong L, Minor W, Dumas P, Boege U, Rossmann MG, Wengler G. 1991. Structure of Sindbis virus core protein reveals a chymotrypsin-like serine proteinase and the organization of the virion. *Nature* 354:37-43.
147. Hahn CS, Strauss JH. 1990. Site-directed mutagenesis of the proposed catalytic amino acids of the Sindbis virus capsid protein autoprotease. *J Virol* 64:3069-73.
148. Solignat M, Gay B, Higgs S, Briant L, Devaux C. 2009. Replication cycle of chikungunya: a re-emerging arbovirus. *Virology* 393:183-97.
149. Perera R, Owen KE, Tellinghuisen TL, Gorbalenya AE, Kuhn RJ. 2001. Alphavirus nucleocapsid protein contains a putative coiled coil alpha-helix important for core assembly. *J Virol* 75:1-10.
150. Firth AE, Chung BY, Fleeton MN, Atkins JF. 2008. Discovery of frameshifting in Alphavirus 6K resolves a 20-year enigma. *Virology* 375:108.
151. Snyder JE, Kulcsar KA, Schultz KL, Riley CP, Neary JT, Marr S, Jose J, Griffin DE, Kuhn RJ. 2013. Functional characterization of the alphavirus TF protein. *J Virol* 87:8511-23.

152. Parrott MM, Sitarski SA, Arnold RJ, Picton LK, Hill RB, Mukhopadhyay S. 2009. Role of conserved cysteines in the alphavirus E3 protein. *J Virol* 83:2584-91.
153. Silva LA, Dermody TS. 2017. Chikungunya virus: epidemiology, replication, disease mechanisms, and prospective intervention strategies. *J Clin Invest* 127:737-749.
154. Ryan C, Ivanova L, Schlesinger MJ. 1998. Effects of site-directed mutations of transmembrane cysteines in sindbis virus E1 and E2 glycoproteins on palmitoylation and virus replication. *Virology* 249:62-7.
155. Simizu B, Yamamoto K, Hashimoto K, Ogata T. 1984. Structural proteins of Chikungunya virus. *J Virol* 51:254-8.
156. Mayne JT, Bell JR, Strauss EG, Strauss JH. 1985. Pattern of glycosylation of Sindbis virus envelope proteins synthesized in hamster and chicken cells. *Virology* 142:121-33.
157. de Curtis I, Simons K. 1988. Dissection of Semliki Forest virus glycoprotein delivery from the trans-Golgi network to the cell surface in permeabilized BHK cells. *Proc Natl Acad Sci U S A* 85:8052-6.
158. Ozden S, Lucas-Hourani M, Ceccaldi PE, Basak A, Valentine M, Benjannet S, Hamelin J, Jacob Y, Mamchaoui K, Mouly V, Despres P, Gessain A, Butler-Browne G, Chretien M, Tangy F, Vidalain PO, Seidah NG. 2008. Inhibition of Chikungunya virus infection in cultured human muscle cells by furin inhibitors: impairment of the maturation of the E2 surface glycoprotein. *J Biol Chem* 283:21899-908.
159. Ivanova L, Schlesinger MJ. 1993. Site-directed mutations in the Sindbis virus E2 glycoprotein identify palmitoylation sites and affect virus budding. *J Virol* 67:2546-51.
160. Ekstrom M, Liljestrom P, Garoff H. 1994. Membrane protein lateral interactions control Semliki Forest virus budding. *EMBO J* 13:1058-64.
161. Suomalainen M, Liljestrom P, Garoff H. 1992. Spike protein-nucleocapsid interactions drive the budding of alphaviruses. *J Virol* 66:4737-47.
162. Powers AM, Brault AC, Tesh RB, Weaver SC. 2000. Re-emergence of Chikungunya and O'nyong-nyong viruses: evidence for distinct geographical lineages and distant evolutionary relationships. *J Gen Virol* 81:471-9.
163. Volk SM, Chen R, Tsetsarkin KA, Adams AP, Garcia TI, Sall AA, Nasar F, Schuh AJ, Holmes EC, Higgs S, Maharaj PD, Brault AC, Weaver SC. 2010. Genome-scale phylogenetic analyses of chikungunya virus reveal independent emergences of recent epidemics and various evolutionary rates. *J Virol* 84:6497-504.
164. Chretien JP, Anyamba A, Bedno SA, Breiman RF, Sang R, Serگون K, Powers AM, Onyango CO, Small J, Tucker CJ, Linthicum KJ. 2007. Drought-associated chikungunya emergence along coastal East Africa. *Am J Trop Med Hyg* 76:405-7.

165. Tsetsarkin KA, Vanlandingham DL, McGee CE, Higgs S. 2007. A single mutation in chikungunya virus affects vector specificity and epidemic potential. *PLoS Pathog* 3:e201.
166. Reiter P, Fontenille D, Paupy C. 2006. *Aedes albopictus* as an epidemic vector of chikungunya virus: another emerging problem? *The Lancet Infectious Diseases* 6:463-464.
167. Vazeille M, Moutailler S, Coudrier D, Rousseaux C, Khun H, Huerre M, Thiria J, Dehecq JS, Fontenille D, Schuffenecker I, Despres P, Failloux AB. 2007. Two Chikungunya isolates from the outbreak of La Reunion (Indian Ocean) exhibit different patterns of infection in the mosquito, *Aedes albopictus*. *PLoS One* 2:e1168.
168. Rezza G, Nicoletti L, Angelini R, Romi R, Finarelli AC, Panning M, Cordioli P, Fortuna C, Boros S, Magurano F, Silvi G, Angelini P, Dottori M, Ciufolini MG, Majori GC, Cassone A. 2007. Infection with chikungunya virus in Italy: an outbreak in a temperate region. *Lancet* 370:1840-6.
169. Grandadam M, Caro V, Plumet S, Thiberge JM, Souares Y, Failloux AB, Tolou HJ, Budelot M, Cosserat D, Leparco-Goffart I, Despres P. 2011. Chikungunya virus, southeastern France. *Emerg Infect Dis* 17:910-3.
170. Leparco-Goffart I, Nougairede A, Cassadou S, Prat C, de Lamballerie X. 2014. Chikungunya in the Americas. *The Lancet* 383:514.
171. Weaver SC, Forrester NL. 2015. Chikungunya: Evolutionary history and recent epidemic spread. *Antiviral Research* 120:32-39.
172. Lanciotti RS, Valadere AM. 2014. Transcontinental movement of Asian Genotype Chikungunya virus. *Emerging Infectious Diseases* 20:1400-1402.
173. Tsetsarkin KA, Chen R, Weaver SC. 2016. Interspecies transmission and chikungunya virus emergence. *Curr Opin Virol* 16:143-150.
174. Teixeira MG, Andrade AM, Costa Mda C, Castro JN, Oliveira FL, Goes CS, Maia M, Santana EB, Nunes BT, Vasconcelos PF. 2015. East/Central/South African genotype chikungunya virus, Brazil, 2014. *Emerg Infect Dis* 21:906-7.
175. Sam IC, Chua CL, Rovie-Ryan JJ, Fu JY, Tong C, Sitam FT, Chan YF. 2015. Chikungunya Virus in Macaques, Malaysia. *Emerg Infect Dis* 21:1683-5.
176. Diallo D, Sall AA, Buenemann M, Chen R, Faye O, Diagne CT, Faye O, Ba Y, Dia I, Watts D, Weaver SC, Hanley KA, Diallo M. 2012. Landscape ecology of sylvatic chikungunya virus and mosquito vectors in southeastern Senegal. *PLoS Negl Trop Dis* 6:e1649.
177. Kraemer MUG, Sinka ME, Duda KA, Mylne AQN, Shearer FM, Barker CM, Moore CG, Carvalho RG, Coelho GE, Van Bortel W, Hendrickx G, Schaffner F, Elyazar IRF, Teng H-J, Brady OJ, Messina JP, Pigott DM, Scott TW, Smith DL, Wint GRW, Golding N,

- Hay SI. 2015. The global distribution of the arbovirus vectors *Aedes aegypti* and *Ae. albopictus*. *eLife* 4:e08347.
178. Vega-Rua A, Zouache K, Girod R, Failloux AB, Lourenco-de-Oliveira R. 2014. High level of vector competence of *Aedes aegypti* and *Aedes albopictus* from ten American countries as a crucial factor in the spread of Chikungunya virus. *J Virol* 88:6294-306.
179. Fischer D, Thomas SM, Suk JE, Sudre B, Hess A, Tjaden NB, Beierkuhnlein C, Semenza JC. 2013. Climate change effects on Chikungunya transmission in Europe: geospatial analysis of vector's climatic suitability and virus' temperature requirements. *Int J Health Geogr* 12:51.
180. Hoarau JJ, Jaffar Bandjee MC, Krejbich Trotot P, Das T, Li-Pat-Yuen G, Dassa B, Denizot M, Guichard E, Ribera A, Henni T, Tallet F, Moiton MP, Gauzere BA, Bruniquet S, Jaffar Bandjee Z, Morbidelli P, Martigny G, Jolivet M, Gay F, Grandadam M, Tolou H, Vieillard V, Debre P, Autran B, Gasque P. 2010. Persistent chronic inflammation and infection by Chikungunya arthritogenic alphavirus in spite of a robust host immune response. *J Immunol* 184:5914-27.
181. Labadie K, Larcher T, Joubert C, Mannioui A, Delache B, Brochard P, Guigand L, Dubreil L, Lebon P, Verrier B, de Lamballerie X, Suhrbier A, Cherel Y, Le Grand R, Roques P. 2010. Chikungunya disease in nonhuman primates involves long-term viral persistence in macrophages. *J Clin Invest* 120:894-906.
182. Ozden S, Huerre M, Riviere J-P, Coffey L, Afonso P. 2007. Human Muscle Satellite Cells as Targets of Chikungunya Virus Infection. *PLoS ONE* 2:527.
183. Gardner J, Anraku I, Le TT, Larcher T, Major L, Roques P, Schroder WA, Higgs S, Suhrbier A. 2010. Chikungunya virus arthritis in adult wild-type mice. *J Virol* 84:8021-32.
184. Morrison TE, Oko L, Montgomery SA, Whitmore AC, Lotstein AR, Gunn BM, Elmore SA, Heise MT. 2011. A mouse model of chikungunya virus-induced musculoskeletal inflammatory disease: evidence of arthritis, tenosynovitis, myositis, and persistence. *Am J Pathol* 178:32-40.
185. Chua HH, Abdul Rashid K, Law WC, Hamizah A, Chem YK, Khairul AH, Chua KB. 2010. A fatal case of chikungunya virus infection with liver involvement. *Med J Malaysia* 65:83-4.
186. Das T, Jaffar-Bandjee MC, Hoarau JJ, Krejbich Trotot P, Denizot M, Lee-Pat-Yuen G, Sahoo R, Guiraud P, Ramful D, Robin S, Alessandri JL, Gauzere BA, Gasque P. 2010. Chikungunya fever: CNS infection and pathologies of a re-emerging arbovirus. *Prog Neurobiol* 91:121-9.
187. Teng TS, Kam YW, Lee B, Hapuarachchi HC, Wimal A, Ng LC, Ng LF. 2015. A Systematic Meta-analysis of Immune Signatures in Patients With Acute Chikungunya Virus Infection. *J Infect Dis* 211:1925-35.

188. Ruiz Silva M, van der Ende-Metselaar H, Mulder HL, Smit JM, Rodenhuis-Zybert IA. 2016. Mechanism and role of MCP-1 upregulation upon chikungunya virus infection in human peripheral blood mononuclear cells. *Sci Rep* 6:32288.
189. Her Z, Malleret B, Chan M, Ong EK, Wong SC, Kwek DJ, Tolou H, Lin RT, Tambyah PA, Renia L, Ng LF. 2010. Active infection of human blood monocytes by Chikungunya virus triggers an innate immune response. *J Immunol* 184:5903-13.
190. Schilte C, Couderc T, Chretien F, Sourisseau M, Gangneux N, Guivel-Benhassine F, Kraxner A, Tschopp J, Higgs S, Michault A, Arenzana-Seisdedos F, Colonna M, Peduto L, Schwartz O, Lecuit M, Albert ML. 2010. Type I IFN controls chikungunya virus via its action on nonhematopoietic cells. *J Exp Med* 207:429-42.
191. Wauquier N, Becquart P, Nkoghe D, Padilla C, Ndjoyi-Mbiguino A, Leroy EM. 2011. The acute phase of Chikungunya virus infection in humans is associated with strong innate immunity and T CD8 cell activation. *J Infect Dis* 204:115-23.
192. Chow A, Her Z, Ong EK, Chen JM, Dimatatac F, Kwek DJ, Barkham T, Yang H, Renia L, Leo YS, Ng LF. 2011. Persistent arthralgia induced by Chikungunya virus infection is associated with interleukin-6 and granulocyte macrophage colony-stimulating factor. *J Infect Dis* 203:149-57.
193. Dupuis-Maguiraga L, Noret M, Brun S, Le Grand R, Gras G, Roques P. 2012. Chikungunya disease: infection-associated markers from the acute to the chronic phase of arbovirus-induced arthralgia. *PLoS Negl Trop Dis* 6:e1446.
194. Brouard C, Bernillon P, Quatresous I, Pillonel J, Assal A, De Valk H, Desenclos JC. 2008. Estimated risk of Chikungunya viremic blood donation during an epidemic on Reunion Island in the Indian Ocean, 2005 to 2007. *Transfusion* 48:1333-41.
195. Borgherini G, Poubeau P, Staikowsky F, Lory M, Le Moullec N, Becquart JP, Wengling C, Michault A, Paganin F. 2007. Outbreak of chikungunya on Reunion Island: early clinical and laboratory features in 157 adult patients. *Clin Infect Dis* 44:1401-7.
196. Economopoulou A, Dominguez M, Helynck B, Sissoko D, Wichmann O, Quenel P, Germonneau P, Quatresous I. 2009. Atypical Chikungunya virus infections: clinical manifestations, mortality and risk factors for severe disease during the 2005-2006 outbreak on Reunion. *Epidemiol Infect* 137:534-41.
197. Tandale BV, Sathe PS, Arankalle VA, Wadia RS, Kulkarni R, Shah SV, Shah SK, Sheth JK, Sudeep AB, Tripathy AS, Mishra AC. 2009. Systemic involvements and fatalities during Chikungunya epidemic in India, 2006. *J Clin Virol* 46:145-9.
198. Rajapakse S, Rodrigo C, Rajapakse A. 2010. Atypical manifestations of chikungunya infection. *Trans R Soc Trop Med Hyg* 104:89-96.
199. Badawi A, Ryoo SG, Vasileva D, Yaghoubi S. 2018. Prevalence of chronic comorbidities in chikungunya: A systematic review and meta-analysis. *Int J Infect Dis* 67:107-113.

200. Pinheiro TJ, Guimaraes LF, Silva MT, Soares CN. 2016. Neurological manifestations of Chikungunya and Zika infections. *Arq Neuropsiquiatr* 74:937-943.
201. Ziegler SA, Lu L, da Rosa AP, Xiao SY, Tesh RB. 2008. An animal model for studying the pathogenesis of chikungunya virus infection. *Am J Trop Med Hyg* 79:133-9.
202. Hawman DW, Stoermer KA, Montgomery SA, Pal P, Oko L, Diamond MS, Morrison TE. 2013. Chronic joint disease caused by persistent chikungunya virus infection is controlled by the adaptive immune response. *J Virol* 87:13878-88.
203. Rohatgi A, Corbo JC, Monte K, Higgs S, Vanlandingham DL, Kardon G, Lenschow DJ. 2014. Infection of myofibers contributes to increased pathogenicity during infection with an epidemic strain of chikungunya virus. *J Virol* 88:2414-25.
204. Krejbich-Trotot P, Denizot M, Hoarau JJ, Jaffar-Bandjee MC, Das T, Gasque P. 2011. Chikungunya virus mobilizes the apoptotic machinery to invade host cell defenses. *FASEB J* 25:314-25.
205. Ng LF, Chow A, Sun YJ, Kwek DJ, Lim PL, Dimatatac F, Ng LC, Ooi EE, Choo KH, Her Z, Kourilsky P, Leo YS. 2009. IL-1beta, IL-6, and RANTES as biomarkers of Chikungunya severity. *PLoS One* 4:e4261.
206. McInnes IB, Schett G. 2011. The pathogenesis of rheumatoid arthritis. *N Engl J Med* 365:2205-19.
207. Manimunda SP, Vijayachari P, Uppoor R, Sugunan AP, Singh SS, Rai SK, Sudeep AB, Muruganandam N, Chaitanya IK, Guruprasad DR. 2010. Clinical progression of chikungunya fever during acute and chronic arthritic stages and the changes in joint morphology as revealed by imaging. *Trans R Soc Trop Med Hyg* 104:392-9.
208. Tanay A. 2017. Chikungunya virus and autoimmunity. *Curr Opin Rheumatol* 29:389-393.
209. Miner JJ, Aw-Yeang HX, Fox JM, Taffner S, Malkova ON, Oh ST, Kim AHJ, Diamond MS, Lenschow DJ, Yokoyama WM. 2015. Chikungunya viral arthritis in the United States: a mimic of seronegative rheumatoid arthritis. *Arthritis Rheumatol* 67:1214-1220.
210. Nakaya HI, Gardner J, Poo YS, Major L, Pulendran B, Suhrbier A. 2012. Gene profiling of Chikungunya virus arthritis in a mouse model reveals significant overlap with rheumatoid arthritis. *Arthritis Rheum* 64:3553-63.
211. Grivard P, Le Roux K, Laurent P, Fianu A, Perrau J, Gigan J, Hoarau G, Grondin N, Staikowsky F, Favier F, Michault A. 2007. Molecular and serological diagnosis of Chikungunya virus infection. *Pathol Biol (Paris)* 55:490-4.
212. Kam YW, Lum FM, Teo TH, Lee WW, Simarmata D, Harjanto S, Chua CL, Chan YF, Wee JK, Chow A, Lin RT, Leo YS, Le Grand R, Sam IC, Tong JC, Roques P, Wiesmuller KH, Renia L, Rotzschke O, Ng LF. 2012. Early neutralizing IgG response to

- Chikungunya virus in infected patients targets a dominant linear epitope on the E2 glycoprotein. *EMBO Mol Med* 4:330-43.
213. Kam YW, Lee WW, Simarmata D, Harjanto S, Teng TS, Tolou H, Chow A, Lin RT, Leo YS, Renia L, Ng LF. 2012. Longitudinal analysis of the human antibody response to Chikungunya virus infection: implications for serodiagnosis and vaccine development. *J Virol* 86:13005-15.
 214. Panning M, Grywna K, van Esbroeck M, Emmerich P, Drosten C. 2008. Chikungunya fever in travelers returning to Europe from the Indian Ocean region, 2006. *Emerg Infect Dis* 14:416-22.
 215. Poo YS, Rudd PA, Gardner J, Wilson JAC, Larcher T, Colle MA, Le TT, Nakaya HI, Warrilow D, Allcock R, Bielefeldt-Ohmann H, Schroder WA, Khromykh AA, Lopez Jé A, Suhrbier A. 2014. Multiple Immune Factors Are Involved in Controlling Acute and Chronic Chikungunya Virus Infection. *PLoS Negl Trop Dis* 8.
 216. Rodriguez-Morales AJ, Cardona-Ospina JA, Villamil-Gomez W, Paniz-Mondolfi AE. 2015. How many patients with post-chikungunya chronic inflammatory rheumatism can we expect in the new endemic areas of Latin America? *Rheumatol Int* 35:2091-4.
 217. Waymouth HE, Zoutman DE, Towheed TE. 2013. Chikungunya-related arthritis: case report and review of the literature. *Semin Arthritis Rheum* 43:273-8.
 218. Y. CA, Liliana E, Alexandra P, Nelly P, Patrick RS, O. MKA, Shamila P, Eyda B, Marianda N, Alejandro RM, Richard A, Priyanka K, S. FG, M. BJ, L. SG. 2018. Frequency of Chronic Joint Pain Following Chikungunya Virus Infection. *Arthritis & Rheumatology* 70:578-584.
 219. Chang AY, Martins KAO, Encinales L, Reid SP, Acuna M, Encinales C, Matranga CB, Pacheco N, Cure C, Shukla B, Ruiz Arteta T, Amdur R, Cazares LH, Gregory M, Ward MD, Porras A, Rico Mendoza A, Dong L, Kenny T, Brueggemann E, Downey LG, Kamalopathy P, Lichtenberger P, Falls O, Simon GL, Bethony JM, Firestein GS. 2017. Chikungunya Arthritis Mechanisms in the Americas: A Cross-Sectional Analysis of Chikungunya Arthritis Patients Twenty-Two Months After Infection Demonstrating No Detectable Viral Persistence in Synovial Fluid. *Arthritis Rheumatol* doi:10.1002/art.40383.
 220. Schilte C, Staikovskiy F, Couderc T, Madec Y, Carpentier F, Kassab S, Albert ML, Lecuit M, Michault A. 2013. Chikungunya virus-associated long-term arthralgia: a 36-month prospective longitudinal study. *PLoS Negl Trop Dis* 7:e2137.
 221. Sissoko D, Malvy D, Ezzedine K, Renault P, Moschetti F, Ledrans M, Pierre V. 2009. Post-Epidemic Chikungunya Disease on Reunion Island: Course of Rheumatic Manifestations and Associated Factors over a 15-Month Period. *PLOS Neglected Tropical Diseases* 3:e389.

222. Heath CJ, Lowther J, Noel TP, Mark-George I, Boothroyd DB, Mitchell G, MacPherson C, Desiree LaBeaud A. 2018. The Identification of Risk Factors for Chronic Chikungunya Arthralgia in Grenada, West Indies: A Cross-Sectional Cohort Study. *Open Forum Infect Dis* 5:ofx234.
223. Delgado-Enciso I, Paz-Michel B, Melnikov V, Guzman-Esquivel J, Espinoza-Gomez F, Soriano-Hernandez AD, Rodriguez-Sanchez IP, Martinez-Fierro ML, Ceja-Espiritu G, Olmedo-Buenrostro BA, Galvan-Salazar HR, Delgado-Enciso OG, Delgado-Enciso J, Lopez-Lemus UA, Montes-Galindo DA. 2018. Smoking and female sex as key risk factors associated with severe arthralgia in acute and chronic phases of Chikungunya virus infection. *Exp Ther Med* 15:2634-2642.
224. Essackjee K, Goorah S, Ramchurn SK, Cheeneebash J, Walker-Bone K. 2013. Prevalence of and risk factors for chronic arthralgia and rheumatoid-like polyarthritis more than 2 years after infection with chikungunya virus. *Postgrad Med J* 89:440-7.
225. Moro ML, Grilli E, Corvetta A, Silvi G, Angelini R, Mascella F, Miserocchi F, Sambo P, Finarelli AC, Sambri V, Gagliotti C, Massimiliani E, Mattivi A, Pierro AM, Macini P. 2012. Long-term chikungunya infection clinical manifestations after an outbreak in Italy: a prognostic cohort study. *J Infect* 65:165-72.
226. Vijayakumar KP, Nair Anish TS, George B, Lawrence T, Muthukkutty SC, Ramachandran R. 2011. Clinical Profile of Chikungunya Patients during the Epidemic of 2007 in Kerala, India. *J Glob Infect Dis* 3:221-6.
227. Larrieu S, Poudroux N, Pistone T, Filleul L, Receveur MC, Sissoko D, Ezzedine K, Malvy D. 2010. Factors associated with persistence of arthralgia among Chikungunya virus-infected travellers: report of 42 French cases. *J Clin Virol* 47:85-8.
228. Gerardin P, Fianu A, Michault A, Mussard C, Boussaid K, Rollot O, Grivard P, Kassab S, Bouquillard E, Borgherini G, Gauzere BA, Malvy D, Breart G, Favier F. 2013. Predictors of Chikungunya rheumatism: a prognostic survey ancillary to the TELECHIK cohort study. *Arthritis Res Ther* 15:R9.
229. Murillo-Zamora E, Mendoza-Cano O, Trujillo-Hernandez B, Guzman-Esquivel J, Higareda-Almaraz E, Higareda-Almaraz MA, Sanchez-Pina RA, Lugo-Radillo A. 2018. Persistent Arthralgia and Related Risks Factors: A Cohort Study at 12 Months from Laboratory-Confirmed Chikungunya Infection. *Arch Med Res* doi:10.1016/j.arcmed.2018.04.008.
230. Huits R, De Kort J, Van Den Berg R, Chong L, Tsoumanis A, Eggermont K, Bartholomeeusen K, Arien KK, Jacobs J, Van Esbroeck M, Bottieau E, Cnops L. 2018. Chikungunya virus infection in Aruba: Diagnosis, clinical features and predictors of post-chikungunya chronic polyarthralgia. *PLoS One* 13:e0196630.
231. Yaseen HM, Simon F, Deparis X, Marimoutou C. 2014. Identification of initial severity determinants to predict arthritis after chikungunya infection in a cohort of French gendarmes. *BMC Musculoskelet Disord* 15:249.

232. Messaoudi I, Vomazke J, Totonchy T, Kreklywich CN, Haberthur K, Springgay L, Brien JD, Diamond MS, Defilippis VR, Streblow DN. 2013. Chikungunya virus infection results in higher and persistent viral replication in aged rhesus macaques due to defects in anti-viral immunity. *PLoS Negl Trop Dis* 7:e2343.
233. Teo TH, Lum FM, Claser C, Lulla V, Lulla A, Merits A, Renia L, Ng LF. 2013. A pathogenic role for CD4+ T cells during Chikungunya virus infection in mice. *J Immunol* 190:259-69.
234. Seymour RL, Adams AP, Leal G, Alcorn MD, Weaver SC. 2015. A Rodent Model of Chikungunya Virus Infection in RAG1 -/- Mice, with Features of Persistence, for Vaccine Safety Evaluation. *PLoS Negl Trop Dis* 9:e0003800.
235. Lee WWL, Teo T-H, Her Z, Lum F-M, Kam Y-W, Haase D, Rénia L, Röttschke O, Ng LFP. 2015. Expanding Regulatory T Cells Alleviates Chikungunya Virus-Induced Pathology in Mice. *Journal of Virology* 89:7893-7904.
236. Long KM, Ferris MT, Whitmore AC, Montgomery SA, Thurlow LR, McGee CE, Rodriguez CA, Lim JK, Heise MT. 2016. $\gamma\delta$ T Cells Play a Protective Role in Chikungunya Virus-Induced Disease. *Journal of Virology* 90:433-443.
237. Kam YW, Ong EK, Renia L, Tong JC, Ng LF. 2009. Immuno-biology of Chikungunya and implications for disease intervention. *Microbes Infect* 11:1186-96.
238. Pal P, Dowd KA, Brien JD, Edeling MA, Gorlatov S, Johnson S, Lee I, Akahata W, Nabel GJ, Richter MK, Smit JM, Fremont DH, Pierson TC, Heise MT, Diamond MS. 2013. Development of a highly protective combination monoclonal antibody therapy against Chikungunya virus. *PLoS Pathog* 9:e1003312.
239. Couderc T, Khandoudi N, Grandadam M, Visse C, Gangneux N, Bagot S, Prost JF, Lecuit M. 2009. Prophylaxis and therapy for Chikungunya virus infection. *J Infect Dis* 200:516-23.
240. Smith SA, Silva LA, Fox JM, Flyak AI, Kose N, Sapparapu G, Khomandiak S, Ashbrook AW, Kahle KM, Fong RH, Swayne S, Doranz BJ, McGee CE, Heise MT, Pal P, Brien JD, Austin SK, Diamond MS, Dermody TS, Crowe JE, Jr. 2015. Isolation and Characterization of Broad and Ultrapotent Human Monoclonal Antibodies with Therapeutic Activity against Chikungunya Virus. *Cell Host Microbe* 18:86-95.
241. Fric J, Bertin-Maghit S, Wang CI, Nardin A, Warter L. 2013. Use of human monoclonal antibodies to treat Chikungunya virus infection. *J Infect Dis* 207:319-22.
242. Fong RH, Banik SS, Mattia K, Barnes T, Tucker D, Liss N, Lu K, Selvarajah S, Srinivasan S, Mabila M, Miller A, Muench MO, Michault A, Rucker JB, Paes C, Simmons G, Kahle KM, Doranz BJ. 2014. Exposure of epitope residues on the outer face of the chikungunya virus envelope trimer determines antibody neutralizing efficacy. *J Virol* 88:14364-79.

243. Selvarajah S, Sexton NR, Kahle KM, Fong RH, Mattia KA, Gardner J, Lu K, Liss NM, Salvador B, Tucker DF, Barnes T, Mabila M, Zhou X, Rossini G, Rucker JB, Sanders DA, Suhrbier A, Sambri V, Michault A, Muench MO, Doranz BJ, Simmons G. 2013. A neutralizing monoclonal antibody targeting the acid-sensitive region in chikungunya virus E2 protects from disease. *PLoS Negl Trop Dis* 7:e2423.
244. Jin J, Liss NM, Chen DH, Liao M, Fox JM, Shimak RM, Fong RH, Chafets D, Bakkour S, Keating S, Fomin ME, Muench MO, Sherman MB, Doranz BJ, Diamond MS, Simmons G. 2015. Neutralizing Monoclonal Antibodies Block Chikungunya Virus Entry and Release by Targeting an Epitope Critical to Viral Pathogenesis. *Cell Rep* 13:2553-2564.
245. Lum FM, Ng L. 2015. Cellular and molecular mechanisms of chikungunya pathogenesis, vol 120.
246. Fox JM, Long F, Edeling MA, Lin H, van Duijl-Richter MKS, Fong RH, Kahle KM, Smit JM, Jin J, Simmons G, Doranz BJ, Crowe JE, Jr., Fremont DH, Rossmann MG, Diamond MS. 2015. Broadly Neutralizing Alphavirus Antibodies Bind an Epitope on E2 and Inhibit Entry and Egress. *Cell* 163:1095-1107.
247. Lee CY, Kam YW, Fric J, Malleret B, Koh EG, Prakash C, Huang W, Lee WW, Lin C, Lin RT, Renia L, Wang CI, Ng LF, Warter L. 2011. Chikungunya virus neutralization antigens and direct cell-to-cell transmission are revealed by human antibody-escape mutants. *PLoS Pathog* 7:e1002390.
248. Porta J, Mangala Prasad V, Wang CI, Akahata W, Ng LF, Rossmann MG. 2016. Structural Studies of Chikungunya Virus-Like Particles Complexed with Human Antibodies: Neutralization and Cell-to-Cell Transmission. *J Virol* 90:1169-77.
249. Masrinoul P, Puiprom O, Tanaka A, Kuwahara M, Chaichana P, Ikuta K, Ramasoota P, Okabayashi T. 2014. Monoclonal antibody targeting chikungunya virus envelope 1 protein inhibits virus release. *Virology* 464-465:111-117.
250. Fox JM, Diamond MS. 2016. Immune-Mediated Protection and Pathogenesis of Chikungunya Virus. *J Immunol* 197:4210-4218.
251. Lum FM, Teo TH, Lee WW, Kam YW, Renia L, Ng LF. 2013. An essential role of antibodies in the control of Chikungunya virus infection. *J Immunol* 190:6295-302.
252. Kam YW, Simarmata D, Chow A, Her Z, Teng TS, Ong EK, Renia L, Leo YS, Ng LF. 2012. Early appearance of neutralizing immunoglobulin G3 antibodies is associated with chikungunya virus clearance and long-term clinical protection. *J Infect Dis* 205:1147-54.
253. Kam YW, Pok KY, Eng KE, Tan LK, Kaur S, Lee WW, Leo YS, Ng LC, Ng LF. 2015. Sero-prevalence and cross-reactivity of chikungunya virus specific anti-E2EP3 antibodies in arbovirus-infected patients. *PLoS Negl Trop Dis* 9:e3445.

254. Levitt NH, Ramsburg HH, Hasty SE, Repik PM, Cole FE, Jr., Lupton HW. 1986. Development of an attenuated strain of chikungunya virus for use in vaccine production. *Vaccine* 4:157-62.
255. Werneke SW, Schilte C, Rohatgi A, Monte KJ, Michault A, Arenzana-Seisdedos F, Vanlandingham DL, Higgs S, Fontanet A, Albert ML, Lenschow DJ. 2011. ISG15 is critical in the control of Chikungunya virus infection independent of UbE1L mediated conjugation. *PLoS Pathog* 7:e1002322.
256. Rudd PA, Wilson J, Gardner J, Larcher T, Babarit C, Le TT, Anraku I, Kumagai Y, Loo YM, Gale M, Jr., Akira S, Khromykh AA, Suhrbier A. 2012. Interferon response factors 3 and 7 protect against Chikungunya virus hemorrhagic fever and shock. *J Virol* 86:9888-98.
257. Schilte C, Buckwalter MR, Laird ME, Diamond MS, Schwartz O, Albert ML. 2012. Cutting edge: independent roles for IRF-3 and IRF-7 in hematopoietic and nonhematopoietic cells during host response to Chikungunya infection. *J Immunol* 188:2967-71.
258. Plante K, Wang E, Partidos CD, Weger J, Gorchakov R, Tsetsarkin K, Borland EM, Powers AM, Seymour R, Stinchcomb DT, Osorio JE, Frolov I, Weaver SC. 2011. Novel chikungunya vaccine candidate with an IRES-based attenuation and host range alteration mechanism. *PLoS Pathog* 7:e1002142.
259. Kam YW, Lee WW, Simarmata D, Le Grand R, Tolou H, Merits A, Roques P, Ng LF. 2014. Unique epitopes recognized by antibodies induced in Chikungunya virus-infected non-human primates: implications for the study of immunopathology and vaccine development. *PLoS One* 9:e95647.
260. Krause CD, Pestka S. 2005. Evolution of the Class 2 cytokines and receptors, and discovery of new friends and relatives. *Pharmacol Ther* 106:299-346.
261. McNab F, Mayer-Barber K, Sher A, Wack A, O'Garra A. 2015. Type I interferons in infectious disease. *Nat Rev Immunol* 15:87-103.
262. Wang BX, Fish EN. 2012. The Yin and Yang of Viruses and Interferon. *Trends in Immunology* 33:190-197.
263. Isaacs A, Lindenmann J. 1957. Virus interference. I. The interferon. *Proc R Soc Lond B Biol Sci* 147:258-67.
264. Pestka S, Krause CD, Walter MR. 2004. Interferons, interferon-like cytokines, and their receptors. *Immunol Rev* 202:8-32.
265. Renauld J-C. 2003. Class II cytokine receptors and their ligands: Key antiviral and inflammatory modulators. *Nature Reviews Immunology* 3:667.

266. van Pesch V, Lanaya H, Renauld JC, Michiels T. 2004. Characterization of the Murine Alpha Interferon Gene Family. *J Virol* 78:8219-28.
267. Ng CT, Mendoza JL, Garcia KC, Oldstone MB. 2016. Alpha and Beta Type 1 Interferon Signaling: Passage for Diverse Biologic Outcomes. *Cell* 164:349-52.
268. Akira S, Uematsu S, Takeuchi O. 2006. Pathogen recognition and innate immunity. *Cell* 124:783-801.
269. Bowie A, O'Neill LA. 2000. The interleukin-1 receptor/Toll-like receptor superfamily: signal generators for pro-inflammatory interleukins and microbial products. *J Leukoc Biol* 67:508-14.
270. Lester SN, Li K. 2014. Toll-like receptors in antiviral innate immunity. *J Mol Biol* 426:1246-64.
271. Medzhitov R, Preston-Hurlburt P, Kopp E, Stadlen A, Chen C, Ghosh S, Janeway CA, Jr. 1998. MyD88 is an adaptor protein in the hToll/IL-1 receptor family signaling pathways. *Mol Cell* 2:253-8.
272. Hoebe K, Du X, Georgel P, Janssen E, Tabeta K, Kim SO, Goode J, Lin P, Mann N, Mudd S, Crozat K, Sovath S, Han J, Beutler B. 2003. Identification of Lps2 as a key transducer of MyD88-independent TIR signalling. *Nature* 424:743-8.
273. Yamamoto M, Sato S, Hemmi H, Hoshino K, Kaisho T, Sanjo H, Takeuchi O, Sugiyama M, Okabe M, Takeda K, Akira S. 2003. Role of adaptor TRIF in the MyD88-independent toll-like receptor signaling pathway. *Science* 301:640-3.
274. Hacker H, Redecke V, Blagoev B, Kratchmarova I, Hsu LC, Wang GG, Kamps MP, Raz E, Wagner H, Hacker G, Mann M, Karin M. 2006. Specificity in Toll-like receptor signalling through distinct effector functions of TRAF3 and TRAF6. *Nature* 439:204-7.
275. Oganessian G, Saha SK, Guo B, He JQ, Shahangian A, Zarnegar B, Perry A, Cheng G. 2006. Critical role of TRAF3 in the Toll-like receptor-dependent and -independent antiviral response. *Nature* 439:208-11.
276. Fitzgerald KA, McWhirter SM, Faia KL, Rowe DC, Latz E, Golenbock DT, Coyle AJ, Liao SM, Maniatis T. 2003. IKKepsilon and TBK1 are essential components of the IRF3 signaling pathway. *Nat Immunol* 4:491-6.
277. Sharma S, tenOever BR, Grandvaux N, Zhou GP, Lin R, Hiscott J. 2003. Triggering the interferon antiviral response through an IKK-related pathway. *Science* 300:1148-51.
278. Honda K, Takaoka A, Taniguchi T. 2006. Type I interferon [corrected] gene induction by the interferon regulatory factor family of transcription factors. *Immunity* 25:349-60.
279. Honda K, Taniguchi T. 2006. IRFs: master regulators of signalling by Toll-like receptors and cytosolic pattern-recognition receptors. *Nat Rev Immunol* 6:644-58.

280. Sato M, Hata N, Asagiri M, Nakaya T, Taniguchi T, Tanaka N. 1998. Positive feedback regulation of type I IFN genes by the IFN-inducible transcription factor IRF-7. *FEBS Lett* 441:106-10.
281. Marie I, Durbin JE, Levy DE. 1998. Differential viral induction of distinct interferon-alpha genes by positive feedback through interferon regulatory factor-7. *EMBO J* 17:6660-9.
282. Ning S, Pagano JS, Barber GN. 2011. IRF7: activation, regulation, modification and function. *Genes and immunity* 12:399-414.
283. Fitzgerald KA, Rowe DC, Barnes BJ, Caffrey DR, Visintin A, Latz E, Monks B, Pitha PM, Golenbock DT. 2003. LPS-TLR4 Signaling to IRF-3/7 and NF- κ B Involves the Toll Adapters TRAM and TRIF. *The Journal of Experimental Medicine* 198:1043-1055.
284. Honda K, Yanai H, Mizutani T, Negishi H, Shimada N, Suzuki N, Ohba Y, Takaoka A, Yeh WC, Taniguchi T. 2004. Role of a transductional-transcriptional processor complex involving MyD88 and IRF-7 in Toll-like receptor signaling. *Proc Natl Acad Sci U S A* 101:15416-21.
285. Chow KT, Gale M, Jr., Loo YM. 2018. RIG-I and Other RNA Sensors in Antiviral Immunity. *Annu Rev Immunol* 36:667-694.
286. Yoneyama M, Kikuchi M, Matsumoto K, Imaizumi T, Miyagishi M, Taira K, Foy E, Loo YM, Gale M, Jr., Akira S, Yonehara S, Kato A, Fujita T. 2005. Shared and unique functions of the DExD/H-box helicases RIG-I, MDA5, and LGP2 in antiviral innate immunity. *J Immunol* 175:2851-8.
287. Saito T, Hirai R, Loo YM, Owen D, Johnson CL, Sinha SC, Akira S, Fujita T, Gale M. 2007. Regulation of innate antiviral defenses through a shared repressor domain in RIG-I and LGP2. *Proc Natl Acad Sci U S A* 104:582-7.
288. Murali A, Li X, Ranjith-Kumar CT, Bhardwaj K, Holzenburg A, Li P, Kao CC. 2008. Structure and function of LGP2, a DEX(D/H) helicase that regulates the innate immunity response. *J Biol Chem* 283:15825-33.
289. Bruns AM, Leser GP, Lamb RA, Horvath CM. 2014. The innate immune sensor LGP2 activates antiviral signaling by regulating MDA5-RNA interaction and filament assembly. *Mol Cell* 55:771-81.
290. Komuro A, Horvath CM. 2006. RNA- and virus-independent inhibition of antiviral signaling by RNA helicase LGP2. *J Virol* 80:12332-42.
291. Kato H, Takeuchi O, Sato S, Yoneyama M, Yamamoto M, Matsui K, Uematsu S, Jung A, Kawai T, Ishii KJ, Yamaguchi O, Otsu K, Tsujimura T, Koh CS, Reis e Sousa C, Matsuura Y, Fujita T, Akira S. 2006. Differential roles of MDA5 and RIG-I helicases in the recognition of RNA viruses. *Nature* 441:101-5.

292. Pichlmair A, Schulz O, Tan CP, Naslund TI, Liljestrom P, Weber F, Reis e Sousa C. 2006. RIG-I-mediated antiviral responses to single-stranded RNA bearing 5'-phosphates. *Science* 314:997-1001.
293. Schmidt A, Schwerd T, Hamm W, Hellmuth JC, Cui S, Wenzel M, Hoffmann FS, Michallet MC, Besch R, Hopfner KP, Endres S, Rothenfusser S. 2009. 5'-triphosphate RNA requires base-paired structures to activate antiviral signaling via RIG-I. *Proc Natl Acad Sci U S A* 106:12067-72.
294. Wang Y, Ludwig J, Schuberth C, Goldeck M, Schlee M, Li H, Juranek S, Sheng G, Micura R, Tuschl T, Hartmann G, Patel DJ. 2010. Structural and functional insights into 5'-ppp RNA pattern recognition by the innate immune receptor RIG-I. *Nat Struct Mol Biol* 17:781-7.
295. Kato H, Takeuchi O, Mikamo-Satoh E, Hirai R, Kawai T, Matsushita K, Hiiragi A, Dermody TS, Fujita T, Akira S. 2008. Length-dependent recognition of double-stranded ribonucleic acids by retinoic acid-inducible gene-I and melanoma differentiation-associated gene 5. *J Exp Med* 205:1601-10.
296. Pichlmair A, Schulz O, Tan CP, Rehwinkel J, Kato H, Takeuchi O, Akira S, Way M, Schiavo G, Reis e Sousa C. 2009. Activation of MDA5 requires higher-order RNA structures generated during virus infection. *J Virol* 83:10761-9.
297. Feng Q, Hato SV, Langereis MA, Zoll J, Virgen-Slane R, Peisley A, Hur S, Semler BL, van Rij RP, van Kuppeveld FJ. 2012. MDA5 detects the double-stranded RNA replicative form in picornavirus-infected cells. *Cell Rep* 2:1187-96.
298. Triantafilou K, Vakakis E, Kar S, Richer E, Evans GL, Triantafilou M. 2012. Visualisation of direct interaction of MDA5 and the dsRNA replicative intermediate form of positive strand RNA viruses. *J Cell Sci* 125:4761-9.
299. Runge S, Sparrer KM, Lassig C, Hembach K, Baum A, Garcia-Sastre A, Soding J, Conzelmann KK, Hopfner KP. 2014. In vivo ligands of MDA5 and RIG-I in measles virus-infected cells. *PLoS Pathog* 10:e1004081.
300. Deddouche S, Goubau D, Rehwinkel J, Chakravarty P, Begum S, Maillard PV, Borg A, Matthews N, Feng Q, van Kuppeveld FJ, Reis e Sousa C. 2014. Identification of an LGP2-associated MDA5 agonist in picornavirus-infected cells. *Elife* 3:e01535.
301. Malathi K, Saito T, Crochet N, Barton DJ, Gale M, Jr., Silverman RH. 2010. RNase L releases a small RNA from HCV RNA that refolds into a potent PAMP. *RNA* 16:2108-19.
302. Hou F, Sun L, Zheng H, Skaug B, Jiang QX, Chen ZJ. 2011. MAVS Forms Functional Prion-Like Aggregates To Activate and Propagate Antiviral Innate Immune Response. *Cell* 146:448-61.

303. Ford E, Thanos D. 2010. The transcriptional code of human IFN-beta gene expression. *Biochim Biophys Acta* 1799:328-36.
304. Kim TK, Maniatis T. 1997. The mechanism of transcriptional synergy of an in vitro assembled interferon-beta enhanceosome. *Mol Cell* 1:119-29.
305. Agalioti T, Lomvardas S, Parekh B, Yie J, Maniatis T, Thanos D. 2000. Ordered Recruitment of Chromatin Modifying and General Transcription Factors to the IFN- β Promoter. *Cell* 103:667-678.
306. Ryals J, Dierks P, Ragg H, Weissmann C. 1985. A 46-nucleotide promoter segment from an IFN-alpha gene renders an unrelated promoter inducible by virus. *Cell* 41:497-507.
307. Tailor P, Tamura T, Kong HJ, Kubota T, Kubota M, Borghi P, Gabriele L, Ozato K. 2007. The feedback phase of type I interferon induction in dendritic cells requires interferon regulatory factor 8. *Immunity* 27:228-39.
308. Levy DE, Marie I, Prakash A. 2003. Ringing the interferon alarm: differential regulation of gene expression at the interface between innate and adaptive immunity. *Curr Opin Immunol* 15:52-8.
309. Genin P, Vaccaro A, Civas A. 2009. The role of differential expression of human interferon--a genes in antiviral immunity. *Cytokine Growth Factor Rev* 20:283-95.
310. Stark GR, Kerr IM, Williams BR, Silverman RH, Schreiber RD. 1998. How cells respond to interferons. *Annu Rev Biochem* 67:227-64.
311. Cohen B, Novick D, Barak S, Rubinstein M. 1995. Ligand-induced association of the type I interferon receptor components. *Molecular and Cellular Biology* 15:4208-4214.
312. Colamonici O, Yan H, Domanski P, Handa R, Smalley D, Mullersman J, Witte M, Krishnan K, Krolewski J. 1994. Direct binding to and tyrosine phosphorylation of the alpha subunit of the type I interferon receptor by p135tyk2 tyrosine kinase. *Mol Cell Biol* 14:8133-42.
313. Gauzzi MC, Velazquez L, McKendry R, Mogensen KE, Fellous M, Pellegrini S. 1996. Interferon-alpha-dependent activation of Tyk2 requires phosphorylation of positive regulatory tyrosines by another kinase. *J Biol Chem* 271:20494-500.
314. Krishnan K, Yan H, Lim JT, Krolewski JJ. 1996. Dimerization of a chimeric CD4-interferon-alpha receptor reconstitutes the signaling events preceding STAT phosphorylation. *Oncogene* 13:125-133.
315. Yan H, Krishnan K, Greenlund AC, Gupta S, Lim JT, Schreiber RD, Schindler CW, Krolewski JJ. 1996. Phosphorylated interferon-alpha receptor 1 subunit (IFN α R1) acts as a docking site for the latent form of the 113 kDa STAT2 protein. *The EMBO Journal* 15:1064-1074.

316. Darnell JE, Jr. 1997. STATs and gene regulation. *Science* 277:1630-5.
317. Levy DE, Kessler DS, Pine R, Reich N, Darnell JE, Jr. 1988. Interferon-induced nuclear factors that bind a shared promoter element correlate with positive and negative transcriptional control. *Genes Dev* 2:383-93.
318. Reich N, Evans B, Levy D, Fahey D, Knight E, Jr., Darnell JE, Jr. 1987. Interferon-induced transcription of a gene encoding a 15-kDa protein depends on an upstream enhancer element. *Proc Natl Acad Sci U S A* 84:6394-8.
319. Nguyen H, Ramana CV, Bayes J, Stark GR. 2001. Roles of phosphatidylinositol 3-kinase in interferon-gamma-dependent phosphorylation of STAT1 on serine 727 and activation of gene expression. *J Biol Chem* 276:33361-8.
320. Wen Z, Zhong Z, Darnell JE, Jr. 1995. Maximal activation of transcription by Stat1 and Stat3 requires both tyrosine and serine phosphorylation. *Cell* 82:241-50.
321. Meinke A, Barahmand-Pour F, Wohrl S, Stoiber D, Decker T. 1996. Activation of different Stat5 isoforms contributes to cell-type-restricted signaling in response to interferons. *Mol Cell Biol* 16:6937-44.
322. Matikainen S, Sareneva T, Ronni T, Lehtonen A, Koskinen PJ, Julkunen I. 1999. Interferon-alpha activates multiple STAT proteins and upregulates proliferation-associated IL-2Ralpha, c-myc, and pim-1 genes in human T cells. *Blood* 93:1980-91.
323. Fasler-Kan E, Pansky A, Wiederkehr M, Battegay M, Heim MH. 1998. Interferon-alpha activates signal transducers and activators of transcription 5 and 6 in Daudi cells. *Eur J Biochem* 254:514-9.
324. van Boxel-Dezaire AH, Rani MR, Stark GR. 2006. Complex modulation of cell type-specific signaling in response to type I interferons. *Immunity* 25:361-72.
325. Plantanias L. 2005. Mechanisms of Type-I- and Type-II-Interferon-Mediated Signalling. *Nature Reviews Immunology* 5:375-386.
326. Li Y, Sassano A, Majchrzak B, Deb DK, Levy DE, Gaestel M, Nebreda AR, Fish EN, Plantanias LC. 2004. Role of p38alpha Map kinase in Type I interferon signaling. *J Biol Chem* 279:970-9.
327. Uddin S, Majchrzak B, Woodson J, Arunkumar P, Alsayed Y, Pine R, Young PR, Fish EN, Plantanias LC. 1999. Activation of the p38 mitogen-activated protein kinase by type I interferons. *J Biol Chem* 274:30127-31.
328. Uddin S, Lekmine F, Sharma N, Majchrzak B, Mayer I, Young PR, Bokoch GM, Fish EN, Plantanias LC. 2000. The Rac1/p38 mitogen-activated protein kinase pathway is required for interferon alpha-dependent transcriptional activation but not serine phosphorylation of Stat proteins. *J Biol Chem* 275:27634-40.

329. Ahmad S, Alsayed YM, Druker BJ, Plataniias LC. 1997. The type I interferon receptor mediates tyrosine phosphorylation of the CrkL adaptor protein. *J Biol Chem* 272:29991-4.
330. Huang CC, You JL, Wu MY, Hsu KS. 2004. Rap1-induced p38 mitogen-activated protein kinase activation facilitates AMPA receptor trafficking via the GDI.Rab5 complex. Potential role in (S)-3,5-dihydroxyphenylglycine-induced long term depression. *J Biol Chem* 279:12286-92.
331. Uddin S, Sassano A, Deb DK, Verma A, Majchrzak B, Rahman A, Malik AB, Fish EN, Plataniias LC. 2002. Protein kinase C-delta (PKC-delta) is activated by type I interferons and mediates phosphorylation of Stat1 on serine 727. *J Biol Chem* 277:14408-16.
332. Bell O, Tiwari VK, Thomä NH, Schübeler D. 2011. Determinants and dynamics of genome accessibility. *Nature Reviews Genetics* 12:554.
333. Cui K, Tailor P, Liu H, Chen X, Ozato K, Zhao K. 2004. The Chromatin-Remodeling BAF Complex Mediates Cellular Antiviral Activities by Promoter Priming. *Molecular and Cellular Biology* 24:4476-4486.
334. Yan Z, Cui K, Murray DM, Ling C, Xue Y, Gerstein A, Parsons R, Zhao K, Wang W. 2005. PBAF chromatin-remodeling complex requires a novel specificity subunit, BAF200, to regulate expression of selective interferon-responsive genes. *Genes & Development* 19:1662-1667.
335. Huang M, Qian F, Hu Y, Ang C, Li Z, Wen Z. 2002. Chromatin-remodelling factor BRG1 selectively activates a subset of interferon- α -inducible genes. *Nature Cell Biology* 4:774.
336. Qureshi SA, Salditt-Georgieff M, Darnell JE. 1995. Tyrosine-phosphorylated Stat1 and Stat2 plus a 48-kDa protein all contact DNA in forming interferon-stimulated-gene factor 3. *Proceedings of the National Academy of Sciences* 92:3829-3833.
337. Zhang JJ, Vinkemeier U, Gu W, Chakravarti D, Horvath CM, Darnell JE, Jr. 1996. Two contact regions between Stat1 and CBP/p300 in interferon gamma signaling. *Proc Natl Acad Sci U S A* 93:15092-6.
338. Bhattacharya S, Eckner R, Grossman S, Oldread E, Arany Z, D'Andrea A, Livingston DM. 1996. Cooperation of Stat2 and p300/CBP in signalling induced by interferon-alpha. *Nature* 383:344-7.
339. Hebbes TR, Thorne AW, Crane-Robinson C. 1988. A direct link between core histone acetylation and transcriptionally active chromatin. *EMBO J* 7:1395-402.
340. Zhang JJ, Zhao Y, Chait BT, Lathem WW, Ritzi M, Knippers R, Darnell JE, Jr. 1998. Ser727-dependent recruitment of MCM5 by Stat1alpha in IFN-gamma-induced transcriptional activation. *EMBO J* 17:6963-71.

341. DaFonseca CJ, Shu F, Zhang JJ. 2001. Identification of two residues in MCM5 critical for the assembly of MCM complexes and Stat1-mediated transcription activation in response to IFN-gamma. *Proc Natl Acad Sci U S A* 98:3034-9.
342. Paulson M, Press C, Smith E, Tanese N, Levy DE. 2002. IFN-Stimulated transcription through a TBP-free acetyltransferase complex escapes viral shutoff. *Nature Cell Biology* 4:140.
343. Nusinzon I, Horvath CM. 2003. Interferon-stimulated transcription and innate antiviral immunity require deacetylase activity and histone deacetylase 1. *Proc Natl Acad Sci U S A* 100:14742-7.
344. Chang HM, Paulson M, Holko M, Rice CM, Williams BR, Marie I, Levy DE. 2004. Induction of interferon-stimulated gene expression and antiviral responses require protein deacetylase activity. *Proc Natl Acad Sci U S A* 101:9578-83.
345. Sakamoto S, Potla R, Lerner AC. 2004. Histone deacetylase activity is required to recruit RNA polymerase II to the promoters of selected interferon-stimulated early response genes. *J Biol Chem* 279:40362-7.
346. Tahk S, Liu B, Chernishof V, Wong KA, Wu H, Shuai K. 2007. Control of specificity and magnitude of NF- κ B and STAT1-mediated gene activation through PIASy and PIAS1 cooperation. *Proceedings of the National Academy of Sciences* 104:11643-11648.
347. Liu B, Gross M, ten Hoeve J, Shuai K. 2001. A transcriptional corepressor of Stat1 with an essential LXXLL signature motif. *Proceedings of the National Academy of Sciences* 98:3203-3207.
348. Morrow AN, Schmeisser H, Tsuno T, Zoon KC. 2011. A Novel Role for IFN-Stimulated Gene Factor 3^{II} in IFN- γ Signaling and Induction of Antiviral Activity in Human Cells. *The Journal of Immunology* 186:1685-1693.
349. Fink K, Grandvaux N. 2013. STAT2 and IRF9. *JAK-STAT* 2:e27521.
350. Fish EN, Uddin S, Korkmaz M, Majchrzak B, Druker BJ, Plataniias LC. 1999. Activation of a CrkL-Stat5 Signaling Complex by Type I Interferons. *Journal of Biological Chemistry* 274:571-573.
351. Xu L, Zhou X, Wang W, Wang Y, Yin Y, Laan LJWvd, Sprengers D, Metselaar HJ, Peppelenbosch MP, Pan Q. 2016. IFN regulatory factor 1 restricts hepatitis E virus replication by activating STAT1 to induce antiviral IFN-stimulated genes. *The FASEB Journal* 30:3352-3367.
352. Harada H, Takahashi E, Itoh S, Harada K, Hori TA, Taniguchi T. 1994. Structure and regulation of the human interferon regulatory factor 1 (IRF-1) and IRF-2 genes: implications for a gene network in the interferon system. *Molecular and Cellular Biology* 14:1500-1509.

353. Ivashkiv LB, Donlin LT. 2014. Regulation of type I interferon responses. *Nat Rev Immunol* 14:36-49.
354. Grandvaux N, Servant MJ, tenOever B, Sen GC, Balachandran S, Barber GN, Lin R, Hiscott J. 2002. Transcriptional profiling of interferon regulatory factor 3 target genes: direct involvement in the regulation of interferon-stimulated genes. *J Virol* 76:5532-9.
355. Collins SE, Noyce RS, Mossman KL. 2004. Innate Cellular Response to Virus Particle Entry Requires IRF3 but Not Virus Replication. *Journal of Virology* 78:1706-1717.
356. E. CN, Bo-Ram B, Purnima G, Meng L, L. CD, Michael UT, P. JL, R. CJ, Takeshi S. 2016. Retinoid regulation of antiviral innate immunity in hepatocytes. *Hepatology* 63:1783-1795.
357. Schneider WM, Chevillotte MD, Rice CM. 2014. Interferon-Stimulated Genes: A Complex Web of Host Defenses. *Annual review of immunology* 32:513-545.
358. Chakrabarti A, Jha BK, Silverman RH. 2011. New insights into the role of RNase L in innate immunity. *J Interferon Cytokine Res* 31:49-57.
359. Munir M, Berg M. 2013. The multiple faces of protein kinase R in antiviral defense. *Virulence* 4:85-9.
360. Rogers RS, Horvath CM, Matunis MJ. 2003. SUMO modification of STAT1 and its role in PIAS-mediated inhibition of gene activation. *J Biol Chem* 278:30091-7.
361. Ungureanu D, Vanhatupa S, Kotaja N, Yang J, Aittomaki S, Janne OA, Palvimo JJ, Silvennoinen O. 2003. PIAS proteins promote SUMO-1 conjugation to STAT1. *Blood* 102:3311-3.
362. Ungureanu D, Vanhatupa S, Gronholm J, Palvimo JJ, Silvennoinen O. 2005. SUMO-1 conjugation selectively modulates STAT1-mediated gene responses. *Blood* 106:224-6.
363. Endo TA, Masuhara M, Yokouchi M, Suzuki R, Sakamoto H, Mitsui K, Matsumoto A, Tanimura S, Ohtsubo M, Misawa H, Miyazaki T, Leonor N, Taniguchi T, Fujita T, Kanakura Y, Komiyama S, Yoshimura A. 1997. A new protein containing an SH2 domain that inhibits JAK kinases. *Nature* 387:921-4.
364. Kamizono S, Hanada T, Yasukawa H, Minoguchi S, Kato R, Minoguchi M, Hattori K, Hatakeyama S, Yada M, Morita S, Kitamura T, Kato H, Nakayama K, Yoshimura A. 2001. The SOCS box of SOCS-1 accelerates ubiquitin-dependent proteolysis of TEL-JAK2. *J Biol Chem* 276:12530-8.
365. Malakhova OA, Kim KI, Luo JK, Zou W, Kumar KG, Fuchs SY, Shuai K, Zhang DE. 2006. UBP43 is a novel regulator of interferon signaling independent of its ISG15 isopeptidase activity. *EMBO J* 25:2358-67.

366. Francois-Newton V, Magno de Freitas Almeida G, Payelle-Brogard B, Monneron D, Pichard-Garcia L, Piehler J, Pellegrini S, Uze G. 2011. USP18-based negative feedback control is induced by type I and type III interferons and specifically inactivates interferon alpha response. *PLoS One* 6:e22200.
367. Makowska Z, Duong FH, Trincucci G, Tough DF, Heim MH. 2011. Interferon-beta and interferon-lambda signaling is not affected by interferon-induced refractoriness to interferon-alpha in vivo. *Hepatology* 53:1154-63.
368. Gao S, von der Malsburg A, Paeschke S, Behlke J, Haller O, Kochs G, Daumke O. 2010. Structural basis of oligomerization in the stalk region of dynamin-like MxA. *Nature* 465:502-6.
369. Klockow B, Tichelaar W, Madden DR, Niemann HH, Akiba T, Hirose K, Manstein DJ. 2002. The dynamin A ring complex: molecular organization and nucleotide-dependent conformational changes. *EMBO J* 21:240-50.
370. Kane M, Yadav SS, Bitzegeio J, Kutluay SB, Zang T, Wilson SJ, Schoggins JW, Rice CM, Yamashita M, Hatzioannou T, Bieniasz PD. 2013. MX2 is an interferon-induced inhibitor of HIV-1 infection. *Nature* 502:563-6.
371. Goujon C, Moncorge O, Bauby H, Doyle T, Ward CC, Schaller T, Hue S, Barclay WS, Schulz R, Malim MH. 2013. Human MX2 is an interferon-induced post-entry inhibitor of HIV-1 infection. *Nature* 502:559-62.
372. Liu Z, Pan Q, Ding S, Qian J, Xu F, Zhou J, Cen S, Guo F, Liang C. 2013. The interferon-inducible MxB protein inhibits HIV-1 infection. *Cell Host Microbe* 14:398-410.
373. Diamond MS, Farzan M. 2013. The broad-spectrum antiviral functions of IFIT and IFITM proteins. *Nat Rev Immunol* 13:46-57.
374. Bluysen HA, Vlietstra RJ, Faber PW, Smit EM, Hagemeyer A, Trapman J. 1994. Structure, chromosome localization, and regulation of expression of the interferon-regulated mouse Ifi54/Ifi56 gene family. *Genomics* 24:137-48.
375. Daugherty MD, Schaller AM, Geballe AP, Malik HS. 2016. Evolution-guided functional analyses reveal diverse antiviral specificities encoded by IFIT1 genes in mammals. *Elife* 5.
376. Daffis S, Szretter KJ, Schriewer J, Li J, Youn S, Errett J, Lin TY, Schneller S, Züst R, Dong H, Thiel V, Sen GC, Fensterl V, Klimstra WB, Pierson TC, Buller RM, Gale M, Jr., Shi PY, Diamond MS. 2010. 2'-O methylation of the viral mRNA cap evades host restriction by IFIT family members. *Nature* 468:452-6.
377. Hyde JL, Gardner CL, Kimura T, White JP, Liu G, Trobaugh DW, Huang C, Tonelli M, Paessler S, Takeda K, Klimstra WB, Amarasinghe GK, Diamond MS. 2014. A viral RNA structural element alters host recognition of nonself RNA. *Science* 343:783-7.

378. Schoggins JW. 2018. Recent advances in antiviral interferon-stimulated gene biology. *F1000Res* 7:309.
379. Huang IC, Bailey CC, Weyer JL, Radoshitzky SR, Becker MM, Chiang JJ, Brass AL, Ahmed AA, Chi X, Dong L, Longobardi LE, Boltz D, Kuhn JH, Elledge SJ, Bavari S, Denison MR, Choe H, Farzan M. 2011. Distinct patterns of IFITM-mediated restriction of filoviruses, SARS coronavirus, and influenza A virus. *PLoS Pathog* 7:e1001258.
380. Feeley EM, Sims JS, John SP, Chin CR, Pertel T, Chen LM, Gaiha GD, Ryan BJ, Donis RO, Elledge SJ, Brass AL. 2011. IFITM3 inhibits influenza A virus infection by preventing cytosolic entry. *PLoS Pathog* 7:e1002337.
381. Anafu AA, Bowen CH, Chin CR, Brass AL, Holm GH. 2013. Interferon-inducible transmembrane protein 3 (IFITM3) restricts reovirus cell entry. *J Biol Chem* 288:17261-71.
382. Li K, Markosyan RM, Zheng YM, Golfetto O, Bungart B, Li M, Ding S, He Y, Liang C, Lee JC, Gratton E, Cohen FS, Liu SL. 2013. IFITM proteins restrict viral membrane hemifusion. *PLoS Pathog* 9:e1003124.
383. Poddar S, Hyde JL, Gorman MJ, Farzan M, Diamond MS. 2016. The Interferon-Stimulated Gene IFITM3 Restricts Infection and Pathogenesis of Arthritogenic and Encephalitic Alphaviruses. *J Virol* 90:8780-94.
384. Gorman MJ, Poddar S, Farzan M, Diamond MS. 2016. The Interferon-Stimulated Gene Ifitm3 Restricts West Nile Virus Infection and Pathogenesis. *J Virol* 90:8212-25.
385. Ryman KD, Meier KC, Nangle EM, Ragsdale SL, Korneeva NL, Rhoads RE, MacDonald MR, Klimstra WB. 2005. Sindbis virus translation is inhibited by a PKR/RNase L-independent effector induced by alpha/beta interferon priming of dendritic cells. *J Virol* 79:1487-99.
386. Wang N, Dong Q, Li J, Jangra RK, Fan M, Brasier AR, Lemon SM, Pfeffer LM, Li K. 2010. Viral induction of the zinc finger antiviral protein is IRF3-dependent but NF-kappaB-independent. *J Biol Chem* 285:6080-90.
387. Zhang Y, Burke CW, Ryman KD, Klimstra WB. 2007. Identification and characterization of interferon-induced proteins that inhibit alphavirus replication. *J Virol* 81:11246-55.
388. Gao G, Guo X, Goff SP. 2002. Inhibition of retroviral RNA production by ZAP, a CCH-type zinc finger protein. *Science* 297:1703-6.
389. Zhu Y, Chen G, Lv F, Wang X, Ji X, Xu Y, Sun J, Wu L, Zheng YT, Gao G. 2011. Zinc-finger antiviral protein inhibits HIV-1 infection by selectively targeting multiply spliced viral mRNAs for degradation. *Proc Natl Acad Sci U S A* 108:15834-9.
390. Muller S, Moller P, Bick MJ, Wurr S, Becker S, Gunther S, Kummerer BM. 2007. Inhibition of filovirus replication by the zinc finger antiviral protein. *J Virol* 81:2391-400.

391. Mao R, Nie H, Cai D, Zhang J, Liu H, Yan R, Cuconati A, Block TM, Guo J-T, Guo H. 2013. Inhibition of Hepatitis B Virus Replication by the Host Zinc Finger Antiviral Protein. *PLoS Pathogens* 9:e1003494.
392. Guo X, Ma J, Sun J, Gao G. 2007. The zinc-finger antiviral protein recruits the RNA processing exosome to degrade the target mRNA. *Proc Natl Acad Sci U S A* 104:151-6.
393. Zhu Y, Wang X, Goff SP, Gao G. 2012. Translational repression precedes and is required for ZAP-mediated mRNA decay. *EMBO J* 31:4236-46.
394. Zhao C, Collins MN, Hsiang TY, Krug RM. 2013. Interferon-induced ISG15 pathway: an ongoing virus-host battle. *Trends Microbiol* 21:181-6.
395. Shi HX, Yang K, Liu X, Liu XY, Wei B, Shan YF, Zhu LH, Wang C. 2010. Positive regulation of interferon regulatory factor 3 activation by Herc5 via ISG15 modification. *Mol Cell Biol* 30:2424-36.
396. Feng Q, Sekula D, Guo Y, Liu X, Black CC, Galimberti F, Shah SJ, Sempere LF, Memoli V, Andersen JB, Hassel BA, Dragnev K, Dmitrovsky E. 2008. UBE1L causes lung cancer growth suppression by targeting cyclin D1. *Mol Cancer Ther* 7:3780-8.
397. Durfee LA, Lyon N, Seo K, Huibregtse JM. 2010. The ISG15 conjugation system broadly targets newly synthesized proteins: implications for the antiviral function of ISG15. *Mol Cell* 38:722-32.
398. Nguyen LH, Espert L, Mechti N, Wilson DM, 3rd. 2001. The human interferon- and estrogen-regulated ISG20/HEM45 gene product degrades single-stranded RNA and DNA in vitro. *Biochemistry* 40:7174-9.
399. Espert L, Degols G, Gongora C, Blondel D, Williams BR, Silverman RH, Mechti N. 2003. ISG20, a new interferon-induced RNase specific for single-stranded RNA, defines an alternative antiviral pathway against RNA genomic viruses. *J Biol Chem* 278:16151-8.
400. Zhou Z, Wang N, Woodson SE, Dong Q, Wang J, Liang Y, Rijnbrand R, Wei L, Nichols JE, Guo JT, Holbrook MR, Lemon SM, Li K. 2011. Antiviral activities of ISG20 in positive-strand RNA virus infections. *Virology* 409:175-88.
401. Espert L, Degols G, Lin YL, Vincent T, Benkirane M, Mechti N. 2005. Interferon-induced exonuclease ISG20 exhibits an antiviral activity against human immunodeficiency virus type 1. *J Gen Virol* 86:2221-9.
402. Feng J, Wickenhagen A, Turnbull ML, Rezelj VV, Kreher F, Tilston-Lunel NL, Slack GS, Brennan B, Koudriakova E, Shaw AE, Rihn SJ, Rice CM, Bieniasz PD, Elliott RM, Shi X, Wilson SJ. 2018. Interferon-Stimulated Gene (ISG)-Expression Screening Reveals the Specific Antibunyaviral Activity of ISG20. *J Virol* 92.
403. Zheng Z, Wang L, Pan J. 2017. Interferon-stimulated gene 20-kDa protein (ISG20) in infection and disease: Review and outlook. *Intractable Rare Dis Res* 6:35-40.

404. Liu Y, Nie H, Mao R, Mitra B, Cai D, Yan R, Guo JT, Block TM, Mechti N, Guo H. 2017. Interferon-inducible ribonuclease ISG20 inhibits hepatitis B virus replication through directly binding to the epsilon stem-loop structure of viral RNA. *PLoS Pathog* 13:e1006296.
405. Indraccolo S, Pfeffer U, Minuzzo S, Esposito G, Roni V, Mandruzzato S, Ferrari N, Anfosso L, Dell'Eva R, Noonan DM, Chieco-Bianchi L, Albin A, Amadori A. 2007. Identification of genes selectively regulated by IFNs in endothelial cells. *J Immunol* 178:1122-35.
406. Severa M, Coccia EM, Fitzgerald KA. 2006. Toll-like receptor-dependent and -independent viperin gene expression and counter-regulation by PRDI-binding factor-1/BLIMP1. *J Biol Chem* 281:26188-95.
407. Chin KC, Cresswell P. 2001. Viperin (cig5), an IFN-inducible antiviral protein directly induced by human cytomegalovirus. *Proc Natl Acad Sci U S A* 98:15125-30.
408. DeFilippis VR, Robinson B, Keck TM, Hansen SG, Nelson JA, Fruh KJ. 2006. Interferon regulatory factor 3 is necessary for induction of antiviral genes during human cytomegalovirus infection. *J Virol* 80:1032-7.
409. Stirnweiss A, Ksienzyk A, Klages K, Rand U, Grashoff M, Hauser H, Kroger A. 2010. IFN regulatory factor-1 bypasses IFN-mediated antiviral effects through viperin gene induction. *J Immunol* 184:5179-85.
410. Helbig KJ, Eyre NS, Yip E, Narayana S, Li K, Fiches G, McCartney EM, Jangra RK, Lemon SM, Beard MR. 2011. The antiviral protein viperin inhibits hepatitis C virus replication via interaction with nonstructural protein 5A. *Hepatology* 54:1506-17.
411. Helbig KJ, Carr JM, Calvert JK, Wati S, Clarke JN, Eyre NS, Narayana SK, Fiches GN, McCartney EM, Beard MR. 2013. Viperin is induced following dengue virus type-2 (DENV-2) infection and has anti-viral actions requiring the C-terminal end of viperin. *PLoS Negl Trop Dis* 7:e2178.
412. Szretter KJ, Brien JD, Thackray LB, Virgin HW, Cresswell P, Diamond MS. 2011. The interferon-inducible gene viperin restricts West Nile virus pathogenesis. *J Virol* 85:11557-66.
413. Wang X, Hinson ER, Cresswell P. 2007. The interferon-inducible protein viperin inhibits influenza virus release by perturbing lipid rafts. *Cell Host Microbe* 2:96-105.
414. Nasr N, Maddocks S, Turville SG, Harman AN, Woolger N, Helbig KJ, Wilkinson J, Bye CR, Wright TK, Rambukwelle D, Donaghy H, Beard MR, Cunningham AL. 2012. HIV-1 infection of human macrophages directly induces viperin which inhibits viral production. *Blood* 120:778-88.

415. Ito T, Amakawa R, Inaba M, Ikehara S, Inaba K, Fukuhara S. 2001. Differential Regulation of Human Blood Dendritic Cell Subsets by IFNs. *The Journal of Immunology* 166:2961-2969.
416. Montoya M, Schiavoni G, Mattei F, Gresser I, Belardelli F, Borrow P, Tough DF. 2002. Type I interferons produced by dendritic cells promote their phenotypic and functional activation. *Blood* 99:3263-3271.
417. Le Bon A, Thompson C, Kamphuis E, Durand V, Rossmann C, Kalinke U, Tough DF. 2006. Cutting Edge: Enhancement of Antibody Responses Through Direct Stimulation of B and T Cells by Type I IFN. *The Journal of Immunology* 176:2074-2078.
418. Brinkmann V, Geiger T, Alkan S, Heusser CH. 1993. Interferon alpha increases the frequency of interferon gamma-producing human CD4+ T cells. *J Exp Med* 178:1655-63.
419. Lee CK, Smith E, Gimeno R, Gertner R, Levy DE. 2000. STAT1 affects lymphocyte survival and proliferation partially independent of its role downstream of IFN-gamma. *J Immunol* 164:1286-92.
420. Tanabe Y, Nishibori T, Su L, Arduini RM, Baker DP, David M. 2005. Cutting edge: role of STAT1, STAT3, and STAT5 in IFN-alpha beta responses in T lymphocytes. *J Immunol* 174:609-13.
421. Nguyen KB, Watford WT, Salomon R, Hofmann SR, Pien GC, Morinobu A, Gadina M, O'Shea JJ, Biron CA. 2002. Critical role for STAT4 activation by type 1 interferons in the interferon-gamma response to viral infection. *Science* 297:2063-6.
422. Nguyen KB, Cousens LP, Doughty LA, Pien GC, Durbin JE, Biron CA. 2000. Interferon alpha/beta-mediated inhibition and promotion of interferon gamma: STAT1 resolves a paradox. *Nat Immunol* 1:70-6.
423. Curtsinger JM, Valenzuela JO, Agarwal P, Lins D, Mescher MF. 2005. Type I IFNs provide a third signal to CD8 T cells to stimulate clonal expansion and differentiation. *J Immunol* 174:4465-9.
424. Agarwal P, Raghavan A, Nandiwada SL, Curtsinger JM, Bohjanen PR, Mueller DL, Mescher MF. 2009. Gene regulation and chromatin remodeling by IL-12 and type I IFN in programming for CD8 T cell effector function and memory. *J Immunol* 183:1695-704.
425. Marshall HD, Prince AL, Berg LJ, Welsh RM. 2010. IFN-alpha beta and self-MHC divert CD8 T cells into a distinct differentiation pathway characterized by rapid acquisition of effector functions. *J Immunol* 185:1419-28.
426. Miyagi T, Gil MP, Wang X, Louten J, Chu WM, Biron CA. 2007. High basal STAT4 balanced by STAT1 induction to control type 1 interferon effects in natural killer cells. *J Exp Med* 204:2383-96.

427. Keppler SJ, Rosenits K, Koegl T, Vucikuja S, Aichele P. 2012. Signal 3 cytokines as modulators of primary immune responses during infections: the interplay of type I IFN and IL-12 in CD8 T cell responses. *PLoS One* 7:e40865.
428. Thompson LJ, Kolumam GA, Thomas S, Murali-Krishna K. 2006. Innate inflammatory signals induced by various pathogens differentially dictate the IFN-I dependence of CD8 T cells for clonal expansion and memory formation. *J Immunol* 177:1746-54.
429. Pinto AK, Daffis S, Brien JD, Gainey MD, Yokoyama WM, Sheehan KC, Murphy KM, Schreiber RD, Diamond MS. 2011. A temporal role of type I interferon signaling in CD8+ T cell maturation during acute West Nile virus infection. *PLoS Pathog* 7:e1002407.
430. Coro ES, Chang WL, Baumgarth N. 2006. Type I IFN receptor signals directly stimulate local B cells early following influenza virus infection. *J Immunol* 176:4343-51.
431. Chang WL, Coro ES, Rau FC, Xiao Y, Erle DJ, Baumgarth N. 2007. Influenza virus infection causes global respiratory tract B cell response modulation via innate immune signals. *J Immunol* 178:1457-67.
432. Heer AK, Shamshiev A, Donda A, Uematsu S, Akira S, Kopf M, Marsland BJ. 2007. TLR signaling fine-tunes anti-influenza B cell responses without regulating effector T cell responses. *J Immunol* 178:2182-91.
433. Fink K, Lang KS, Manjarrez-Orduno N, Junt T, Senn BM, Holdener M, Akira S, Zinkernagel RM, Hengartner H. 2006. Early type I interferon-mediated signals on B cells specifically enhance antiviral humoral responses. *Eur J Immunol* 36:2094-105.
434. Bach P, Kamphuis E, Odermatt B, Sutter G, Buchholz CJ, Kalinke U. 2007. Vesicular stomatitis virus glycoprotein displaying retrovirus-like particles induce a type I IFN receptor-dependent switch to neutralizing IgG antibodies. *J Immunol* 178:5839-47.
435. Watson AM, Lam LK, Klimstra WB, Ryman KD. 2016. The 17D-204 Vaccine Strain-Induced Protection against Virulent Yellow Fever Virus Is Mediated by Humoral Immunity and CD4+ but not CD8+ T Cells. *PLoS Pathog* 12:e1005786.
436. Mandl JN, Barry AP, Vanderford TH, Kozyr N, Chavan R, Klucking S, Barrat FJ, Coffman RL, Staprans SI, Feinberg MB. 2008. Divergent TLR7 and TLR9 signaling and type I interferon production distinguish pathogenic and nonpathogenic AIDS virus infections. *Nat Med* 14:1077-87.
437. Jacquelin B, Mayau V, Targat B, Liovat AS, Kunkel D, Petitjean G, Dillies MA, Roques P, Butor C, Silvestri G, Giavedoni LD, Lebon P, Barre-Sinoussi F, Benecke A, Muller-Trutwin MC. 2009. Nonpathogenic SIV infection of African green monkeys induces a strong but rapidly controlled type I IFN response. *J Clin Invest* 119:3544-55.
438. Rotger M, Dalmau J, Rauch A, McLaren P, Bosinger SE, Martinez R, Sandler NG, Roque A, Liebner J, Battegay M, Bernasconi E, Descombes P, Erkizia I, Fellay J,

- Hirschel B, Miro JM, Palou E, Hoffmann M, Massanella M, Blanco J, Woods M, Gunthard HF, de Bakker P, Douek DC, Silvestri G, Martinez-Picado J, Telenti A. 2011. Comparative transcriptomics of extreme phenotypes of human HIV-1 infection and SIV infection in sooty mangabey and rhesus macaque. *J Clin Invest* 121:2391-400.
439. Teijaro JR, Ng C, Lee AM, Sullivan BM, Sheehan KC, Welch M, Schreiber RD, de la Torre JC, Oldstone MB. 2013. Persistent LCMV infection is controlled by blockade of type I interferon signaling. *Science* 340:207-11.
440. Wilson EB, Yamada DH, Elsaesser H, Herskovitz J, Deng J, Cheng G, Aronow BJ, Karp CL, Brooks DG. 2013. Blockade of chronic type I interferon signaling to control persistent LCMV infection. *Science* 340:202-7.
441. Tansey EA, Johnson CD. 2015. Recent advances in thermoregulation. *Advances in Physiology Education* 39:139-148.
442. Parsons K. 2014. *Human Thermal Environments: The Effects of Hot, Moderate, and Cold Environments on Human Health, Comfort, and Performance*, Third ed. Taylor & Francis, Abingdon, UK.
443. A B Craig J, Dvorak M. 1966. Thermal regulation during water immersion. *Journal of Applied Physiology* 21:1577-1585.
444. Wilkerson JE, Raven PB, Horvath SM. 1972. Critical temperature of unacclimatized male Caucasians. *J Appl Physiol* 33:451-5.
445. Erikson H, Krog J, Andersen KL, Scholander PF. 1956. The critical temperature in naked man. *Acta Physiol Scand* 37:35-9.
446. Yoshimura M, Yoshimura H. 1969. Cold tolerance and critical temperature of the Japanese. *Int J Biometeorol* 13:163-72.
447. Kurz A. 2008. Physiology of Thermoregulation. *Best Practice & Research Clinical Anaesthesiology* 22:627-644.
448. Castellani JW, Young AJ. 2016. Human physiological responses to cold exposure: Acute responses and acclimatization to prolonged exposure. *Auton Neurosci* 196:63-74.
449. McAllen RM, Tanaka M, Ootsuka Y, McKinley MJ. 2010. Multiple thermoregulatory effectors with independent central controls. *Eur J Appl Physiol* 109:27-33.
450. Romanovsky AA. 2007. Thermoregulation: some concepts have changed. *Functional architecture of the thermoregulatory system. Am J Physiol Regul Integr Comp Physiol* 292:R37-46.
451. Veicsteinas A, Ferretti G, Rennie DW. 1982. Superficial shell insulation in resting and exercising men in cold water. *J Appl Physiol Respir Environ Exerc Physiol* 52:1557-64.

452. Thompson-Torgerson CS, Holowatz LA, Flavahan NA, Kenney WL. 2007. Cold-induced cutaneous vasoconstriction is mediated by Rho kinase in vivo in human skin. *Am J Physiol Heart Circ Physiol* 292:H1700-5.
453. Brajkovic D, Ducharme MB, Frim J. 1998. Influence of localized auxiliary heating on hand comfort during cold exposure. *J Appl Physiol* (1985) 85:2054-65.
454. Martin K. 2003. Cold-Induced Recruitment of Brown Adipose Tissue Thermogenesis. *Experimental Physiology* 88:141-148.
455. Dawkins MJ, Scopes JW. 1965. Non-shivering thermogenesis and brown adipose tissue in the human new-born infant. *Nature* 206:201-2.
456. van der Lans AA, Wierts R, Vosselman MJ, Schrauwen P, Brans B, van Marken Lichtenbelt WD. 2014. Cold-activated brown adipose tissue in human adults: methodological issues. *Am J Physiol Regul Integr Comp Physiol* 307:R103-13.
457. Just B, Delva E, Camus Y, Lienhart A. 1992. Oxygen uptake during recovery following naloxone. Relationship with intraoperative heat loss. *Anesthesiology* 76:60-4.
458. Frank SM, Raja SN, Bulcao CF, Goldstein DS. 1999. Relative contribution of core and cutaneous temperatures to thermal comfort and autonomic responses in humans. *J Appl Physiol* (1985) 86:1588-93.
459. Castellani JW, Young AJ, Ducharme MB, Giesbrecht GG, Glickman E, Sallis RE. 2006. American College of Sports Medicine position stand: prevention of cold injuries during exercise. *Med Sci Sports Exerc* 38:2012-29.
460. Turk EE. 2010. Hypothermia. *Forensic Sci Med Pathol* 6:106-15.
461. Elenius K, Jalkanen M. 1994. Function of the syndecans--a family of cell surface proteoglycans. *J Cell Sci* 107 (Pt 11):2975-82.
462. Greenfield AD. 1963. The circulation through the skin, p 1325-1351, *Handbook of Physiology Circulation*, vol 2. American Physiological Society, Washington D.C.
463. Johnson JM, Pergola PE, Liao FK, Kellogg DL, Jr., Crandall CG. 1995. Skin of the dorsal aspect of human hands and fingers possesses an active vasodilator system. *J Appl Physiol* (1985) 78:948-54.
464. Taylor NA, Machado-Moreira CA, van den Heuvel AM, Caldwell JN. 2014. Hands and feet: physiological insulators, radiators and evaporators. *Eur J Appl Physiol* 114:2037-60.
465. Hart SR, Bordes B, Hart J, Corsino D, Harmon D. 2011. Unintended Perioperative Hypothermia. *Ochsner J* 11:259-70.

466. Matsukawa T, Sessler DI, Sessler AM, Schroeder M, Ozaki M, Kurz A, Cheng C. 1995. Heat Flow and Distribution during Induction of General Anesthesia. *Anesthesiology* 82:662-673.
467. Ducharme MB, VanHelder WP, Radomski MW. 1991. Tissue temperature profile in the human forearm during thermal stress at thermal stability. *J Appl Physiol* (1985) 71:1973-8.
468. Rajek A, Greif R, Sessler DI, Baumgardner J, Laciny S, Bastanmehr H. 2000. Core cooling by central venous infusion of ice-cold (4 degrees C and 20 degrees C) fluid: isolation of core and peripheral thermal compartments. *Anesthesiology* 93:629-37.
469. Deakin CD. 1998. Changes in core temperature compartment size on induction of general anaesthesia. *Br J Anaesth* 81:861-4.
470. Matsukawa T, Kashimoto S, Ozaki M, Shindo S, Kumazawa T. 1996. Temperatures measured by a deep body thermometer (Coretemp) compared with tissue temperatures measured at various depths using needles placed into the sole of the foot. *Eur J Anaesthesiol* 13:340-5.
471. Kurz A, Sessler DI, Narzt E, Lenhardt R, Lackner F. 1995. Morphometric influences on intraoperative core temperature changes. *Anesth Analg* 80:562-7.
472. McFadden ER, Jr., Pichurko BM, Bowman HF, Ingenito E, Burns S, Dowling N, Solway J. 1985. Thermal mapping of the airways in humans. *J Appl Physiol* (1985) 58:564-70.
473. Durairajanayagam D, Agarwal A, Ong C. 2015. Causes, effects and molecular mechanisms of testicular heat stress. *Reprod Biomed Online* 30:14-27.
474. North BJ, Sinclair DA. 2012. The Intersection Between Aging and Cardiovascular Disease. *Circ Res* 110:1097-108.
475. Holowatz LA, Thompson-Torgerson C, Kenney WL. 2010. Aging and the control of human skin blood flow. *Front Biosci (Landmark Ed)* 15:718-39.
476. Blatteis CM. 2012. Age-dependent changes in temperature regulation - a mini review. *Gerontology* 58:289-95.
477. Anonymous. !!! INVALID CITATION !!! (393, 411).
478. Messner B, Bernhard D. 2014. Smoking and cardiovascular disease: mechanisms of endothelial dysfunction and early atherogenesis. *Arterioscler Thromb Vasc Biol* 34:509-15.
479. Criqui MH, Aboyans V. 2015. Epidemiology of peripheral artery disease. *Circ Res* 116:1509-26.

480. Akishima S, Matsushita S, Sato F, Hyodo K, Imazuru T, Enomoto Y, Noma M, Hiramatsu Y, Shigeta O, Sakakibara Y. 2007. Cigarette-smoke-induced vasoconstriction of peripheral arteries: evaluation by synchrotron radiation microangiography. *Circ J* 71:418-22.
481. Liew NC, Lee L, Nor Hanipah Z, Gee T, Jabar MF. 2015. Pathogenesis and Management of Buerger's Disease. *Int J Low Extrem Wounds* 14:231-5.
482. Kenny GP, Sigal RJ, McGinn R. 2016. Body temperature regulation in diabetes. *Temperature (Austin)* 3:119-45.
483. Savastano DM, Gorbach AM, Eden HS, Brady SM, Reynolds JC, Yanovski JA. 2009. Adiposity and human regional body temperature. *The American Journal of Clinical Nutrition* 90:1124-1131.
484. Temprano KK. 2016. A Review of Raynaud's Disease. *Mo Med* 113:123-6.
485. Evans SS, Repasky EA, Fisher DT. 2015. Fever and the thermal regulation of immunity: the immune system feels the heat. *Nat Rev Immunol* 15:335-49.
486. Hasday JD, Thompson C, Singh IS. 2014. Fever, immunity, and molecular adaptations. *Compr Physiol* 4:109-48.
487. Niven DJ, Gaudet JE, Laupland KB, Mrklas KJ, Roberts DJ, Stelfox H. 2015. Accuracy of peripheral thermometers for estimating temperature: A systematic review and meta-analysis. *Annals of Internal Medicine* 163:768-777.
488. Van Breukelen F, Martin SL. 2002. Invited review: molecular adaptations in mammalian hibernators: unique adaptations or generalized responses? *J Appl Physiol (1985)* 92:2640-7.
489. Richter K, Haslbeck M, Buchner J. 2010. The heat shock response: life on the verge of death. *Mol Cell* 40:253-66.
490. Toivola DM, Strnad P, Habtezion A, Omary MB. 2010. Intermediate filaments take the heat as stress proteins. *Trends Cell Biol* 20:79-91.
491. Welch WJ, Suhan JP. 1985. Morphological study of the mammalian stress response: characterization of changes in cytoplasmic organelles, cytoskeleton, and nucleoli, and appearance of intranuclear actin filaments in rat fibroblasts after heat-shock treatment. *J Cell Biol* 101:1198-211.
492. Buchan JR, Parker R. 2009. Eukaryotic stress granules: the ins and outs of translation. *Mol Cell* 36:932-41.
493. Velichko AK, Markova EN, Petrova NV, Razin SV, Kantidze OL. 2013. Mechanisms of heat shock response in mammals. *Cell Mol Life Sci* 70:4229-41.

494. Park HG, Han SI, Oh SY, Kang HS. 2005. Cellular responses to mild heat stress. *Cell Mol Life Sci* 62:10-23.
495. Punyiczki M, Fesus L. 1998. Heat shock and apoptosis. The two defense systems of the organism may have overlapping molecular elements. *Ann N Y Acad Sci* 851:67-74.
496. Ananthan J, Goldberg AL, Voellmy R. 1986. Abnormal proteins serve as eukaryotic stress signals and trigger the activation of heat shock genes. *Science* 232:522-4.
497. Wu C. 1995. Heat shock transcription factors: structure and regulation. *Annu Rev Cell Dev Biol* 11:441-69.
498. Diller KR. 2006. Stress protein expression kinetics. *Annu Rev Biomed Eng* 8:403-24.
499. Schroder M, Kaufman RJ. 2005. The mammalian unfolded protein response. *Annu Rev Biochem* 74:739-89.
500. Mayer MP, Bukau B. 2005. Hsp70 chaperones: cellular functions and molecular mechanism. *Cell Mol Life Sci* 62:670-84.
501. Mehlen P, Arrigo AP. 1994. The serum-induced phosphorylation of mammalian hsp27 correlates with changes in its intracellular localization and levels of oligomerization. *Eur J Biochem* 221:327-34.
502. Calderwood SK, Murshid A, Prince T. 2009. The shock of aging: molecular chaperones and the heat shock response in longevity and aging--a mini-review. *Gerontology* 55:550-8.
503. Garrido C, Solary E. 2003. A role of HSPs in apoptosis through "protein triage"? *Cell Death Differ* 10:619-20.
504. Garrido C, Gurbuxani S, Ravagnan L, Kroemer G. 2001. Heat shock proteins: endogenous modulators of apoptotic cell death. *Biochem Biophys Res Commun* 286:433-42.
505. Mahat DB, Salamanca HH, Duarte FM, Danko CG, Lis JT. 2016. Mammalian Heat Shock Response and Mechanisms Underlying Its Genome-wide Transcriptional Regulation. *Mol Cell* 62:63-78.
506. Streffer C. 1982. Aspects of biochemical effects by hyperthermia. *Natl Cancer Inst Monogr* 61:11-7.
507. Voellmy R, Boellmann F. 2007. Chaperone regulation of the heat shock protein response. *Adv Exp Med Biol* 594:89-99.
508. Ciuzan O, Hancock J, Pamfil D, Wilson I, Lodomery M. 2015. The evolutionarily conserved multifunctional glycine-rich RNA-binding proteins play key roles in development and stress adaptation. *Physiol Plant* 153:1-11.

509. Leonart ME. 2010. A new generation of proto-oncogenes: Cold-inducible RNA binding proteins. *Biochimica et Biophysica Acta (BBA) - Reviews on Cancer* 1805:43-52.
510. Tong G, Endersfelder S, Rosenthal L-M, Wollersheim S, Sauer IM, Bühner C, Berger F, Schmitt KRL. 2013. Effects of moderate and deep hypothermia on RNA-binding proteins RBM3 and CIRP expressions in murine hippocampal brain slices. *Brain Research* 1504:74-84.
511. Wellmann S, Bühner C, Moderegger E, Zelmer A, Kirschner R, Koehne P, Fujita J, Seeger K. 2004. Oxygen-regulated expression of the RNA-binding proteins RBM3 and CIRP by a HIF-1-independent mechanism. *Journal of Cell Science* 117:1785-1794.
512. Sheikh MS, Carrier F, Papathanasiou MA, Hollander MC, Zhan Q, Yu K, Fornace AJ, Jr. 1997. Identification of several human homologs of hamster DNA damage-inducible transcripts. Cloning and characterization of a novel UV-inducible cDNA that codes for a putative RNA-binding protein. *J Biol Chem* 272:26720-6.
513. Haley B, Paunesku T, Protić M, Woloschak GE. 2009. Response of heterogeneous ribonuclear proteins (hnRNP) to ionising radiation and their involvement in DNA damage repair. *International Journal of Radiation Biology* 85:643-655.
514. Rzechorzek NM, Connick P, Patani R, Selvaraj BT, Chandran S. 2015. Hypothermic Preconditioning of Human Cortical Neurons Requires Proteostatic Priming. *EBioMedicine* 2:528-535.
515. Aoki K, Ishii Y, Matsumoto K, Tsujimoto M. 2002. Methylation of *Xenopus* CIRP2 regulates its arginine- and glycine-rich region-mediated nucleocytoplasmic distribution. *Nucleic Acids Res* 30:5182-92.
516. Nishiyama H, Danno S, Kaneko Y, Itoh K, Yokoi H, Fukumoto M, Okuno H, Millan JL, Matsuda T, Yoshida O, Fujita J. 1998. Decreased expression of cold-inducible RNA-binding protein (CIRP) in male germ cells at elevated temperature. *Am J Pathol* 152:289-96.
517. Danno S, Itoh K, Matsuda T, Fujita J. 2000. Decreased Expression of Mouse *Rbm3*, a Cold-Shock Protein, in Sertoli Cells of Cryptorchid Testis. *The American Journal of Pathology* 156:1685-1692.
518. Zhu X, Bühner C, Wellmann S. 2016. Cold-inducible proteins CIRP and RBM3, a unique couple with activities far beyond the cold. *Cellular and Molecular Life Sciences* 73:3839-3859.
519. Pilotte J, Cunningham BA, Edelman GM, Vanderklish PW. 2009. Developmentally regulated expression of the cold-inducible RNA-binding motif protein 3 in euthermic rat brain. *Brain Research* 1258:12-24.

520. Chip S, Zelmer A, Ogunshola OO, Felderhoff-Mueser U, Nitsch C, Bühner C, Wellmann S. 2011. The RNA-binding protein RBM3 is involved in hypothermia induced neuroprotection. *Neurobiology of Disease* 43:388-396.
521. Danno S, Nishiyama H, Higashitsuji H, Yokoi H, Xue JH, Itoh K, Matsuda T, Fujita J. 1997. Increased transcript level of RBM3, a member of the glycine-rich RNA-binding protein family, in human cells in response to cold stress. *Biochem Biophys Res Commun* 236:804-7.
522. Sumitomo Y, Higashitsuji H, Higashitsuji H, Liu Y, Fujita T, Sakurai T, Candeias MM, Itoh K, Chiba T, Fujita J. 2012. Identification of a novel enhancer that binds Sp1 and contributes to induction of cold-inducible RNA-binding protein (cirp) expression in mammalian cells. *BMC Biotechnology* 12:72.
523. Al-Fageeh MB, Smales CM. 2009. Cold-inducible RNA binding protein (CIRP) expression is modulated by alternative mRNAs. *RNA* 15:1164-76.
524. Yang C, Carrier F. 2001. The UV-inducible RNA-binding Protein A18 (A18 hnRNP) Plays a Protective Role in the Genotoxic Stress Response. *Journal of Biological Chemistry* 276:47277-47284.
525. Liu Y, Hu W, Murakawa Y, Yin J, Wang G, Landthaler M, Yan J. 2013. Cold-induced RNA-binding proteins regulate circadian gene expression by controlling alternative polyadenylation. *Scientific Reports* 3:2054.
526. Barbosa-Morais NL, Carmo-Fonseca M, Aparicio S. 2006. Systematic genome-wide annotation of spliceosomal proteins reveals differential gene family expansion. *Genome Res* 16:66-77.
527. Yang R, Weber DJ, Carrier F. 2006. Post-transcriptional regulation of thioredoxin by the stress inducible heterogenous ribonucleoprotein A18. *Nucleic Acids Research* 34:1224-1236.
528. De Leeuw F, Zhang T, Wauquier C, Huez G, Kruijs V, Gueydan C. 2007. The cold-inducible RNA-binding protein migrates from the nucleus to cytoplasmic stress granules by a methylation-dependent mechanism and acts as a translational repressor. *Experimental Cell Research* 313:4130-4144.
529. Kaliandra dAG, Costa BG, Ângela S, Gustavo ML, T. ZNI, Jörg K. 2011. Evidence for the association of the human regulatory protein Ki-1/57 with the translational machinery. *FEBS Letters* 585:2556-2560.
530. Xun G, Yuehan W, S. HR. 2010. Cold-inducible RNA-binding protein contributes to human antigen R and cyclin E1 deregulation in breast cancer. *Molecular Carcinogenesis* 49:130-140.

531. Wu Y, Guo X, Brandt Y, Hathaway HJ, Hartley RS. 2011. Three-dimensional collagen represses cyclin E1 via β 1 integrin in invasive breast cancer cells. *Breast Cancer Research and Treatment* 127:397-406.
532. Masuda T, Itoh K, Higashitsuji H, Higashitsuji H, Nakazawa N, Sakurai T, Liu Y, Tokuchi H, Fujita T, Zhao Y, Nishiyama H, Tanaka T, Fukumoto M, Ikawa M, Okabe M, Fujita J. 2012. Cold-inducible RNA-binding protein (Cirp) interacts with Dyrk1b/Mirk and promotes proliferation of immature male germ cells in mice. *Proceedings of the National Academy of Sciences* 109:10885-10890.
533. Saito K, Fukuda N, Matsumoto T, Iribe Y, Tsunemi A, Kazama T, Yoshida-Noro C, Hayashi N. 2010. Moderate low temperature preserves the stemness of neural stem cells and suppresses apoptosis of the cells via activation of the cold-inducible RNA binding protein. *Brain Research* 1358:20-29.
534. Zhang H-T, Xue J-H, Zhang Z-W, Kong H-B, Liu A-J, Li S-C, Xu D-G. 2015. Cold-inducible RNA-binding protein inhibits neuron apoptosis through the suppression of mitochondrial apoptosis. *Brain Research* 1622:474-483.
535. Li S, Zhang Z, Xue J, Liu A, Zhang H. 2012. Cold-inducible RNA binding protein inhibits H₂O₂-induced apoptosis in rat cortical neurons. *Brain Research* 1441:47-52.
536. Zhou KW, Zheng XM, Yang ZW, Zhang L, Chen HD. 2009. Overexpression of CIRP may reduce testicular damage induced by cryptorchidism. *Clin Invest Med* 32:E103-11.
537. Lee HN, Ahn S-M, Jang HH. 2015. Cold-inducible RNA-binding protein, CIRP, inhibits DNA damage-induced apoptosis by regulating p53. *Biochemical and Biophysical Research Communications* 464:916-921.
538. Sakurai T, Kudo M, Watanabe T, Itoh K, Higashitsuji H, Arizumi T, Inoue T, Hagiwara S, Ueshima K, Nishida N, Fukumoto M, Fujita J. 2013. Hypothermia Protects against Fulminant Hepatitis in Mice by Reducing Reactive Oxygen Species Production. *Digestive Diseases* 31:440-446.
539. Hofmann S, Cherkasova V, Bankhead P, Bukau B, Stoecklin G. 2012. Translation suppression promotes stress granule formation and cell survival in response to cold shock. *Mol Biol Cell* 23:3786-800.
540. Smart F, Aschrafi A, Atkins A, Owens GC, Pilotte J, Cunningham BA, Vanderklish PW. 2007. Two isoforms of the cold-inducible mRNA-binding protein RBM3 localize to dendrites and promote translation. *J Neurochem* 101:1367-79.
541. Dresios J, Aschrafi A, Owens GC, Vanderklish PW, Edelman GM, Mauro VP. 2005. Cold stress-induced protein Rbm3 binds 60S ribosomal subunits, alters microRNA levels, and enhances global protein synthesis. *Proc Natl Acad Sci U S A* 102:1865-70.
542. Sureban SM, Ramalingam S, Natarajan G, May R, Subramaniam D, Bishnupuri KS, Morrison AR, Dieckgraefe BK, Brackett DJ, Postier RG, Houchen CW, Anant S. 2008.

- Translation regulatory factor RBM3 is a proto-oncogene that prevents mitotic catastrophe. *Oncogene* 27:4544-56.
543. Lin JH, Li H, Yasumura D, Cohen HR, Zhang C, Panning B, Shokat KM, LaVail MM, Walter P. 2007. IRE1 Signaling Affects Cell Fate During the Unfolded Protein Response. *Science* 318:944-949.
544. Zhu X, Zelmer A, Kapfhammer JP, Wellmann S. 2016. Cold-inducible RBM3 inhibits PERK phosphorylation through cooperation with NF90 to protect cells from endoplasmic reticulum stress. *The FASEB Journal* 30:624-634.
545. Poone GK, Hasseldam H, Munkholm N, Rasmussen RS, Gronberg NV, Johansen FF. 2015. The Hypothermic Influence on CHOP and Ero1-alpha in an Endoplasmic Reticulum Stress Model of Cerebral Ischemia. *Brain Sci* 5:178-87.
546. Roobol A, Carden MJ, Newsam RJ, Smales CM. 2009. Biochemical insights into the mechanisms central to the response of mammalian cells to cold stress and subsequent rewarming. *FEBS Journal* 276:286-302.
547. Knight JR, Bastide A, Roobol A, Roobol J, Jackson TJ, Utami W, Barrett DA, Smales CM, Willis AE. 2015. Eukaryotic elongation factor 2 kinase regulates the cold stress response by slowing translation elongation. *Biochem J* 465:227-238.
548. Xia Z, Zheng X, Zheng H, Liu X, Yang Z, Wang X. 2012. Cold-inducible RNA-binding protein (CIRP) regulates target mRNA stabilization in the mouse testis. *FEBS Lett* 586:3299-308.
549. Horvath SM, Spurr GB, Hutt BK, Hamilton LH. 1956. Metabolic cost of shivering. *J Appl Physiol* 8:595-602.
550. Manthous CA, Hall JB, Olson D, Singh M, Chatila W, Pohlman A, Kushner R, Schmidt GA, Wood LD. 1995. Effect of cooling on oxygen consumption in febrile critically ill patients. *Am J Respir Crit Care Med* 151:10-4.
551. Schumacker PT, Rowland J, Saltz S, Nelson DP, Wood LD. 1987. Effects of hyperthermia and hypothermia on oxygen extraction by tissues during hypovolemia. *J Appl Physiol* (1985) 63:1246-52.
552. Young PJ, Saxena MK, Beasley RW. 2011. Fever and antipyresis in infection. *Med J Aust* 195:458-9.
553. Graham NM, Burrell CJ, Douglas RM, Debelle P, Davies L. 1990. Adverse effects of aspirin, acetaminophen, and ibuprofen on immune function, viral shedding, and clinical status in rhinovirus-infected volunteers. *J Infect Dis* 162:1277-82.
554. Doran TF, De Angelis C, Baumgardner RA, Mellits ED. 1989. Acetaminophen: more harm than good for chickenpox? *J Pediatr* 114:1045-8.

555. Earn DJ, Andrews PW, Bolker BM. 2014. Population-level effects of suppressing fever. *Proc Biol Sci* 281:20132570.
556. Prymula R, Siegrist CA, Chlibek R, Zemlickova H, Vackova M, Smetana J, Lommel P, Kaliskova E, Borys D, Schuerman L. 2009. Effect of prophylactic paracetamol administration at time of vaccination on febrile reactions and antibody responses in children: two open-label, randomised controlled trials. *Lancet* 374:1339-50.
557. Launey Y, Nessler N, Malledant Y, Seguin P. 2011. Clinical review: fever in septic ICU patients--friend or foe? *Crit Care* 15:222.
558. Polderman KH. 2008. Induced hypothermia and fever control for prevention and treatment of neurological injuries. *Lancet* 371:1955-69.
559. Osawa E, Muschel LH. 1964. STUDIES RELATING TO THE SERUM RESISTANCE OF CERTAIN GRAM-NEGATIVE BACTERIA. *J Exp Med* 119:41-51.
560. Hasday JD, Singh IS. 2000. Fever and the heat shock response: distinct, partially overlapping processes. *Cell Stress Chaperones* 5:471-80.
561. Girard JP, Moussion C, Forster R. 2012. HEVs, lymphatics and homeostatic immune cell trafficking in lymph nodes. *Nat Rev Immunol* 12:762-73.
562. von Andrian UH, Mempel TR. 2003. Homing and cellular traffic in lymph nodes. *Nat Rev Immunol* 3:867-78.
563. Griffith JW, Sokol CL, Luster AD. 2014. Chemokines and chemokine receptors: positioning cells for host defense and immunity. *Annu Rev Immunol* 32:659-702.
564. Ostberg JR, Ertel BR, Lanphere JA. 2005. An important role for granulocytes in the thermal regulation of colon tumor growth. *Immunol Invest* 34:259-72.
565. Takada Y, Sato EF, Nakajima T, Hosono M, Tsumura M, Inoue M, Yamada R. 2000. Granulocyte-colony stimulating factor enhances anti-tumour effect of hyperthermia. *Int J Hyperthermia* 16:275-86.
566. Rice P, Martin E, He JR, Frank M, DeTolla L, Hester L, O'Neill T, Manka C, Benjamin I, Nagarsekar A, Singh I, Hasday JD. 2005. Febrile-range hyperthermia augments neutrophil accumulation and enhances lung injury in experimental gram-negative bacterial pneumonia. *J Immunol* 174:3676-85.
567. Zanker KS, Lange J. 1982. Whole body hyperthermia and natural killer cell activity. *Lancet* 1:1079-80.
568. Pritchard MT, Li Z, Repasky EA. 2005. Nitric oxide production is regulated by fever-range thermal stimulation of murine macrophages. *J Leukoc Biol* 78:630-8.

569. Vega VL, Rodriguez-Silva M, Frey T, Gehrman M, Diaz JC, Steinem C, Multhoff G, Arispe N, De Maio A. 2008. Hsp70 translocates into the plasma membrane after stress and is released into the extracellular environment in a membrane-associated form that activates macrophages. *J Immunol* 180:4299-307.
570. Noessner E, Gastpar R, Milani V, Brandl A, Hutzler PJ, Kuppner MC, Roos M, Kremmer E, Asea A, Calderwood SK, Issels RD. 2002. Tumor-derived heat shock protein 70 peptide complexes are cross-presented by human dendritic cells. *J Immunol* 169:5424-32.
571. Hatzfeld-Charbonnier AS, Lasek A, Castera L, Gosset P, Velu T, Formstecher P, Mortier L, Marchetti P. 2007. Influence of heat stress on human monocyte-derived dendritic cell functions with immunotherapeutic potential for antitumor vaccines. *J Leukoc Biol* 81:1179-87.
572. Ostberg JR, Gellin C, Patel R, Repasky EA. 2001. Regulatory potential of fever-range whole body hyperthermia on Langerhans cells and lymphocytes in an antigen-dependent cellular immune response. *J Immunol* 167:2666-70.
573. Frink M, Flohe S, van Griensven M, Mommsen P, Hildebrand F. 2012. Facts and fiction: the impact of hypothermia on molecular mechanisms following major challenge. *Mediators Inflamm* 2012:762840.
574. Webster CM, Kelly S, Koike MA, Chock VY, Giffard RG, Yenari MA. 2009. Inflammation and NF κ B activation is decreased by hypothermia following global cerebral ischemia. *Neurobiology of Disease* 33:301-312.
575. Du G, Liu Y, Li J, Liu W, Wang Y, Li H. 2013. Hypothermic microenvironment plays a key role in tumor immune subversion. *Int Immunopharmacol* 17:245-253.
576. Horosz B, Malec-Milewska M. 2013. Inadvertent intraoperative hypothermia. *Anaesthesiol Intensive Ther* 45:38-43.
577. Foxman EF, Storer JA, Fitzgerald ME, Wasik BR, Hou L, Zhao H, Turner PE, Pyle AM, Iwasaki A. 2015. Temperature-dependent innate defense against the common cold virus limits viral replication at warm temperature in mouse airway cells. *Proc Natl Acad Sci U S A* doi:10.1073/pnas.1411030112.
578. Letchworth GJ, Carmichael LE. 1984. Local tissue temperature: a critical factor in the pathogenesis of bovid herpesvirus 2. *Infect Immun* 43:1072-9.
579. Matsui T, Motoki Y, Yoshida Y. 2013. Hypothermia reduces toll-like receptor 3-activated microglial interferon-beta and nitric oxide production. *Mediators Inflamm* 2013:436263.
580. van den Broek MF, Muller U, Huang S, Zinkernagel RM, Aguet M. 1995. Immune defence in mice lacking type I and/or type II interferon receptors. *Immunol Rev* 148:5-18.

581. McFadden G, Mohamed MR, Rahman MM, Bartee E. 2009. Cytokine determinants of viral tropism. *Nat Rev Immunol* 9:645-55.
582. Goubau D, Deddouche S, Reis ESC. 2013. Cytosolic sensing of viruses. *Immunity* 38:855-69.
583. MacMicking JD. 2012. Interferon-inducible effector mechanisms in cell-autonomous immunity. *Nat Rev Immunol* 12:367-82.
584. Sadler AJ, Williams BR. 2008. Interferon-inducible antiviral effectors. *Nat Rev Immunol* 8:559-68.
585. Garcia-Sastre A, Durbin RK, Zheng H, Palese P, Gertner R, Levy DE, Durbin JE. 1998. The role of interferon in influenza virus tissue tropism. *J Virol* 72:8550-8.
586. Brajkovic D, Ducharme MB, Frim J. 2001. Relationship between body heat content and finger temperature during cold exposure. *J Appl Physiol* (1985) 90:2445-52.
587. Garmel GM. 2012. Fever in adults, p 375-392. *In* Mahadevan SV, Garmel GM (ed), *An Introduction to Clinical Emergency Medicine*, 2 ed. Cambridge University Press.
588. Boonarkart C, Suptawiwat O, Sakorn K, Puthavathana P, Auewarakul P. 2017. Exposure to cold impairs interferon-induced antiviral defense. *Arch Virol* 162:2231-2237.
589. Ruiz-Gomez J, Sosa-Martinez J. 1965. Virus multiplication and interferon production at different temperatures in adult mice infected with Coxsackie B 1 Virus. *Archiv für die gesamte Virusforschung* 17:295-299.
590. Postic B, DeAngelis C, Breinig MK, Ho M. 1966. Effect of Temperature of the Induction of Interferons by Endotoxin and Virus. *Journal of Bacteriology* 91:1277-1281.
591. Hirai N, Hill NO, Oshier K. 1984. Temperature Influences on Different Human Alpha Interferon Activities. *Journal of Interferon Research* 4:507-516.
592. Letchworth GJ, 3rd, Carmichael LE. 1984. The effect of temperature on production and function of bovine interferons. *Arch Virol* 82:211-21.
593. Groveman DS, Borden EC, Merritt JA, Robins HI, Steeves R, Bryan GT. 1984. Augmented antiproliferative effects of interferons at elevated temperatures against human bladder carcinoma cell lines. *Cancer Res* 44:5517-21.
594. Fleischmann Jr. WR, Fleischmann CM, Gindhart TD. 1986. Effect of Hyperthermia on the Antiproliferative Activities of Murine α -, β -, and γ -Interferon: Differential Enhancement of Effect of Hyperthermia on the Antiproliferative Activities of Murine γ -Interferon. *Cancer Research* 46:8-13.
595. Gifford GE. 1963. Effect of Environmental Changes upon Antiviral Action of Interferon. *Proceedings of the Society for Experimental Biology and Medicine* 114:644-649.

596. Kirn A, Schieffer A, Tinland R. 1967. Lack of Correlation between Production of Interferon and Protection of Temperature in Mice infected with Sindbis Virus. *Nature* 215:86.
597. Lockart RZ, Jr., Bayliss NL, Toy ST, Yin FH. 1968. Viral events necessary for the induction of interferon in chick embryo cells. *J Virol* 2:962-5.
598. Skehel JJ, Burke DC. 1968. A Temperature-sensitive Event in Interferon Production. *Journal of General Virology* 3:191-199.
599. Cole GA, Wisseman CL. 1969. The Effect of Hyperthermia on Dengue Virus Infection of Mice. *Proceedings of the Society for Experimental Biology and Medicine* 130:359-363.
600. Pusztai R, Béládi I, Bakay M, Mucsi I. 1969. Effect of Ultraviolet Irradiation and Heating on the Interferon-inducing Capacity of Human Adenoviruses. *Journal of General Virology* 4:169-176.
601. Ahl R. 1970. Temperature-dependent Interferon-sensitivity of Foot-and-Mouth Disease Virus. *Archiv für die gesamte Virusforschung* 32:163-170.
602. Haahr S, Teisner B. 1973. The influence of different temperatures on mortality, virus multiplication and interferon production in adult mice infected with Coxsackie B1 virus. *Archiv für die gesamte Virusforschung* 42:273-277.
603. Murphy BR, Baron S, Chalhub EG, Uhlenhof CP, Chanock RM. 1973. Temperature-Sensitive Mutants of Influenza Virus. IV. Induction of Interferon in the Nasopharynx by Wild-Type and a Temperature-Sensitive Recombinant Virus. *The Journal of Infectious Diseases* 128:488-493.
604. Atkins GJ, Johnston MD, Westmacott LM, Burke DC. 1974. Induction of Interferon in Chick Cells by Temperature-sensitive Mutants of Sindbis Virus. *Journal of General Virology* 25:381-390.
605. Atkins GJ, Lancashire CL. 1976. The induction of interferon by temperature-sensitive mutants of Sindbis virus: its relationship to double-stranded RNA synthesis and cytopathic effect. *J Gen Virol* 30:157-65.
606. Stanton GJ, Langford MP, Baron S. 1977. Effect of interferon, elevated temperature, and cell type on replication of acute hemorrhagic conjunctivitis viruses. *Infection and Immunity* 18:370-376.
607. Yin J, Gardner CL, Burke CW, Ryman KD, Klimstra WB. 2009. Similarities and differences in antagonism of neuron alpha/beta interferon responses by Venezuelan equine encephalitis and Sindbis alphaviruses. *J Virol* 83:10036-47.
608. Verbruggen P, Ruf M, Blakqori G, Overby AK, Heidemann M, Eick D, Weber F. 2011. Interferon antagonist NSs of La Crosse virus triggers a DNA damage response-like degradation of transcribing RNA polymerase II. *J Biol Chem* 286:3681-92.

609. Branca AA, Faltynek CR, D'Alessandro SB, Baglioni C. 1982. Interaction of interferon with cellular receptors. Internalization and degradation of cell-bound interferon. *J Biol Chem* 257:13291-6.
610. Himms-Hagen J. 1985. Food restriction increases torpor and improves brown adipose tissue thermogenesis in ob/ob mice. *American Journal of Physiology - Endocrinology And Metabolism* 248:E531-E539.
611. Cox B, Tha SJ. 1975. The role of dopamine and noradrenaline in temperature control of normal and reserpine-pretreated mice. *J Pharm Pharmacol* 27:242-7.
612. Zeisberger E. 1987. The roles of monoaminergic neurotransmitters in thermoregulation. *Can J Physiol Pharmacol* 65:1395-401.
613. Sun C, Gardner CL, Watson AD, Ryman KD, Klimstra WB. 2013. Stable, high-level expression of reporter proteins from improved alphavirus expression vectors to track replication and dissemination during encephalitic and arthritogenic disease. *J Virol* doi:10.1128/jvi.02990-13.
614. Russwurm S, Stonans I, Schwerter K, Stonane E, Mieissner W, Reinhart K. 2002. Direct Influence of Mild Hypothermia on Cytokine Expression and Release in Cultures of Human Peripheral Blood Mononuclear Cells. *Journal of Interferon and Cytokine Research* 22:215-221.
615. Fairchild KD, Singh IS, Patel S, Drysdale BE, Viscardi RM, Hester L, Lazusky HM, Hasday JD. 2004. Hypothermia prolongs activation of NF- κ B and augments generation of inflammatory cytokines, vol 287.
616. Hagiwara S, Iwasaka H, Matsumoto S, Noguchi T. 2007. Changes in cell culture temperature alter release of inflammatory mediators in murine macrophagic RAW264.7 cells. *Inflammation Research* 56:297-303.
617. Foxman EF, Storer JA, Vanaja K, Levchenko A, Iwasaki A. 2016. Two interferon-independent double-stranded RNA-induced host defense strategies suppress the common cold virus at warm temperature. *Proc Natl Acad Sci U S A* doi:10.1073/pnas.1601942113.
618. Smale ST, Plevy SE, Weinmann AS, Zhou L, Ramirez-Carrozzi VR, Pope SD, Bhatt DM, Tong A-J. 2013. Toward an Understanding of the Gene-Specific and Global Logic of Inducible Gene Transcription. *Cold Spring Harbor Symposia on Quantitative Biology* 78:61-68.
619. Au-Yeung N, Mandhana R, Horvath CM. 2013. Transcriptional regulation by STAT1 and STAT2 in the interferon JAK-STAT pathway. *Jakstat* 2:e23931.
620. Chang H-M, Paulson M, Holko M, Rice CM, Williams BRG, Marié I, Levy DE. 2004. Induction of interferon-stimulated gene expression and antiviral responses require protein

- deacetylase activity. Proceedings of the National Academy of Sciences of the United States of America 101:9578-9583.
621. Kadota S, Nagata K. 2014. Silencing of IFN-stimulated gene transcription is regulated by histone H1 and its chaperone TAF-I. *Nucleic Acids Research* 42:7642-7653.
 622. Medzhitov R, Horng T. 2009. Transcriptional control of the inflammatory response. *Nat Rev Immunol* 9:692-703.
 623. Vilcek J, Havell EA. 1973. Stabilization of interferon messenger RNA activity by treatment of cells with metabolic inhibitors and lowering of the incubation temperature. *Proc Natl Acad Sci U S A* 70:3909-3913.
 624. Al-Fageeh MB, Smales CM. 2006. Control and regulation of the cellular responses to cold shock: The responses in yeast and mammalian systems. *Biochemical Journal* 397:247-259.
 625. Roobol A, Carden MJ, Newsam RJ, Smales CM. 2009. Biochemical insights into the mechanisms central to the response of mammalian cells to cold stress and subsequent rewarming. *Febs j* 276:286-302.
 626. Aguilar PV, Adams AP, Wang E, Kang W, Carrara AS, Anishchenko M, Frolov I, Weaver SC. 2008. Structural and nonstructural protein genome regions of eastern equine encephalitis virus are determinants of interferon sensitivity and murine virulence. *J Virol* 82:4920-30.
 627. Garmashova N, Atasheva S, Kang W, Weaver SC, Frolova E, Frolov I. 2007. Analysis of Venezuelan equine encephalitis virus capsid protein function in the inhibition of cellular transcription. *J Virol* 81:13552-65.
 628. Ramseur JM, Friedman RM. 1977. Prolonged Infection of Interferon-Treated Cells by Vesicular Stomatitis Virus: Possible Role of Temperature-Sensitive Mutants and Interferon. *Journal of General Virology* 37:523-533.
 629. Barrett PN, Atkins GJ. 1981. Establishment of persistent infection in mouse cells by Sindbis virus and its temperature-sensitive mutants. *J Gen Virol* 54:57-65.
 630. Chaloner Larsson G, Johnson-Lussenburg CM. 1981. Establishment and maintenance of a persistent infection of L132 cells by human coronavirus strain 229E. *Arch Virol* 69:117-29.
 631. Cunningham AL, Fraser JR. 1985. Persistent rubella virus infection of human synovial cells cultured in vitro. *J Infect Dis* 151:638-45.
 632. Gercel C, Mahan KB, Hamparian VV. 1985. Preliminary characterization of a persistent infection of HeLa cells with human rhinovirus type 2. *J Gen Virol* 66 (Pt 1):131-9.

633. Joguet G, Mansuy JM, Matusali G, Hamdi S, Walschaerts M, Pavili L, Guyomard S, Prisant N, Lamarre P, Dejucq-Rainsford N, Pasquier C, Bujan L. 2017. Effect of acute Zika virus infection on sperm and virus clearance in body fluids: a prospective observational study. *Lancet Infect Dis* 17:1200-1208.
634. Biava M, Caglioti C, Castilletti C, Bordi L, Carletti F, Colavita F, Quartu S, Nicastri E, Iannetta M, Vairo F, Liuzzi G, Taglietti F, Ippolito G, Capobianchi MR, Lalle E. 2017. Persistence of ZIKV-RNA in the cellular fraction of semen is accompanied by a surrogate-marker of viral replication. Diagnostic implications for sexual transmission. *New Microbiol* 40.
635. Garcia-Bujalance S, Gutierrez-Arroyo A, De la Calle F, Diaz-Menendez M, Arribas JR, Garcia-Rodriguez J, Arsuaga M. 2017. Persistence and infectivity of Zika virus in semen after returning from endemic areas: Report of 5 cases. *J Clin Virol* 96:110-115.
636. Morrison TE. 2014. Reemergence of chikungunya virus. *J Virol* 88:11644-7.
637. Yactayo S, Staples JE, Millot V, Cibrelus L, Ramon-Pardo P. 2016. Epidemiology of Chikungunya in the Americas. *J Infect Dis* 214:S441-S445.
638. Kendrick K, Stanek D, Blackmore C. 2014. Transmission of Chikungunya Virus in the Continental United States — Florida, 2014. *MMWR Morbidity and Mortality Weekly Report* 63:1137-1137.
639. Lindsey NP, Staples JE, Fischer M. 2018. Chikungunya Virus Disease among Travelers-United States, 2014-2016. *Am J Trop Med Hyg* 98:192-197.
640. van Aalst M, Nelen CM, Goorhuis A, Stijnis C, Grobusch MP. 2017. Long-term sequelae of chikungunya virus disease: A systematic review. *Travel Med Infect Dis* 15:8-22.
641. Hawman DW, Carpentier KS, Fox JM, May NA, Sanders W, Montgomery SA, Moorman NJ, Diamond MS, Morrison TE. 2017. MUTATIONS IN THE E2 GLYCOPROTEIN AND THE 3' UNTRANSLATED REGION ENHANCE CHIKUNGUNYA VIRUS VIRULENCE IN MICE. *J Virol* doi:10.1128/jvi.00816-17.
642. Hall MP, Unch J, Binkowski BF, Valley MP, Butler BL, Wood MG, Otto P, Zimmerman K, Vidugiris G, Machleidt T, Robers MB, Benink HA, Eggers CT, Slater MR, Meisenheimer PL, Klaubert DH, Fan F, Encell LP, Wood KV. 2012. Engineered luciferase reporter from a deep sea shrimp utilizing a novel imidazopyrazinone substrate. *ACS Chem Biol* 7:1848-57.
643. Cook MJ. 1965. *The anatomy of the laboratory mouse*. Academic Press.
644. Snell LM, Brooks DG. 2015. New insights into type I interferon and the immunopathogenesis of persistent viral infections. *Curr Opin Immunol* 34:91-8.
645. Murira A, Lamarre A. 2016. Type-I Interferon Responses: From Friend to Foe in the Battle against Chronic Viral Infection. *Front Immunol* 7:609.

646. Levine B, Griffin DE. 1992. Persistence of viral RNA in mouse brains after recovery from acute alphavirus encephalitis. *J Virol* 66:6429-35.
647. Levine B, Hardwick JM, Trapp BD, Crawford TO, Bollinger RC, Griffin DE. 1991. Antibody-mediated clearance of alphavirus infection from neurons. *Science* 254:856-60.
648. Burdeinick-Kerr R, Wind J, Griffin DE. 2007. Synergistic roles of antibody and interferon in noncytolytic clearance of Sindbis virus from different regions of the central nervous system. *J Virol* 81:5628-36.
649. Burke CW, Gardner CL, Steffan JJ, Ryman KD, Klimstra WB. 2009. Characteristics of alpha/beta interferon induction after infection of murine fibroblasts with wild-type and mutant alphaviruses. *Virology* 395:121-132.
650. Klimstra WB, Ryman KD, Johnston RE. 1998. Adaptation of Sindbis virus to BHK cells selects for use of heparan sulfate as an attachment receptor. *J Virol* 72:7357-66.
651. Tsetsarkin K, Higgs S, McGee CE, De Lamballerie X, Charrel RN, Vanlandingham DL. 2006. Infectious clones of Chikungunya virus (La Reunion isolate) for vector competence studies. *Vector Borne Zoonotic Dis* 6:325-37.
652. Anishchenko M, Paessler S, Greene IP, Aguilar PV, Carrara AS, Weaver SC. 2004. Generation and characterization of closely related epizootic and enzootic infectious cDNA clones for studying interferon sensitivity and emergence mechanisms of Venezuelan equine encephalitis virus. *J Virol* 78:1-8.
653. Frolov I, Agapov E, Hoffman Jr TA, Prágai BM, Lippa M, Schlesinger S, Rice CM. 1999. Selection of RNA replicons capable of persistent noncytopathic replication in mammalian cells. *Journal of Virology* 73:3854-3865.
654. Gardner CL, Hritz J, Sun C, Vanlandingham DL, Song TY, Ghedin E, Higgs S, Klimstra WB, Ryman KD. 2014. Deliberate attenuation of chikungunya virus by adaptation to heparan sulfate-dependent infectivity: a model for rational arboviral vaccine design. *PLoS Negl Trop Dis* 8:e2719.
655. Davis NL, Willis LV, Smith JF, Johnston RE. 1989. In vitro synthesis of infectious venezuelan equine encephalitis virus RNA from a cDNA clone: analysis of a viable deletion mutant. *Virology* 171:189-204.
656. Bird BH, Albariño CG, Nichol ST. 2007. Rift Valley fever virus lacking NSm proteins retains high virulence in vivo and may provide a model of human delayed onset neurologic disease. *Virology* 362:10-15.
657. Caroline AL, Powell DS, Bethel LM, Oury TD, Reed DS, Hartman AL. 2014. Broad Spectrum Antiviral Activity of Favipiravir (T-705): Protection from Highly Lethal Inhalational Rift Valley Fever. *PLOS Neglected Tropical Diseases* 8:e2790.

658. Livak KJ, Schmittgen TD. 2001. Analysis of relative gene expression data using real-time quantitative PCR and the $2^{-\Delta\Delta C(T)}$ Method. *Methods* 25:402-8.
659. Trgovcich J, Aronson JF, Johnston RE. 1996. Fatal Sindbis virus infection of neonatal mice in the absence of encephalitis. *Virology* 224:73-83.
660. Bick MJ, Carroll JW, Gao G, Goff SP, Rice CM, MacDonald MR. 2003. Expression of the zinc-finger antiviral protein inhibits alphavirus replication. *J Virol* 77:11555-62.
661. Tesfay MZ, Yin J, Gardner CL, Khoretonenko MV, Korneeva NL, Rhoads RE, Ryman KD, Klimstra WB. 2008. Alpha/beta interferon inhibits cap-dependent translation of viral but not cellular mRNA by a PKR-independent mechanism. *J Virol* 82:2620-30.